Contributions Towards Positioning Normal Form Method as a Tool for Analysing Future Power Transmission Grid

Nnaemeka Ugwuanyi

HESAM UNIVERSITÉ

Arts et Métiers Sciences et Technologies

2020HESAE0020

ÉCOLE DOCTORALE SCIENCES ET MÉTIERS DE L'INGÉNIEUR

[L2EP - Campus de Lille]

THÈSE

présentée par : **Nnaemeka UGWUANYI**

soutenue le : **26 June, 2020**

pour obtenir le grade de : **Docteur d'HESAM Université**

préparée à : **École Nationale Supérieure d'Arts et Métiers**

Spécialité : **Génie électric**

Contributions Towards Positioning Normal Form Method as a Tool for Analysing Future Power Transmission Grid

THÈSE dirigée par :

[M. KESTELYN Xavier]

et co-encadrée par :

[M. MARINESCU Bogdan]
[M. THOMAS Olivier]

Jury

M. MESSINA Arturo,	Prof., Electr. Eng., CINVESTAV	Président
Mme. SECHILARIU Manuela,	Prof., AVENUES EA 7284, UTC Compiègne	Rapporteur
M. EKWUE Arthur,	Prof., Electr. Eng., University of Nigeria, Nsukka	Rapporteur
M. THOMAS Olivier,	Prof., LISPEN EA 7515, ENSAM	Examinateur
M. MARINESCU Bogdan,	Prof., LS2N UMR 6004, Ecole centrale de Nantes	Examinateur
M. KESTELYN Xavier,	Prof., L2EP EA 2697, ENSAM	Examinateur

THÈSE

Dedicated to my little daughter Chidazie Ugwuanyi.

Acknowledgement

This thesis is a success not only because I worked hard but also because other persons formed a ladder for me to climb. Some have played easily visible roles while others have worked in the background. I would mention just a few, but I sincerely appreciate all that contributed in one way or the other to bring about the success of the thesis.

Foremost, I would like to express my profound gratitude to my advisors Prof. Xavier Kestelyn, Prof. Bogdan Marinescu and Prof. Olivier Thomas for their continuous research support, motivation, enthusiasm, and wealth of knowledge. They really made a good research team for me and I could not have imagined having better advisors and mentors for my PhD.

I would like to thank all members of my thesis committee, in particular, the president, Prof. Arturo Messina and the two rapporteurs, Prof. Manuella Sechilariu and Prof. Arthur Ekwue, for their encouragement, insightful comments, and thought-provoking questions.

My sincere thanks also goes to Dr. Bin Wang for all his suggestions and help despite being far away. Although, we did not meet physically, each e-mail from him was really helpful.

My special thanks also goes to Dr. Frédéric Colas who was not directly my advisor but always was ready to help me out.

I would like to thank all the doctoral and postdoctoral fellows in L2EP, LISPEN and LMFL laboratories of ENSAM, Lille campus, where I worked during this thesis. In particular, I thank my colleagues in the office, Quentin Cossart, Martin Legry, Pierre Vermeersch, Jérôme Buire, Artur Avazov and Taoufik Qoria for their ideas shared and for the good moments we spent together.

My profound gratitude goes to my family and in particular, my mother, Theresa Ugwuanyi, firstly, for giving birth to me and for her moral and spiritual support throughout my life.

I would like to sincerely thank my lovely wife Eberechukwu for her support, understanding and patience during the period of this PhD.

I would like to thank the Tertiary Education Trust Fund (TETFUND) Nigeria for financially supporting this thesis.

Above all, there is one behind all the above human connections. He is the almighty God and He has arranged every plan and made it possible to bring the needed people together, thereby ensuring that this thesis is a success. I personally believe that God leads those who believe in Him, and He did lead me through this journey.

Abstract

Given several economic, technical and environmental constraints, today's power systems are operated very close to their limits, which means they exhibit nonlinear behaviour more than in the past. In addition, the transfer of large amount of power over long distances common nowadays leads to nonlinear interactions, a phenomenon which challenges the traditional power system analysis tools. Furthermore, high penetration of renewable energies and the accompanying power electronics, which are evident in today's power systems, increase the nonlinearities of the systems. As a result, the well-established modal analysis tools become insufficient for the analysis of present and future power systems; making the development of alternative tools necessary. The inclusion of higher order terms in modal analysis, possible with Normal Form (NF) method, augments the information it provides, and enables better dynamic studies of systems exhibiting high nonlinear behaviour. However, NF method requires the preliminary Taylor expansion of the nonlinear system, which generates several higher order Hessian matrices and coefficients to be computed, an operation impracticable with standard methods, when considering large scale systems. In this thesis, to answer to this problem, an efficient numerical method for accelerating those computations, by avoiding the usual Taylor expansion is developed. The new computations consist in prescribing the linear eigenvectors as unknown field in the initial nonlinear system, which leads to solving linear-only equations to obtain all needed coefficients. In this way, the computation of the nonlinear model up to third order, and nonlinear modal analysis become fast, and achievable in a convenient computation time. Moreover, NF-based indices for power system stability and operation monitoring are proposed and tested on several systems.

Key words: Computation reduction, nonlinear modal analysis, normal form method, power system analysis.

Résumé

Compte tenu de plusieurs contraintes économiques, techniques et environnementales, les systèmes électriques actuels fonctionnent très près de leurs limites, ce qui fait qu'ils présentent de plus en plus des comportements non linéaires. De plus, le transfert d'une grande quantité d'énergie sur de longues distances n'est pas rare aujourd'hui, cela conduit à des interactions non linéaires, conduisant à un réel défit; celui de l'utilisation des outils traditionnels d'analyse du système électrique en présence de fortes non linéarités. En outre, la forte pénétration des énergies renouvelables et de l'électronique de puissance qui l'accompagne viennent augmenter ces non linéarités du système électrique. En conséquence, les outils d'analyse modale bien établis utilisés par le passé deviennent insuffisants pour l'analyse du système électrique aujourd'hui et celui du futur; d'où le besoin d'outils alternatifs. L'inclusion de termes d'ordres supérieurs dans l'analyse modale, possible avec la méthode de forme normale (NF), augmente les informations qu'elle fournit et permet de mieux étudier les aspects dynamiques sur un système d'alimentation présentant un comportement fortement non linéaire. Cependant, la méthode NF nécessite au préalable la décomposition de Taylor du système non linéaire, qui produit plusieurs matrices et coefficients de Hesse d'ordre supérieur, une opération non réalisable avec les méthodes standard lorsque l'on considère les systèmes à grande échelle. Dans cette thèse, pour répondre à cette problématique, une méthode numérique efficace pour accélérer ces calculs, en évitant l'expansion de Taylor habituelle, est développée. Les nouveaux calculs consistent à définir les vecteurs propres linéaires comme champ inconnu dans le système non linéaire initial, ce qui conduit à résoudre des équations linéaires uniquement pour obtenir tous les coefficients nécessaires. De cette façon, le calcul du modèle non linéaire jusqu'au troisième ordre et l'analyse modale non linéaire deviennent simples et réalisables avec un temps de calcul raisonnable. De plus, des indices basés sur la NF pour la stabilité du système électrique et la surveillance du fonctionnement sont proposés et testés sur plusieurs systèmes.

Mots clés: Réduction du calcul, analyse modale non linéaire, méthode de forme normale, analyse du système d'alimentation.

Contents

List of Tables

List of Figures

Chapter 1

Introduction

"*Things change. And friends leave. Life doesn't stop for anybody.*"

Stephen Chbosky

Contents

1.1 General Context and Motivation

1.1.1 The Changing Grid

Power system is an interconnection of many components such as generators, transformers, transmission lines and so on. The electric power is produced by the generators and transported to the loads through the transmission lines. These lines can be short or long depending on the separation between the generation and loads. The electric power seems to be the most beneficial engineering innovation today. Therefore, to ensure a reliable and efficient power delivery, several intelligent techniques are being introduced into the power system. However, due to ratings and other constraints of the power system components, there is always a limit for operating the system, so called stability margins.

In the traditional power systems, the generators are mainly synchronous machines, mainly powered by environmentally-unfriendly sources like fossil fuel. Fossil fuel in turn is a key player in environmental degradation due to the accompanying emissions. The reduction of gas emissions and hence, fossil fuel, has been a worldwide concern owing to several negative environmental changes. With several economic, technical and environmental constraints, today's power system is operated very close to its margins, making the system to be stressed. A stressed system has operating condition near, for example, the voltage stability limit and may be as a result of — 1) a higher level of system loadings, 2) heavy power transfer across some transmission interfaces, and 3) heavy loading of certain plants. This can be represented by a power-voltage (P-V) curve for bus voltage stability as shown in Figure 1.1. Stressed power system can lead to complex dynamic behaviour. That is, unusual nonlinear behaviour that could be difficult to explain.

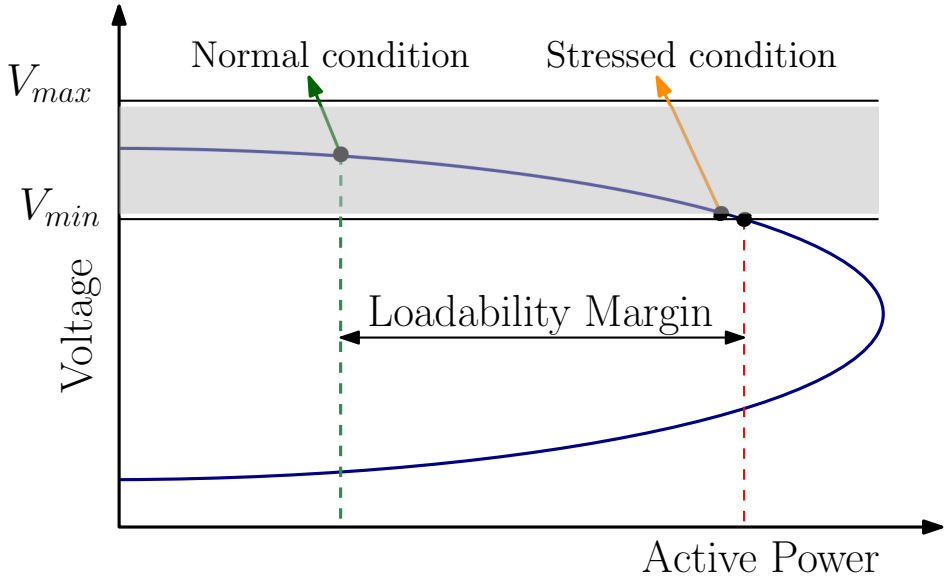

Figure 1.1 – P-V curve showing normal and stressed conditions

The depletion of fossil fuel has forced a shift from traditional energy resources to renewable energies (REs) such as solar thermal, solar photovoltaic, wind, and biogas [1]. Each year, more electricity is generated from renewable energy than in the previous year (see Figure 1.2). The integration of these renewable energies into the grid is now feasible due to the technological advancements in power-electronic-based (PE) converters. The emergence of new PE devices onto the power scene and the increasing number of distributed generation power systems in electrical grids contribute to changing the structure of the traditional grid. This outburst seems to be the fastest growing trend in power system [2, 3] with proliferation of DC/AC inverters, switch mode power supplies, High Voltage DC (HVDC) links, distributed renewable energy systems, Static VAr Compensator (SVC), and other Flexible AC Transmission Systems (FACTS) devices.

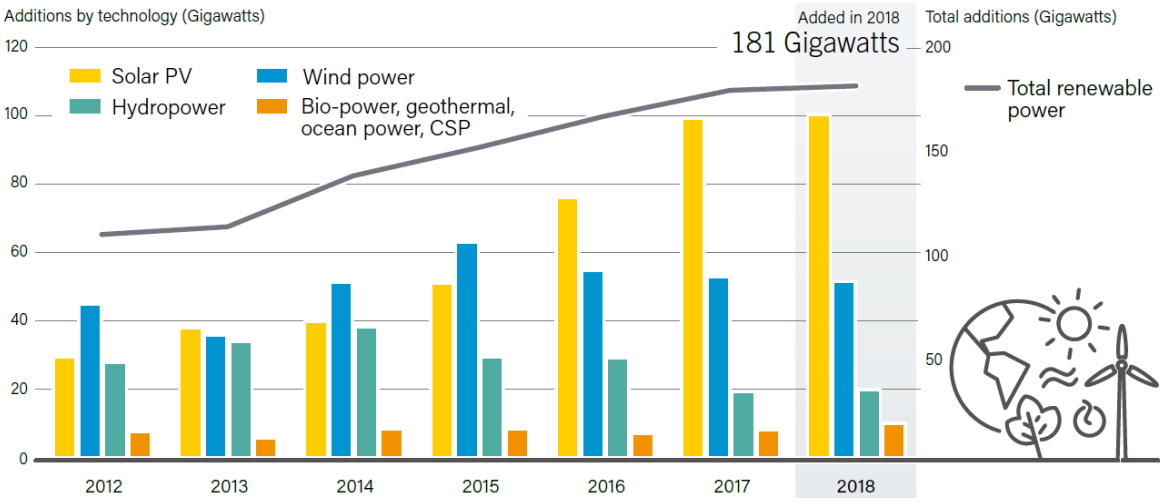

Figure 1.2 – Annual Global Additions of Renewable Power Capacity, by Technology and Total, 2012-2018 [4]

1.1.2 Present and Potential Future Challenges of the Grid

The system stress together with the integration of RE increases the system nonlinearities and hence, creates new challenges to power systems. It can lead to nonlinear interactions of the system modes of oscillation, which alter the dynamic behaviour of the system. *Mode* is the technical term for a particular oscillation pattern (see detailed explanation in section 1.3). The system nonlinearities and modal interactions are impacted by system operating conditions, control strategy, and control system parameters [5]. The transfer of large amount of power over long distances are not uncommon nowadays due to inter-area connections (example Scotland-England) and the growth of RE sources. Moreover, most viable RE sources like wind farms are usually far from load centre. The transfer of large power over long distances leads to power oscillations and nonlinear interactions in a High Voltage AC (HVAC) system.

HVDC links can be used instead, in order to damp the oscillations. However, the controls for HVDC can lead to strong nonlinear interactions, though these interactions are not always necessarily negative. Earlier investigation of nonlinear modal interaction in a HVDC/AC system with DC modulation indicated that strong nonlinear modal interaction can result from higher AC and DC loading and with well-tuned DC power modulation [5]. Perhaps, with the development of Modular Multilevel Converters (MMC) technologies, the situation may be different. Other PE devices also lead to increased nonlinearity. For example, the control parameter of SVCs can lead to strong nonlinear interactions in a stressed system, which gives rise to unstable oscillations [6]. Note that the controls of synchronous machines can equally introduce nonlinearities especially if not properly tuned [7]. However, [8] reported that nonlinear interaction is stronger when PE controls are in the system. With the growth of REs, utilising an additional device, such as battery energy storage (BES) in power systems is inevitable. A current research reported that increasing BES's gain controller could lead to interaction events [9]. Since REs inject power into the network through PE converters, resulting in the lack of inertia and synchronising torque in the grid, de-commitment of the synchronous generators would increase the effect of nonlinearity [10] and will affect the rotor angle stability. Also, the PE converters could form a virtual capacitance, which could interact with the AC grid to trigger an unstable oscillation in relatively weak (i.e high impedance) system [11].

As highlighted in [12, 13], apart from contributing to nonlinearity, REs and their accompanying PEs introduce new modes of oscillation to the grid due to displacement of synchronous machines. It was noted in [12] that these new modes of oscillation are highly sensitive to control parameter variations, and can make the system more unpredictable and hard to monitor or control.

The challenges of RE/PE penetration to the grid have triggered serious researches in Europe, mainly anchored by Massive Integration of Power Electronic Devices (MIGRATE) [14], which aims at finding solutions to the technical challenges. The MIGRATE's report on systemic issues are summarised in Table 1.1. The manifestations of these challenges abound in practical power systems with significant RE integration. For example, on 19 February 2011, inter-area oscillations within the Continental Europe (CE) power system occurred. Similar oscillations reoccurred on 24 February, 2011. The oscillation frequency was 0.25 Hz and lasted for 15 minutes (see Figure 1.3). There was no clear clue on the cause of the oscillation initially. Modal calculations in [16] later revealed that two modes superimposed at 0.25 Hz with participation of Turkey, Spain/Portugal and Italy against North of Europe. The following conclusions were made in [16]: (1) there was an interaction of 0.18 Hz (East-West mode) and

Table 1.1 – Ranking of the power system stability issues as identified by European TSOs in the context of the MIGRATE Project [15]

Ranking	Ranking score	Issue
1	17.35	Decrease of inertia
2	10.16	Resonances due to cables and PE
3	9.84	Reduction of transient stability margins
4	8.91	Missing or wrong participation of PE-connected generators and loads in frequency containment
5	8.19	PE Controller interaction with each other and passive AC components
6	7.50	Loss of devices in the context of fault-ride-through capability
7	7.00	Lack of reactive power
8	6.91	Introduction of new power oscillations and/or reduced damping of existing power oscillations
9	6.09	Excess of reactive power
10	4.27	Voltage Dip-Induced Frequency Dip
11	3.87	Altered static and dynamic voltage dependence of loads

0.25 Hz (North-south mode) modes, (2) synchronous connection of Turkey displaces 0.3Hz mode to 0.25 Hz (new mode), (3) the RE generators subtracted inertia from the system by replacing generators equipped with power system stabilzer (PSS). Consequently, the Italian TSO immediately reinforced PSSs in Italy. Another severe oscillation occurred in Hami wind

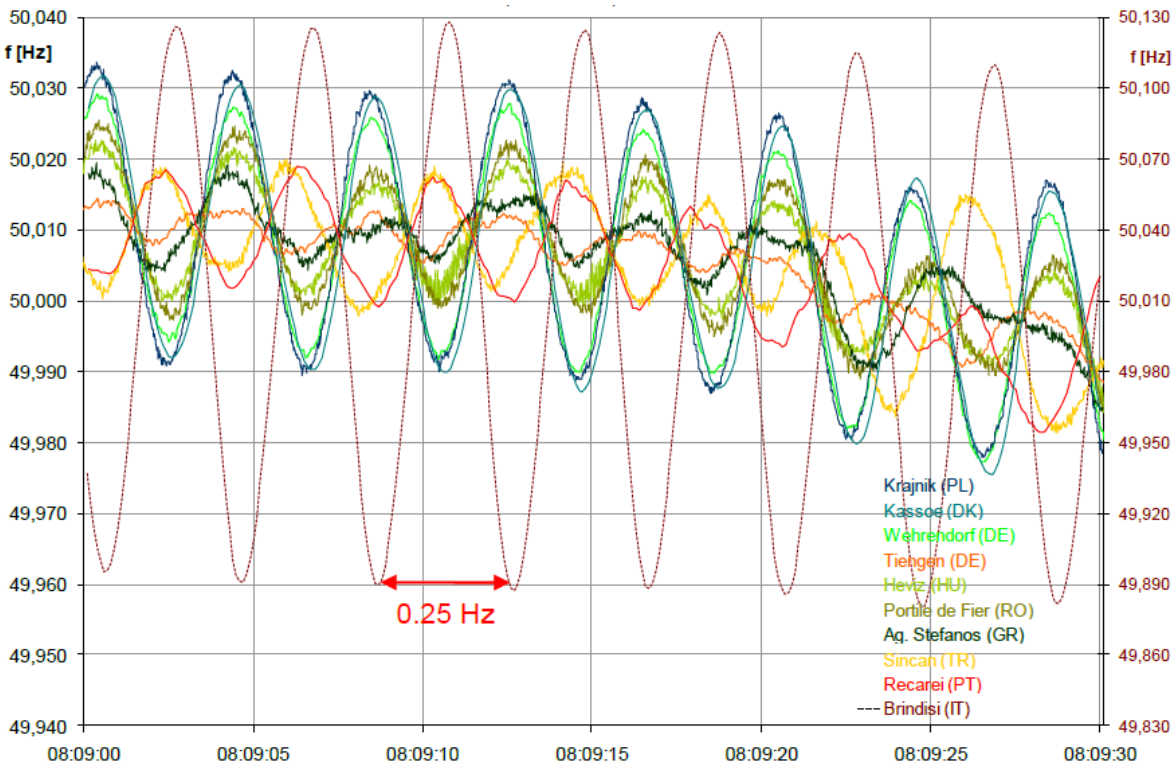

Figure 1.3 – Detailed view of system frequency (measurements) for 19 February 2011— Brindisi (IT) in phase with Sincan (TR) and Recarei (PT) opposite to Portile de Fier (RO) and Kassoe (DK) [[16]

power system, Xinjiang, China on July the 1st, 2015 and lasted for 3 hours and 20 minutes.

It was later found out that this oscillation was caused by the interaction between multiple wind turbine converters (WTCs) of permanent magnet synchronous generators (PMSGs) and the weak AC grid [17].

In the light of all these present and anticipated changes in the grid, it becomes necessary to extend the analysis of the grid in order to properly characterise its dynamic behaviour and to better design its controls. This will require more sophisticated tools to cope with the evolution. Although, there are several studies going on in respect to the increased nonlinearity and consequent unusual behaviour of the grid, not much attention is being paid to the nonlinear interactions, which can reveal a lot of hidden information in the system. The effect of nonlinear interactions in a system can be negative or positive, depending on the condition of the system. This is perhaps, among other things, the reason why in literature, both positive and negative effects of RE/PE integration are being reported. For instance, improved damping of oscillations in case of an increasing share of PE-interfaced generation was reported in [18].

1.1.3 Need for Developing Tools in Continuity of the Existing Ones

As mentioned earlier, stressed systems exhibit strong nonlinear behaviour and the RE/PE integration into the grid further contributes to this stress. More sophisticated tools are needed to cope with the complexity of the system. Advanced tools such as Pattern Recognition methods [19], Expert Systems (ES) methods [20], Robust-control-based tools [21], are being developed for the study of complex systems. However, these tools are too far from the knowledge of an average power system operation engineer. Most often, they do not present quantifiable physical parameters to enable the engineer make decisions or plannings. The best known tool for studying oscillations in power system is modal analysis. The conventional modal analysis tools such as small-signal stability are commonly used. However, they are linear tools and will no more be sufficient to accurately characterise the behaviour of the grid when there is high penetration of RE/PE. There is therefore, a need to provide alternative tools with features common to the engineers and yet, with extended capabilities. *Normal Form (NF)* is a good alternative but it is difficult to apply to systems with large number of state variables.

1.1.4 Defining a Large Grid

Often times, when large grid/system is mentioned, what comes to mind is a power system with so many buses, lines, generators and so on. While this is logical, the meaning of large grid can be somewhat confusing. A grid could be large in the sense that there are many

interconnections and buses. A grid may also be considered large because of the computational difficulty in its analysis. The latter implies that, if power flow computation is considered, a 39-bus system for instance, is larger than a 9-bus system. This is because, the voltages at each bus and line flows have to be computed. On the other hand, if the dynamics of the state variables are to be considered, a 9-bus system with four machines, each modelled with 6 state variables may be considered larger that a 39-bus system with ten machines, each modelled with 2 state variables. Large system is used in this work in the sense of more state variables. The European interconnected system with about 20,000 state variables is commonly considered a large system. However, some new tools being developed for the future grid; such as the one considered in this work are extremely computation-intensive. As such, a system of 100 state variables for example may be considered large if a system with, say 20 variables, are sufficiently difficult to analyse. It is in this narrow context that *large grid* is used in this work.

1.2 Tools for Power System Dynamic Performance Analysis

The tools for the analysis of power system dynamic behaviour can be classified into two:

- nonlinear tools, which are suited for transient stability analysis.
- linear or small-signal analysis (SSA), which is based on the linear techniques and employed for small-signal stability analysis.

1.2.1 Transient Stability Analysis

Transient stability is the capacity of the power system to remain in synchronism following a large disturbance. There are several methods for transient stability analysis, which are basically grouped into time domain simulations (TDS) and direct methods. TDS remains the most reliable method to investigate nonlinear systems. However, simulating a high dimensional power grid could be very time consuming if oscillators are coupled and interact nonlinearly [22, 23]. Moreover, it does not provide information regarding the degree of stability or instability of a power system. It lacks in qualitative and structural information about the system.

Direct methods such as equal area criterion (EAC) and energy function techniques like *boundary of stability region based controlling unstable equilibrium point method* (BCU method) have their own strengths and weaknesses. EAC uses graphical visualisation to simplify stability assessment, but limited to two-machine systems. Energy function methods are fast but not every post-fault transient stability model admits an energy function [24]. In addition

finding the controlling unstable equilibrium point (CUEP) by BCU is difficult. To enhance the transient stability analysis, it could be gainful to combine the TDS and the direct methods. This will reduce the challenges in each method.

1.2.2 Small-signal Stability Analysis

When a disturbance to the system is small enough, the system can be assumed to exhibit linear behaviour and can be analysed by linearising the system model around its steady-state operating points. The linearised model can provide many information not explicit in time-domain simulation. Stability determined with such model and with such assumption is called small-signal stability.

The first step involved is to linearise the power system differential equations in the neighbourhood of stable operating point. Then, the eigenvalues of the system are used to characterise the stability. The real part and the imaginary parts of an eigenvalue give damping and frequency information respectively. If the real part of the eigenvalue is negative, the amplitude of the oscillation decays and the system is stable. If the real part is positive, the amplitude increases and the system is not stable. For zero real part, the amplitude remains constant and more information is required for the stability. With the eigenvalues and eigenvectors, it is possible to obtain an approximate close-form solution of the nonlinear differential equations with a given initial condition.

Small-signal stability analysis is a powerful tool for engineers. It presents the numerous mathematics describing the system in terms that are easy to understand and interpret. Just by observing the real part of an eigenvalue, an engineer has a feel of the likely behaviour of the system. SSA tool is almost indispensable in dynamic analysis. The challenge however, is that the analysis is limited to a neighbourhood of the operating point which the linearisation is valid.

1.3 Modes of Oscillation

There are several modes of oscillations in an interconnected system. Mathematically, a mode (or an eigenmode)/natural mode is the term for one eigenvalue/eigenvector pair of the linear part of a dynamical system. Physically, a mode can be viewed as a unique pattern in which the stored energy in the system is expended when the system is disturbed. As an illustration, consider in Figure 1.4, two masses m_1, m_2, attached to three springs k_1, k_2 , and k_{12} . Assume the end points are fixed, this system has two natural modes of oscillation.

Let the displacements of the first mass be $x_1(t)$ and that of the second mass $x_2(t)$. The

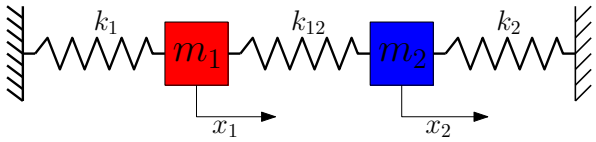

Figure 1.4 – Mass-spring system exhibiting two natural modes of oscillation.

equations of motion of the system are given by

$$m\ddot{x}_1 = -k_1x_1 - 0.3k_1x_1^2 - 0.4k_1x_1^3 + k_{12}(x_2 - x_1) \tag{1.1a}$$

$$m\ddot{x}_2 = -k_2x_2 + 0.4k_1x_2^2 + 0.3k_1x_2^3 + k_{12}(x_1 - x_2), \tag{1.1b}$$

where nonlinearities (arbitrarily chosen) in the springs are intentionally added for demonstrations.

If we assume that the displacements are small enough and the equilibrium of the system is at the origin, the effects of the nonlinear terms (blue in (1.1)) can be neglected and it is possible to compute the natural frequencies in Hertz for identical springs and masses (i.e., $k_1 = k_2 = k_{12} = k,\ m_1 = m_2 = m$) as

$$f_1 = \frac{1}{2\pi}\sqrt{\frac{k}{m}}, \quad f_2 = \frac{1}{2\pi}\sqrt{\frac{3k}{m}}. \tag{1.2}$$

Having assumed a linear system, when the mass m_1 is moved by x_1 to the right, the spring k_1 pulls the mass to the left with a reaction force k_1x_1, and the spring k_{12} pushes the mass to the left with a reaction force $k_{12}(x_1 - x_2)$. Similarly, when the mass m_2 is moved by x_2 to the left, the spring k_2 pulls the mass to the right with a reaction force k_2x_2, and the spring k_{12} pushes the mass to the right with a reaction force $k_{12}(x_2 - x_1)$. Assume $k = 5,\ m = 1$, $f_1 = 0.36\ Hz$ and $f_2 = 0.62\ Hz$. Thus, the two modes are described below :

- **Mode 1 -** both masses move together at frequency $f_1 = 0.36\ Hz$, with the same amplitude and in the same direction so that the connecting spring (k_{12}) between them is neither stretched nor compressed. This motion is shown in Figure 1.5a and is obtained by simulating the nonlinear system (1.1) with small and equal initial conditions for $x_1,\ x_2$. The FFT of Figure 1.5b confirms the frequency of the oscillation.

- **Mode 2 -** both masses move at frequency $f_2 = 0.62\ Hz$, with the same amplitude but in opposite directions so that the connecting spring (k_{12}) between them is alternately stretched and compressed. In this case, the center (node) of the connecting spring is stationary. This motion is shown in Figure 1.5c and is obtained by simulating the nonlinear system (1.1) with small, equal but opposite initial conditions for $x_1,\ x_2$. The FFT of Figure 1.5d confirms the frequency of the oscillation.

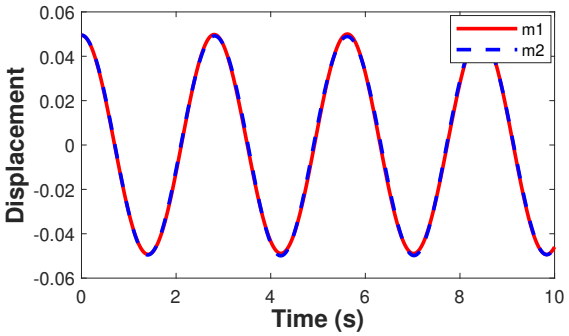

(a) Mode 1—0.36 Hz

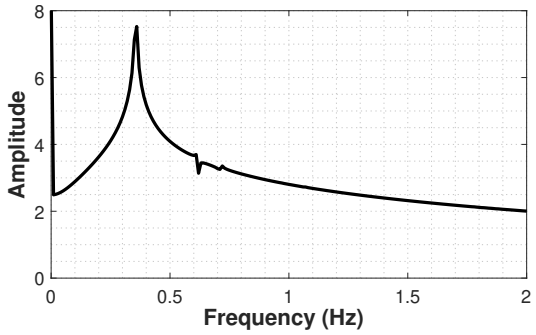

(b) Mode 1—FFT spectrum

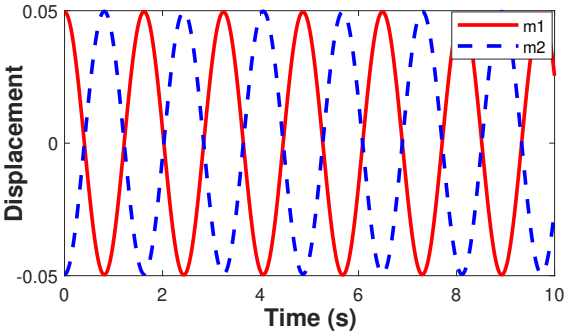

(c) Mode 2—0.62 Hz.

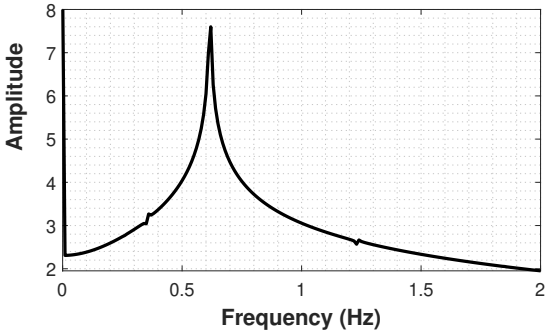

(d) Mode 2—FFT spectrum.

Figure 1.5 – Natural modes of Oscillation of two-mass three-spring system.

Any other motion of the bodies in Figure 1.4 is not natural but a linear combination of the two natural modes. The two modes described above have two distinct frequencies. Thus, mode is often used, more loosely, to refer to an oscillation at a characteristic frequency.

Power system can be modelled similar to the system in Figure 1.4, whereby the spring constant and the displacement are equivalent to the line impedance and rotor deviation respectively. The reaction force is analogous to the synchronising power of the power system. Let the force moving these masses represent the generator or fault power transported through the line. It can be seen from (1.1) and (1.2) that:

- Power flow on the lines can lead to oscillations.
- Higher impedance of the lines can lead to low frequency oscillation.
- Higher impedance of the lines can weaken the ties between machines.

Using more elaborate models, major oscillations in power systems include: electromechanical, control, and torsional modes of oscillation. For electromechanical modes, the most involved variables are the internal angles and the rotor speeds of the generators. Generally speaking, power systems low-frequency oscillations are a result of electromechanical coupling between the transmission network and generators. Control modes are associated with generator or the exciter units and other control equipment, such as poorly tuned exciters, HVDC converters, and static var compensators. Torsional oscillation modes are associated with the

turbine generator shaft rotational system. The major challenge of the power system is the low frequency electromechanical oscillations which can either be *local* or inter-area. When a machine or group of machines that have strong electric ties in an area oscillates and their oscillations are dominant in the area they are located, it is known as local oscillation. Inter-area mode involves machines in one area swinging against machines in other areas. It usually has lower natural frequency in the range of 0.1-0.8Hz [25]. However, with several converter control-based generators (CCBG) devices in the grid, the above characteristics may not always be true signatures of electromechanical modes. This is because the CCBGs lead to new low oscillatory modes akin to the inter-area electromechanical modes of oscillation [12]. This phenomenon poses a problem in identifying clearly, the actual electromechanical modes. New methods are being developed to tackle this problem [26]. Analysis of large systems has to necessarily focus on the critical modes of importance, usually the inter-area modes.

The study of the behaviour of these modes is known as modal analysis. The most common tool for modal analysis is the SSA which provides much information regarding these oscillations. Since SSA explains only linear behaviour, it is more precisely referred to as Linear Modal Analysis (LMA).

1.4 Modal Interactions and Nonlinear Modes

When the power system is stressed, the dynamics are not completely described by the natural modes. In addition to the natural modes, the dynamics can be affected by some higher order combinations of the natural modes. The effect of these higher order combinations is called *nonlinear modal interaction*. The nonlinear modal interaction gives rise to "other modes", which may significantly affect the dynamics of the system. The mechanism, by which these "other modes" are formed, will be clearly explained, mathematically, in later chapters. The concept of *nonlinear mode* allows for proper understanding, and interpretation of the phenomenon—nonlinear modal interaction, since it helps to explain the "other modes", with the eigenspectrum. Nonlinear mode is used to describe the extension of a linear mode to the nonlinear regime. Thus, it is an extension of the invariance property of a linear mode to the nonlinear regime. Physically, it is the rendering of nonlinear modal couplings, in a way that, if a particular motion is initiated on a particular mode only; no energy is given to the others, such that the motion remains on this mode only.

Modal interaction is critical and can either stabilise or destabilise the system. For instance, the excitation system can introduce modes which interact with the electromechanical modes of the system, resulting in angle instability. When nonlinear modal interaction occurs, the

dynamics become difficult to explain with LMA. The modal analysis which takes into account the nonlinear interactions of modes is known as Nonlinear Modal Analysis (NLMA).

A simple illustration of nonlinear modal interactions can be shown by simulating the system (1.1) with higher initial conditions (i.e larger displacements of x_1, x_2). The effect of the nonlinearities will no longer be negligible and the oscillation will be composed of the linear (natural) and significant combinations of the linear modes. This is shown in Figure 1.6. It is clear from Figure 1.6a that mode 1 is dominant. At least, the response resembles the one in Figure 1.5a. However, the conclusion that linear mode is sufficient

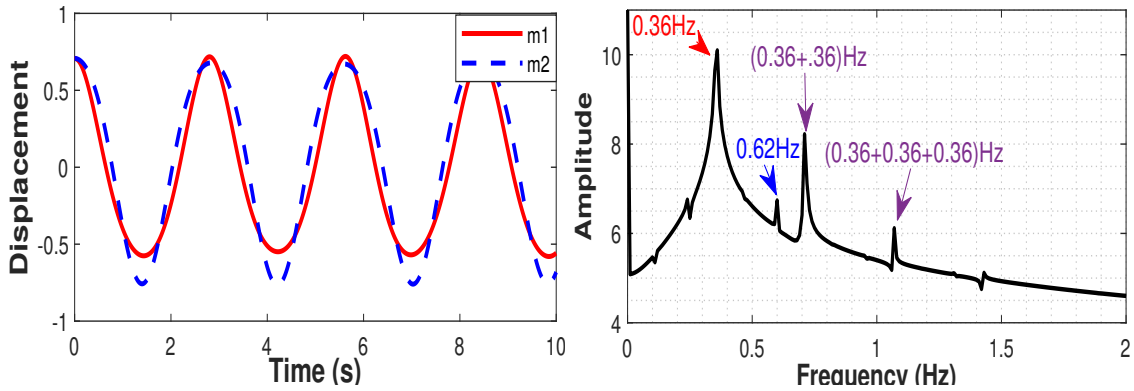

(a) Mode 1—0.36 Hz (b) FFT showing—linear and nonlinear modes.

Figure 1.6 – Example of modal interactions

to understand the behaviour of that system can be deceptive. The FFT in Figure 1.6b clearly reveals the significant presence of other frequencies, in this case, due to nonlinear distortions of the natural modes. For example, the two linear modes are identified (0.36 Hz and 0.62 Hz) with mode 2 having smaller peak. Observe that there is a frequency of 0.72Hz (i.e., $0.36 + 0.36 = 2 \times$ mode 1), whose amplitude is high. There is also a frequency of 1.08 Hz (i.e., $0.36 + 0.36 + 0.36 = 3 \times$ mode 1), although with smaller peak. In a way, one can loosely say, there are "new modes" in the dynamics other than the linear modes. A common term usually used to describe these new frequencies is *nonlinear harmonics*, since they are multiples of the fundamental modes. However, as we shall see in later chapters, these new frequencies are not necessarily multiples of a fundamental mode but can come from combinations of different modes. NF provides analytical way to clearly explain the sources of these frequencies. When a power system is stressed, this phenomenon is present. Therefore, other information is needed in addition to linear analysis to properly understand the behaviour.

There are basically two approaches for detecting nonlinear modal interactions in a system—time-domain-simulation-based methods and closed-form solution methods. In case of time domain simulation, the time responses are extracted, and then, their spectral components

decomposed with some tools like Hilbert spectra analysis (HSA), Prony analysis or FFT (though other methods have been proven to be more efficient). By evaluating the damping and the frequency, the mode combination leading to a new mode with significant amplitude can be predicted. The comparison of the new mode with the natural modes can show possible interaction. The second method extends the LMA to obtain closed-form solution of the nonlinear approximate model of the system. Then, it enables some definitions which exactly detect the interacting modes and the new frequency. The most common tool in the second category is the NF tool. NF method has advantage in that it does not only detect the nonlinear interaction, but also, it renders the system in such a way that the convenient techniques in LMA can still be employed to describe the system. In other words, it provides a good way to explain the concept of nonlinear modes. However, it has very serious computational challenges. The two approaches can be used in a complementary way. Thus, time domain simulation can be used to verify the solutions from NF method.

1.5 Normal Form Method

The term *Normal Form* is used in several domains for various connotations. For example, it is used to refer to database normalisation. In mathematics and computer science, it can mean any standard way of presenting object as a mathematical expression. Example in this case is the Jordan normal form. Normal Form as used in this work is a mathematical technique that simplifies a set of nonlinear differential equations into a simplified one, which can be linear in some particular cases. The simplification is achieved by introducing sequential nonlinear coordinate transformations. The resulting equations are then in their simplest form (Normal Form) [27–30]. This definition of *Normal Form* is often precisely referred to, as Poincaré Normal Form, after the work of Poincaré [27]. It is based on the series expansion of a system of nonlinear differential equations. The NF technique itself is very old but its power system application to nonlinear modal analysis is quite on the trend. In the last two decades, researchers at Iowa state university made several publications and promoted the need to study higher order modal analysis with Normal Form. Their propositions received concern and in 2005, an IEEE task-force was formed to investigate on the need for inclusion of the higher order terms in small-signal analysis. The task-force highlighted the potentials of NF technique and recommended its higher order development in future [31].

The NF approach consists of obtaining a higher order Taylor series expansion of the nonlinear equations around a stable equilibrium point (SEP). The linear part of the series expansion is analysed to extract the modal contents. With the modal parameters of the linear

part, it is possible to define some coordinate change of variables which simplify the nonlinear parts.

The higher order NF accounts for sufficient nonlinearities and hence, will be suitable for studying the developments in today's grid, and even in future. This has been demonstrated on grid with high penetration of RE/PE in [10].

1.6 Objective and Scope of the Research

The implication of all the changes going on in today's grid is that the LMA tools designed for its analysis begin to fail. Yet, the features of LMA tools are so attractive that losing them will be difficult. Among the nonlinear alternatives, NF method has received highest research interest up till present day. NF tool has however, a major setback that limits its application in power system. It is computationally very expensive. Traditional approach requires the preliminary evaluation of Hessian matrices and eigenvalue expansion, which are impracticable with standard methods when considering large scale systems. The process of the eigenvalue expansion is very difficult and needs to be accelerated. In order to improve on this global power system problem and make nonlinear modal analysis of the future grid possible, this thesis principally deals with one issue:

- **The drastic reduction of the computations needed to apply NF method to power systems with large number of state variables (so-called large systems).**

The thrust of the work is therefore, the simplification of processes for NF application in power systems. A new method for rapidly evaluating all polynomial coefficients (termed *nonlinear coefficients* in this work) needed for NF application is proposed. It is assumed that the computation of all eigenvalues is possible and the power system network is already reduced if necessary. Proposed method was applied to four different systems: the IEEE 3-, the IEEE 10-, the IEEE 16-, and the IEEE 50-machine systems. Known applications of NF, such as participation factor analysis, stability and nonlinear frequency shift predictions are reviewed and implemented with drastically reduced computation. The other scopes of the research work are as follow:

- It is assumed that the nonlinearities are smooth and static. By smooth nonlinearities, it means that the system nonlinearities considered are that which can be represented by the higher order terms in the Taylor series expansion for the set of system differential equations. By static nonlinearities, it means that the nonlinearities are not on the differential parts (terms) of the system model but on the algebraic parts (terms). The second and third order terms of the equations of the power system are considered in

this research work. However, higher orders can be considered if deemed necessary and practicable.

- The LMA is performed to extract the fundamental mode of oscillations of power system and associated eigenvectors. Then with the eigenvectors, the original system is transformed to Jordan form.
- The same Jordan transformation is extended to the nonlinear parts of the Taylor expansion. But the Jordan transform equivalent for the second and third order terms are estimated with the modal parameters obtained from the LMA. The original system is perturbed using the eigenvectors to evaluate the components of the Jordan transform of the higher order terms (i.e. nonlinear coefficients).
- Both real-valued and complex-valued NF are considered for second order and first order power system models respectively. For the second order model, the theory of nonlinear normal mode (NNM) adapted from mechanical engineering domain is extended to study power system oscillation.
- New method for selective application of NF to the study of nonlinear modal interactions was proposed. Previous indices for nonlinear modal interactions were used to study modal interactions based on the selective method for NF proposed.
- Based on NNM theory, a new method for monitoring instability of modes in a multi-machine power system was developed.
- The time simulations were conducted to verify inferences made from NF technique, regarding the system dynamic behaviour.

Therefore, the research work utilises a combination of normal form theory, nonlinear normal mode theory, linear system techniques, Taylor series expansion, mode excitation technique, and time-domain simulation.

1.7 Contributions of this PhD Research Work

In response to the research problem, this thesis has made the following contributions:

1. To the knowledge of the author, this thesis is the first application of NF to power system study without the usual preliminary Taylor series expansion. This thesis proposes a fast method to obtain the needed nonlinear coefficient for NF model without Taylor expansion and the associated Hessian matrices computation. By avoiding the building of Hessians, the NF analysis becomes fast.

2. In terms of NF application to second order power system model, this thesis reports the largest test case ever, considering third order nonlinearities. The application of NF to second order power system model without any complex variables, using NNM is a new concept not well exploited. To the author's knowledge, the largest reported test case of such application involves only four generators. The technique developed in this thesis allows the extension of the capability of the previous proposals to the study of more than fifty machines in a convenient computational time.

3. This thesis introduces new and computationally-reduced tool for monitoring electromechanical mode instability in an interconnected power system. The proposed method has potential for on-line application and can be used by power system operators to make quick and rough estimation of modes' proximity to instability.

4. The new approach to NF analysis proposed in this thesis opens the way for selective NF application in power systems. For example, this thesis proposes a fast NF technique for power system modal interaction investigation, which uses characteristics of system modes to carefully select relevant terms to be considered in the analysis. This leads to a very rapid nonlinear modal analysis.

5. To the author's knowledge, there is no dedicated software for NF application due to its computational complexities. The proposed method allows the reuse of only the information from linear analysis, to evaluate the coefficients of all nonlinear terms, in a linearly-simple and computer-friendly fashion. Thus, the implementation of NF with power system commercial software like EUROSTAG®, which already has linear and transient analysis tools embedded, is achievable.

6. Although certain constraints precluded some further experimentation and validation, this thesis opens up several research problems for future researchers. For instance, the criteria proposed for selective NF applications can be investigated for 100% PE grid. Also, further computational reduction using balanced realisation technique was suggested. This could be well explored for very large systems.

Some of the main contributions of this thesis are validated by the following articles which were drawn from it:

- **N. S. Ugwuanyi**, X. Kestelyn, O. Thomas, B. Marinescu and A.R. Messina, "A New Fast Track to Nonlinear Modal Analysis of Power System Using Normal Form," IEEE Trans. Power Syst., vol. 35, no. 4, pp. 3247-3257, 2020.

- **N. S. Ugwuanyi**, X. Kestelyn, B. Marinescu and O. Thomas, "Power System Nonlinear Modal Analysis using Computationally Reduced Normal Form Method,"Energies, vol. 13, no. 5, p. 1249, 2020.

- **N. S. Ugwuanyi**, X. Kestelyn, O. Thomas, and B. Marinescu, "A Novel Method for Accelerating the Analysis of Nonlinear Behaviour of Power Grids using Normal Form Technique," in Innovative Smart Grid Technologies Europe (ISGT Europe), 2019.

- **N. S. Ugwuanyi**, X. Kestelyn, O. Thomas, and B. Marinescu, "Selective Nonlinear Coefficients Computation for Modal Analysis of The Emerging Grid," in Conférence des Jeunes chercheurs en Génie Eléctrique, 2019.

- **N. S. Ugwuanyi**, X. Kestelyn, B. Marinescu, and O. Thomas, "Speedy Technique for Selective Nonlinear Analysis of Electromechanical Modes of Future Grids," European Journal of Electrical Engineering: **UNDER REVIEW**.

1.8 Thesis Outline

The thesis is divided into 6 chapters described as follows.

Chapter 1 provides context as well as the statement of the problem. The motivation, objectives and the main contributions of this research work are also presented in this chapter.

Chapter 2 presents a detailed literature review dedicated to Normal Form applications in power systems, challenges, and the existing proposals to mitigate these challenges. Some background information are presented as well. Also, the scientific position of the current work globally and in L2EP[1] is established in this chapter.

Chapter 3 describes the power system models used in this work and the Normal Form method due to these models. Simple examples are used to explain the NF method. Also, in this chapter, the challenges encountered in NF applications are discussed and demonstrated.

Chapter 4 presents a detailed documentation of the proposed method for computing all the nonlinear coefficients, both for second and first order power system models. Examples are presented to explain the method. Thereafter, several larger systems are tested. The proposed method is compared with symbolic tool and the computational efficiency and accuracy

[1] **L2EP** is the french research laboratory in which the present PhD was prepared. L2EP stands for Laboratory of Electrical Engineering and Power Electronics

extensively discussed in this chapter. Also, the time domain simulations are presented to support the results.

Chapter 5 presents the practical power system applications of NF method facilitated by the proposed method. In this chapter, new proposals for studying power systems based on NNM are presented and validated with numerical simulations on IEEE 3- and IEEE 50-machine power systems. Also in this chapter, new approaches for selective study of modal interactions and participation factors are presented.

Chapter 6 presents conclusions of this work and suggestions for future work.
Finally, the details of the third order normal form for the power system equations and the data for the IEEE 3-machine system are given in Appendices D and E respectively. Other interesting appendices are also presented.

Chapter 2

Literature Review

> "*That is part of the beauty of all literature. You discover that your longings are universal longings, that you're not lonely and isolated from anyone. You belong.*"
>
> F. Scott Fitzgerald

Contents

Introduction

In chapter 1, it was stated that the thrust of the thesis is the simplification of the process involved in Normal Form application. It was also stated that stressed systems exhibit increased nonlinearities which lead to nonlinear modal interactions. These interactions can be positive or negative, phenomena beyond the scope of linear analysis. The exploration on the NF method, advocated since last two decades by researchers in IOWA state university; and later by other laboratories in USA, Mexico, Japan, China, and recently France (L2EP[1]), highlights NF's potentials for better analysis of stressed systems (hence, for present and future grids). Several other research laboratories worldwide are working on Normal Form method and its applications to modal analysis, both in power systems and in other fields. This chapter is dedicated to the review of NF applications in power systems. The aim of the reviews is to bring out the relevance of Normal Form as a tool in power systems; its challenges and the existing proposals to mitigate these challenges. The position of the thesis globally is then established. The reviews are sectioned for easy reading and some background information are provided. The chapter starts with a concise appraisal of linear modal analysis, upon which the developments of nonlinear modal analysis are based. The idea is to show the rich features of linear analysis which are emulated and expanded by the Normal Form.

2.1 Revisiting Linear Modal Analysis Tools

Linear modal analysis is widely applied in power systems to study and provide solutions to oscillation problems. The dynamical behaviour of power systems can be represented by

$$\dot{\mathbf{x}} = \mathbf{f}(\mathbf{x}, \mathbf{u}), \tag{2.1a}$$

$$\mathbf{0} = \mathbf{g}(\mathbf{x}, \mathbf{u}). \tag{2.1b}$$

In (2.1), $\mathbf{x}$ is a vector of the state variables and $\mathbf{u}$ is a vector of input. The expressions of $\mathbf{x}$ depend on the model being considered. A system described with differential equation (2.1a) and the algebraic equation (2.1b) is said to be a differential-algebraic-equations (DAEs) system. A linear model is obtained by linearising the nonlinear system around an operating point, usually performed in the neighbourhood of SEP.

Assume $\mathbf{x_0}, \mathbf{u_0}$ to be initial state vector and the input vector respectively, which correspond to the equilibrium point, then, $\mathbf{x}(\mathbf{x_0}, \mathbf{u_0})$ is the solution of (2.1) with $\dot{\mathbf{x}} = \mathbf{0}$. For small perturbation, the new states and inputs are denoted as $\mathbf{x} = \mathbf{x_0} + \mathbf{\Delta x}$, $\mathbf{u} = \mathbf{u_0} + \mathbf{\Delta u}$, where

[1] **L2EP** is the french research laboratory in which the present PhD was prepared. L2EP stands for Laboratory of Electrical Engineering and Power Electronics

Δ stands for increment. Linearisation is an assumption that if the perturbation is sufficiently small, first term of the Taylor series expansion can approximate the dynamics of the nonlinear system. It is possible to put the algebraic equations into the differential ones. Therefore, the linear model is given by

$$\boldsymbol{\Delta}\dot{\mathbf{x}} = \mathbf{A}\boldsymbol{\Delta}\mathbf{x} + \mathbf{B}\boldsymbol{\Delta}\mathbf{u}, \tag{2.2a}$$

$$\tag{2.2b}$$

where the Jacobians, evaluated at the SEP are:

$$\mathbf{A} = \frac{\partial \mathbf{f}}{\partial \mathbf{x}}|_{\mathbf{x_0},\mathbf{u_0}},\ \mathbf{B} = \frac{\partial \mathbf{f}}{\partial \mathbf{u}}|_{\mathbf{x_0},\mathbf{u_0}}.$$

Under free motion (i.e. zero input), the system (2.2a) can be be written as

$$\boldsymbol{\Delta}\dot{\mathbf{x}} = \mathbf{A}\boldsymbol{\Delta}\mathbf{x}. \tag{2.3}$$

The equilibrium can be shifted to the origin so that the vector of state variables $\mathbf{x}$ represents perturbations from the equilibrium. Therefore, the linear model under free oscillation is given as

$$\dot{\mathbf{x}} = \mathbf{A}\mathbf{x}. \tag{2.4}$$

The eigenvalues and eigenvectors are computed from $\mathbf{A}$ by solving the following eigenvalue problem $(\mathbf{A} - \lambda\mathbf{I})\mathbf{U} = \mathbf{0}$, where $\mathbf{I}$ is an identity matrix, $\mathbf{U}$ is a matrix with each column corresponding to one eigenvalue λ_i of the system, so called *right eigenvectors*. With the right eigenvectors determined, the complementary vector $\mathbf{V}$ is determined by solving $\mathbf{VA} = \lambda\mathbf{V}$, where $\mathbf{V}$ is a matrix with each row corresponding to an eigenvalue, so called *left eigenvectors*. **Participation factor** is defined with left and right eigenvectors as

$$P_{ki} = v_{ki}u_{ki}. \tag{2.5}$$

where v_{ki} and u_{ki} denote the k-th components of the eigenvectors v_i and u_i. The participation factor is a dimensionless quantity which represents the measure of the participation of the state variable x_k in the i-th mode.

In LMA, it is not always easy to isolate the parameters that significantly affect the dynamics due to the cross-couplings existing among the state variables. These cross-couplings are removed by putting the linear model in Jordan form. Jordan form is obtained by introducing a new state variable through a linear transformation, using the eigenvectors. The

linear transformation (also called similarity or near identity transformation) is of the form

$$\mathbf{x} = \mathbf{U}\mathbf{y}, \tag{2.6}$$

where $\mathbf{y}$ is the vector of the new state variable.

Differentiating (2.6) and substituting into (2.4) yields

$$\mathbf{U}\dot{\mathbf{y}} = \mathbf{A}\mathbf{U}\mathbf{y}. \tag{2.7}$$

Pre-multiplying both sides of (2.7) by the left eigenvector matrix yields

$$\dot{\mathbf{y}} = \mathbf{\Lambda}\mathbf{y}, \tag{2.8}$$

where $\mathbf{\Lambda} = \mathbf{V}\mathbf{A}\mathbf{U}$ is a diagonal matrix with the eigenvalues on the diagonal. The system (2.8) is said to be in Jordan form since the eigenvalues are distinct. Since the system is now decoupled, each element of $\mathbf{y}$ corresponds to a particular eigenvalue (mode). Thus, the variable $\mathbf{y}$ is also called modal variable and the model (2.8), *modal model*.
Hence, the solution of (2.8) for the i-th Jordan form variable can be written as

$$y_j(t) = y_{j0}e^{\lambda_j t}, \tag{2.9}$$

where y_{j0} is the j-th initial condition in the Jordan form coordinate system. Then the closed-form linear solution in the original machine states for an N-differential system is obtained by using the transformation in (2.6) as

$$x_i(t) = \sum_{j=1}^{N} u_{ij}y_{j0}e^{\lambda_j t} \quad \forall i, j = 1, 2, \ldots, N, \tag{2.10}$$

where u_{ij} is the element in the i-th row and j-th column of the right eigenvector $\mathbf{U}$.

Countless number of researches and publications exist, based on linear analysis. It has been used to analyse power system's inter-area oscillation phenomenon in [25, 32–34]. Sensitivity analysis performed in linear analysis helps to understand which state variable (and from which machine) participates more in a particular mode. It also helps to know which groups of machines will swing together or against themselves when a mode is excited. With the linear techniques such as observability and controllability, the system eigenvectors can help in designing power system controls [35]. Also, it helps to know the optimum location for siting PSS [36]. Linear tools have gained even much wider usage with the developments in power electronic converters. Researchers in L2EP are developing several control strategies

for power electronic (PE) converters for power grid, based on the linear analysis [37–39].

To illustrate the benefits of LMA, let us consider the system in Figure 2.1. The complete data for the system are presented in Appendix E. Each of the machines is represented with 2 state variables (rotor angle and speed), which means the size of the system is 6.

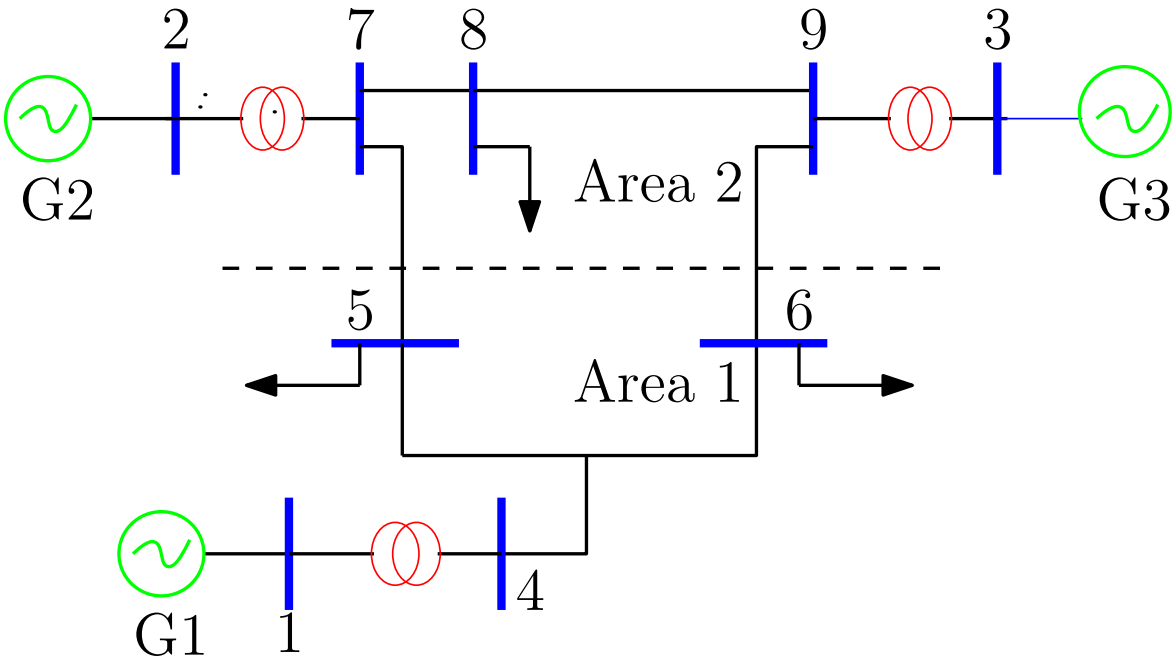

Figure 2.1 – IEEE 3-machine 9-bus power system

The eigenvalues of the system are given in Table 2.1. Without time-domain simulation, Table 2.1 shows immediately, at least, three important features of the system—(1) there are two modes of oscillation with frequencies 2.2 Hz (local) and 1.4 Hz (inter-area)[2]; (2) these modes are stable since they have negative real parts; and (3) these modes are poorly damped since they have real parts near to zero and damping ratios much less than 5%. The work of a control designer, is to "push" the real parts of these modes (*eigenvalues*) far into the negative half-plane.

Table 2.1 – Eigenvalues

Mode	Eigenvalue	Frequency (Hz)	Damping ratio (%)
$\lambda_{1,2}$	-0.0147±13.72j	2.20	0.11
$\lambda_{3,4}$	-0.0075 ± 8.82j	1.40	0.09
λ_5	-0.0087	0	100
λ_6	-0.00	0	-

Table 2.2 shows the participation factor analysis corresponding to the system modes. The participation factors give another vital information not apparent in time-domain simulations.

[2]Recalled from chapter 1, Inter-area oscillation mode involves machines from different areas, while local oscillation mode involves machines in a particular area.

It is clear that mode 1 is more associated with G2 and G3, while mode 2 is more associated to G1 and G2. To improve the damping of mode 1 for instance, it is better to locate the PSS in the area of the system closer to G3. The location of the PSS in the area closer to G1 may be a bad choice. In the same vein, location of the PSS in area of G2 is more preferable for improving the damping of mode 2.

Table 2.2 – Mode-in-state participation factors (absolute values) for the system modes

λ_1	λ_2	λ_3	λ_4	λ_5	λ_6	State
0.0032	0.0032	**0.1284**	**0.1284**	0.3564	0.3804	δ_1
0.0032	0.0032	**0.1284**	**0.1284**	0.0000	0.7368	ω_1
0.1033	**0.1033**	**0.3081**	**0.3081**	0.3163	0.1393	δ_2
0.1033	**0.1033**	**0.3081**	**0.3081**	0.0000	0.1770	ω_2
0.3934	**0.3934**	0.0635	0.0635	0.3273	0.2411	δ_3
0.3934	**0.3934**	0.0635	0.0635	0.0000	0.0862	ω_3
Mode 1		Mode 2				

Furthermore, by plotting the right eigenvectors corresponding to the angles of the machines, it is possible to determine how the machines in the system will swing, should any of the modes be excited. Such plots are known as the *mode shapes* and are shown in Figure 2.2.

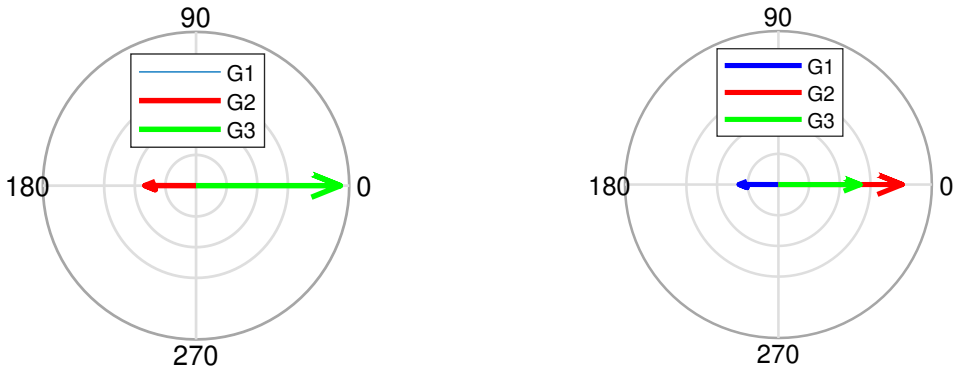

(a) Mode 1 (b) Mode 2

Figure 2.2 – Mode shapes for the two oscillatory modes

Figure 2.2a shows that if mode 1 is excited, G2 and G3 will swing in 180° phase opposition. G1 is not apparent in the figure because its participation to this mode is very low. If the system in Figure 2.1 is considered a two-area power system, then mode 1 can be viewed as local modes, since G2 and G3 are in one area. Figure 2.2b shows that when mode 2 is excited, G2 and G3 will swing together and in 180° phase opposition with G1. This mode can be viewed as inter-area, since G1 is in one area while G2 and G3 are in another area. The information provided by mode shapes can be used as a guide in aggregating machines or

model order reductions [see, 40].

To observe these oscillations in time-domain simulation, let us try to excite these modes almost separately. Since mode 1 is more associated to G3, it can be excited by a disturbance near G3. A three-phase fault at bus 9, applied at 1 s and cleared after 0.01 s produces the response in Figure 2.3a. It is clear that G2 and G3 are in phase opposition at approximately

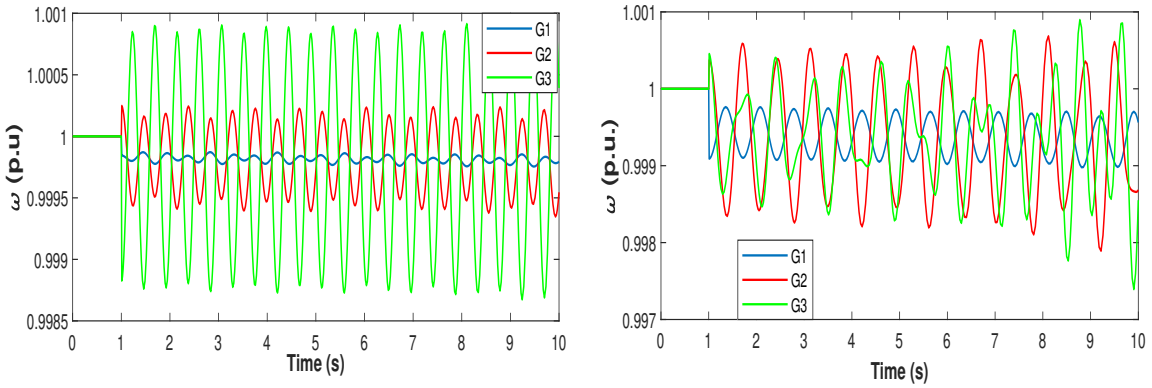

(a) Mode 1 (b) Mode 2

Figure 2.3 – Excitation of the two oscillatory modes

2.2 Hz, with G1 almost unaffected. This is in agreement with the LMA in Figure 2.2a. A disturbance at bus 2 will excite mode 2, but also significantly excite mode 1. This is because G2 has also significant participation in mode 1. In general, inter-area modes involve many machines in the system and can be difficult to excite without significant excitation of some local modes. Since G1 has very low participation in mode 1, a disturbance near G1 will excite mode 2 with minimum excitation of mode 1. A three-phase fault at bus 4, applied at 1 s and cleared after 0.01 s produces the response in Figure 2.3b. The observed oscillation is coherent with the LMA result of Figure 2.2b.

Notice that in Figure 2.3, it is easy to observe the pattern of the oscillations, but it is not easy to pinpoint the exact states responsible. Indeed, linear analysis provide very interesting characteristics of a system which are not very apparent in time-domain simulation tools.

As seen in chapter 1, the response of the power system is considered most often as a combination of natural modes of oscillations present in the system. The eigenvalues obtained from linear analysis should represent the fundamental frequencies which are observed in the motions of the different machines in the system. It was also shown in chapter 1 that in a stressed system with significant nonlinearity, the linear analysis may not be able to characterise properly the dynamics due to significant modal interactions and harmonic distortions. However, as seen above, it will be difficult to totally get rid of LMA due to the information it provides. Moreover, the nonlinear effects can be better understood as the combinations of these linear modes. As [41] says, "The nonlinear effects should be considered as additions

to the linear-modal picture, not as replacements for it". Research interest has been kindled towards developing nonlinear modal analysis tools (such as NF), able to conserve the kind of information available with LMA but in extended manner. Such tool can be called *extended linear analysis* tool.

2.2 Basic Idea of Normal Form

When approximating the nonlinear system model, the inclusion of higher order terms, which leads to NLMA, augments the information provided by LMA and enables better dynamic characteristic studies of the power systems. Normal Form uses sequence of nonlinear coordinate transformations to remove the nonlinearities in the approximate Taylor expansion model, to obtain a simplified system, easy to analyse [30].

The basic idea of NF is depicted with Figure 2.4, while more details are presented in the next chapter. Notice that the operations from block 1 and block 2 are the same operations discussed for the linear model in the Section 2.1. The only difference is that the expansion is extended to higher orders. While the Jordan transformation in linear case totally decouples the system (see (2.8)), it does not decouple the nonlinear parts for the higher order model. The job of NF is to use block 3 to remove these nonlinear couplings and obtain a simple system similar to (2.8).

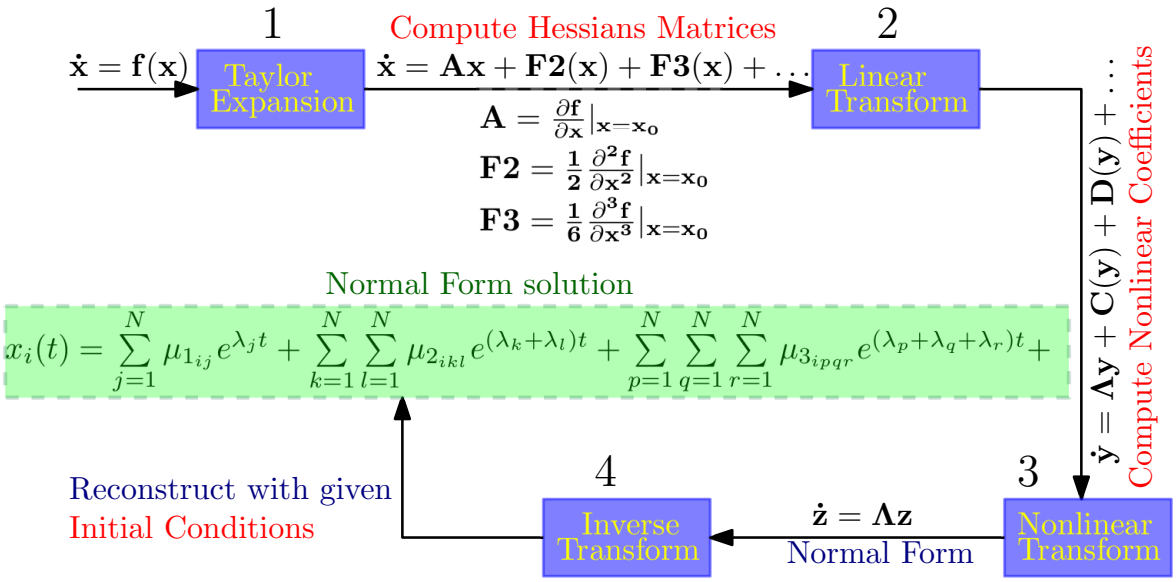

Figure 2.4 – Representation of the Basic idea of Normal Form Method

Although the simplified system $\dot{\mathbf{z}} = \mathbf{\Lambda z}$ resembles (2.8), the solution is different. The difference is in the change of variables which is linear in LMA (2.6) and nonlinear in NF. Thus, the "magic" of NF is the inclusion of nonlinear information in a linear dynamical system. The resulting simplified system has many advantages and allows the extension of

many linear techniques. For instance, (1) it provides information on nonlinear interactions of modes, which help to design better controls for power systems; (2) nonlinear mode-in-state participation factors can be defined for better siting of PSS; (3) modal interaction also gives insights into the stability of the nonlinear system; (4) the nonlinear interaction enables one to explain the sources of unknown frequencies appearing in time responses.

2.3 Applications of Normal Form in Power Systems

As earlier mentioned, the nonlinear contents of the NF solution add several vital information to the linear analysis. These extra information make NF a veritable tool in power system studies. Several works have been reported on the applications of NF in power system.

As highlighted in chapter 1, power system controls can lead to some nonlinear behaviour depending on the control parameters and the designs. The authors in [42, 43] used NF to investigate the effects of modal interactions on the control performance. The results showed that modal interaction can have significant effects on the control performance. The results aroused interest in the use of NF for control designs. In [44], an approach is proposed to reduce the nonlinear modal interactions of a stressed power system and improve the transient stability of the system through re-tuning some parameters of the generator excitation system. A nonlinearity index was developed using NF, then based on the index, a sensitivity function was formed to indicate the dominant excitation system parameters in the nonlinear behaviour of the system. These parameters are tuned to reduce the nonlinearity index, and hence reduce nonlinear modal interactions. A bifurcation subsystem-based control design methodology to study nonlinear effects of a robust μ-synthesis power system stabiliser (MPSS) was proposed in [45]. In order to include nonlinear information, the authors introduced NF which enabled them to define second order interaction indices used in the design. In [46], a decentralised method for nonlinear control of oscillatory dynamics in power systems was proposed. The nonlinear control scheme was derived using NF and the scheme ensures both transient stability and small-signal stability.

Linear analysis is suited for power system control designs due to some linear techniques like observability and controllability of states/modes. The linear analysis was extended to define nonlinear measures of modal controllability and observability based on NF method in [47]. These nonlinear measures for modal controllability and observability, allow for the definition of nonlinear participation factors. Participation factor analysis is very crucial in siting PSS in a power system. Various research works show that the nonlinear participation factors analysis, possible with NF, could provide more reliable information than the linear

one (see for example [31, 48, 49]). As a result, better methods for designing [50, 51] and siting [52, 53] PSS using NF have been developed.

In a stressed power system, modal interaction can seriously affect the entire stability. The authors in [54] showed that power system stability sub-modes interact with each other, especially when the power system presents strong nonlinear characteristics. Stability sub-modes were defined as the modes which participate more in voltage and angle state variables. Since nonlinear modal interactions can be either negative or positive, they shade lights on the system stability. By studying the nonlinear interactions of modes during disturbance, stability indices using NF were proposed in [55, 56]. The authors focused on the interaction of weakly damped oscillatory modes, which determine to a larger extent, the stability of the system. The effect of higher order nonlinearity was described in the form of the change in oscillation characteristics (damping factor and period) with respect to the change in amplitude. Then, using NF, approximated stability regions of oscillation modes in state space were obtained. Similar approach was followed to define a stability index in [57]. However, the authors added a nonlinear term omitted in earlier works and reported improved stability analysis.

The SVC has been widely employed in power systems to provide reactive power and maintain busbar voltages. Studies have shown that the controllers of PE devices such as SVC, unified power flow controller (UPFC), and other FACTS devices, can have unusual nonlinear interactions in the system. A main feature of a UPFC is its multiple control function that may be implemented by multiple controllers (i.e power flow controller, AC voltage controller and DC voltage controller). Zou, *et. al.* [58] investigated the interactions among the multi-control channels of UPFCs using NF. The nonlinear participation factor was developed with NF and used as an index to indicate the extent of nonlinear interaction among these UPFC controllers. The results showed that the negative interactions among the stable UPFC individual controllers result in poor control performance and even the closed-loop instability. Also, the interaction between DC voltage controller and active power flow is stronger than that between DC and AC voltage controller. Similar study was done in [59] where the NF method was used to analyse the interaction of SVC with inter-area modes and the interaction among multiple SVCs. A study case showed negative interactions among multiple SVC controllers.

When there is a severe contingency in power systems such as a loss of a major HVDC system, different machines can separate to form groups. This further cascades the protection system. Identification of the grouping pattern, which would account for the nonlinear behavior of the system and the nonlinear interaction between modes of oscillation, would provide a basis for developing a systematic procedure to create islands in the remaining system. The

authors in [60] used NF to develop an analytically based index which identifies the onset of the inter-area separation of the generators. This index was used in [61] to determine the natural groupings which are formed by the machines in Manitoba Hydro power system due to nonlinear interaction.

Contrary to the assumption in the traditional LMA applied to power system studies, when a nonlinear system is subjected to large disturbance, the frequencies of the modes are not constant. The frequency of oscillation is changing with the amplitude. In the field of mechanics, NF has been employed to accurately explain the amplitude-dependent frequency shifts exhibited by nonlinear system under disturbance [62–64]. This concept can easily be adapted for the study of power system electromechanical modes, under large disturbance.

The nonlinear transformation involved in NF leads to a complex representation of the state variables, thereby befuddling its physical meaning. Also, NF operates with differential-only equations which makes proper utilisation of the sparsity of power system DAEs difficult. The authors in [65] proposed a method of applying NF, which exploits the sparsity of the power system structure and preserves the physical meaning of the original variables. Real valued NF transformation has also been proposed and used for predicting the stability boundary of the power systems in [66].

The usefulness of NF analysis in power system triggered more researches to ensure its accuracy. A fundamental study was conducted in [65, 67] to investigate the effect of higher order modal interactions on the system dynamics. Reference [68] proposed some indices based on Neumann series convergence, for validating the NF solutions. Only quadratic nonlinearities were considered. Recently, [69] extended the Neumann series convergence to study the accuracy of higher order Normal Forms. It was concluded that higher order NF could have a smaller convergence zone. The implication of the results however, requires further verification as it was based on a single-machine-infinite-bus (SMIB) power system. An upper bound for validity limits of NF was proposed in [70], where NF was done up to order 25. Generally, determining the validity region of NF without the comparison of its solution with the original solution is difficult.

Indeed, there are so many applications of Normal Form in power systems and different versions of NF exist in literature as discussed in the next subheading.

2.3.1 Higher Order Normal Form Methods Existing in Literature

Depending on the order of the Taylor series expansion, two Normal Form approximations are recently reported. They are: (1) Second order Normal Form (NF2) and Third order Normal Form (NF3). Most of the works reported so far in literature are based on second

order approximation, as in [7, 44, 49, 52, 61]. As reported in the previous section, NF2 has been used for: predicting the inter-area separation and grouping of generators under fault; defining 2nd order nonlinear participation factors; designing and siting of PSS. A lot of improvement has been done to linear analysis by including second order terms in the analysis. However, there are some issues with second order approximations: 1) it can study only second order interactions but the third order modal interaction can be significant; 2) the stability of the system when studied by second order approximation is same with linear analysis; 3) its validity region is still small and not remarkably far from the LMA. With these shortcomings, researchers started exploring higher order NF tools.

With third order Normal Form approach, it is possible to study both second and third order modal interactions and obtain some insights into the system stability. Applying nonlinear transformation to third order Taylor expansion can generate third order terms due to residuals from second order transformation. In literature, different third order Normal Forms have been proposed, many not including the second order residuals in the system dynamics. In [51] a new parameter for siting PSS based on third order Normal Form was proposed but the residual term was neglected. Similar omission was also observed in [71]. A fundamental study was done based on third order approximation in [72] and [67] but the validity of their approach is very small because they not only neglected the residual term but also neglected the inherent third order resonance in poorly damped system. At L2EP, Tian [57] showed that the accuracy of the third order approximation is affected if both or either of the residual and third order resonance terms are neglected. Currently, at L2EP Arts et Métiers Institute of Technology, we are investigating the feasibility of NF3 method in characterisation of the stressed power system's dynamic behaviour with emphasis on its computational reduction. The preliminary results are reported in [73–76] in addition to this present report. To summarise, two approximations for NF exist:

- **Second Order Normal Form**, where the Taylor series expansion is truncated at order 2. That is

$$\dot{\mathbf{x}} = \mathbf{A}\mathbf{x} + \mathbf{F_2}(\mathbf{x}), \tag{2.11}$$

  where, $\mathbf{F_2}(\mathbf{x})$ contains only second order terms. This type of NF is well developed in literature, although applications are mostly on very small test cases.

- **Third Order Normal Form**, where the Taylor series expansion is truncated at order 3. That is

$$\dot{\mathbf{x}} = \mathbf{A}\mathbf{x} + \mathbf{F_2}(\mathbf{x}) + \mathbf{F_3}(\mathbf{x}), \tag{2.12}$$

  where, $\mathbf{F_3}(\mathbf{x})$ contains only third order terms. Existing NF3 versions are summarized

in [57].

Although, higher order NF gives more accurate results in analysis, the improvement is basically due to the order of nonlinearity considered in the Taylor expansion and not because of NF application. What NF does is to simplify the nonlinearities. Figure 2.5 shows typical behaviour of 1st, 2nd and 3rd order Taylor series approximation for no stress and stressed conditions.

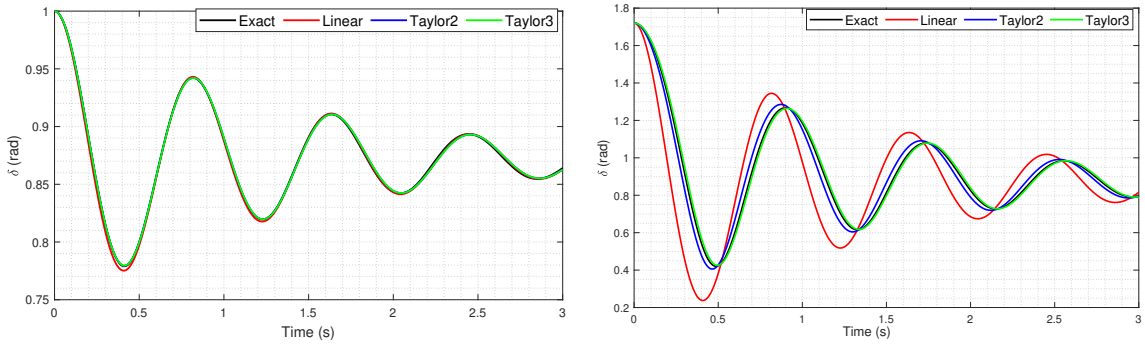

(a) No stress condition

(b) Stressed condition

Figure 2.5 – Typical responses for 1st, 2nd , and 3rd order Taylor approximations under no stressed/stressed condition for a two-state variable SMIB system.

It can be seen that the more the order of Taylor expansion, the closer the approximation to the exact (original) system. For this reason, the accuracy of NF solutions are sometimes determined by comparing with its Taylor expansion model instead of the original system.

2.3.2 Real Normal Form Transformation

The strength of the conventional NF is its ability to decouple or simplify the model of a nonlinear system. However, it usually operates with first order system models, which lead to complex variables in NF coordinate. As noted earlier, when the variables in NF coordinates are complex, the physical meanings of the states are lost. One starts with physical variables (e.g speed, angle, ...) but ends in a simplified system whose meanings are difficult to interpret. To overcome this challenge, a real NF approach for studying resonant power system was proposed in [77]; however, it is based on 2nd order approximation. As a result, it has little or no stability information.

In vibration mechanics, the theory of Nonlinear Normal Modes (NNM) is common. According to Shaw and Pierre [78], Nonlinear Normal Mode is defined when all displacements and velocities can be related to a single pair of displacement and velocity. In the theory of normal modes, a *master* mode (i.e. the mode of interest) is chosen, and the normal mode is then defined by a formulation such that the remaining linear modes of the system (the *slave* modes) depend on the *master* mode in a manner which is consistent with system dynamics.

This approach allows some manipulations that get rid of the complex quantities. NNM has also been adapted for studying power system electromechanical oscillations in [79, 80]. The above works are still based on 2nd order approximation and are bereft of stability information. In [62, 63] it was shown that NNM can also be obtained up to 3rd order, by just nonlinear change of variable defined in such a way that complex quantities are avoided. The approach follows same Poincaré and Poincé-Dulac NF theory [27, 81]. The difference here is that there is no preliminary complex quantity computed. Also, the determination of Taylor series coefficients is done with 2nd order differential equations. With this approach, an analytical expression of the nonlinear frequent shifts can be easily defined. Recently, NF-like nonlinear modal decoupling approach based on 3rd order approximation has been proposed in [82, 83]. Here the multi-machine power system is decoupled into independent oscillators. In these works, complex quantities are first computed and later got rid of, by some modal transformations. A real Normal Form is eventually obtained, however, the preliminary complex quantities increase the computation. Decoupled system has advantage in that analysis on the dynamics and stability related to each mode can be performed on the corresponding oscillator, which will be easier than on the original system.

2.3.3 Summary of NF Applications in Power Systems

From the above reviews, the application of NF in power systems can be summarised as follows:

1. Enables better power system control design and tuning. The nonlinear mode-in-state participation factors can offer better location for placement of PSS to damp inter-area modes.

2. Unravels the sources of unknown frequencies observed in the system.

3. NF3 particularly, provides expanded stability insights not possible with linear and NF2.

4. NF3 explains the proper behaviour of the natural frequency when subjected to disturbance. In other words, it explains the amplitude-dependent frequency shifts inherent in a nonlinear dynamics.

2.4 Present Challenges with Normal Form Method

The precious NF technique has been challenged by its computational complexity arising from the inclusion of higher order terms in the Taylor series expansion. As a result, most studies are based on inclusion of 2nd order terms. Current researches emphasize the deficits of 2nd order NF in the light of nonlinearly growing power systems [57]. Consequently, it is not

possible with the present computing technologies to apply NF to large power system. Thus, the benefits of NF can not be fully exploited. To extend the NF application to large power systems and exploit all its benefits, preliminary steps must include solving this computation problem.

In order to reduce the computational burden, the authors in [31, 84] opined that if the interacting modes are accurately determined by higher order spectra (HOS) analysis or prony method, several computations can be restricted to the interacting modes. The implementation of this suggestion for NF however, does not exist in literature. Moreover, these preliminary works are not in themselves simple, since they are sensitive to simulation data considered and prony is also computationally demanding. The authors in [82] suggested that if there is no strong resonance, coupling terms associated with non-conjugate eigenvalues may not have significant contribution to the system nonlinearity in a classical power system. Therefore, selective computation can reduce the computational burden. Two challenges however are—(1) a prior knowledge of the significant terms; (2) convenient computational technique to focus on the significant terms.

A reduced order NF study was proposed in [85], where some interactions were neglected based on their damping rates and nearness to resonance. In order to estimate the NF coefficients relating to these interactions, the time-domain signal is fitted to the needed coefficients in least square (LS) sense, which makes the modal reconstruction fast. The algorithm requires prerequisite time-domain simulation data which determine the accuracy of LS. More data for accuracy increases the computation which makes the claimed NF reduction unclear. Also, while this method makes simulation in NF space fast, it hides the actual contribution of each eigenvalue combination which is key to the study of modal interaction. Moreover, NF is developed for analytical results and not for time-domain simulations.

Some researchers advocated for Modal series (MS) method in order to do the same analysis as with NF [86, 87]. MS is similar to NF, but nonlinear transformation is avoided. MS applies Voltera series theory to approximate the system response as an infinite series [88]. Since nonlinear transformation is avoided, it is claimed to have advantage of always retaining the physical meaning of the state variables. However, most recent comparison of both methods shows NF to be more accurate and less burdensome under 3rd order consideration [89]. Moreover, processes involved in block 1 and block 2 in Figure 2.4, which are burdensome in NF are exactly the same for MS.

Inspired by the NF potentials, Netto *et al.* [90] proposed an alternative method based on Koopman Mode Decomposition (KMD), which enables the computation of nonlinear participation factor in similar manner as done with NF. However, a comparison of both approaches

showed same computation complexity [91]. A Very recent work reveals that the efficiency of KMD largely depends on the choice of the observable state variables, and one is never sure the exact states to observe to ensure good results [90]. This review motivates the need to expand Normal Form analysis to adapt to more complex system representations.

The major difficulty in NF is encountered in:

- *Building the approximate model and computing its numerous nonlinear coefficients.* That is, computation of the Hessian matrices in block 1 and the nonlinear coefficients (which also form Hessian matrices) in block 2 (see Figure 2.4).
- *Finding the initial condition in NF space from initial values in physical space.* That is, the initial condition needed in block 4 to "move" the NF system back to physical space.

The latter involves solving nonlinear optimisation problem, which may be difficult to converge, or may even converge to a wrong solution. The former arises due to the numerous coefficients needed for the analysis, which have to be computed. These coefficients increase exponentially with system size.

In order to exploit in details the benefits of Normal Form, several types of power system models such as grids including virtual synchronous machines (VSM), HVDC links, wind farms, and PVs have to be investigated. This means that tools developed for NF have to be easily adapted to a change of model in order to be applicable to different types of grid. The conventional method for building Normal Form approximate models is not convenient since it involves the expansion of the system equations by Taylor series up to desired order. This gives rise to higher order derivatives and Hessian matrices difficult to evaluate for large number of variables.

Basically, four approaches may be used to build the Hessian matrices and then compute NF coefficients:

- The expressions for the Hessian derivatives may be pre-defined and then stored as a library in advance (Hand-derived differentiation),
- Symbolic tools can be used to perform the higher order Hessian derivative,
- Numerical differentiation technique is achievable,
- Automatic differentiation (AD) method also exists [92–96].

Hand-derived differentiation entails deriving traditionally, all possible derivatives needed in the analysis. If the expressions for the Hessian derivatives are defined in advance, only substitution of the operating point is needed (e.g. in [7, 8] for NF2). As a result, this

approach is expected to be faster once the expressions are defined. However, any change in the model overhauls the whole exercise. At 3rd order, this approach can be cumbersome. It can take days and it is easy to make mistakes after the painstaking work. In this aspect, this method is very conservative and therefore not good for different models. This is probably the reason why most NF applications to a relatively large system follow similar power system model (see [53, 91]).

Symbolic differentiation programs manipulate formulas to produce new formulas, rather than performing numeric calculations based on formulas. Examples of popular commercial software with symbolic computing capability include, MATLAB®, Maple® and Mathematica®. Symbolic tools have been employed in evaluating NF coefficients in [82, 83, 97–99]. Symbolic computation minimizes error while dealing with higher order differentiation, but it is generally too slow and does not scale to large system.

Numerical differentiation computes an approximation to the derivative of a function by suitable combinations of the known values of the function. It simplifies derivative problems, however it accumulates error. The higher the derivative, the more problematic is the round-off error. For 2nd and higher order derivatives where possible, and often, for cross-derivatives, the error can become substantial. This is not desirable especially since the Taylor series is in itself an approximation.

Automatic differentiation is a method for efficiently augmenting computer programs with statements for the computation of derivatives; motivated by the fact that every computation is made up of elementary mathematical operations like sine, cosine, multiplications, and so on [92]. Considering the various combinations of these elementary operations, AD exploits the structure of the chain rule to evaluate differential operators of a function as the function itself is being evaluated as a computer program [94]. AD overcomes the problems of numerical and symbolic differentiation and has similar efficiency as hand derived derivatives but there are also some concerns. AD implementation requires high level skills almost reserved for the experts and AD software developers. Decomposing a computer program into the necessary component functions required in AD is far from simple. A computationally naive implementation of AD can result in outrageously slow code and excessive use of memory [93, 95]. There exists no standard set of problems cutting across the varieties of AD applications, and the development of a package is usually driven by a specific class of problems [93]. AD implementation for higher order derivatives is very complicated and far from the well established first order implementation. A common method is to repeat AD of

the first order till the desired order is obtained, an approach which Betancourt [94] described as inefficient.

For polynomial nonlinearity, such as assumed in NF, not all terms will be very important for some studies. This necessitates selective evaluation of certain terms in the polynomial approximation. With selective NF application in view, the above methods are not very convenient. All the reviewed methods have their strengths and weaknesses, however, one may ask: can actual Taylor expansion in NF application be avoided entirely? A positive answer to this question will mean significant improvement in the NF methods.

2.5 Power System Model Order Reductions

Whether linear, *extended linear*, or full nonlinear analysis, dealing with very large power system is a huge task, even with advances in modern computing. In dealing with very large power systems, computations may be lessened by first reducing the size of the grid. This reduction can be done in many ways, depending on the type of analysis required. For example, the machines located in the area of interest can be modelled as detailed as possible, while the machines far from the studied area represented with classical models. This approach was used in [7] to apply NF2 to a 50-machine power system. The 6 machines in the area of interest were represented with 4th order model while the remaining 44 machines were represented with classical model. Another option is to represent the areas not of interest with an equivalent shunt. This approach has been used in [61] to apply NF2 to a system with over 300 generators. The challenge with the later is that the effects of inter-area mode involve always many machines in different areas. Since the inter-area modes are more associated with the angle and speed of the machines, representing an area with a static shunt equivalence may sometimes introduce significant dynamic inaccuracy. A popular technique for reducing the grid size is the *synchronic modal equivalencing* (SME) [100–102], which uses the mode shape to classify the machines as either more relevant or less relevant. The less relevant machines can be replaced by equivalent current injectors at the buses where they are connected. Extended versions of SME, called *border synchrony*, employing participation factor analysis, mode shape, and *balanced realisation techniques* have been advocated in [40, 103, 104]. With *border synchrony*, the reduction of the European system, containing about 400 generators and 2000 buses to 20 generators has been reported in [40].

In order to study large grid with 100% PE, new reduction techniques are being developed based on *residualisation* of some states or discarding of some modes in the system [105, 106]. To residualise states, the differential equations corresponding to these states are converted

to algebraic equations. Depending on the reduction objective, some strategies are developed for choosing either the states to residualise or the system modes to discard. The different strategies for this type of reduction are reported in [107].

Apparently, model order reduction is an initial step that will ease computations. However, they do not reduce any operation in NF analysis other than the grid size. It is acknowledged that computations in very large power systems are generally difficult, but in the case of Normal Form method, the difficulty is not only in the size of the power system, but also in the way the method is applied. Application of NF3 to a grid of even 20 state variables is enough burden with the current methods.

2.6 Summary

Linear analysis is a powerful tool in the field of engineering. It quickly reveals the system characteristics with well known concepts like eigenvalues and eigenvectors. As a result, it has been employed in various aspects of engineering and power systems for control designs. As it offers mainly *single-mode* information, it fails to adequately characterise the system behaviour under stress, since the modal interactions become significant. To improve the linear tools, higher order terms are included in the analysis. This inclusion reveals many other characteristics of the system not possible with the linear analysis. The analysis of the resulting model is made possible using tools like Normal Form method. The NF tool has been widely used in various aspects of power system analysis and control. Although powerful, NF is difficult to realise in larger systems due to its computational complexity. Large power systems can be first reduced before applying the NF analysis. Various techniques for model reduction exist, but the current method for NF analysis is still very difficult to go by, even when the network is well reduced.

Chapter 3

Normal Form for Power System Models

"The secret to modeling is not being perfect. What one needs is a face that people can identify in a second. You have to be given what's needed by nature, and what's needed is to bring something new. "

Karl Lagerfeld

Contents

Introduction

In chapter 2, we saw the several applications of NF method in power systems. A basic idea of NF method was presented, including the existing higher order approximations in literature. It was highlighted that NF requires computations of Hessian matrices, which are difficult in large systems. In this chapter, a more detailed presentation of NF method is made and the computational burden brought to the fore. Both NF of first order (leading to complex quantities) and second order (retaining real quantities) systems are presented. Since this thesis is building on already existing NF methods, some numerous mathematical derivations are considered boring for the reader. The main ideas are presented, while supplementary ideas can be found in the appendices and/or other sources referenced in the thesis. As NF is a simplified representation of a system model, the power system models used throughout this PhD are briefly discussed before describing their NF.

3.1 Power System Models

NF method usually operates with differential-only equations. Since power system is represented by DAEs, the algebraic equations are substituted in the differential ones to obtain differential-only equations before applying NF. However, a structure-preserving application is possible. The application of NF to power system structure-preserving DAEs models has been addressed before in [65], but that is outside the scope of the present work. The models generating the DAEs are first of all briefly presented. The components of interest are: synchronous generators, the excitation system, and the power network. The two generator models used throughout the PhD are the classical and the two-axis models, however, the method developed in this thesis is general and can be used for any model.

3.1.1 Classical Generator Model

The so-called classical model is the simplest model representing a multi-machine power system. Though simple, it is not trivial especially when interest is only on the study of electromechanical modes. Irrespective of the model used, the nature of electromechanical oscillations remains the same [108]. Such models are widely used for NF and NF-like stability studies of power systems (see for examples [66, 82, 83]).

Based on the assumptions [109], a power system composed of generators modelled as

classical can be represented by first order swing equations

$$\dot{\omega}_i = \frac{1}{M_i}[P_{m_i} - P_{e_i} - \mathcal{D}_i(\omega_i - 1)] \tag{3.1}$$

$$\dot{\delta}_i = \omega_s(\omega_i - 1) \tag{3.2}$$

$$P_{e_i} = E_i^2 \mathcal{G}_{ii} + \sum_{j=1, j\neq i}^{N} E_i E_k [\mathcal{G}_{ij} \cos\delta_{ij} + \mathcal{B}_{ij} \sin\delta_{ij}] \tag{3.3}$$

$$\delta_{ij} = \delta_i - \delta_j, \tag{3.4}$$

where

N:	number of generators
E_i:	internal bus voltage of generator i
M_i:	inertia constant of generator i
P_{m_i}:	mechanical power input of generator i
P_{e_i}:	electrical power of generator i
$\mathcal{G}_{ii}$:	driving point conductance of node i
$\mathcal{G}_{ij} + j\mathcal{B}_{ij}$:	the transfer admittance in the system reduced to the internal nodes between generators i and j
δ_i:	rotor angle of generator i
ω_i:	rotor speed of generator i
ω_s:	synchronous speed
$\mathcal{D}_i$:	damping coefficient of generator i.

Damping coefficient $\mathcal{D}$ can be set to zero if necessary.

3.1.2 Two-axis Generator Model

For analysis of the power system with excitation system controls, the synchronous generator is represented by the two-axis model [Section 4.15, 109]. For a generator i, the variables and the generator equations are given by

$$\dot{\delta}_i = \omega_s(\omega_i - 1), \tag{3.5}$$

$$\dot{E}'_{q_i} = \frac{1}{T'_{d0}}[-E'_{q_i} - (x_{d_i} - x'_{d_i})I_{d_i} + E_{fd_i}], \tag{3.6}$$

$$\dot{E}'_{d_i} = \frac{1}{T'_{q0}}[-E'_{d_i} + (x_{q_i} - x'_{q_i})I_{q_i}], \tag{3.7}$$

$$\dot{\omega}_i = \frac{1}{M_i}[P_{m_i} - (E'_{q_i} I_{q_i} + E'_{d_i} I_{d_i}) - \mathcal{D}_i(\omega_i - 1)], \tag{3.8}$$

where

E'_{d_i}, E'_{q_i}: direct and quadrature axes stator EMFs of generator i which correspond to rotor transient flux components, respectively

I_{d_i}, I_{q_i}: the d- and q- axes stator currents of generator i

τ'_{d0_i}, τ'_{q0_i}: open-circuit direct and quadrature axes transient time constants of generator i

x_{d_i}, x_{q_i}: direct and quadrature axes synchronous reactances of generator i

x'_{d_i}, x'_{q_i}: direct and quadrature axes transient reactances of generator i

E_{fd_i}: stator EMF corresponding to the field voltage of generator i

If the N-th machine is used as a reference to other machines, then, the order of the model is reduced by defining a new state $\delta_{iN} = \delta_i - \delta_N$. This is proper since loss of synchronism is determined by the relative angles. Then (3.5) and (3.2) are redefined as (3.9), all other equations remaining unchanged.

$$\dot{\delta}_{iN} = \omega_s(\omega_i - \omega_N). \tag{3.9}$$

3.1.3 Network Equations

Assuming constant impedance loads, the network is reduced to the internal generator nodes by eliminating all the load nodes. The $\mathbf{Y}$bus of the reduced network is obtained with its diagonal elements $Y_{ii} = \mathcal{G}_{ii} + j\mathcal{B}_{ii}$, and off-diagonal elements $Y_{ij} = \mathcal{G}_{ij} - j\mathcal{B}_{ij}$. With the procedure described in [Section 12.3, 110], the generator currents I_q and I_d are given by

$$I_{qi} = \sum_{j=i}^{N}[(\mathcal{B}_{ij}\cos\delta_{ij} - \mathcal{G}_{ij}\sin\delta_{ij})E'_{qj} + (\mathcal{B}_{ij}\sin\delta_{ij} + \mathcal{G}_{ij}\cos\delta_{ij})E'_{dj}] \tag{3.10}$$

$$I_{di} = \sum_{j=i}^{N}[(\mathcal{B}_{ij}\sin\delta_{ij} + \mathcal{G}_{ij}\cos\delta_{ij})E'_{qj} - (\mathcal{B}_{ij}\cos\delta_{ij} - \mathcal{G}_{ij}\sin\delta_{ij})E'_{dj}]. \tag{3.11}$$

The electrical power P_e for the 2-axis model becomes

$$P_{e_i} = E'_{q_i}I_{q_i} + E'_{d_i}I_{d_i} + (x'_{d_i} - x'_{q_i})I_{d_i}I_{q_i}. \tag{3.12}$$

3.1.4 Exciter Equations

The exciter model shown in Figure 3.1 is a simple AVR model which can be used for rough stability evaluations. The equations are given as

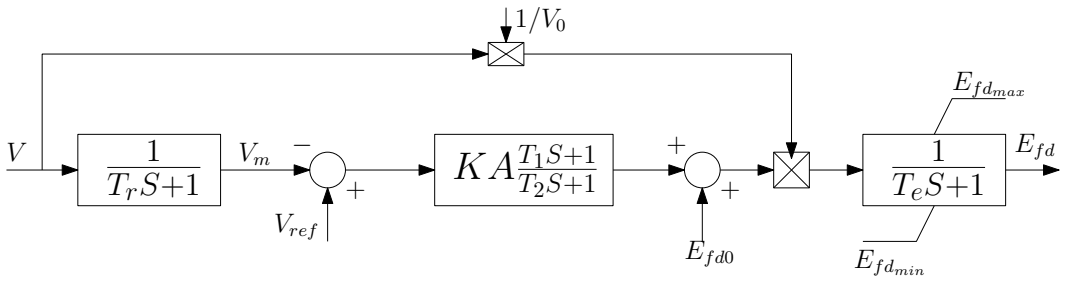

Figure 3.1 – Simple excitation system

$$\dot{V}_{m_i} = (V_i - V_{m_i})/T_{r_i}, \tag{3.13}$$

$$\dot{V}_{r_i} = (KA_i(1 - \frac{T_{1_i}}{T_{2_i}})(V_{ref_i} - V_{m_i}) - V_{r_i})/T_{2_i}, \tag{3.14}$$

$$\dot{E}_{fd_i} = ((V_{r_i} + KA_i\frac{T_{1_i}}{T_{2_i}}(V_{ref_i} - V_{m_i}) + E_{fd_{0_i}})\frac{V_i}{V_{0_i}} - E_{fd_i})/T_{e_i}, \tag{3.15}$$

$$V_i = V_{d_i} + jV_{q_i} = (E'_{qi} + x'_{q_i}I_{q_i}) + j(E'_{q_i} - x'_{d_i}I_{d_i}), \tag{3.16}$$

$$V_i = \sqrt{V_{q_i}^2 + V_{d_i}^2}, \tag{3.17}$$

where all the variables and parameters are shown in Figure 3.1 and

V_i: terminal voltage of generator i

V_{ref_i}: exciter reference voltage of generator i

KA_i: regulator gain for exciter connected to generator i

T_{1_i}: regulator zero for exciter connected to generator i

T_{2_i}: regulator pole for exciter connected to generator i

T_{e_i}: field circuit time constant for exciter connected to generator i

T_{r_i}: measurement time constant of generator i

E_{fd_0i}: field voltage offset of generator i

S: laplace operator

If there is no bus voltage offset (V_{0_i}), the term $\frac{V_i}{V_{0_i}}$ is set to 1.

3.2 General Normal Form Theory

NF main idea consists in simplifying all nonlinear terms that are not very relevant to the system dynamics in the neighbourhood of an equilibrium point. Consider the power system models discussed in the previous section, represented generally as

$$\dot{\mathbf{x}} = \mathbf{f}(\mathbf{x}). \tag{3.18}$$

In (3.18), $\mathbf{x}$ is the vector containing N state variables, $\mathbf{f}$ is a smooth vector field. The expressions of $\mathbf{x}$ for the classical model and two-axis with AVR are given by:

$$\mathbf{x} = \left[\delta_1, \delta_2, \ldots, \delta_{N-1}, \omega_1, \omega_2, \ldots, \omega_N \right]^T \quad \text{classical model} \tag{3.19}$$

$$\mathbf{x} = \left[\delta_1, \omega_1, E'_{q_1}, E'_{d_1}, E_{fd_1}, V_{m_1}, V_{r_1} \ \ldots, \ \delta_{N-1}, \omega_N, E'_{q_N}, E'_{d_N}, E_{fd_N}, V_{m_N}, V_{r_N} \right]^T \quad \text{2-axis} \tag{3.20}$$

where the superscript T means transpose. The notation δ_i has been retained for relative angle δ_{iN}, where the meaning is not confusing. It is assumed that the system in (3.18) has an equilibrium point at the origin (or can be moved to the origin by a coordinate transformation) and can be approximated by Taylor series around the equilibrium point.

Therefore, system (3.18) can be written as

$$\dot{\mathbf{x}} = \mathbf{A}\mathbf{x} + \mathbf{\Gamma}(\mathbf{x}), \tag{3.21}$$

where $\mathbf{A}$ is the Jacobian of $\mathbf{f}$, $\mathbf{\Gamma}(\mathbf{x})$ represents nonlinear terms expanded in polynomial series and $\mathbf{\Gamma}(\mathbf{0}) = \mathbf{0}$.

As in the previous chapter, let us denote by $\mathbf{U}_i$, and $\mathbf{V}_i$ the i-th columns of right and left eigenvectors respectively, $\mathbf{U} = [u_{ij}]$, $\mathbf{V} = [v_{ij}]$, the corresponding matrices and $\mathbf{\Lambda} = \mathbf{V}^T\mathbf{A}\mathbf{U} = \text{diag}(\lambda_\mathbf{p})$[1], the diagonal matrix of its eigenvalues, $p, i, j = 1, \ldots N$. It is assumed that matrix $\mathbf{A}$ is diagonalisable. Using the linear transformation

$$\mathbf{x} = \mathbf{U}\mathbf{y} \tag{3.22}$$

in (3.21) and multiplying the result by the left eigenvectors yields

$$\dot{\mathbf{y}} = \mathbf{\Lambda}\mathbf{y} + \mathbf{\Gamma}(\mathbf{y}). \tag{3.23}$$

NF theorem states that if no internal resonance exist among the eigenvalues of $\mathbf{A}$, there exists a nonlinear transformation

$$\mathbf{y} = \mathbf{z} + \mathbf{h}(\mathbf{z}) \tag{3.24}$$

which simplifies the system (3.21) to

$$\dot{\mathbf{z}} = \mathbf{\Lambda}\mathbf{z}. \tag{3.25}$$

In other words, the nonlinear part of the system of (3.23) is removed. $\mathbf{h}(\mathbf{z})$ is a polynomial of

[1]Note that if the left vector is normalised as inverse of the right vector (i.e., $\mathbf{V} = \mathbf{U}^{-1}$), the transpose is not used. Instead, $\mathbf{VAU}$ is used.

higher order terms. If a resonant relation exists, then all mononomial terms in $\mathbf{\Gamma}(\mathbf{y})$ that are resonant cannot be removed [62, 70]. NF finds $\mathbf{h}$ to remove the removable nonlinear terms.

3.2.1 Normal Form at a Certain Order

To perform Normal Form at a certain order, consider the nonlinear part of (3.21) sorted by orders:

$$\dot{\mathbf{x}} = \mathbf{A}\mathbf{x} + \mathbf{F_2}(\mathbf{x}) + \mathbf{F_3}(\mathbf{x}) + H.O.T, \tag{3.26}$$

where, $\mathbf{F_2}$ contains only second order terms, $\mathbf{F_3}$ contains only third order terms, $H.O.T$ stands for higher order terms.

As recalled in chapter 2, depending on the order of truncation of the Taylor series, different NFs are obtained. Each NF has different domain of validity and therefore, performs differently. The higher the order of truncation, the better the NF. In other words, the higher the truncation order, the closer the NF solution is to the original nonlinear system. As will be seen later, components of these higher order terms are simply the eigenvalue expansion. Although higher order truncation gives results closer to the original nonlinear system, the complexity increases tremendously. Inclusion of third other terms, is enormous complexity compared to the second order approximations.

3.2.2 Third Order Normal Form NF3

Suppose the expansion (3.26) is truncated to order 3 and the term H.O.T omitted in all subsequent equations for simplicity, we obtain

$$\dot{\mathbf{x}} = \mathbf{A}\mathbf{x} + \underbrace{\mathbf{F_2}(\mathbf{x}) + \mathbf{F_3}(\mathbf{x})}_{\mathbf{\Gamma}(\boldsymbol{x})}, \tag{3.27}$$

where $\mathbf{\Gamma}(\mathbf{x})$ collects all second and third order terms. In power system modal analysis, the mechanical input is often assumed to be constant for small disturbances. That is, the governor's action can be neglected. This assumption is implied in this section. Equation (3.27) can be written as

$$\dot{x}_i = \sum_{m=1}^{N} A_{im}x_m + \sum_{m=1}^{N}\sum_{n=1}^{N} F2^i_{mn}x_m x_n + \sum_{m=1}^{N}\sum_{n=1}^{N}\sum_{l=1}^{N} F3^i_{mnl}x_m x_n x_l, \tag{3.28}$$

where

$$\forall i,m,n,l=1,2,\dots N: \quad A_{im}=\frac{\partial f_i}{\partial x_m}|_{\mathbf{x}=\mathbf{x_0}}, \quad F2^i_{mn}=\frac{1}{2}\frac{\partial^2 f_i}{\partial x_m \partial x_n}|_{\mathbf{x}=\mathbf{x_0}}, \\ F3^i_{mnl}=\frac{1}{6}\frac{\partial^3 f_i}{\partial x_m \partial x_n \partial x_l}|_{\mathbf{x}=\mathbf{x_0}}. \tag{3.29}$$

Notice that the first indices for the elements of multidimensional matrices **F2**, and **F3** have been written as superscripts in (3.28) and (3.29). This is the convention adopted for all elements of multidimensional matrices in this thesis.

Using the linear transformation (3.22), (3.27) is put in Jordan form as

$$\dot{\mathbf{y}}=\mathbf{\Lambda y}+\mathbf{f}_{\mathrm{NL}}(y_1,y_2,\dots,y_N), \tag{3.30}$$

or

$$\forall j=1\dots N: \qquad \dot{y_j}=\lambda_j y_j+\sum_{k=1}^{N}\sum_{l=1}^{N}C^j_{kl}y_k y_l+\sum_{p=1}^{N}\sum_{q=1}^{N}\sum_{r=1}^{N}D^j_{pqr}y_p y_q y_r, \tag{3.31}$$

and

$$\mathbf{f}_{\mathrm{NL}}=\mathbf{V^T\Gamma(Uy)}, \tag{3.32}$$

where the eigenvalue λ_j is the j^{th} element of $\mathbf{\Lambda}$,

$$\begin{cases} C^j_{kl}=F2^i_{mn}v_{ij}u_{mk}u_{nl} \\ D^j_{pqr}=F3^i_{mnl}v_{ij}u_{mp}u_{nq}u_{lr} \end{cases} \tag{3.33}$$

are the *nonlinear coefficients*, while u_{ij} and v_{ij} are the ij-th elements of **U** and **V** respectively. Currently there is no special software dedicated to NF application in power systems. Therefore, the above presentations are commonly implemented by symbolic manipulations using some software. Consequently, the processes taken to arrive at (3.33) are very difficult to follow for large systems because of the need to evaluate the Hessians in (3.29).

Equation (3.31) is the modal model of the original system where the states are now represented with the modal variable **y**. Observe that the linear part of (3.31) is totally decoupled but the nonlinear part remains coupled. NF theory leads to simplifying the nonlinear terms in (3.30) by a nonlinear polynomial change of variables, written as [30]

$$\mathbf{y}=\mathbf{z}+\mathbf{h2}(\mathbf{z})+\mathbf{h3}(\mathbf{z}), \tag{3.34}$$

or

$$\forall j = 1 \dots N : \qquad y_j = z_j + \sum_{k=1}^{N}\sum_{l=1}^{N} h2_{kl}^{j} z_k z_l + \sum_{p=1}^{N}\sum_{q=1}^{N}\sum_{r=1}^{N} h3_{pqr}^{j} z_p z_q z_r, \tag{3.35}$$

where z is the state variable in NF coordinate, $h2_{kl}^{j}$ and $h3_{pqr}^{j}$ are respectively complex valued quadratic and cubic coefficients, determined such that (3.30) is simplified, so-called *normal form coefficients*.

Differentiating (3.34) and substituting into (3.30) yields after some simplifications (see [(D.32), Appendix D])

$$\dot{\mathbf{z}} = \mathbf{\Lambda z} + \hat{\mathbf{F}}(\mathbf{z}). \tag{3.36}$$

where

$$\hat{\boldsymbol{F}}(\boldsymbol{z}) = -\boldsymbol{\Lambda z}\bar{\boldsymbol{D}}\boldsymbol{h3}(\boldsymbol{z}) + \boldsymbol{\Lambda h3}(\boldsymbol{z}) + \bar{\boldsymbol{D}}\boldsymbol{C}(\boldsymbol{z})\boldsymbol{h2}(\boldsymbol{z}) + \boldsymbol{D}(\boldsymbol{z}) \tag{3.37}$$

and $\bar{\boldsymbol{D}}$ is a derivative operator, with terms of order higher than 3 neglected. Removing nonlinear terms from (3.36) implies setting the second term on the right hand side of (3.36) to zero (i.e equating (3.37) to zero). It can be shown that if there is no internal resonance relationship among the eigenvalues, setting (3.37) to zero yields

$$h2_{kl}^{j} = \frac{C_{kl}^{j}}{\lambda_k + \lambda_l - \lambda_j}, \tag{3.38a}$$

$$h3_{pqr}^{j} = \frac{D_{pqr}^{j} + Cres_{pqr}^{j}}{\lambda_p + \lambda_q + \lambda_r - \lambda_j}. \tag{3.38b}$$

where $Cres$ is a residual term from second order transformation and is expressed as $\sum_{l=1}^{N}(C_{pl}^{j} + C_{lp}^{j})h2_{qr}^{p}$ [57] and D_{pqr}^{j} is the original third order term. Details of derivations leading to (3.38) are documented in Appendix D. Notice that the NF coefficients are simply algebraic functions of the nonlinear coefficients and the linear modes. The NF coefficients (3.38a) removes second order nonlinearities from (3.31), while (3.38b) removes third order nonlinearities.

Generally, the removal of a certain order of nonlinearities introduces higher order nonlinearities (*residuals*) due to the transformation. These higher order nonlinearities are then neglected for being weak compared to the considered order of nonlinearities. In other words, NF transformation at a certain order, "pushes" the nonlinearities to higher orders. Consequently, for NF3, the removal of second order nonlinearities introduces new third order nonlinearities, so-called *second order residuals*. Similarly, the removal of third order nonlin-

earities introduces fourth and higher order nonlinearities which are neglected. In many cases the effects of the second order residuals can be neglected without significant error. Thus, (3.38b) is simplified to

$$h3^j_{pqr} = \frac{D^j_{pqr}}{\lambda_p + \lambda_q + \lambda_r - \lambda_j}. \tag{3.39}$$

It can be seen that if the denominators of (3.38) are close to zero with non zero absolute value of the numerators, the value of the coefficients will be very large, which would lead to a inconsistent change of variables. The nullity of the denominators leads to particular relations between the complex eigenvalues called internal resonances. If no internal resonance occurs, (3.36) reduces to a fully linear system:

$$\dot{z}_j = \lambda_j z_j, \tag{3.40}$$

with solution given as

$$z_j(t) = z_{j_0} e^{\lambda_j t}. \tag{3.41}$$

In (3.41), the initial conditions z_{j_0} of the variables z_j are computed by solving a system of nonlinear equations (3.42), formulated from (3.35) for given initial conditions $\mathbf{y_0}$.

$$\forall j = 1 \dots N: \quad f_j(\mathbf{z_0}) = z_{j_0} - y_{j_0} + \sum_{k=1}^{N}\sum_{l=1}^{N} h2^j_{kl} z_{k_0} z_{l_0} + \sum_{p=1}^{N}\sum_{q=1}^{N}\sum_{r=1}^{N} h3^j_{pqr} z_{p_0} z_{q_0} z_{r_0} = 0. \tag{3.42}$$

The algorithm for obtaining the initial condition is presented in section 3.2.3.

In the other cases where internal resonances occur, some nonlinear terms cannot be eliminated from (3.31) and (3.40) becomes

$$\dot{z}_j = \lambda_j z_j + g_j(z), \tag{3.43}$$

where $g_j(z)$ gathers the terms that cannot be removed. If 3rd order nonlinear terms are considered and there exist lightly damped modes, there are always inherent near resonances so that $g_j(z)$ is never zero. Such near resonances exist because if $\lambda_j, \lambda_{2j-1}, \forall j \in M$ lightly damped modes are complex conjugates, $\lambda_j + \lambda_{2j-1} + \lambda_i - \lambda_i$ will always lead to very small divisor (near resonance) which translates to ill-conditioning. Technique for handling internal resonances is outside the scope of this thesis. Interested readers can refer to [89] where a method is proposed for getting closed-form solution under resonance.

At the end, system (3.43) has two advantages. Due to the normal transform, it is first, much simpler than system (3.28), since it has much less nonlinear terms and second, it can be consistently truncated to a few modes, thanks to the concept of nonlinear modes and

invariant manifolds (see [62, 111, 112] and references therein). System (3.43) can then be used for nonlinear modal analyses, time integration and many more, and can be reversed to its original coordinates $\mathbf{x}$ by applying successively, the change of variables (3.35) and (3.22).

The solution of (3.28) after back transformation of z is of the form [71]

$$\boxed{x_i(t) = \sum_{j=1}^{N} \mu_{1_{ij}} e^{\lambda_j t} + \sum_{k=1}^{N}\sum_{l=1}^{N} \mu^i_{2_{kl}} e^{(\lambda_k+\lambda_l)t} + \sum_{p=1}^{N}\sum_{q=1}^{N}\sum_{r=1}^{N} \mu^i_{3_{pqr}} e^{(\lambda_p+\lambda_q+\lambda_r)t}}, \tag{3.44}$$

where

$$\mu_{1_{ij}} = u_{ij} z_{j_0}, \quad \mu^i_{2_{kl}} = z_{k_0} z_{l_0} \sum_{j=1}^{N} u_{ij} h2^j_{kl}, \quad \mu^i_{3_{pqr}} = z_{p_0} z_{q_0} z_{r_0} \sum_{j=1}^{N} u_{ij} h3^j_{pqr}.$$

The boxed equation (3.44) is very important in understanding the motivation for NF analysis, since it explains clearly its gains. For instance:

- The 2nd and 3rd terms on the right hand side of (3.44) represent the effects of nonlinear modal interactions in addition to the linear modes on the dynamics of state i.
- $\mu_{1_{ij}}$, $\mu^i_{2_{kl}}$, and $\mu^i_{3_{pqr}}$ indicate the sizes of the contributions of the linear mode j, nonlinear mode $(k+l)$, and nonlinear mode $(p+q+r)$ to the oscillations of state i respectively.
- The nonlinear modal interactions $(k+l)$ and $(p+q+r)$ are both corrections and extra information added to linear analysis.

3.2.3 Normal form initial condition

The initial condition plays a key role since all the indices depend on it. A robust Newton-Raphson solution technique proposed in [31] for second order NF is extended here for third order NF as follow:

1. $\mathbf{x_0}$: Define $\mathbf{x_0}$, the initial condition of the power system after disturbance as $\mathbf{x_0} = \mathbf{x_{cl}} - \mathbf{x_{SEP}}$, where $\mathbf{x_{SEP}}$ is the post disturbance equilibrium solution and $\mathbf{x_{cl}}$ is the system condition at the end of the disturbance.
2. $\mathbf{y_0}$: Use the eigenvector to obtain the initial condition in Jordan coordinate as $\mathbf{y_0} = \mathbf{U}^{-1}\mathbf{x_0}$.
3. To compute $\mathbf{z_0}$:

   I. Formulate the solution problem as (3.42).

   II. Choose the initial guess for $\mathbf{z_0}$. $\mathbf{z_0} = \mathbf{y_0}$ recommended.

   III. Compute the mismatch function for iteration s as:

$$\forall j,k,l,p,q,r = 1\ldots N:$$
$$f_j(z^{(s)}) = z_j^{(s)} - y_j + \sum_{k=1}^{N}\sum_{l=1}^{N} h2_{kl}^{j} z_k^{(s)} z_l^{(s)} + \sum_{p=1}^{N}\sum_{q=1}^{N}\sum_{r=1}^{N} h3_{pqr}^{j} z_p^{(s)} z_q^{(s)} z_r^{(s)} = 0.$$

IV. Compute the Jacobian of $\mathbf{f}(\mathbf{z})$ at $\mathbf{z^{(s)}}$ as $\left[\mathbf{A}(\mathbf{z^{(s)}})\right] = \left[\frac{\partial \mathbf{f}}{\partial \mathbf{z}}\right]_{\mathbf{z}=\mathbf{z^{(s)}}}$

V. Compute the increment $\Delta\mathbf{z}^{(s)} = -\left[\mathbf{A}(\mathbf{z^{(s)}})\right]^{-1}\mathbf{f}(\mathbf{z^{(s)}})$

VI. Obtain the optimal step length ρ with cubic interpolation or any other appropriate procedure and compute $\mathbf{z^{(s+1)}} = \mathbf{z^{(s)}} + \rho\Delta\mathbf{z}^{(s)}$.

VII. Iterate till a specific tolerance is met. The value of $\mathbf{z^{(s)}}$ meeting the tolerance gives the solution $\mathbf{z_0}$.

Note that it is possible for the iteration to converge to a false solution. Several methods can be used to verify the initial condition, such as backward transformation to compare with the $\mathbf{x_0}$. Reference [68] gives other guides.

3.2.4 Didactic Example

Consider a classical single machine connected to an infinite bus shown in Figure 3.2. The machine data are $x'_d = 0.3, M = 7$. The network reactances are given on 220MVA, 24kV, 60Hz base and the post-fault values are given as: $P = 0.9$ p.u., $Q = 0.3$ p.u. (overexcited), terminal voltage $= 1\angle 36°$, total line impedance $X_s = 0.95p.u.$ The stable operating condition $\delta_{SEP} = 49.92°$, $\omega_{SEP} = 1$, $\mathcal{D} = 0$. The state vector $\mathbf{x} = [\delta,\ \omega]^T$, and the general nonlinear

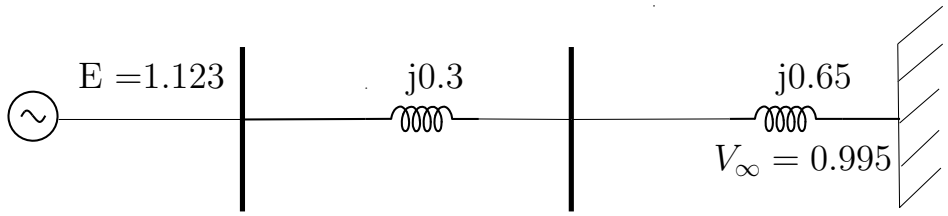

Figure 3.2 – Single machine-infinite-bus system

function $\mathbf{f}(\mathbf{x})$ is given by

$$\dot{\delta} = f_1(\delta,\omega) = \omega_s(\omega - 1)$$
$$\dot{\omega} = f_2(\delta,\omega) = \frac{1}{M}\left[P_m - P_e - \mathcal{D}(\omega - 1)\right]$$
$$P_e = \frac{EV_\infty}{X_s}\sin\delta.$$

With $\omega_s = 2\pi f \approx 377$ rad/s, the Jacobian and Hessians are defined as shown below:

***Evaluation of Jacobian and modal contents* (3.29)**

$$\mathbf{A} = \begin{bmatrix} \frac{\partial f_1}{\partial \delta} & \frac{\partial f_1}{\partial \omega} \\ \frac{\partial f_2}{\partial \delta} & \frac{\partial f_2}{\partial \omega} \end{bmatrix}_{\mathbf{x}=\mathbf{x_0}} = \begin{bmatrix} 0 & 377 \\ -0.1082 & 0 \end{bmatrix}$$

$$\mathbf{\Lambda} = \begin{bmatrix} 6.38i & 0 \\ 0 & -6.38i \end{bmatrix}, \quad \mathbf{U} = \begin{bmatrix} 0.9999 & 0.9999 \\ 0.0169i & -0.0169i \end{bmatrix}, \quad \mathbf{V^T} = \begin{bmatrix} 0.5001 & -29.5205i \\ 0.5001 & 29.5205i \end{bmatrix}.$$

***Evaluation of multidimensional Hessian matrices* (3.29)**

$$\mathbf{F}_2 = \frac{1}{2}\begin{bmatrix} \begin{bmatrix} \frac{\partial^2 f_1}{\partial \delta^2} & \frac{\partial^2 f_1}{\partial \delta \partial \omega} \\ \frac{\partial^2 f_2}{\partial \delta^2} & \frac{\partial^2 f_2}{\partial \delta \partial \omega} \end{bmatrix} & \begin{bmatrix} \frac{\partial^2 f_1}{\partial \omega \partial \delta} & \frac{\partial^2 f_1}{\partial \omega^2} \\ \frac{\partial^2 f_2}{\partial \omega \partial \delta} & \frac{\partial^2 f_2}{\partial \omega^2} \end{bmatrix} \end{bmatrix}_{\mathbf{x}=\mathbf{x_0}} = \begin{bmatrix} \begin{bmatrix} 0 & 0 \\ 0.0643 & 0 \end{bmatrix} & \begin{bmatrix} 0 & 0 \\ 0 & 0 \end{bmatrix} \end{bmatrix}$$

$$\mathbf{F}_3 = \frac{1}{6}\begin{bmatrix} \begin{bmatrix} \frac{\partial^3 f_1}{\partial \delta^3} & \frac{\partial^3 f_1}{\partial \delta^2 \partial \omega} \\ \frac{\partial^3 f_2}{\partial \delta^3} & \frac{\partial^3 f_2}{\partial \delta^2 \partial \omega} \end{bmatrix} & \begin{bmatrix} \frac{\partial^3 f_1}{\partial \omega \partial \delta^2} & \frac{\partial^3 f_1}{\partial \omega \partial \delta \partial \omega} \\ \frac{\partial^3 f_2}{\partial \omega \partial \delta^2} & \frac{\partial^3 f_2}{\partial \omega \partial \delta \partial \omega} \end{bmatrix} \\ \begin{bmatrix} \frac{\partial^3 f_1}{\partial \delta \partial \omega \partial \delta} & \frac{\partial^3 f_1}{\partial \delta \partial \omega^2} \\ \frac{\partial^3 f_2}{\partial \delta^2 \partial \omega} & \frac{\partial^3 f_2}{\partial \delta \partial \omega \partial \delta} \end{bmatrix} & \begin{bmatrix} \frac{\partial^3 f_1}{\partial \omega^2 \partial \delta} & \frac{\partial^3 f_1}{\partial \omega^3} \\ \frac{\partial^3 f_2}{\partial \omega^2 \partial \delta} & \frac{\partial^3 f_2}{\partial \omega^3} \end{bmatrix} \end{bmatrix}_{\mathbf{x}=\mathbf{x_0}} = \begin{bmatrix} \begin{bmatrix} 0 & 0 \\ 0.018 & 0 \end{bmatrix} & \begin{bmatrix} 0 & 0 \\ 0 & 0 \end{bmatrix} \\ \begin{bmatrix} 0 & 0 \\ 0 & 0 \end{bmatrix} & \begin{bmatrix} 0 & 0 \\ 0 & 0 \end{bmatrix} \end{bmatrix}$$

***Modal expansion/Evaluation of nonlinear coefficients* $\mathbf{C}$ *and* $\mathbf{D}$ (3.32)**

$$\begin{aligned} \mathbf{C} = \mathbf{V}^T\mathbf{F_2}\mathbf{U} &= \begin{bmatrix} \begin{bmatrix} -1.89i & -1.89i \\ 1.89i & 1.89i \end{bmatrix} & \begin{bmatrix} -1.89i & -1.89i \\ 1.89i & 1.89i \end{bmatrix} \end{bmatrix} \\ \implies \mathbf{C}(\mathbf{y}) &= \begin{matrix} -1.89iy_1^2 & -3.79iy_1y_2 & -1.89iy_2^2 \\ 1.89iy_1^2 & +3.79iy_1y_2 & +1.89iy_2^2 \end{matrix} \end{aligned} \tag{3.45}$$

$$\begin{aligned} \mathbf{D} = \mathbf{V}^T\mathbf{F_3}\mathbf{U} &= \begin{bmatrix} \begin{bmatrix} -0.53i & -0.53i \\ 0.53i & 0.53i \\ -0.53i & -0.53i \\ 0.53i & 0.53i \end{bmatrix} & \begin{bmatrix} -0.53i & -0.53i \\ 0.53i & 0.53i \\ -0.53i & -0.53i \\ 0.53i & 0.53i \end{bmatrix} \end{bmatrix} \\ \implies \mathbf{D}(\mathbf{y}) &= \begin{matrix} -0.53iy_1^3 & -1.59iy_1^2y_2 & -1.59iy_1y_2^2 & -0.53iy_2^3 \\ 0.53iy_1^3 & +1.59iy_1^2y_2 & +1.59iy_1y_2^2 & +0.53iy_2^3 \end{matrix} \end{aligned} \tag{3.46}$$

Note that by symmetry, Hessian evaluation splits diagonal elements such that $C^j_{kl} = C^j_{lk}$, $D^j_{kkl} = D^j_{lkk} = D^j_{klk}$. Therefore, the actual coefficients are $C^j_{kl_{actual}} = 2C^j_{lk}$, $D^j_{kkl_{actual}} = 3D^j_{lkk}$, where the residual $\mathbf{C_{res}}$ is at this point neglected. Therefore, (3.31) becomes

$$\dot{y}_1 = 6.38iy_1 - 1.89iy_1^2 - 3.79iy_1y_2 - 1.89iy_2^2 - 0.53iy_1^3 - 1.59iy_1^2y_2 - 1.59iy_1y_2^2 - 0.53iy_2^3 \tag{3.47a}$$

$$\dot{y}_2 = -6.38iy_2 + 1.89iy_1^2 + 3.79iy_1y_2 + 1.89iy_2^2 + 0.53iy_1^3 + 1.59iy_1^2y_2 + 1.59iy_1y_2^2 + 0.53iy_2^3. \tag{3.47b}$$

Evaluation of NF coefficients *h2 and h3* **(3.38)**

The NF transformation polynomials can be defined as

$$y_1 = z_1 + h2^1_{11}z_1^2 + h2^1_{12}z_1z_2 + h2^1_{22}z_2^2 + h3^1_{111}z_1^3 + h3^1_{112}z_1^2z_2 + h3^1_{221}z_2^2z_1 + h3^1_{222}z_2^3 \tag{3.48a}$$

$$y_2 = z_1 + h2^2_{11}z_1^2 + h2^2_{12}z_1z_2 + h2^2_{22}z_2^2 + h3^2_{111}z_1^3 + h3^2_{112}z_1^2z_2 + h3^2_{221}z_2^2z_1 + h3^2_{222}z_2^3. \tag{3.48b}$$

Since the nonlinear coefficients (**C** and **D**) have been computed in (3.47), the NF coefficients ($h2$ and $h3$) are easily evaluated by implementing (3.38a) and (3.38b). Implementation of (3.38a) obtains the $h2$ coefficients as:

$$h2^1_{11} = -0.29, \quad h2^1_{12} = 0.59, \quad h2^1_{22} = 0.099$$
$$h2^2_{11} = 0.099, \quad h2^2_{12} = 0.59, \quad h2^2_{22} = -0.29.$$

To implement (3.38b), we first need to evaluate the second order residuals $\mathbf{C_{res}}$ defined as:

$$C_{res_1}(\mathbf{y}) = (2C^1_{11}h2^1_{11})y_1^3 + (C^1_{12}h2^1_{12})y_1^2y_2 + (C^1_{12}h2^1_{12})y_1y_2^2 + (2C^1_{22}h2^1_{22})y_2^3 \tag{3.49a}$$

$$C_{res_2}(\mathbf{y}) = (2C^2_{11}h2^2_{11})y_1^3 + (C^2_{12}h2^2_{12})y_1^2y_2 + (C^2_{12}h2^2_{12})y_1y_2^2 + (2C^2_{22}h2^2_{22})y_2^3. \tag{3.49b}$$

Definition (3.49) is obtained by differentiating (3.45) and multiplying by $h2$ coefficients (i.e., $\bar{\mathbf{D}}\mathbf{C}(\mathbf{z})\mathbf{h2}(\mathbf{z})$, the third term on the right hand side of (3.37)). The reader may refer to [Section D.2, Appendix D] for details. Substituting the values of $h2$ and C coefficients in (3.49) yields

$$C_{res_1}(\mathbf{y}) = 1.10y_1^3 - 2.24y_1^2y_2 - 2.24y_1y_2^2 - 0.37y_2^3 \tag{3.50a}$$

$$C_{res_2}(\mathbf{y}) = 0.37y_1^3 + 2.24y_1^2y_2 + 2.24y_1y_2^2 - 1.10y_2^3. \tag{3.50b}$$

Equations (3.50) contain only cubic terms which are then added to the cubic terms of (3.47). Therefore, (3.47) are updated as:

$$\dot{y}_1 = 6.38iy_1 - 1.89iy_1^2 - 3.79iy_1y_2 - 1.89iy_2^2 + 0.57iy_1^3 - 3.83iy_1^2y_2 - 3.83iy_1y_2^2 - 0.9iy_2^3 \tag{3.51a}$$

$$\dot{y}_2 = -6.38iy_2 + 1.89iy_1^2 + 3.79iy_1y_2 + 1.89iy_2^2 + 0.9iy_1^3 + 3.83iy_1^2y_2 + 3.83iy_1y_2^2 - 0.57iy_2^3. \tag{3.51b}$$

Considering the updated cubic terms of (3.51), the $h3$ coefficients are computed as:

$$h3^1_{111} = 0.045, \quad h3^1_{122} = 0.3, \quad h3^1_{222} = 0.035$$
$$h3^2_{111} = 0.035, \quad h3^2_{112} = 0.3, \quad h3^2_{222} = 0.045.$$

Therefore, the nonlinear transformation (3.35) can be defined as

$$y_1 = z_1 - 0.29z_1^2 + 0.59z_1z_2 + 0.099z_2^2 + 0.045z_1^3 + 0.3z_1z_2^2 + 0.035z_2^3 \tag{3.52a}$$
$$y_2 = z_2 + 0.099z_1^2 + 0.59z_1z_2 - 0.29z_2^2 + 0.035z_1^3 + 0.3z_1^2z_2 + 0.045z_2^3. \tag{3.52b}$$

If the second order residual terms are not considered, $h3$ coefficients are determined directly from (3.47) and (3.39). Notice that $h3^1_{112}$ and $h3^2_{221}$ are not determined since they correspond to resonant conditions (i.e. $\lambda_1 + \lambda_1 + \lambda_2 - \lambda_1 = 0, \quad \lambda_2 + \lambda_2 + \lambda_1 - \lambda_2 = 0$). Therefore, their corresponding mononomial terms must not be removed from the NF. With all the possible coefficients determined, the NF is then obtained by substituting (3.52) into (3.51) which yields

$$\dot{z}_1 = \quad 6.38iz_1 - 3.83iz_1^2z_2 \tag{3.53a}$$
$$\dot{z}_2 = -6.38iz_2 + 3.83iz_1z_2^2. \tag{3.53b}$$

It can be seen that the system of (3.53) is very simplified compared to the system of (3.51), since it has mush less nonlinear terms. System (3.51) has 14 nonlinear terms while system (3.53) has just 2.

Remark. *The computed nonlinear coefficients in the above example are symmetrical, which leads to the symmetry of (3.47). This is because the classical SMIB power system used has one mode of oscillation, since the two eigenvalues are conjugate pair. This symmetry can be lost when there are some real eigenvalues in the system.*

Numerical simulations

For any initial condition in the physical space (x-coordinate), the initial conditions in NF-coordinate are obtained by the algorithm described in section 3.2.3. The system is stressed by increasing the operating point by: (a) $\Delta\delta = 5^\circ$ ($\frac{\pi}{36}$ rad) ; (b) $\Delta\delta = 15^\circ$ ($\frac{\pi}{12}$ rad) , and (c) $\Delta\delta = 25^\circ$ ($\frac{5\pi}{36}$ rad) . The NF results of these stress conditions are shown in Figure 3.3. For less stressed condition, the linear, the NF2, and the NF3 approximations work quite well compared

to the the original (exact) system. This is seen in Figure 3.3a, where all curves approximately match the exact one. As the operating point increases by $\Delta\delta = 15°$, the linear model begins to deviate in the amplitude, while the NF2 and NF3 still approximate well, the original system (see Figure 3.3b). Further increase of the operating point by $\Delta\delta = 25°$, increases significantly,

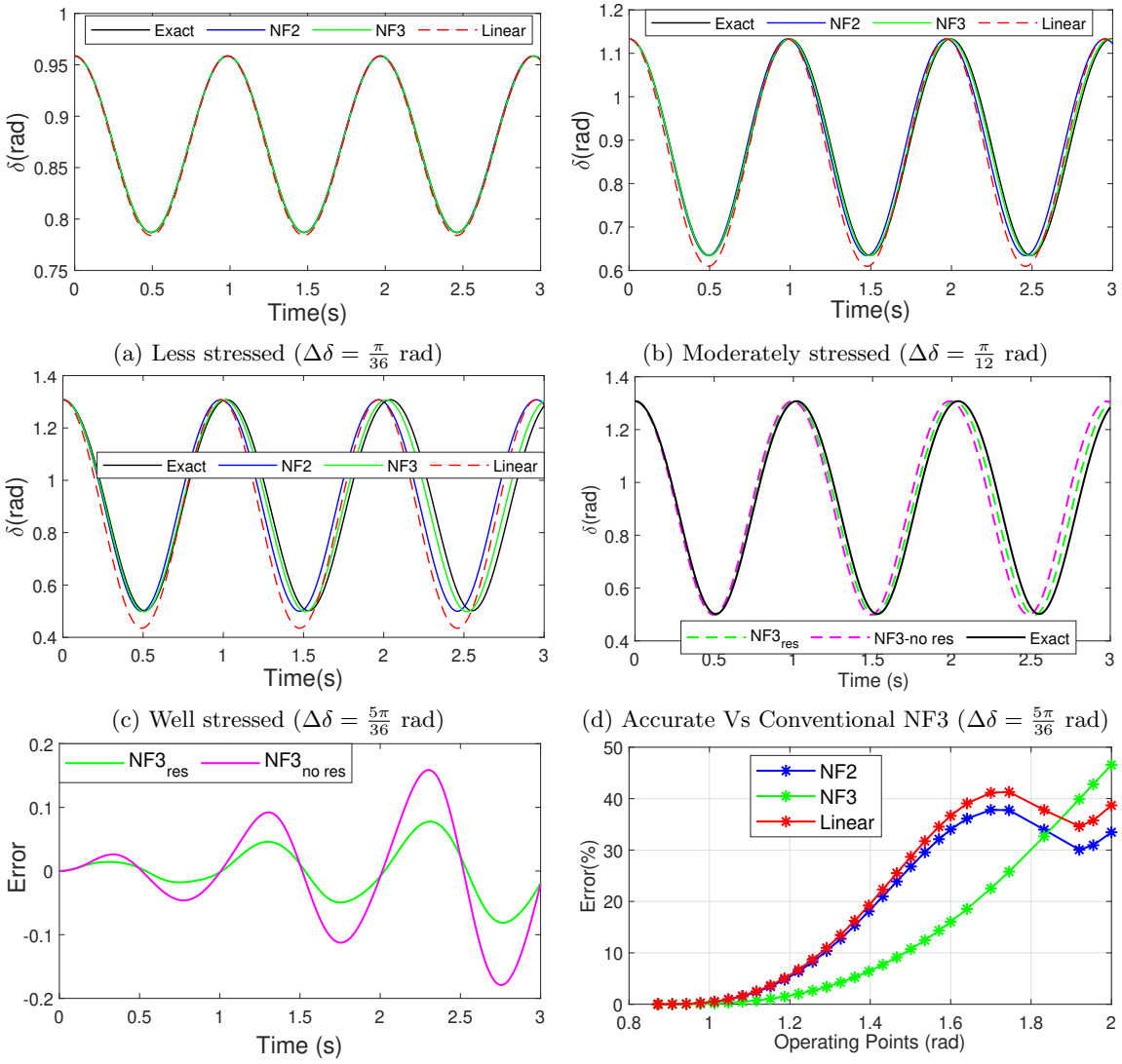

(a) Less stressed ($\Delta\delta = \frac{\pi}{36}$ rad)

(b) Moderately stressed ($\Delta\delta = \frac{\pi}{12}$ rad)

(c) Well stressed ($\Delta\delta = \frac{5\pi}{36}$ rad)

(d) Accurate Vs Conventional NF3 ($\Delta\delta = \frac{5\pi}{36}$ rad)

(e) Error—NF$_{\text{res}}$ Vs NF$_{\text{no res}}$

(f) Approximation errors

Figure 3.3 – Comparison of different approximate models for NF analysis

the nonlinearity. As a result, both linear and NF2 deviate in the frequency, although NF2 captures the amplitude. On the other hand, NF3 captures the amplitude and the frequency of the original system. These are seen in Figure 3.3c. Figure 3.3d shows a comparison of NF3 performed by neglecting (NF3$_{\text{no res}}$) and retaining (NF3$_{\text{res}}$), the second order residual terms. This figure shows that neglecting the residual term can introduce some errors. The errors of (NF3$_{\text{no res}}$) and (NF3$_{\text{res}}$) are plotted in Figure 3.3e, which clearly shows the merit of (NF3$_{\text{res}}$) over (NF3$_{\text{no res}}$). However, in some specific NF studies, the effects of the error do not play significant roles and can therefore be neglected [55].

Finally, Figure 3.3f presents the average errors on 20s time window for linear, NF2, and NF3 as functions of the operating point. As the operating point increases (increase in stress), the error increases for all the approximations. It is clear from the figure that NF3 incurs least error over large range of operating points compared to the linear and NF2. It is clear from the figure that the improvement brought by adding second order nonlinearities is not remarkably far from the linear approximation. The errors due to linear and NF2 seem to be very near. It seems that there are some operating points where the NF3 produces result worse than even linear and NF2. For instance, after 1.82 rad, the error of NF3 keeps increasing while the linear and NF2 dropped before rising again. The determination of the exact validity region of NF a priori is still an open problem. However, since NF is based on asymptotic expansion, one can envisage that before reaching the point at which the linear and NF2 give better results, the underlying assumption that the Taylor expansion around the operating point is sufficient to describe the dynamic behaviour of the system would have been broken. Hence, NF3 is judged to have effectively higher validity limit than linear and NF2.

From the didactic example above, one can identify the challenges with the traditional method for NF application. Some of these challenges are discussed in the next subsections.

3.2.5 Computational Burden

For better understanding of the main issue this thesis aims at solving, we can compute the number of nonlinear coefficients required for NF application. Considering an N-dimensional dynamical system and the symmetries of the Hessian matrices in (3.29), the number of nonlinear terms (which is equivalent to number of computations) that need to be computed in $\mathbf{\Gamma}(\mathbf{x})$ (i.e (3.27)) is

$$N_c = N\left[\frac{(N+1)!}{2!(N-1)!} + \frac{(N+2)!}{3!(N-1)!}\right] = \frac{N^4}{6} + N^3 + \frac{5N^2}{6}, \tag{3.54}$$

where $N!$ is the factorial of integer N. Furthermore, the number of coefficients C^j_{kl} and D^j_{pqr} in the modal model (3.31) that have to be computed using (3.32) is again N_c. Equation (3.54) shows that the computational burden increases with the power of four of the number of state variables of the initial system. Also, from the didactic example above, it is seen that the Hessians computed by (3.29) can be sparse, but the computation of the nonlinear coefficients using (3.32) leads to full matrices. Then, the overall implication in terms of memory and computation time can be huge, even impracticable for large systems with large N.

As an illustration, the evolution of the number of coefficients with respect to the linear basis size (i.e. number of state variables) is shown in Figure 3.4. A small change in size

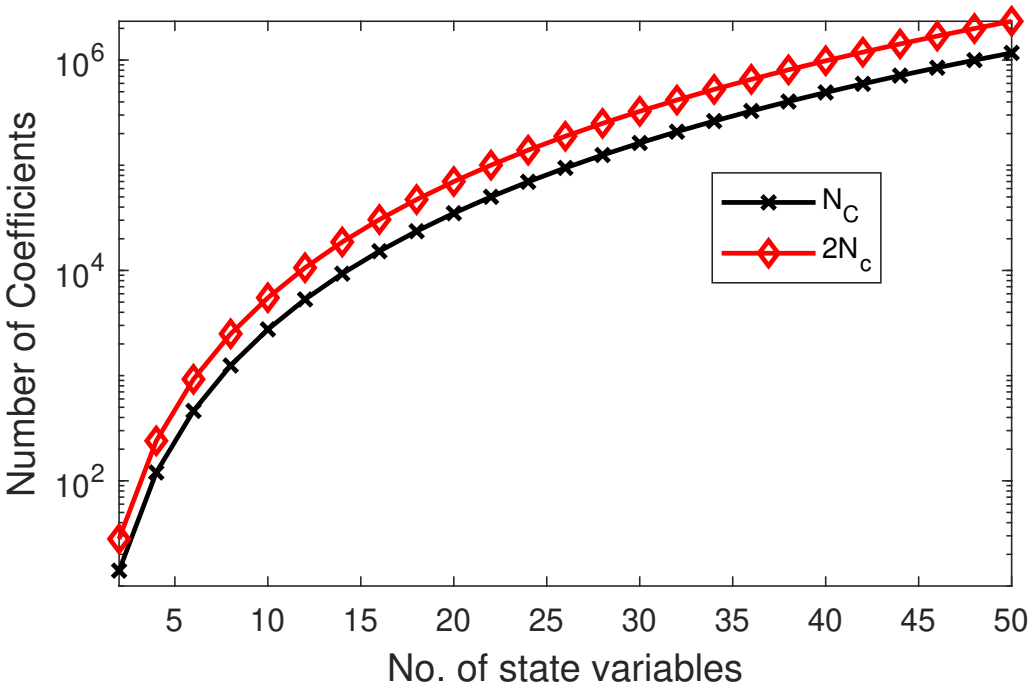

Figure 3.4 – Computational Burden of NF3

leads to a huge computational burden. As shall be seen in the next chapter, the major advantage of the method proposed in this thesis is that it enables one to compute directly, the nonlinear coefficients C^j_{kl} and D^j_{pqr} without requiring the preliminary computation of the Taylor expansion of (3.29) and the modal expansion by the use of (3.32). Moreover, the final number of nonlinear coefficients in the modal model (3.31) is equal to N_c since it is naturally written in upper triangular form (The sums $\sum_{k,l=1}^{N}, \sum_{k,l,s=1}^{N}$ are replaced by $\sum_{k=1,l>k}^{N}, \sum_{k=1,l>k,s>l}^{N}$) [113]. It means that instead of $2N_c$ computations, it is sufficient to perform only N_c computations in an easier way.

3.2.6 Model Flexibility

As seen earlier in chapter 2, higher order differentiation in (3.29) can be implemented by symbolic method, or by defining the expressions for those derivatives in advance. We assume that symbolic approach is avoided for being slow and one is able to painstakingly define those derivatives for a particular power system. Assuming for the same power system, the type of exciter used changes, or a static var compensator (SVC) is introduced, or a PE converter integrated or other changes that introduce modifications of the model, then definitions of (3.29) have to be extended to accommodate the new models. One has to repeat the process for the added model by defining the derivatives of the new variables with respect to the old ones and vice versa, in order to study these changes. Unfortunately, the above changes are typical of real power system.

The method proposed in this thesis is both efficient in reducing the computational burden and also very convenient for real life power system operators since it adapts easily to any addition of new component. The next chapter will show that the method acts only on the output of the overall system to formulate linear system of equations that obtain the needed coefficients. It is not necessary to obtain the derivative of the new model, hence, the method can easily adapt to changes in models.

Recapitulation

Let us quickly remind some major points so far in this chapter. Power systems are usually represented by first order DAEs models. For classical model, second order DAEs representations are possible. The DAEs models can be formulated as differential-only models suitable for NF application. These models can be approximated by Taylor series expansion which describe the nonlinear model with polynomials. The higher order approximations which have several nonlinear terms can be simplified using NF method. Moreover, the evaluation of these nonlinear terms is very difficult since it involves higher order derivatives and Hessian matrices. NF method uses nonlinear change of variable/nonlinear transformation (or simply NF transformation) to remove the nonlinear terms in order to obtain a simplified system. The NF procedures involve the computation of higher order Hessian matrices and numerous nonlinear coefficients which are computationally demanding in terms of time and memory. Since, conventional way to apply NF requires preliminary higher order derivative of the system model, slight change in the model will introduce significant changes in the Hessian matrices. Hence, the conventional method is less flexible in terms of model variations. A didactic example has been used to show the main steps and computations.

3.3 Normal Form of Second Order System Models

Till now, we have considered only first order model which is standard in power systems. The didactic example showed that this model presents the state variables as complex quantities. For mechanical systems, second order models are standard. In power systems, many direct methods for quick stability assessments such as equal area criteria, Lyapunov energy functions and Zubov's method are usually based on the classical model of power systems. Classical models of power systems are similar to mechanical systems and can equally be modelled with second order differential equations. Second order model has two main advantages:

- It has less number of variables, hence, less computational demand;
- It allows for convenient computation of only real eigenvalues.

The 2nd order classical modelling of power system can be described similar to mechanical system as

$$\mathbf{M}\ddot{\mathbf{x}} + \bar{\mathbf{C}}\dot{\mathbf{x}} + \mathbf{f}(\mathbf{x}) = \mathbf{P_T}, \tag{3.55}$$

where $\mathbf{M}$ and $\bar{\mathbf{C}}$ are symmetric matrices which respectively correspond to inertia and damping of the electric machine. $\mathbf{P_T}$ is a vector of mechanical power input of the machines, $\mathbf{x}$ is an N-dimensional vector of the state variables, and $\mathbf{f}(\mathbf{x})$ corresponds to $\mathbf{P_e}$ in (3.3). Similar to the first order model, the nonlinear coefficients are computed first and thereafter, a nonlinear change of variable is defined. The Taylor expansion model of (3.55) can be obtained at order 3 as

$$\mathbf{M}\ddot{\mathbf{x}} + \bar{\mathbf{C}}\dot{\mathbf{x}} + \mathbf{K}\mathbf{x} + \underbrace{\mathbf{F2}(\mathbf{x}) + \mathbf{F3}(\mathbf{x})}_{\mathbf{\Gamma(x)}} = \mathbf{P}, \tag{3.56}$$

or

$$\forall i = 1 \dots N: \;\; M_{ij}\ddot{x}_j + \bar{C}_{ij}\dot{x}_j + \sum_{j=1}^{N} K_{ij}x_j + \sum_{j=1}^{N}\sum_{k=1}^{N} F2^i_{jk}x_j x_k + \sum_{j=1}^{N}\sum_{k=1}^{N}\sum_{l=1}^{N} F3^i_{jkl}x_j x_k x_l = P_i, \tag{3.57}$$

where $\mathbf{P} = \Delta\mathbf{P_T}$, $\mathbf{K}$, the Jacobian of $\mathbf{f}(\mathbf{x})$ and differs from $\mathbf{A}$, defined for first order model, in that its eigenvalues are all real.

Let $\mathbf{\Omega^2}$ be a vector of the eigenvalues, obtained by solving $(\mathbf{K} - \Omega_i^2\mathbf{M})\mathbf{\Phi}_i = \mathbf{0}$. Let the i-th element be Ω_i^2 and $\mathbf{\Phi}$ be the right eigenvector. Exploiting the orthogonality properties of eigenmodes, the following statements are true

$$\begin{cases} \mathbf{\Phi}_i^T \boldsymbol{M} \mathbf{\Phi}_j = \sigma_{ij} \quad \forall i,j \\ \mathbf{\Phi}_i^T \mathbf{K} \mathbf{\Phi}_j = \Omega_i^2 \sigma_{ij} \quad \forall i,j \\ \mathbf{\Phi}_i^T \bar{\boldsymbol{C}} \mathbf{\Phi}_j \approx 2\zeta_i \Omega_i^2 \sigma_{ij} \quad \forall i,j \text{ (for low damping)}, \end{cases} \tag{3.58}$$

where ζ is the damping constant and the left eigenvector is the transpose of the right eigenvector. The Kronecker-σ is defined as $\sigma_{ij} = \begin{cases} 1 & \forall i = j \\ 0 & \forall i \neq j. \end{cases}$

If Φ_{ip} implies the i^{th} element of $\mathbf{\Phi}_p$, and Φ_{jq} implies the j^{th} element of $\mathbf{\Phi}_q$ (p,q = 1...N), then (3.58) can be re-written in scalar form as

$$\begin{cases} \Phi_{pi}^T M_{ij} \Phi_{jq} = \sigma_{pq} \quad \forall p,q \\ \Phi_{pi}^T K_{ij} \Phi_{jq} = \Omega_p^2 \sigma_{pq} \quad \forall p,q \\ \Phi_{pi}^T \bar{C}_{ij} \Phi_{jq} = 2\zeta_p \Omega_p^2 \sigma_{pq} \quad \forall p,q. \end{cases} \tag{3.59}$$

Similar to the case of first order model, (3.56) is transformed to modal coordinate by

$$\mathbf{x} = \boldsymbol{\Phi}\boldsymbol{\eta} \implies x_i = \Phi_{ip}\eta_p, \tag{3.60}$$

where $\boldsymbol{\eta}$ is now the modal variable equivalence of $\mathbf{y}$ for first order model. Putting equation (3.60) into (3.56) using (3.59) yields

$$\boldsymbol{M}\boldsymbol{\Phi}\ddot{\boldsymbol{\eta}} + \bar{\boldsymbol{C}}\boldsymbol{\Phi}\dot{\boldsymbol{\eta}} + \boldsymbol{K}\boldsymbol{\Phi}\boldsymbol{\eta} + \boldsymbol{\Gamma}_{NL}(\eta_1, \eta_2, \ldots, \eta_N) = \boldsymbol{\Phi}^T\mathbf{P}. \tag{3.61}$$

or

$$M_{ij}\Phi_{jq}\ddot{\eta}_q + \bar{C}_{ij}\Phi_{jq}\dot{\eta}_q + K_{ij}\Phi_{jq}\eta_q + F2^i_{jk}\Phi_{jp}\Phi_{kq}\eta_p\eta_q + F3^i_{jkl}\Phi_{jp}\Phi_{kq}\Phi_{lr}\eta_p\eta_q\eta_r = P_i. \tag{3.62}$$

Pre-multiplying (3.62) with $\boldsymbol{\Phi}_p^T (= \Phi_{pi})$, paying attention to (3.59) yields

$$\ddot{\eta}_p + 2\zeta_p\Omega_p\dot{\eta}_p + \Omega_p^2\eta_p + \sum_{q=1}^{N}\sum_{r=1}^{N} G^p_{qr}\eta_p\eta_r + \sum_{q=1}^{N}\sum_{r=1}^{N}\sum_{s=1}^{N} H^p_{qrs}\eta_q\eta_r\eta_s = \Phi_{pi}P_i, \forall p = 1, \ldots N, \tag{3.63}$$

where

$$\begin{cases} G^p_{qr} = F2^i_{jk}\Phi_{ip}\Phi_{jq}\Phi_{kr}, \\ H^p_{qrs} = F3^i_{jkl}\Phi_{ip}\Phi_{jq}\Phi_{kr}\Phi_{ls}. \end{cases} \tag{3.64}$$

or compactly,

$$\ddot{\boldsymbol{\eta}} + 2\boldsymbol{\zeta}\boldsymbol{\Omega}\dot{\boldsymbol{\eta}} + \boldsymbol{\Omega}^2\boldsymbol{\eta} + \boldsymbol{f}_{NL}(\eta_1, \eta_2, \ldots, \eta_N) = \boldsymbol{\Phi}^T\mathbf{P}, \tag{3.65}$$

where $\mathbf{f}_{\text{NL}} = \boldsymbol{\Phi}^T\boldsymbol{\Gamma}(\boldsymbol{\Phi}\boldsymbol{\eta})$. Equations (3.63)—(3.65) are written based on the normalisation, $\boldsymbol{\Phi}_p^T\boldsymbol{M}\boldsymbol{\Phi}_p = 1$. The nonlinear coefficients G and H in (3.64) are equivalence of C and D for first order models. However, while C and D are complex valued, G and H are only real.

Having obtained the nonlinear coefficients, the nonlinear change of variable (NF transformation) is used to obtain a simplified form of (3.63) called *nonlinear normal mode* (NNM)[2]. Recall from chapter 2 that NNM is defined according to Shaw and Pierre [78], when all displacements and velocities can be related to a single pair of displacement and velocity.

[2]The invariance property of NNM is equally maintained in the structure of (3.43), which was obtained for first order system. The only challenge is that the physical meaning of such expression is difficult to interpret, since the state variables are complex-valued

3.3.1 Nonlinear Change of Variables

References [62, 63] showed that NNM can be obtained by just nonlinear change of variable defined in such a way that complex quantities are avoided. That is, the NF transformation is performed similar to that of first order models, but with complex quantities avoided. The second order model considered in this thesis is a specific power system model, so-called classical model, however, we can imagine that the same nonlinear change of variables can be applied to systems more complex (if they can be put in second order form). If constant mechanical input is assumed and the damping neglected, (3.63) becomes

$$\forall p = 1 \dots N : \ddot{\eta}_p + \Omega_p^2 \eta_p + \sum_{i=1}^{N} \sum_{j \geq i}^{N} G_{ij}^p \eta_i \eta_j + \sum_{i=1}^{N} \sum_{j \geq i}^{N} \sum_{k \geq j}^{N} H_{ijk}^p \eta_i \eta_j \eta_k = 0. \tag{3.66}$$

To avoid complex quantities, (3.66) can be put to first order using the velocity $\varpi_p = \dot{\eta}_p$ as auxiliary variable and then each oscillator represented by a block diagonal matrix

$$\begin{pmatrix} 0 & 1 \\ -\Omega_p^2 & 0 \end{pmatrix}. \tag{3.67}$$

The auxiliary variable allows (3.66) to be written as $\dot{\eta}_p = f_p(\eta)$ and can always be cancelled to recover 2nd-order-like oscillator equations. Using (3.67), the system in (3.66) is rendered in first order and a nonlinear change of variable (i.e nonlinear transformation) is defined to remove the nonlinear terms. This is done sequentially, first, the quadratic and next, the cubic terms are removed. The first difference compared to conventional NF method discussed earlier is that, the 2nd order system model is expanded by Taylor series before putting to first order. The linear mode is unchanged while maintaining simpler computation.

As clearly stated in chapter 1, the focus of this thesis is not deriving new NF but facilitating the processes, especially the computation of the nonlinear coefficients (G and H in this case). Full derivations of nonlinear change of variables for second order models can be found in [62, 63, 114]. Only necessary equations considered useful in this work are presented next.

Quadratic Nonlinear Transformation

The system of (3.66) up to 2nd order becomes

$$\dot{\eta}_p = \varpi_p \tag{3.68a}$$

$$\dot{\varpi}_p = -\Omega_p^2 \eta_p - \sum_{i=1}^{N}\sum_{j\geq i}^{N} G_{ij}^p \eta_i \eta_j. \tag{3.68b}$$

Equation (3.68) suggests that at each point, one is working with N pairs of displacement-velocity variables. The nonlinear change of variable is defined as

$$\eta_p = U_p + \sum_{i=1}^{N}\sum_{j\geq i}^{N}(a_{ij}^p U_i U_j + b_{ij}^p V_i V_j) + \sum_{i=1}^{N}\sum_{j=1}^{N} c_{ij}^p U_i V_j \tag{3.69a}$$

$$\varpi_p = V_p + \sum_{i=1}^{N}\sum_{j\geq i}^{N}(\varphi_{ij}^p U_i U_j + \beta_{ij}^p V_i V_j) + \sum_{i=1}^{N}\sum_{j=1}^{N} \gamma_{ij}^p U_i V_j. \tag{3.69b}$$

where U_p and V_p are the new variables. Notice that the transformation in (3.69) is similar to that in (3.35) for first order model. However, it has been written in such a way as to take into account commuting and non-commuting terms differently. It is different in that it is defined as displacement-velocity pair.

To determine the unknown coefficients a_{ij}^p, b_{ij}^p, c_{ij}^p, φ_{ij}^p, β_{ij}^p, γ_{ij}^p (equivalence of $h2$ coefficients in first order case), one has to use (3.69) to re-write (3.68),[3] which yields

$$\begin{aligned}\dot{U}_p + \sum_{i=1}^{N}\sum_{j\geq i}^{N}[(a_{ij}^p - \Omega_j^2 b_{ij}^p)V_i U_j + (a_{ij}^p - \Omega_j^2 b_{ij}^p)U_i V_j] + \sum_{i=1}^{N}\sum_{j=1}^{N} c_{ij}^p (V_i V_j - \Omega_j^2 U_i U_j) \\ = V_p + \sum_{i=1}^{N}\sum_{j\geq i}^{N}(\varphi_{ij}^p U_i U_j + \beta_{ij}^p V_i V_j) + \sum_{i=1}^{N}\sum_{j=1}^{N}\gamma_{ij}^p U_i V_j\end{aligned} \tag{3.70a}$$

$$\begin{aligned}\dot{V}_p + \sum_{i=1}^{N}\sum_{j\geq i}^{N}[(\varphi_{ij}^p - \Omega_j^2 \beta_{ij}^p)V_i U_j + (a_{ij}^p - \Omega_j^2 b_{ij}^p)U_i V_j] + \sum_{i=1}^{N}\sum_{j=1}^{N}\gamma_{ij}^p (V_i V_j - \Omega_j^2 U_i U_j) \\ = -\sum_{i=1}^{N}\sum_{j=1}^{N} c_{ij}^p U_i V_j - \Omega_p\left[U_p + \sum_{i=1}^{N}\sum_{j\geq i}^{N}(\varphi_{ij}^p U_i U_j + \beta_{ij}^p V_i V_j) + \sum_{i=1}^{N}\sum_{j=1}^{N} c_{ij}^p U_i V_j\right] - \sum_{1=1}^{N}\sum_{j\geq i}^{N} G_{ij}^p U_i U_j.\end{aligned} \tag{3.70b}$$

Then, terms of like powers are equated, leading to a set of linear equations, which are easily solved. At last, the unknown coefficients required to remove second order nonlinearities from (3.66) are determined as [114]

[3] This generates terms of the form $\dot{U}_i U_j, \dot{V}_i V_j, \dot{U}_i V_j \ldots$ which is simplified by observing that at lower order $\dot{U}_p = V_p, \dot{V}_p = -V_p^2 U_p$ [114]

$\forall i = 1 \dots N \ , \forall j \geq i \dots N$

$$a_{ij}^p = \frac{\Omega_i^2 + \Omega_j^2 - \Omega_p^2}{\bar{\Delta}_{ijp}} G_{ij}^p \tag{3.71a}$$

$$b_{ij}^p = \frac{2}{\bar{\Delta}_{ijp}} G_{ij}^p \tag{3.71b}$$

$$c_{ij}^p = 0, \ \varphi_{ij}^p = 0, \ \beta_{ij}^p = 0 \tag{3.71c}$$

$$\gamma_{ii}^p = \frac{2}{4\Omega_i^2 - \Omega_p^2} G_{ij}^p \tag{3.71d}$$

$$\forall i = 1 \dots N-1, \quad \forall j > i \dots N \tag{3.71e}$$

$$\gamma_{ij}^p = \frac{\Omega_j^2 - \Omega_i^2 - \Omega_p^2}{\bar{\Delta}_{ijp}} G_{ij}^p \tag{3.71f}$$

$$\gamma_{ji}^p = \frac{\Omega_i^2 - \Omega_j^2 - \Omega_p^2}{\bar{\Delta}_{ijp}} G_{ij}^p \tag{3.71g}$$

where $\bar{\Delta}_{ijp} = (\Omega_i + \Omega_j - \Omega_p)(\Omega_i + \Omega_j + \Omega_p)(-\Omega_j + \Omega_i + \Omega_p)(\Omega_i - \Omega_j - \Omega_p)$. Notice that $\bar{\Delta}_{ijp}$ is composed of all possible second order resonant relations, implying that some second order nonlinearities cannot be removed in the case of resonance. Unlike the NF coefficients $(h2)$ in (3.38a), the above coefficients are all real valued. Note that to remove the second order nonlinearities, (3.66) is first of all written in first order. Then, the results of (3.71) are substituted in (3.69) and back to (3.66). This leaves only third and higher order terms in (3.66).

Cubic Nonlinear Transformation

For cubic change of variables, the technique is the same although tedious. Since the second order nonlinearities are removed, considering only third order terms, (3.66) becomes

$$\dot{U}_p = V_p \tag{3.72a}$$

$$\dot{V}_p = -\Omega_p^2 U_p - \sum_{i=1}^{N}\sum_{j\geq i}^{N}\sum_{k\geq j}^{N} H_{ijk}^p U_i U_j U_k - \sum_{i=1}^{N}\sum_{j=1}^{N}\sum_{k\geq j}^{N} [A_{ijk}^p U_i U_j U_k + B_{ijk}^p U_i U_j U_k], \tag{3.72b}$$

where A_{ijk}^p and B_{ijk}^p are cubic terms (residuals) introduced by the quadratic transformation[4] and are expressed as

$$\begin{aligned} A_{ijk}^p &= \sum_{l\geq i}^{N} G_{il}^p a_{jk}^l + \sum_{l\leq i}^{N} G_{il}^p a_{jk}^l \\ B_{ijk}^p &= \sum_{l\geq i}^{N} G_{il}^p b_{jk}^l + \sum_{l\leq i}^{N} G_{il}^p b_{jk}^l. \end{aligned} \tag{3.73}$$

[4]The reader is reminded that elimination of nonlinear term of a particular order in NF transformation normally introduces higher order terms

A similar change of variable is defined and similar procedure is followed to obtained all unknown coefficients. The overall expression for the nonlinear change of variables reads

$$\eta_p = R_p + \sum_{i=1}^{N}\sum_{j\geq i}^{N}(a_{ij}^p R_i R_j + b_{ij}^p S_i S_j) + \sum_{i=1}^{N}\sum_{j\geq i}^{N}\sum_{k\geq j}^{N} r_{ijk}^p R_i R_j R_k + \sum_{i=1}^{N}\sum_{j\geq i}^{N}\sum_{k\geq j}^{N} u_{ijk}^p R_i S_j S_k \tag{3.74a}$$

$$\varpi_p = S_p + \sum_{i=1}^{N}\sum_{j=1}^{N}\gamma_{ij}^p R_i S_j + \sum_{i=1}^{N}\sum_{j\geq i}^{N}\sum_{k\geq j}^{N}\mu_{ijk}^p S_i S_j S_k + \sum_{i=1}^{N}\sum_{j\geq i}^{N}\sum_{k\geq j}^{N} v_{ijk}^p S_i R_j R_k, \tag{3.74b}$$

where R_p and S_p are new variables (i.e. in NF coordinate), $u_{ijk}^p, r_{ijk}^p, v_{ijk}^p, \mu_{ijk}^p$ are coefficients determined in similar manner as in the previous case of quadratic transformation. Detailed presentation of their computations can be found in [Appendix C, 114].

The nonlinear dynamics in the new coordinate is obtained by substituting (3.74) in (3.66) which yields [114]

$$\dot{R}_p = S_p. \tag{3.75a}$$

$$\begin{aligned}\dot{S}_p = -\Omega_p^2 R_p - (A_{ppp}^p + H_{ppp}^p)R_p^3 - B_{ppp}^p R_p S_p^2 - R_p[\sum_{j>p}^{N}[(A_{jpj}^p + A_{pjj}^p + H_{pjj}^p)R_j^2 + B_{pjj}^p S_j^2] \\ + \sum_{i<p}[(A_{iip}^p + A_{pii}^p + H_{iip}^p)R_i^2 + B_{pii}^p S_i^2]] - S_p[\sum_{j>p}^{N} B_{jpj}^p R_j S_j + \sum_{i<p}^{N} B_{iip}^p R_i S_i].\end{aligned} \tag{3.75b}$$

3.3.2 Simplification to NNM

The NNM is obtained by cancelling all other variables except the displacement-velocity pair considered [62, 63] in (3.75). For instance, for mode p, the NNM will be defined as:

$$\forall q \neq p : R_q = 0, S_q = 0, \tag{3.76a}$$

$$\dot{R}_p = S_p, \tag{3.76b}$$

$$\dot{S}_p = -\Omega_p^2 R_p - (A_{ppp}^p + H_{ppp}^p)R_p^3 - B_{ppp}^p R_p S_p^2 \tag{3.76c}$$

Notice that for p-th mode, (3.76) is a function of only one displacement-velocity pair. The highly coupled system of (3.57) can now be studied analytically with the uncoupled and simpler model of (3.76), which preserves the system dynamics but in a new coordinate. Justification for (3.76a)—(3.76c) is on the assumption that effects of any cross-coupling nonlinearity is weak compared to any self-coupling nonlinearity, provided no internal resonance occurs.

As in the case of first order model, the initial conditions $\mathbf{R_0}$ are determined by formulating nonlinear optimisation problem from (3.74), with $\mathbf{S_0} = \mathbf{0}$.

3.3.3 NF of Second Order Models versus NF of First Order Models

Although the two models describe the same system behaviour, they do not give exactly the same results under NF analysis. The previous NF analysis on a SMIB power system is repeated with second order model (i.e. following NNM). The analyses from the two models are compared in Figure 3.5. Notice that for the linear case, both models give exactly the

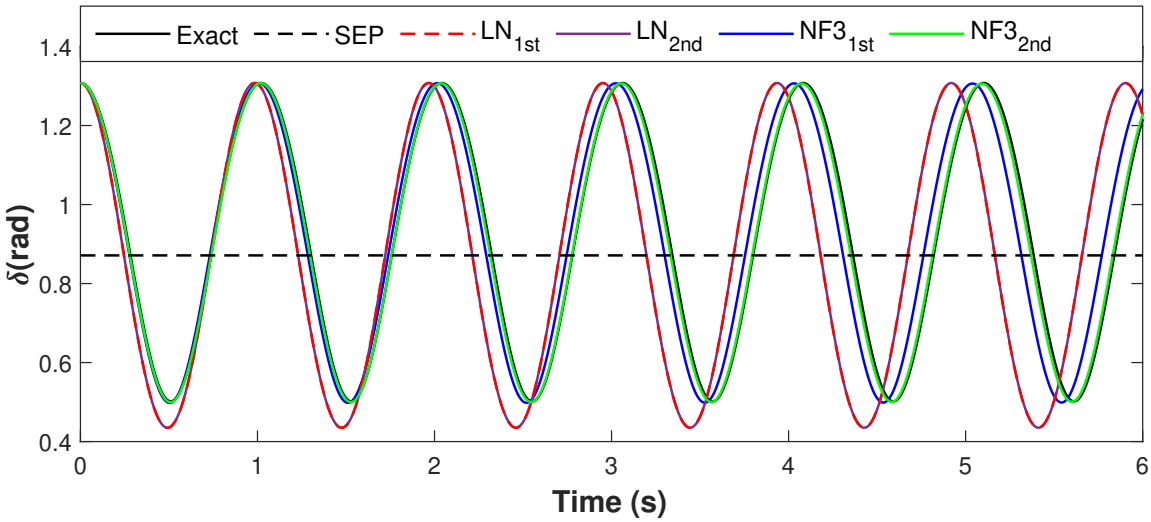

Figure 3.5 – NF— Second order versus First order Models for a SMIB power system.

same result (i.e. purple and red curves). However, for a third order NF (i.e. blue and green curves) analysis, there is a slight difference, both in the amplitude and in the frequency. In fact, the second order model is closer to the exact solution (i.e black curve). The difference in the first and second order methods comes from a difference in their invariance properties [115]. In the first order form, the eigenvalue decomposition results in the natural frequency ω_n being split into two eigenvalue components $j\omega_n$ and $-j\omega_n$. In contrast, the second order form has eigenvalues of ω_n^2 for each ω_n. Although, first order NF application is predominant in power system, for classical models, its second order counterpart is more accurate and less computation-intensive since the number of state variables is lesser. Moreover, the physical meaning is well preserved for second order model since there is no complex quantities in the process.

3.4 Summary of Normal Form Steps in Power System

Normal Form analysis can be applied to classical models of power system as well as to the detailed model. A classical model can be written either as set of first order differential

equations or as a set of second order differential equations. The application of NF to second order model is more accurate than that of first order [115], however, in taking into account the excitation controls, power systems are usually represented with first order models. The detailed model adopted in this work is the two-axis model. The power system DAEs is formulated as differential-only equations suitable for NF. The basic steps of NF application to power systems can be summarised with Figure 3.6 and described below:

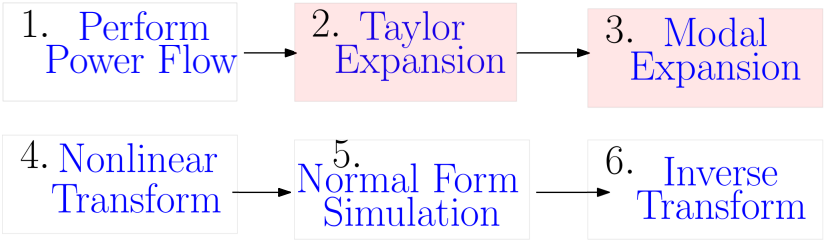

Figure 3.6 – Main steps in NF application to power systems.

1. *Formulate the DAEs of the system*: The power flow solutions are obtained and the stable equilibrium point (SEP) for the post-fault system is determined.

2. *Taylor expansion:* The algebraic equations are substituted into the differential ones and the resulting differential-only equations are expanded by Taylor series up to desired order around the SEP. The Taylor expansion can also be done on structure preserving power system DAEs [65]. The Jacobian of the system (i.e the first order term in the Taylor expansion.) is used to extract the system eigenvalues and vectors.

3. *Modal expansion:* The system of step 2 is expanded onto the eigenvectors basis obtained at step 2 and a new dynamical system with Jordan linear part is obtained, with nonlinear terms that couple the equations. The coefficients of the nonlinear terms, referred to as *nonlinear coefficients*, have to be computed.

4. *Normal form transformation:* The nonlinear part is further simplified by applying the normal form technique, based on successive nonlinear change of variables. This step leads to evaluation of other polynomial coefficients, so-called NF coefficients.

5. *NF initial conditions and simulation:* For transient simulations, the initial conditions of the NF system are determined, usually by combination of Newton-Raphson method and optimisation techniques. The system is then simulated in NF coordinates.

6. *Inverse NF and modal transformation:* The original dynamics can be reconstructed by using the change of coordinates of steps 4 and 3.

For power system applications, step 6 is often only used as a verification of the method. Meanwhile, most analyses are based on the investigation of the information in steps 3-4 and the initial condition of step 5. Evaluation of NF coefficients in step 4 finally boils down to simple division of the nonlinear coefficients (computed in step 3) by different combinations of the linear eigenvalues (computed in step 2). Hence the major computational burden is in steps 2 to step 3 and evaluation of initial condition in step 5. As will be seen, the method promoted in this work aims at significantly simplifying steps 2 to 3. In the next chapter, the proposed method for facilitating the NF3 application is systematically presented.

Chapter 4

Developed Method for Facilitating Normal Form Applications

"*Out of intense complexities, intense simplicities emerge.*"

Winston Churchill

Contents

Introduction

In the previous chapter, the theories of Normal Form were presented. We have seen that NF can be applied to first order system models as well as second order system models. It was shown, how the nonlinear normal mode (NNM) can be defined for second order models, following NF procedure. Whether first or second order model, the evaluation of Hessian matrices and numerous nonlinear coefficients as a result of Taylor expansion, and its associated higher order derivatives is common. It was noted that the evaluations of Hessians and these nonlinear coefficients are very difficult, especially for systems with large number of variables. In this chapter, we proposed a method that avoids the evaluation of Hessians and higher order derivatives but obtains the nonlinear coefficients by solving sets of linear equations. The proposed method is originally based on second order system model. In this chapter, it will be shown how to generalise it to power system first order model. Thus, the second order models are taken first and thereafter, the first order models. In each case, simple example is used to demonstrate the technique, followed by the implementation on larger power systems. We recall that in the previous chapter, the mechanical input power of the generator turbine was assumed constant. It will be seen in this chapter that the proposed method has to assume non-constant mechanical input for the evaluation of the nonlinear coefficients. The efficiency and accuracy of the proposed method are accessed by comparison with symbolic computation as well as with time domain simulations.

4.1 Motivation for the Proposed Method

In this thesis, we propose a method that avoids all the Hessian matrices and simultaneously obtains the nonlinear coefficients. The proposed method is motivated by a technique introduced in the mechanical engineering field [116], and widely applied since, to compute the coefficients of nonlinear modal reduced order models of mechanical structures discretized by a finite-elements method [113, 117]. Effort in the following section is to exploit the similarities between second order mechanical and electrical systems, in order to adapt this technique for power system studies.

Motivation

For better understanding of the proposed method, let us consider a simple motivating example. Figure 4.1 shows a mass connected to a rigid body through a spring of stiffness K. The mass rests on some rollers, such that it can move. Assume that an external force F_{ext} causes the movement of the mass, which in turn causes the spring to extend through a distance x.

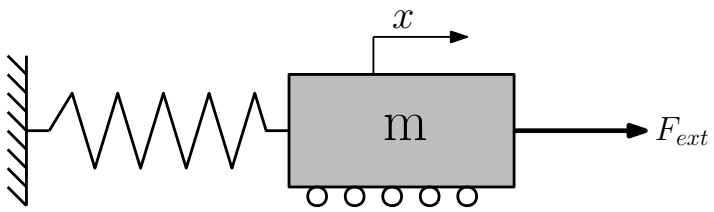

Figure 4.1 – One mass-spring system

The nonlinear behaviour of the spring can be modelled as:

$$m\ddot{x} + f(x) = F_{ext}. \tag{4.1}$$

System (4.1) can be approximated with nonlinearities up to third order as

$$m\ddot{x} + Kx + \beta x^2 + \gamma x^3 = F_{ext}, \tag{4.2}$$

where β, γ are unknown coefficients. Let us try to solve for the unknown coefficients by taking the stiffness (i.e. assuming a steady-state condition) part of (4.2). But since it contains two unknowns in one equation, solving for β, γ is mathematically difficult; requiring perhaps, iterations. It is assumed that we know the range of x for which the approximation (4.2) is valid and we can always compute $f(x)$; then it is possible to solve (4.2) linearly to obtain the unknown coefficients. Let us select two arbitrary values of x, equal in amplitude but opposite in sign (i.e. $\pm x \equiv x,\ -x$) from the range of values of x. For simplicity, the value of m is equal to unity. Then, it is possible to obtain two different equations, one for each value of x as

$$Kx^{\pm} + \beta x^{2\pm} + \gamma x^{3\pm} = F_{ext}^{\pm} \implies \begin{cases} Kx^{+} + \beta x^{2+} + \gamma x^{3+} = F_{ext}^{+} \\ Kx^{-} + \beta x^{2-} + \gamma x^{3-} = F_{ext}^{-}, \end{cases} \tag{4.3}$$

where the positive and negative superscripts are used to refer to equation relating to x and $-x$ respectively. Thus, F_{ext}^{+} and F_{ext}^{-} correspond to $f(x)$ and $f(-x)$ respectively in the static part of (4.1). The more compact form $\pm$ will henceforth, be used where the meaning is not confusing.

System of equations (4.3) is linear and totally defined and can then be solved to find the unknown coefficients β and γ. The above operation is exactly the idea proposed in this work, except that the proposed method deals with vector field instead of scalar equation as (4.2). The method is presented next.

4.2 Computation of Nonlinear Coefficients: 2nd Order Model

Let us recall that the 2nd order classical model of power system with negligible damping can be described as

$$\mathbf{M}\ddot{\mathbf{x}} + \mathbf{f}(\mathbf{x}) = \mathbf{P_T}, \tag{4.4}$$

where $\mathbf{M}$ is diagonal matrix, which corresponds to inertia constant of the electric machine. $\mathbf{P_T}$ is a vector of mechanical power input of the machines, $\mathbf{x}$ is an N-dimensional vector of the state variables, and $\mathbf{f}$ is a smooth vector field collecting all nonlinearities. Also, we recall from section 3.3 that (4.4) can be expanded as

$$\mathbf{M}\ddot{\mathbf{x}} + \mathbf{K}\mathbf{x} + \underbrace{\mathbf{F2}(\mathbf{x}) + \mathbf{F3}(\mathbf{x})}_{\mathbf{\Gamma(x)}} = \mathbf{P}, \tag{4.5}$$

and transformed by

$$\boldsymbol{x} = \mathbf{\Phi}\eta \implies x_i = \Phi_{ip}\eta_p, \tag{4.6}$$

to

$$\ddot{\boldsymbol{\eta}} + \mathbf{\Omega^2}\boldsymbol{\eta} + \boldsymbol{f}_{NL}(\eta_1, \eta_2, \ldots, \eta_N) = \mathbf{\Phi^T P}, \tag{4.7}$$

or

$$\ddot{\eta}_p + \Omega_p^2\eta_p + \sum_{q=1}^{N}\sum_{r=1}^{N} G_{qr}^p \eta_p\eta_r + \sum_{q=1}^{N}\sum_{r=1}^{N}\sum_{s=1}^{N} H_{qrs}^p \eta_q\eta_r\eta_s = \Phi_{pi}P_i, \forall p = 1, \ldots N, \tag{4.8}$$

where

$$\mathbf{f}_{\mathrm{NL}} = \mathbf{\Phi^T \Gamma}(\mathbf{\Phi}\eta). \tag{4.9}$$

$\mathbf{K}$ is the linear part, $\mathbf{\Gamma}(\mathbf{x})$ collects all the 2nd and 3rd order terms, $\mathbf{P} = \Delta\mathbf{P_T}$, while G and H are the nonlinear coefficients that must be computed.

To describe the new method for computing these nonlinear coefficients, we first consider in (4.4), the static part (i.e. $\mathbf{f}(\mathbf{x}) = \mathbf{P_T}$) and we assume that we are able to compute $\mathbf{f}(\mathbf{x})$ for any $\mathbf{x}$. The reader is reminded from chapter 2 that if the equilibrium is shifted to the origin, the state variable $\mathbf{\Delta x}$ is retained as $\mathbf{x}$. Therefore, taking up to 3rd order for a perturbation, the static part of (4.4) can be written as

$$\mathbf{P_T} = \mathbf{f}(\mathbf{x_0} + \mathbf{x}) \approx \mathbf{f}(\mathbf{x_0}) + \mathbf{K}\mathbf{x} + \mathbf{\Gamma}(\mathbf{x}). \tag{4.10}$$

Then, for a given SEP $\mathbf{x}_0$ and a given disturbance $\mathbf{x}$, the definition

$$\mathbf{P} = \Delta\mathbf{P_T} = \mathbf{P_T} - \mathbf{f}(\mathbf{x_0}) \tag{4.11}$$

and the nonlinear part can be written

$$\mathbf{P}_{\mathrm{NL}} = \mathbf{\Gamma}(\mathbf{x}) = \mathbf{P_T} - \mathbf{f}(\mathbf{x_0}) - \mathbf{K}\mathbf{x} = \mathbf{P} - \mathbf{K}\mathbf{x}. \tag{4.12}$$

Then, considering the static part of (4.8) and (4.7), the expression of the r-th component of $\mathbf{f}_{\mathrm{NL}}$ can be written:

$$f^r_{NL}(\eta_1, \eta_2, ...\eta_N) = \sum_{j=1}^{N}\sum_{k=1}^{N} G^r_{jk}\eta_j\eta_k + \sum_{j=1}^{N}\sum_{k=1}^{N}\sum_{l=1}^{N} H^r_{jkl}\eta_j\eta_k\eta_l = \mathbf{\Phi}_r^T\mathbf{P}_{\mathrm{NL}}, \tag{4.13}$$

where (4.12) has been used to cancel the linear part.

The method proposed here consists of two successive steps:

- First, one has to prescribe a set of displacement vectors $\mathbf{x}$, which are linear combinations of selected eigenvectors $\mathbf{\Phi}_i$ and compute the corresponding nonlinear force vector $\mathbf{P}_{\mathrm{NL}} = \mathbf{\Gamma}(\mathbf{x})$. The above operation is possible as soon as one can compute $\mathbf{P_T}$ or $\mathbf{f}(\mathbf{x})$ in (4.4) for a given $\mathbf{x}$. It does not require to solve any nonlinear system, for instance, with a Newton-Raphson technique. In time-domain simulation, the above operation implies the initialisation of the nonlinear system with a chosen initial condition.

- Second, the unknown coefficients G^r_{jk} and H^r_{jkl} are found by solving a linear system of equations, for which the second members are known functions of $\mathbf{P}_{\mathrm{NL}} = \mathbf{\Gamma}(\mathbf{x})$, computed at the previous step.

It is worthy of note that any SEP and model can be considered, with (4.13). To illustrate the method, we first consider prescribing the following perturbation of the SEP:

$$\mathbf{x}_1^{\pm} = \pm\alpha_i\Phi_i \quad \Rightarrow \quad \begin{cases} \eta_i = \alpha_i, \\ \eta_j = 0 \ \forall j \neq i, \end{cases} \tag{4.14}$$

where α_i, called *modal deviation amplitude* in this thesis is an arbitrary constant whose value will be addressed hereafter. The second part of the above equation comes from the orthogonality of the eigenmodes and (4.6). As explained earlier in the motivating example, the reason for the negative and positive prescriptions is to make it possible for creating two equations to be solved simultaneously. Prescribing a perturbation α_i on a given eigenmode $\mathbf{\Phi}_i$ leads to set to zero, all the other modal coordinates η_j. That is to say that passing $\mathbf{x} = \mathbf{\Phi}_i\alpha_i$

to linear and nonlinear static models will have effect, approximately, only on the node ii, $\mathbf{x} = \mathbf{\Phi}_i\alpha_i + \mathbf{\Phi}_j\alpha_j$ will have effect on ii, jj, and ij. By prescribing series of $\mathbf{x}$, one obtains sets of linear equations whose solutions are the coefficients. Considering (4.14) and (4.13), one obtains:

$$\alpha_i^2 G_{ii}^r + \alpha_i^3 H_{iii}^r = \mathbf{\Phi}_r^T \mathbf{P}_{\mathrm{NL}}^+ \tag{4.15}$$

$$\alpha_i^2 G_{ii}^r - \alpha_i^3 H_{iii}^r = \mathbf{\Phi}_r^T \mathbf{P}_{\mathrm{NL}}^-, \tag{4.16}$$

where $\mathbf{P}_{\mathrm{NL}}^{\pm} = \mathbf{\Gamma}(\mathbf{x}_1^{\pm}) = \mathbf{\Gamma}(\pm\alpha_i\mathbf{U}_i)$. As a consequence, coefficients G_{ii}^r and H_{iii}^r are solutions of a linear system whose second member is easily computed with the static part of the initial system $\mathbf{f}(\mathbf{x})$. This linear system can be generally written as $\mathbf{A_c}\mathbf{x_c} = \mathbf{B_c}$, where

$$\mathbf{A_c} = \begin{bmatrix} \alpha_i^2 & \alpha_i^3 \\ \alpha_i^2 & -\alpha_i^3 \end{bmatrix}, \mathbf{x_c} = \begin{bmatrix} G_{ii}^r \\ H_{iii}^r \end{bmatrix}, \mathbf{B_c} = \begin{bmatrix} \mathbf{\Phi}_r^T \mathbf{P}_{\mathrm{NL}}^+ \\ \mathbf{\Phi}_r^T \mathbf{P}_{\mathrm{NL}}^- \end{bmatrix}. \tag{4.17}$$

For other coefficients, such as G_{ij}^r, H_{iij}^r, H_{jji}^r, $i \neq j$ and H_{ijk} $i \neq j \neq k$, 16 different prescriptions of $\mathbf{x}$ are needed as:

$$\mathbf{x} = \begin{cases} \pm\mathbf{\Phi_i}\alpha_i \\ \pm\mathbf{\Phi_j}\alpha_j \\ \pm\mathbf{\Phi_k}\alpha_k \\ \mathbf{\Phi_i}\alpha_i + \mathbf{\Phi_j}\alpha_j \\ \mathbf{\Phi_i}\alpha_i - \mathbf{\Phi_j}\alpha_j \\ -\mathbf{\Phi_i}\alpha_i + \mathbf{\Phi_j}\alpha_j \\ \mathbf{\Phi_i}\alpha_i + \mathbf{\Phi_k}\alpha_k \\ \mathbf{\Phi_i}\alpha_i - \mathbf{\Phi_k}\alpha_k \\ -\mathbf{\Phi_i}\alpha_i + \mathbf{\Phi_k}\alpha_k \\ \mathbf{\Phi_j}\alpha_j + \mathbf{\Phi_k}\alpha_k \\ \mathbf{\Phi_j}\alpha_j - \mathbf{\Phi_k}\alpha_k \\ -\mathbf{\Phi_j}\alpha_j + \mathbf{\Phi_k}\alpha_k \\ \mathbf{\Phi_i}\alpha_i + \mathbf{\Phi_j}\alpha_j + \mathbf{\Phi_k}\alpha_k \end{cases} \tag{4.18}$$

Then a new linear system is obtained with $\mathbf{A_c} =$

$$\begin{bmatrix}
\alpha_i^2 & \alpha_i^3 & 0 & 0 & 0 & 0 & 0 & 0 & 0 & 0 & 0 & 0 & 0 & 0 & 0 & 0 \\
\alpha_i^2 & -\alpha_i^3 & 0 & 0 & 0 & 0 & 0 & 0 & 0 & 0 & 0 & 0 & 0 & 0 & 0 & 0 \\
0 & 0 & \alpha_j^2 & \alpha_j^3 & 0 & 0 & 0 & 0 & 0 & 0 & 0 & 0 & 0 & 0 & 0 & 0 \\
0 & 0 & \alpha_j^2 & -\alpha_j^3 & 0 & 0 & 0 & 0 & 0 & 0 & 0 & 0 & 0 & 0 & 0 & 0 \\
0 & 0 & 0 & 0 & \alpha_k^2 & \alpha_k^3 & 0 & 0 & 0 & 0 & 0 & 0 & 0 & 0 & 0 & 0 \\
0 & 0 & 0 & 0 & \alpha_k^2 & -\alpha_k^3 & 0 & 0 & 0 & 0 & 0 & 0 & 0 & 0 & 0 & 0 \\
\alpha_i^2 & \alpha_i^3 & \alpha_j^2 & \alpha_j^3 & 0 & 0 & \alpha_i\alpha_j & \alpha_i^2\alpha_j & \alpha_i\alpha_j^2 & 0 & 0 & 0 & 0 & 0 & 0 & 0 \\
\alpha_i^2 & \alpha_i^3 & \alpha_j^2 & -\alpha_j^3 & 0 & 0 & -\alpha_i\alpha_j & -\alpha_i^2\alpha_j & \alpha_i\alpha_j^2 & 0 & 0 & 0 & 0 & 0 & 0 & 0 \\
\alpha_i^2 & -\alpha_i^3 & \alpha_j^2 & \alpha_j^3 & 0 & 0 & -\alpha_i\alpha_j & \alpha_i^2\alpha_j & -\alpha_i\alpha_j^2 & 0 & 0 & 0 & 0 & 0 & 0 & 0 \\
\alpha_i^2 & \alpha_i^3 & 0 & 0 & \alpha_k^2 & \alpha_k^3 & 0 & 0 & 0 & \alpha_i\alpha_k & \alpha_i^2\alpha_k & \alpha_i\alpha_k^2 & 0 & 0 & 0 & 0 \\
\alpha_i^2 & \alpha_i^3 & 0 & 0 & \alpha_k^2 & -\alpha_k^3 & 0 & 0 & 0 & -\alpha_i\alpha_k & -\alpha_i^2\alpha_k & \alpha_i\alpha_k^2 & 0 & 0 & 0 & 0 \\
\alpha_i^2 & -\alpha_i^3 & 0 & 0 & \alpha_k^2 & \alpha_k^3 & 0 & 0 & 0 & -\alpha_i\alpha_k & \alpha_i^2\alpha_k & -\alpha_i\alpha_k^2 & 0 & 0 & 0 & 0 \\
0 & 0 & \alpha_j^2 & \alpha_j^3 & \alpha_k^2 & \alpha_k^3 & 0 & 0 & 0 & 0 & 0 & 0 & \alpha_j\alpha_k & \alpha_j^2\alpha_k & \alpha_j\alpha_k^2 & 0 \\
0 & 0 & \alpha_j^2 & \alpha_j^3 & \alpha_k^2 & -\alpha_k^3 & 0 & 0 & 0 & 0 & 0 & 0 & -\alpha_j\alpha_k & -\alpha_j^2\alpha_k & \alpha_j\alpha_k^2 & 0 \\
0 & 0 & \alpha_j^2 & -\alpha_j^3 & \alpha_k^2 & -\alpha_k^3 & 0 & 0 & 0 & 0 & 0 & 0 & -\alpha_j\alpha_k & \alpha_j^2\alpha_k & -\alpha_j\alpha_k^2 & 0 \\
\alpha_i^2 & \alpha_i^3 & \alpha_j^2 & \alpha_j^3 & \alpha_k^2 & \alpha_k^3 & \alpha_i\alpha_j & \alpha_i^2\alpha_j & \alpha_i\alpha_j^2 & \alpha_i\alpha_k & \alpha_i^2\alpha_k & \alpha_i\alpha_k^2 & \alpha_j\alpha_k & \alpha_j^2\alpha_k & \alpha_j\alpha_k^2 & \alpha_i\alpha_j\alpha_k
\end{bmatrix}$$

$$\mathbf{X_c} = \left[G^r_{ii}, H^r_{iii}, G^r_{jj}, H^r_{jjj}, G^r_{kk}, H^r_{kkk,} \, G^r_{ij}, H^r_{iij}, H^r_{ijj}, G^r_{ik}, H^r_{iik}, H^r_{ikk}, G^r_{jk}, H^r_{jjk}, H^r_{jkk}, G^r_{ijk} \right]^T$$

$$\mathbf{B_c} = \begin{bmatrix}
\boldsymbol{\Phi}_r^T \mathbf{P}^+_{NL_i}, & \boldsymbol{\Phi}_r^T \mathbf{P}^-_{NL_i}, \, \boldsymbol{\Phi}_r^T \mathbf{P}^+_{NL_j}, \, \boldsymbol{\Phi}_r^T \mathbf{P}^-_{NL_j}, \, \boldsymbol{\Phi}_r^T \mathbf{P}^+_{NL_k}, \, \boldsymbol{\Phi}_r^T \mathbf{P}^-_{NL_k}, \, \boldsymbol{\Phi}_r^T \mathbf{P}^{++}_{NL_{ij}}, \, \dots \\
\dots \, \boldsymbol{\Phi}_\mathbf{r}^\mathbf{T} \mathbf{P}^{+-}_{NL_{ij}}, \, \boldsymbol{\Phi}_r^T \mathbf{P}^{-+}_{NL_{ij}}, \boldsymbol{\Phi}_r^T \mathbf{P}^{++}_{NL_{ik}}, \boldsymbol{\Phi}_r^T \mathbf{P}^{+-}_{NL_{ik}}, \boldsymbol{\Phi}_r^T \mathbf{P}^{-+}_{NL_{ik}}, \boldsymbol{\Phi}_r^T \mathbf{P}^{++}_{NL_{jk}}, \boldsymbol{\Phi}_r^T \mathbf{P}^{+-}_{NL_{jk}}, \dots \\
\dots \, \boldsymbol{\Phi}_r^T \mathbf{P}^{-+}_{NL_{jk}}, \boldsymbol{\Phi}_r^T \mathbf{P}^{+++}_{NL_{ijk}}
\end{bmatrix}^T,$$

where the superscripts correspond to the signs of the different prescriptions of $\mathbf{x}$ in (4.18). The 16 different prescriptions can be done simultaneously through a parallel computation software. The challenge however, is that the big matrix $\mathbf{A_c}$ is rebuilt for every set of coefficients, leading to repeated computations which are not desired. It is possible to reuse the previous computations for the subsequent ones. It is better to solve a lot of small systems and not a big one, computationally speaking.

Suppose all G^r_{ii} and H^r_{iii} are computed with (4.17), for the other coefficients such as

G^r_{ij}, H^r_{iij} and H^r_{jji}, $i \neq j$, $\mathbf{x}$ can be prescribed as:

$$\mathbf{x} = \begin{cases} \mathbf{\Phi_i}\alpha_i + \mathbf{\Phi_j}\alpha_j \\ \mathbf{\Phi_i}\alpha_i - \mathbf{\Phi_j}\alpha_j \\ -\mathbf{\Phi_i}\alpha_i + \mathbf{\Phi_j}\alpha_j \end{cases} \tag{4.19}$$

A new linear system is obtained with unknown G^r_{ij}, H^r_{iij} and H^r_{jji} and with the previously obtained coefficients G^r_{ii} and H^r_{iii} in the second member. Therefore, using (4.14) and (4.13) we get a set of linear equations

$$\mathbf{A_c x_c} = \mathbf{B_c} \tag{4.20}$$

with:

$$\begin{aligned} \mathbf{A_c} &= \begin{bmatrix} \alpha_i\alpha_j & \alpha_i^2\alpha_j & \alpha_i\alpha_j^2 \\ -\alpha_i\alpha_j & -\alpha_i^2\alpha_j & \alpha_i\alpha_j^2 \\ -\alpha_i\alpha_j & \alpha_i^2\alpha_j & -\alpha_i\alpha_j^2 \end{bmatrix}, \qquad \mathbf{x_c} = \begin{bmatrix} G^r_{ij} \\ H^r_{iij} \\ H^r_{jji} \end{bmatrix}, \\ \mathbf{B}_c &= \begin{bmatrix} \mathbf{\Phi}_r^T\mathbf{P}^{++}_{NL_{ij}} - G^r_{ii}\alpha_i^2 - H^r_{iii}\alpha_i^3 - G^r_{jj}\alpha_j^2 - H^r_{jjj}\alpha_j^3 \\ \mathbf{\Phi}_r^T\mathbf{P}^{+-}_{NL_{ij}} - G^r_{ii}\alpha_i^2 - H^r_{iii}\alpha_i^3 - G^r_{jj}\alpha_j^2 + H^r_{jjj}\alpha_j^3 \\ \mathbf{\Phi}_r^T\mathbf{P}^{-+}_{NL_{ij}} - G^r_{ii}\alpha_i^2 + H^r_{iii}\alpha_i^3 - G^r_{jj}\alpha_j^2 - H^r_{jjj}\alpha_j^3 \end{bmatrix}. \end{aligned} \tag{4.21}$$

Note that all self-coupled coefficients have been previously determined with (4.17).

Finally, the last coefficients H^r_{ijk}, $k \neq i \neq j$, $\mathbf{x}$ are obtained by prescribing:

$$\mathbf{x} = \mathbf{\Phi_i}\alpha_i + \mathbf{\Phi_j}\alpha_j + \mathbf{\Phi_k}\alpha_k. \tag{4.22}$$

Then all H^r_{ijk} can be obtained from

$$\begin{aligned} G^r_{ii}\alpha_i^2 + H^r_{iii}\alpha_i^3 + G^r_{jj}\alpha_j^2 + H^r_{jjj}\alpha_j^3 + G^r_{kk}\alpha_k^2 + H^r_{kkk}\alpha_k^3 + G^r_{ij}\alpha_i\alpha_j + H^r_{iij}\alpha_i^2\alpha_j + \ \ldots \\ \ldots\ H^r_{ijj}\alpha_i\alpha_j^2 + G^r_{ik}\alpha_i\alpha_k + H^r_{iik}\alpha_i^2\alpha_k + H^r_{ikk}\alpha_i\alpha_k^2 + G^r_{jk}\alpha_j\alpha_k + H^r_{jjk}\alpha_j^2\alpha_k + H^r_{jkk}\alpha_j\alpha_k^2 \ldots \\ + H^r_{ijk}\alpha_i\alpha_j\alpha_k = \mathbf{\Phi}_r^T\mathbf{P}^{+}_{NL_{ijk}}. \end{aligned} \tag{4.23}$$

Equation (4.23) contains only one unknown term H^r_{ijk}, since all other terms have been previously determined in (4.17) and (4.21).

Observe the following:

- The actual Taylor expansion and associated higher order derivatives and Hessian computations in (4.5) have been avoided. Therefore, instead of building Hessians, one needs only to solve linear system of equations.

- The computation of nonlinear coefficients via the modal expansion (4.9) has been avoided. Implementation of (4.9) leads to full matrices (not always symmetrical) even with sparse Hessian matrices of ((4.5)), thus symmetry cannot always be exploited.

- It is important to note that any desired coefficients can be computed easily by such a formulation as in (4.15) and (4.16). This is a major advantage of the proposed method, since not all terms will be needed for every analysis. It has to be emphasised that it is not practically impossible to compute a term selectively with the conventional method; the proposed method is only more convenient and faster.

4.2.1 Choosing the Modal Deviation Amplitude (α)

Although the amplitude of the deviation α is chosen arbitrarily, it should neither be too small nor too big. Very small value of α does not trigger the nonlinearity very well; hence, the system is more or less linear. On the other hand, too large value of α leads to higher nonlinearity, hence the domain of validity of 3rd order approximation is exceeded. Figure 4.2 shows the sensitivity of α for the system demonstrated in subsection 4.3.1. The modulus of some nonlinear coefficients is shown as a function of α. We observe that the coefficients

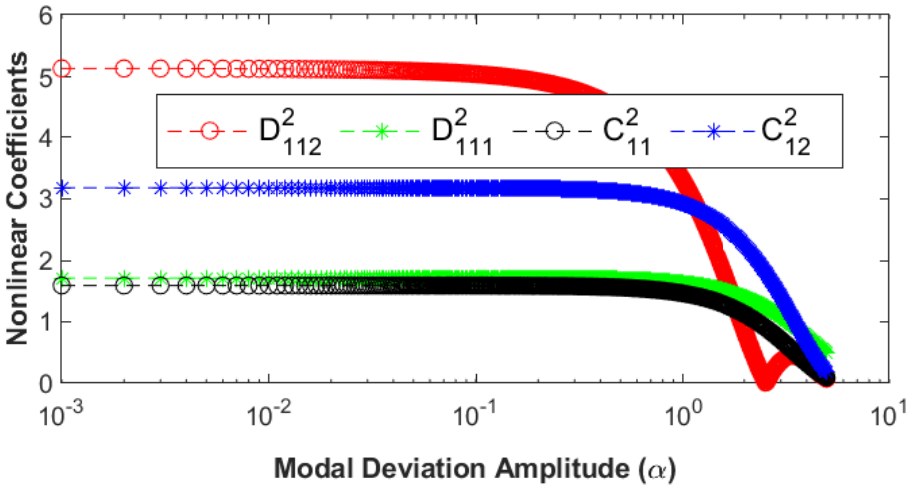

Figure 4.2 – Sensitivity of Modal deviation amplitude (α)

are consistent for α within certain range. As α becomes large, the nonlinearity increases beyond the validity of the third order approximation. This is evident from Figure 4.2 as the curves deviate from the actual results. In all the cases we have tried, a value in the range of $0.001 \leq \alpha \leq 0.9$ seems to give good result. However, it is necessary to know in advance, the actual value of α that gives the correct result for any given system. The modal deviation amplitude α is now chosen empirically, but future work should be able to define its value in advance, considering the degree of nonlinearity of the studied system.

A summary of the steps involved in the proposed method is depicted with Figure 4.3. The first two steps can be obtained with a commercial software and the other steps can also be implemented.

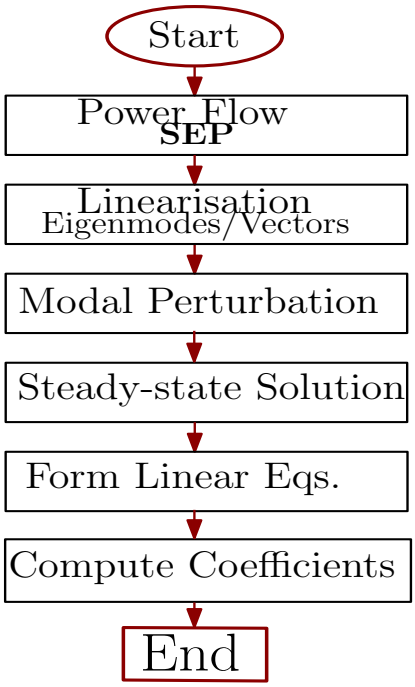

Figure 4.3 – Flow Chart of the Proposed Method

4.2.2 Benefits of the Proposed Method Summarised

The benefits of the proposed method are highlighted as follows:

- Both second and third order nonlinear coefficients are computed simultaneously.
- With good knowledge of the coefficients of interest, they can be selectively computed rapidly.
- It requires only the state matrix used for the linear analysis. No further differentiation needed.
- It is easy to implement and can easily adapt to model variations.
- It can be convenient to integrate in a commercial software, since there are many small signal analysis software that generate the state matrix.

Remark. *The developed method assumes that the nonlinearities are smooth and static. This implies that the nonlinearities are not on the differential parts of the equations.*

4.2.3 Illustrative Example

Firstly, the IEEE 3-machine 9-bus power system (Figure 2.1) is used to demonstrate the method. The full data of the system can be found in Appendix E. The numerical results are compared to that obtained by symbolic method. Symbolic method is also called Hessian approach in this thesis, since it involves the actual Taylor expansions and Hessian evaluations. Each of the three machines can be expressed as

$$M_i\ddot{\delta}_i + \bar{C}_i\dot{\delta}_i + P_{e_i} = P_{m_i} \tag{4.24a}$$

$$P_{e_i} = E_i^2\mathcal{G}_{ii} + \sum_{k=1,k\neq i}^{N} E_iE_k\left[\mathcal{G}_{ik}\cos\delta_{ik} + \mathcal{B}_{ik}\sin\delta_{ik}\right]. \tag{4.24b}$$

$M_i,\ \bar{C}_i\ , P_{e_i},\ P_{m_i},\ \delta_i$ have their meanings as defined in chapter 3. The damping constant $\bar{C}_i$ is set to zero for simplicity. The system of (4.24) is linearised and the Jacobian matrix $\mathbf{K}$ built as:

$$\forall\ (i,j=1\ldots N): \quad K_{ij} = \frac{\partial P_{e_i}}{\partial\delta_j}|_{\delta=\delta_\mathbf{0}}. \tag{4.25}$$

With last machine used as a reference, the size of $\mathbf{K}$ becomes $(N-1)\times(N-1)$, which corresponds to two[1] oscillators. The quadratic and cubic nonlinear coefficients for the two modes using the proposed method are presented in Table 4.1 and Table 4.2 . The results from the conventional Hessian approach (symbolic) are also presented for comparison. As can be seen from the tables, the two results perfectly agree. The superiority of the proposed method is seen immediately by comparing the computation costs. With an Intel CoreTM i7-4610M, 3Gz personal computer, the allocated memory and time consumed are estimated as shown in Figure 4.4. It is clear that the computational burden is significantly reduced, especially in time and memory consumption. As, shall be seen later, for more state variables, the proposed method shows almost incomparable results with the symbolic method in terms of computation cost.

[1] The fact that the left eigenvector is the transpose of the right eigenvector has a computational advantage since matrix inversion is avoided. However, the right eigenvector should be normalised such that $\Phi_{pi}^T M_{ij}\Phi_{jq} = 1$, given that the eigenvalues are computed as the solution of $(\mathbf{K}-\Omega_i^2\mathbf{M})\mathbf{\Phi}_i = \mathbf{0}$. In an interconnected power system, at least one of the eigenvalues of $\mathbf{K}$ is zero. Thus, there are at most $(N-1)$ modes in an N-machine system, where one machine is used as reference. The equation corresponding to the reference machine is subtracted from all other equations in order to get rid of the zero eigenvalue. This modifies $\mathbf{K}$ and $\mathbf{M}$ which makes the eigenvector normalisation more rigorous. The simplest normalisation is to define the left vector as the inverse of the right vector, but then, a price is paid for matrix inversion.

Table 4.1 – Proposed versus Symbolic—Quadratic coefficients for the 9-Bus Power System

r-th Mode	Symbolic			Proposed		
	G_{11}	G_{12}	G_{22}	G_{11}	G_{12}	G_{22}
1	-8.3772	-1.0724	0.1855	-8.3772	-1.0724	0.1855
2	-0.0098	-9.5637	5.1094	-0.0098	-9.5637	5.1094

Table 4.2 – Proposed versus Symbolic—Cubic coefficients for the 9-Bus Power System

r-th Mode	Symbolic				Proposed			
	H_{111}	H_{112}	H_{122}	H_{222}	H_{111}	H_{112}	H_{122}	H_{222}
1	-17.5849	0.2575	-5.9340	-0.1392	-17.5849	0.2571	-5.9336	-0.1392
2	0.8617	-42.7540	-3.2966	-16.0409	0.8617	-42.7542	-3.2964	-16.0408

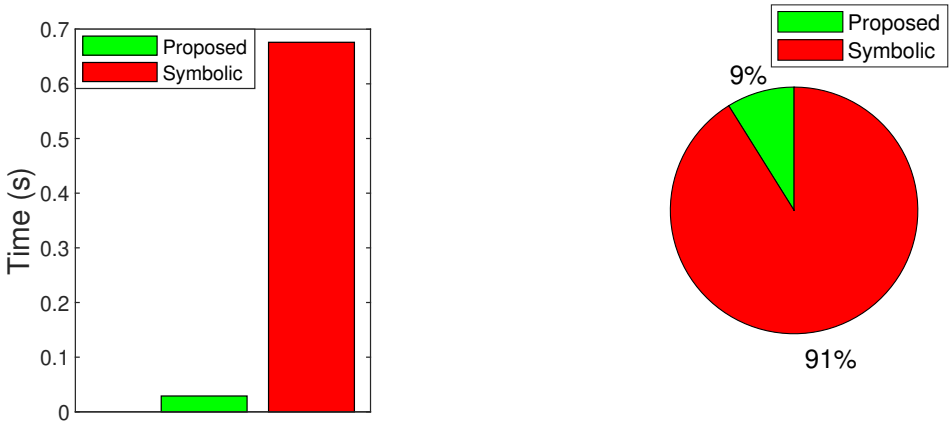

(a) Time-memory cost

(b) Memory cost (kB)

Figure 4.4 – Proposed vs Symbolic—Computation costs for the 9-Bus Power system

4.2.4 Implementation on Larger Power Systems

The power systems selected in this section are the 39-bus, 10-machine power system shown in Figure 4.5, and the 145-bus, 50-machine system shown in Figure 4.13. The 39-bus system is basically a two-area system where G1 represents an equivalent New York system and G2 to G10 New England system [118]. The system exhibits 9 natural modes of oscillation and mode 1 (slowest) is an inter-area mode, with major participation from generator 1. The inter-area mode is regarded as a New England versus New York oscillation, with all generators within New England area oscillating coherently, against the New York equivalent [118]. The 145-bus system on the other hand, has 49 electromechanical modes, most of which are local.

With second order modelling, and the last generator as a reference, the 10-machine system and 50-machine system have 9 and 49 state variables respectively. The number of nonlinear coefficients (G, H) needed for NF transformation, according to (3.54) are $1,890$ and $1,080,450$ for the 10- and 50-machine systems respectively. These are obviously too large numerical results to present on paper. Therefore, to validate the computed coefficients, we

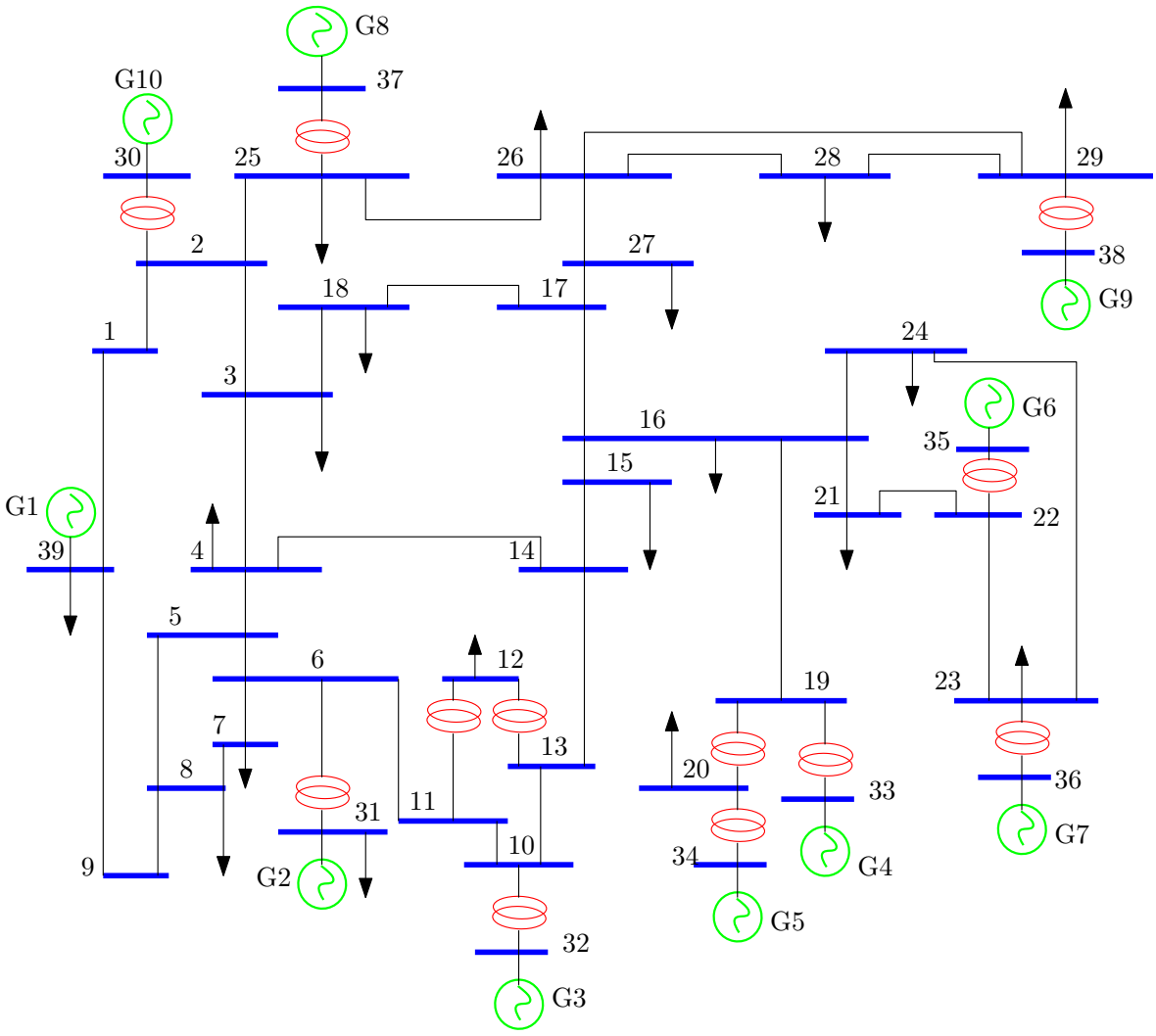

Figure 4.5 – One line diagram of 39-bus New England power system

simulated the modal model (4.8), with nonlinear coefficients computed by the symbolic tools and with nonlinear coefficients computed by the proposed method, under the same initial conditions. Using symbolic method as a standard, the result from the proposed method is being compared in Figure 4.6 for the 10-machine system. It is clear that the two curves are in good match. The error evolution indicates a maximum error of $2.2e^{-5}$ (i.e. $Hessian - Proposed$) at the end of 20s, which confirms the accuracy of the proposed method. Note that this is a cumulative error while using the method in the simulation. Further error analysis specifically related to the coefficients will be presented later in the chapter. In the second case, the limit of symbolic method is reached (i.e based on the personal computer and MATLAB® used). The computation could not be completed even after 12 hours. However, with the proposed method, all the $1,080,450$ coefficients were computed in approximately 131 seconds. The magnitude of these coefficients are plotted in Figure 4.8.

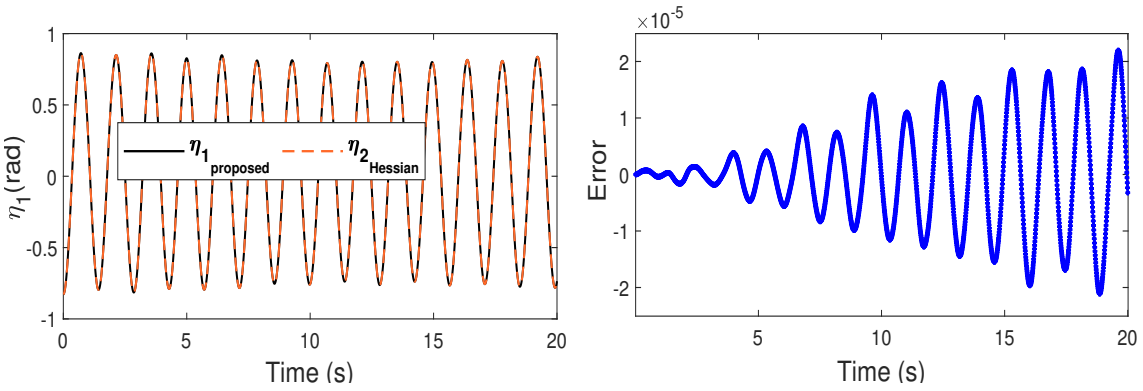

(a) Response for modal variable η_1 (b) Error evolution

Figure 4.6 – Proposed versus Symbolic (direct Hessian) method for 39-Bus Power system

Computational Analysis

As announced, the proposed and the symbolic methods become incomparable with the increased number of state variables. This is clearly seen in Figure 4.7, where the bar corresponding to the proposed method (Figure 4.7a) is almost invisible and the sector corresponding to the proposed method in Figure 4.7b is less than 1%.

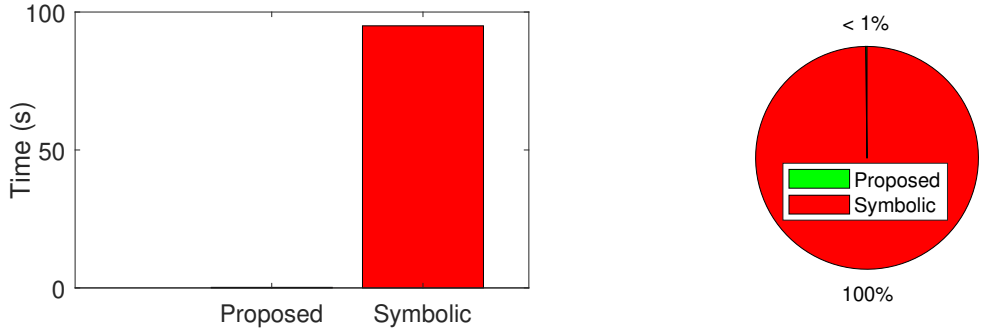

(a) Time-memory cost (b) Memory cost (kB)

Figure 4.7 – Proposed vs Symbolic—Computation costs for 39-Bus Power System

The computational analyses of the proposed method, in comparison with the symbolic method for the two power systems are summarised in Table 4.3. The table shows that the proposed method leads to remarkable gain, both in memory and in time, compared with the symbolic method, where Hessians are evaluated. For instance, the memory saving factor (MSF) and the time saving factor (TSF) for the case of the 10-machine system are respectively, $1.52e^3$ and 475. Saving factor is defined as the ratio of the computation cost by symbolic method to the computation cost by the proposed method. This implies that for the 10-machine system, the proposed method is 475 times faster and $1.52e^3$ times less costly (in terms of memory) than the symbolic method.

From Figure 4.8 and Tables 4.1, 4.2, the following observations can be made about nonlinearities for the test case:

Table 4.3 – Computational efficiency of the proposed method—2nd Order Model

System	Symbolic		Proposed			
	Time (s)	Mem. (kb)	Time (s)	Mem. (kb)	MSF*	TSF**
10-Machines	95	91e^3	0.20	60	1.52e^3	475
50-Machines	–	–	131	49e^3	–	–

*MSF =Memory saving factor; **TSF = Time saving factor.

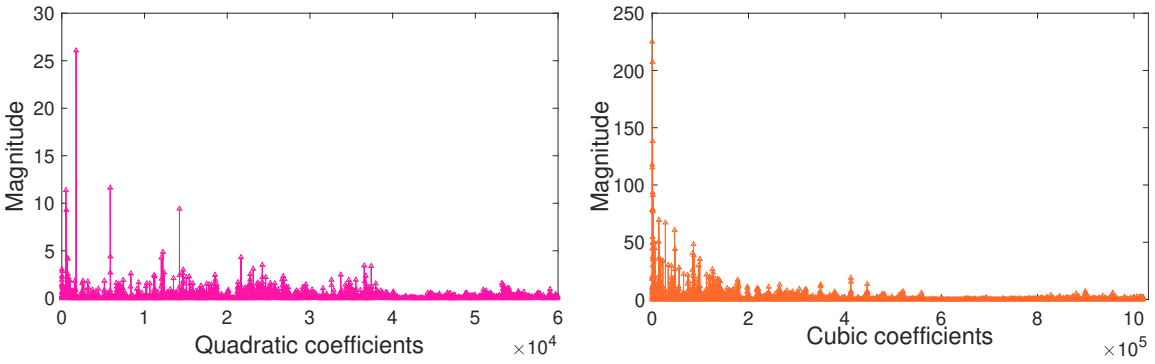

(a) Quadratic coefficients (G)

(b) Cubic coefficients (H)

Figure 4.8 – Distribution of G and H coefficients for the 145-Bus Power system

- The nonlinearities are not uniformly distributed among the modes. They are instead, localised on few modes in the system.

- Third order nonlinearities can be stronger than second order nonlinearities.

The implication of the first observation is that it may be possible to build a reduced order model, whereby, not all the nonlinear coefficients are computed. Currently, researchers in mechanical domain are already exploiting this benefit [62, 63, 113, 117]. This of course, can be extended to power system analysis. The implication of the second observation is that third order nonlinearities can play very significant role in the system dynamics. Therefore, if NF is performed with classical model (e.g. [60, 79]), at least third order nonlinearities should be considered. In fact, in vibrational mechanics, for some models, second order nonlinearities are sometimes negligible compared to third order nonlineairties. This point can be shown clearly by simulation.

Consider a three-phase solid fault at bus 4 of the 10-machine system shown in Figure 4.5. We know from previous works that a fault added to bus 4 of that system, will excite significantly the inter-area mode. The fault was cleared after 0.35 seconds. Three approximate modal models, namely— linear, second order and third order, obtained from (4.8) are simulated. The responses of the first modal variable due to these models are plotted in Figure 4.9. It can be seen that for the test case:

- The inclusion of second order nonlinearities for classical model do not show very signif-

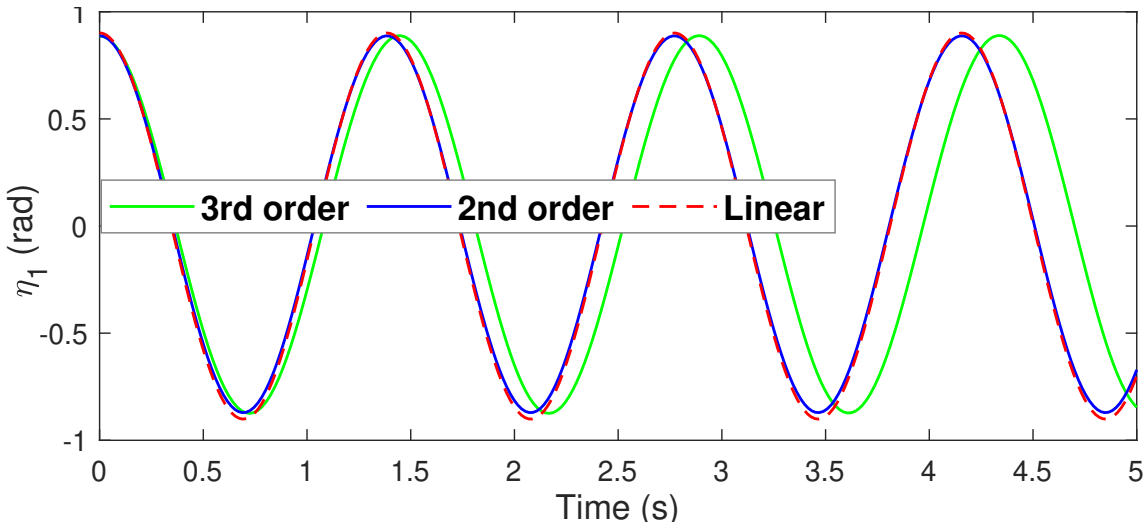

Figure 4.9 – Comparison of Linear, 2nd and 3rd order modal model for 39-bus system

icant difference from linear one.

- The three models had initially, nearly same frequency and amplitude, but the frequency of third order model keeps shifting as time evolves.

A characteristic behaviour of nonlinear system is this shifting of frequency with respect to amplitude during a disturbance. It is possible to study the amplitude-frequency shifts using third order nonlinearities. This is one of the major achievements of NF application using second order differential equations.

Recapitulation

As discussed above, the proposed method is very efficient, since no Taylor expansion is involved, and since the evaluation of the nonlinear coefficients reduces to (i) the evaluation of $\mathbf{f}(\mathbf{x})$ *for a given* $\mathbf{x}$ *and (ii) the solving of linear systems. Consequently, huge computations are avoided, leading to significant reduction in memory and time of computations. Another interesting feature of this method is that if one has good information regarding the coefficients of interest, they can be selectively computed without having to do the whole computation. In general, all that are needed are the state matrix, which is readily available in many commercial SSA software, and the exact nonlinear equations that model the system. With nonlinear coefficients computed, the NF coefficients are computed easily by direct substitution. The next challenging step is the evaluation of NF initial conditions, which is not directly dealt with in this work. Note that the first steps (linear analysis) of our method can be obtained with a commercial software and the implementation of other steps is achievable.*

4.3 Computation of Nonlinear Coefficients: 1st Order Model

In the previous section, the computations of the nonlinear coefficients for second order models were discussed and a faster method was proposed. As noted, the new method is an extension of a technique already existing in the mechanical engineering field. However, this method has been applied only to systems of second order differential equations with real eigenvalues/vectors. On the contrary, power systems are modelled usually, as first order systems with complex eigenvalues/vectors. First order models are more convenient for the incorporation of other elements of power systems like, exciters and PSS. Furthermore, when power system is represented with second order model, each machine is represented by a differential equation with a corresponding mechanical input power. This mechanical input power is a *forcing* term, compulsory for the proposed technique. On the contrary, with first order representation, only one out of many differential equations describing the machine, has a mechanical input power.

As a further extension of the technique proposed in the previous section, the formulation in this section considers the following:

- first order complex differential systems;
- differential equations without input, or with other input other than mechanical power (e.g. Voltage);
- detailed model generator; and
- other conditions for good results with first order model.

Consider a power system modelled with N-dimensional first order differential equations

$$\dot{\mathbf{x}} + \mathbf{f}(\mathbf{x}) = \mathbf{P_T}, \tag{4.26}$$

where $\mathbf{x}$ and $\mathbf{P_T}$ are vectors of state and external input respectively. Though, $\mathbf{P_T}$ does not apply to all the equations if the system is in first order differential equations (since some equations have zero input), the idea is to put element of $\mathbf{P_T} = 0$ where they do not apply. The representation in (4.26) is a specific form of the general representation in (3.18), and is chosen to emulate the previous proposal. $\mathbf{f}(\mathbf{x})$ is a nonlinear function and its expression and degree of nonlinearity depends on the particular model adopted. Let the Taylor expansion of (4.26) be expressed as

$$\dot{\mathbf{x}} + \mathbf{A}\mathbf{x} + \mathbf{\Gamma}(\mathbf{x}) = \mathbf{P}, \tag{4.27}$$

where $\mathbf{A}$ is the Jacobian, $\mathbf{\Gamma}(\mathbf{x})$ collects all second and third order terms and $\mathbf{P} = \Delta\mathbf{P_T}$. Recall from chapter 3, the following definitions: $\mathbf{U}_i$, and $\mathbf{V}_i$ are the i-th columns of right and left

eigenvectors respectively, $\mathbf{U} = [u_{ij}]$, $\mathbf{V} = [v_{ij}]$, the corresponding matrices and $\mathbf{\Lambda} = \mathbf{V}^T\mathbf{A}\mathbf{U} =$ diag (λ_p), the diagonal matrix of its eigenvalues, $p, i, j = 1, \ldots N$.

As shown in chapter 3, with the transformation

$$\mathbf{x} = \mathbf{U}\mathbf{y} \tag{4.28}$$

one obtains the r-th component of the nonlinear part (4.27) similar to that obtained for second order model (4.13) and is given by

$$f^r_{NL} = \sum_{j=1}^{N}\sum_{k=1}^{N} C^r_{jk} y_j y_k + \sum_{j=1}^{N}\sum_{k=1}^{N}\sum_{l=1}^{N} D^r_{jkl} y_j y_k y_l = \mathbf{V}_r^T \mathbf{P}, \tag{4.29}$$

where

$$\mathbf{f}_{\mathrm{NL}} = \mathbf{V}^{\mathbf{T}}\mathbf{\Gamma}(\mathbf{U}\mathbf{y}) \tag{4.30}$$

and C, D are nonlinear coefficients to be computed. Apart from the definition of the left eigenvector $\mathbf{V}$ (defined as $\mathbf{U}^{-1}$ to ensure proper normalisation), the procedures are the same as in the previous section, the major difference is in the treatment of $\mathbf{P_T}$ in the right hand side of (4.26), which is discussed next.

In order to make the proposed method work for first order power system models, the following changes relating to the treatment of $\mathbf{P_T}$ are proposed.

1. Define dummy parameters at the right hand side of all equations without input in (4.26).

2. Identify any constant terms (i.e. non-state variables that are not multipliers) in $\mathbf{f}(\mathbf{x})$ (i.e. in (4.26)) and move them to the right hand side.

3. Assign zeros as the initial values of the dummy parameters defined above.

4.3.1 Didactic Examples

Example 1—Classical SMIB model

We consider a 2-state-variable system verifying the following equations:

$$\dot{\omega} + \frac{1}{M}\left[\frac{EV}{X_s}\sin\delta + \mathcal{D}(\omega - 1)\right] = P_T \tag{4.31a}$$

$$\dot{\delta} - \omega_s(\omega - 1) = P_T^* \tag{4.31b}$$

M and $\mathcal{D}$ are respectively the inertia and damping[2] constants. X_s is the total reactance between the machine and infinite bus, P_T is the mechanical input power while P_T^* in (4.31) is a dummy parameter. For the SMIB system above, P_T^* is zero at SEP since $\omega_s(\omega - 1)$ is zero. After perturbation, P_T^* will not necessarily be zero since $\omega_s(\omega - 1)$ is no longer zero (i.e. considering the static part of (4.31)). Assume the system parameters to be: $M = 1, E = 1.123$ p.u., $V = 0.995$ p.u., $X_s = 0.95$ p.u., $\mathcal{D} = 2$, $SEP = [0.3 \text{ rad}, 1 \text{ p.u.}]$, $P_{T_0} = 0.35$ $p.u.$. The right and left eigenvectors are computed as:

$$\mathbf{U} = \begin{bmatrix} -0.0026 + 0.0544i & -0.0026 - 0.0544i \\ 0.9985 & 0.9985 \end{bmatrix}, \quad \mathbf{V} = \begin{bmatrix} 0.4383 - 9.1702i & 0.5008 \\ -0.4383 + 9.1702i & 0.5008 \end{bmatrix}$$

The necessary deviations are defined as (4.28):

$$\mathbf{x_1^{\pm}} = \pm 0.1 * \begin{pmatrix} -0.0026 + 0.0544i \\ 0.9985 \end{pmatrix} \quad \mathbf{x_2^{\pm}} = \pm 0.1 * \begin{pmatrix} -0.0026 - 0.0544i \\ 0.9985 \end{pmatrix}$$

The $r-$th quadratic and cubic coefficients of the SMIB system using the symbolic and proposed methods are presented in Table 4.4 and Table 4.5. As can be seen from the tables, the two results are in agreement.

Table 4.4 – Proposed Vs Symbolic—Quadratic coefficients for SMIB example

r-th Mode	Symbolic			Proposed		
	C_{11}	C_{12}	C_{22}	C_{11}	C_{12}	G_{22}
1	-1.59j	-3.18j	-1.59j	-1.59j	-3.18j	-1.59j
2	1.59j	3.18j	1.59j	1.59j	3.18j	1.59j

Table 4.5 – Proposed Vs Symbolic—Cubic coefficients for SMIB example

r-th Mode	Symbolic				Proposed			
	D_{111}	D_{112}	D_{122}	D_{222}	D_{111}	D_{112}	D_{122}	D_{222}
1	-1.71j	-5.14j	-5.14j	-1.71j	-1.71j	-5.14j	-5.14j	-1.71j
2	1.71j	5.14j	5.14j	1.71j	1.71j	5.14j	5.14j	1.71j

Example 2—Two-axis machine model

The second example is the 9-bus power system previously studied (Figure 2.1). Each of the three machines is represented with a two-axis model described in section 3.1.2 by (3.5) — (3.8). With the last generator as a reference, the number of differential equations will be 11, which translate to $3,872$ coefficients (i.e., C, D).

[2] For specific case of classical model, it is recommended to define a damping coefficient (≥ 0.1 recommended) to avoid unnecessary rearrangement of equations. If there is no damping, the magnitudes of the coefficients will be same, but the signs may rotate, due to the splitting of eigenvalues.

Firstly, rearrange (3.5)—(3.8) in the form (4.26) and create dummy parameters where necessary

$$\begin{bmatrix} \dot{\delta}_i - \omega_s(\omega_i - \omega_N) \\ \dot{E'}_{q_i} - \frac{1}{T'_{d0}}[-E'_{q_i} - (x_{d_i} - x'_{d_i})I_{d_i}] \\ \dot{E'}_{d_i} - \frac{1}{T'_{q0}}[-E'_{d_i} + (x_{q_i} - x'_{q_i})I_{q_i}] \\ \dot{\omega}_i - \frac{1}{M_i}[-(E'_{q_i}Iq_i + E'_{d_i}Id_i) - \mathcal{D}_i(\omega_i - 1)] \end{bmatrix} = \begin{bmatrix} P^*_{T_{\delta_i}} \\ P_{T_{E_{fd_i}}} \\ P^*_{T_{E'_{di}}} \\ P_{T_{\omega i}} \end{bmatrix} \equiv \begin{bmatrix} 0 \\ E_{fd_i} \\ 0 \\ \frac{P_{m_i}}{M_i} \end{bmatrix}, \tag{4.32}$$

where the asterisk (*) denotes dummy parameters while the subscripts in P_T indicates the corresponding equation.

Secondly, set all derivatives to zero to obtain the static model

$$\mathbf{f(x)} = \begin{bmatrix} -\omega_s(\omega_i - \omega_N) \\ -\frac{1}{T'_{d0}}[-E'_{q_i} - (x_{d_i} - x'_{d_i})I_{d_i}] \\ -\frac{1}{T'_{q0}}[-E'_{d_i} + (x_{q_i} - x'_{q_i})I_{q_i}] \\ -\frac{1}{M_i}[-(E'_{q_i}Iq_i + E'_{d_i}Id_i) - \mathcal{D}_i(\omega_i - 1)] \end{bmatrix} = \mathbf{P_T} \tag{4.33}$$

and the initial ***forcing vector***,

$$\mathbf{f(x_0)} = \mathbf{P_T} = \begin{bmatrix} 0 \\ E_{fd_{0i}} \\ 0 \\ \frac{P_{m_{0i}}}{M_i} \end{bmatrix} \tag{4.34}$$

where

$$I_{qi} = \sum_{j=i}^{N}[(\mathcal{B}_{ij}\cos\delta_{ij} - \mathcal{G}_{ij}\sin\delta_{ij})E'_{qj} + (\mathcal{B}_{ij}\sin\delta_{ij} + \mathcal{G}_{ij}\cos\delta_{ij})E'_{dj}] \tag{4.35a}$$

$$I_{di} = \sum_{j=i}^{N}[(\mathcal{B}_{ij}\sin\delta_{ij} + \mathcal{G}_{ij}\cos\delta_{ij})E'_{qj} - (\mathcal{B}_{ij}\cos\delta_{ij} - \mathcal{G}_{ij}\sin\delta_{ij})E'_{dj}] \tag{4.35b}$$

Prescribe deviations $\mathbf{x}$ ***to compute the nonlinear coefficients:***

(a.) For $\mathbf{x}$, the nonlinear algebraic equations (4.35) are solved to obtain I_{q_i}, I_{d_i};

(b.) Then I_{q_i}, I_{d_i} replaced in (4.33) to get new $\mathbf{P_T}$;

(c.) Then $\mathbf{P_{NL}}$ is obtained from (4.12) as $\mathbf{P}_{\mathrm{NL}} = \mathbf{P_T} - \mathbf{f(x_0)}$.

The quadratic and cubic coefficients of the r^{th} equation are presented in Table 4.7 and Table 4.9. The results from the conventional direct Hessian approach (symbolic in this case)

are also presented (Table 4.6 and Table 4.8) for comparison. Note that not all coefficients are shown in the tables, since the data are too large and inconvenient to show on paper.

Table 4.6 – Quadratic Coefficients —Hessian Method (symbolic) for 2-axis Model

r^{th}	C_{11}	C_{23}	C_{45}
1	0.3249 + 0.2378i	0.5124 + 0.3663i	0.6631 - 3.0947i
3	-0.0105 - 0.0028i	0.0406 + 0.1353i	0.2577 - 0.8525i
4	-0.1323 - 0.0191i	0.0641 + 0.1335i	0.3234 - 0.8295i
6	0.6383 - 0.0433i	-0.0824 + 0.0197i	0.1117 + 0.0280i
7	-0.1193 + 0.0151i	0.0264 - 0.0059i	-0.0597 + 0.0051i
10	0.1617 + 0.0732i	-0.0088 - 0.0036i	-0.1960 - 0.0368i
11	0.0140 +0.0099i	-0.0469 +0.0075i	-0.2191 - 0.0653i

Table 4.7 – Quadratic Coefficients — Proposed Method for 2-axis Model

r^{th}	C_{11}	C_{23}	C_{45}
1	0.3249 + 0.2376i	0.5124 + 0.3661i	0.6631 - 3.0948i
3	-0.0104 + 0.0027i	0.0410 + 0.1508i	0.2581 - 0.8370i
4	-0.1323 - 0.0189i	0.0641 + 0.1337i	0.3234 - 0.8293i
6	0.6309 - 0.0433i	-0.0897 + 0.0197i	0.1043 + 0.0280i
7	-0.1191 - 0.0151i	0.0264 - 0.0059i	-0.0597 + 0.0051i
10	0.1649 + 0.0732i	-0.0086 - 0.0036i	-0.1928 - 0.0368i
11	0.0150 + 0.0100i	-0.0468 + 0.0075i	-0.2191 - 0.0653i

Table 4.8 – Cubic Coeff. Hessian Method (symbolic) for 2-axis Model

r^{th}	D_{222}	$D_{4,8,8}$	$D_{9,10,11}$
1	-0.3191 - 0.3763i	-0.0015 - 0.0188i	-0.2008 - 1.0589i
3	-0.0043 - 0.0121i	-0.0027 + 0.0208i	0.0210 + 0.2150i
4	0.0034 + 0.0091i	0.0077 - 0.0214i	0.0210 - 0.2150i
6	-0.0278 - 0.0519i	-0.0489 - 0.0052i	-0.2819 - 0.0000i
7	-0.0046 - 0.0104i	0.0104 + 0.0015i	0.0633 + 0.0000i
10	0.0036 + 0.0113i	-0.0266 - 0.0024i	-0.2473 - 0.0000i
11	-0.0022 - 0.0067i	0.0013 - 0.0000i	0.0071 + 0.0000i

Table 4.9 – Cubic Coeff. Proposed Method for 2-axis Model

r^{th}	D_{222}	$D_{4,8,8}$	$D_{9,10,11}$
1	-0.3191 - 0.3763i	-0.0015 - 0.0188i	-0.2010 - 1.0584i
3	-0.0043 - 0.0121i	-0.0028 + 0.0208i	0.0209 + 0.2150i
4	0.0034 + 0.0091i	0.0077 - 0.0213i	0.0209 - 0.2150i
6	-0.0278 - 0.0519i	-0.0490 - 0.0052i	-0.2819 - 0.0000i
7	-0.0046 - 0.0104i	0.0104 + 0.0015i	0.0632 + 0.0000i
10	0.0036 + 0.0113i	-0.0266 - 0.0024i	-0.2472 - 0.0000i
11	-0.0022 - 0.0067i	0.0013 - 0.0000i	0.0071 + 0.0000i

As could be seen from the tables, the two results highly agree.

4.3.2 Application to Larger Power Systems

In this section, we will progressively investigate the application of the proposed method to the IEEE 3-Machine system with excitation controls, the IEEE 16-Machine, and the IEEE 50-Machine systems. In all cases, the number of coefficients becomes too large to show due to lack of paper space. We will focus on the computation time and memory consumption. However, the accuracy will be investigated by checking the maximum error compared to the direct Hessian approach (where possible), which is used here as standard. The modal deviation amplitude (α) of 0.1 was used in all cases. The state matrix employed by the proposed method was obtained from a commercial software. It is important to note that the complexity arises from the number of state variables (linear basis size) in the system, and not from the size of network. Clearly, it is possible for a small network to have a very large computational burden due to the number of state variables. One power electronic (PE) converter, for instance, can have up to 13 state variables [105], which is computationally larger than 6-machine system with classical model.

Test on IEEE 3-Machine System with Detailed Model and Excitation Control

The proposed method is now investigated for two-axis model with control. The excitation model described in (3.13)—(3.17) was added to the previous 9-bus system (i.e. Figure 2.1). With machine 3 used as reference, the linear basis size is 20, which from (3.54) amounts to 35,000 nonlinear coefficients . The procedures discussed in section 4.3 were followed to compute all the coefficients.

A further comparison by numerical simulation is provided by Figure 4.10a,b. A 3-phase fault was applied to bus 4 and cleared in 0.184 s. This clearing time is almost the critical clearing time[3], and was chosen to ensure a very severe condition where there should be significant difference in the methods. Then, a 3rd order NF model was built using the conventional Hessian and the proposed methods. As expected, the NF solutions show some remarkable deviations from the exact solution due to the severity of the stress. However, the results from the proposed method and the conventional Hessian approach are matched to very high extent, which confirms that the proposed method reduces the computational burden without the accuracy compromised. The maximum errors in percentage were computed as $\xi_2 = \max|\frac{C2^j_{kl_{\mathbf{h}}} - C2^j_{kl_{\mathbf{p}}}}{C2^j_{kl_{\mathbf{h}}}}| \times 100$ and $\xi_3 = \max|\frac{D3^j_{pqr_{\mathbf{h}}} - D3^j_{pqr_{\mathbf{p}}}}{D3^j_{pqr_{\mathbf{h}}}}| \times 100$ for quadratic and cubic coefficients respectively. The errors were estimated to be $2e^{-5}\%$ and $1.8e^{-3}\%$ for quadratic and cubic coefficients respectively. The error distribution, taking into account all quadratic and cubic coefficients is shown with the red line (Case-A) in Figure 4.11b.

[3]The critical clearing time is 0.185 s which was obtained by several simulation runs.

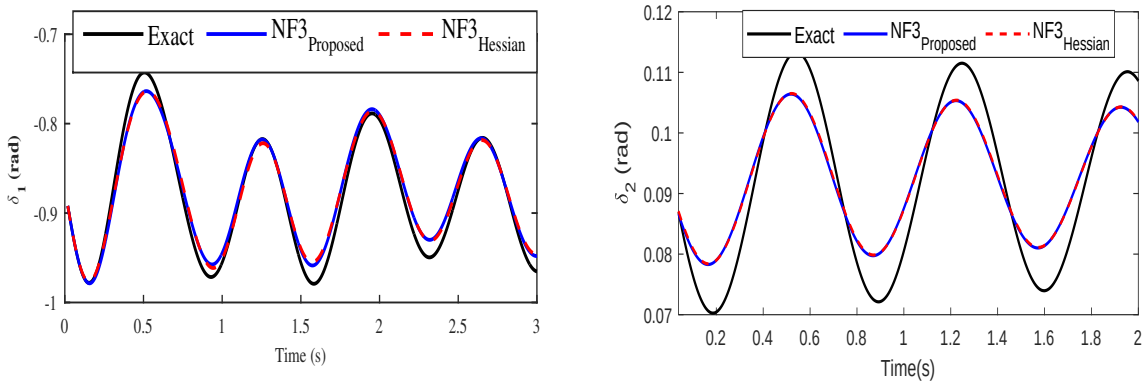

(a) Machine-1 Relative Angle (b) Machine-2 Relative Angle

Figure 4.10 – Accuracy of the proposed method on detailed model with control

To validate the method, further investigation was performed on relatively larger systems in the next subsections.

Test on IEEE 16-Machine System

The New England/New York System [119] is a widely used 5-Area system consisting of 16 generators, 68 buses and 83 lines. The classical model was used with machine 16 as a reference, making the total number of differential equations 31 and total of $186,434$ C and D coefficients.

Again, time-domain solution Figure 4.11a for a 0.02s short-circuit at bus 53, coming from models built by both the proposed and the conventional Hessian methods show the accuracy of both methods to be same. Note that this system is unstable when no PSS or only one PSS

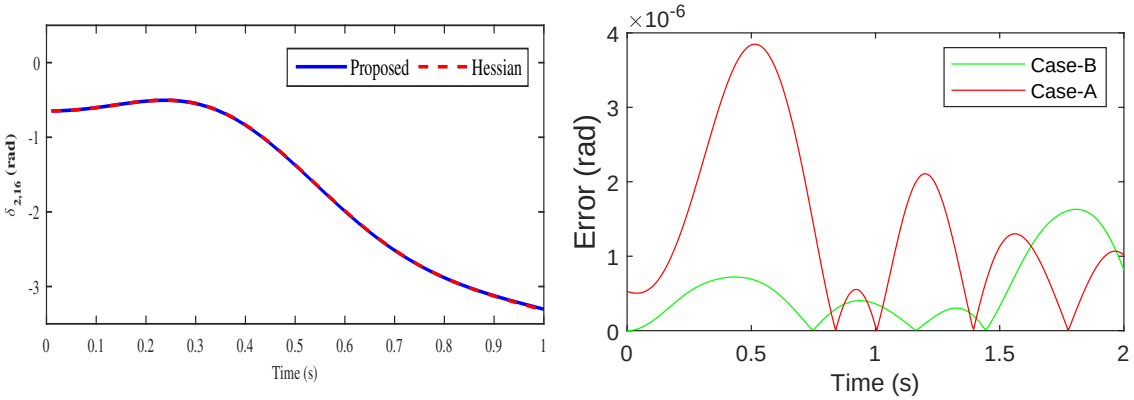

(a) Machine-2 Relative Angle (b) Error distribution

Figure 4.11 – Accuracy of the proposed method on 20- and 31-state system

is installed [119]. As we did not consider PSS, the system is unstable; the interest in Figure 4.11a is only to show the accuracy of the proposed method compared with the standard Hessian approach even for unstable system.

The maximum errors were estimated to be $1.7e^{-7}\%$ and $7.3e^{-5}\%$, for quadratic and cubic

coefficients respectively. The error here is very infinitesimal compared to the errors in the previous subsection (see case-B in Figure 4.11b). The reason, is likely due to degree of nonlinearity. When there is control in the system such as AVR and PSS, the nonlinearity increases compared to that of classical model. In general, the error incurred by the proposed method is small and is a good compromise for the time and memory saved.

Test on IEEE 50-Machine System

In the previous subsections, we have verified the accuracy of the proposed method by comparing with symbolic computation. Here, we focus on the number of coefficients and the time for their computation. We applied our method to the IEEE 50-Machine system shown in Figure 4.13 and modelled as classical, with machine 50 taken as reference. There are 16,988,400 C and D coefficients which were computed in approximately 4 hours. Table 4.10 shows some selected coefficients. All the coefficients were computed. The presented coefficients were only selected randomly. Figure 4.12a–d show the absolute value distributions of C and D coefficients for some modes. Figure 4.12a–b represent a complete plot of all the C and D coefficients of the first row in Table 4.10 (mode 1), while Figure 4.12c–d represent a complete plot of all the C and D coefficients in row 70 (mode 70), not shown in Table 4.10. It is evident from the figures that both numerically significant and insignificant values are computed.

Table 4.10 – Quadratic & Cubic Coeff.Proposed Method

r^{th}	$C_{1,1}$	$C_{10,50}$	$D_{1,60,80}$	$D_{90,90,90}$
1	9.6e-3j	- 1.6e-3j	-2e-4 + 6.1e-3j	9e-6 - 3e-4j
45	1e-4 - 11.9e-3j	2e-4 - 7e-4j	-1e-5 - 1e-4j	3e-5 + 1e-4j
99	-1e-3 + 3e-3j	2e-5 - 2e-4j	2e-4 - 2.5e-3j	11.9e-3j

In addition to huge computational success already brought by the proposed method, another major advantage is that it allows with convenience, the application of NF to power system, focusing only on some selected terms. We note that to reduce NF computational burden, earlier researches had suggested that higher order spectra (HOS) or prony analyses be used to detect the interacting modes, and then, only terms relating to these modes can be selectively computed [31, 84]. With the proposed method, any terms of interest can be easily computed. Table 4.10 and Figure 4.12 lend more credence to the fact that some terms can be negligible in NF application. With the proposed method, one can reduce the computational burden drastically by neglecting some terms due to the particular modes excited. Certainly, there are some coefficients in NF application that can be neglected, even if we are not precise now and in pursuance of such selective NF applications, the proposed method is apt.

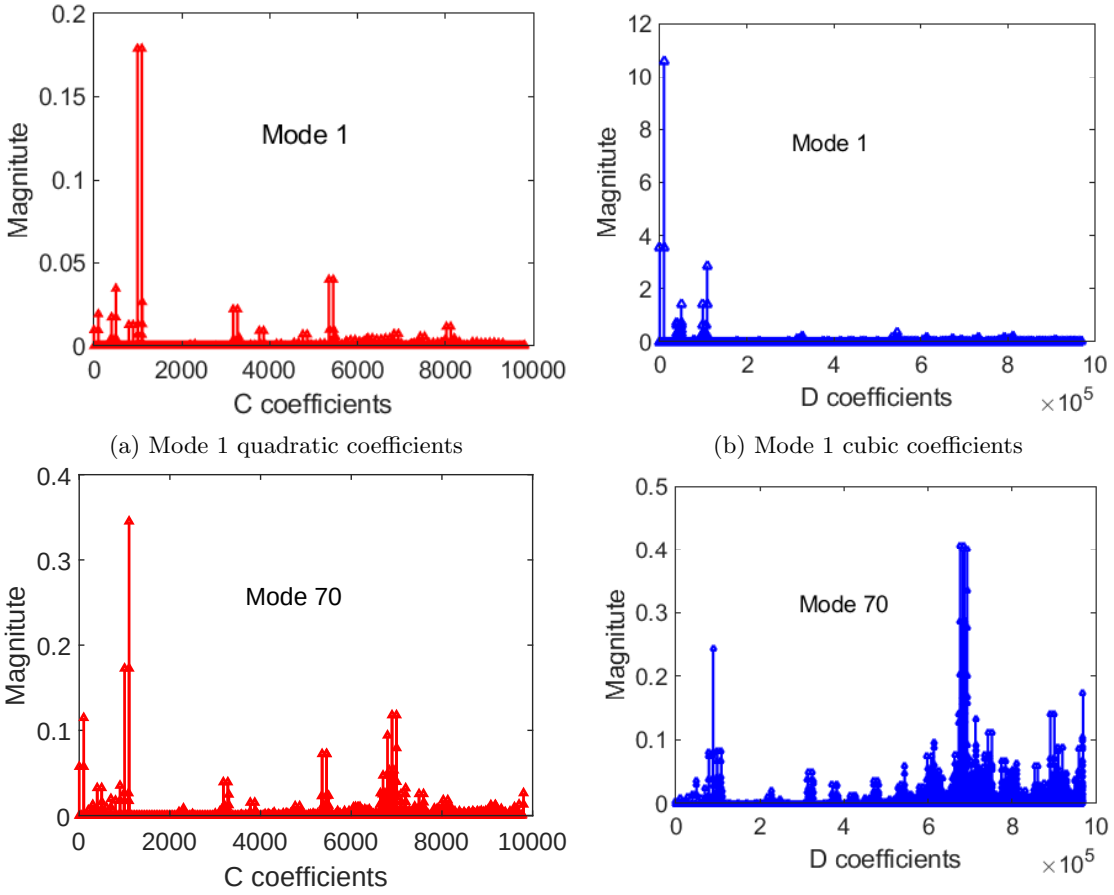

(a) Mode 1 quadratic coefficients

(b) Mode 1 cubic coefficients

(c) Mode 70 quadratic coefficients

(d) Mode 70 cubic coefficients

Figure 4.12 – Distribution of C and D coefficients for 147-Bus Power System

4.3.3 Computational Efficiency

A summary of the computational analysis of some tested cases is shown in Table 4.11. N/A in Table 4.11 means *not applied*. For the 3-machine system, the time and memory costs were investigated on an Intel CoreTM i7-3520M 2.9GHz laptop computer, and compared with computation, using the Symbolic Math Toolbox in MATLAB®. The proposed method achieved time and memory saving factors of 43 and 49 respectively (please see columns 8-9 of Table 4.11). Saving factor is computed as the ratio of the symbolic time/memory consumption to that of the proposed method. Similar comparison for the 16-machine system yielded time and memory saving factors of 472 and 776 respectively (see columns 8-9 of Table 4.11). In comparison with the symbolic method, this method is indeed a huge success and good news for power system researchers interested in Normal Form based analysis. For further assessment of the computational efficiency, we investigated the time and memory consumption on various system sizes. Figure 4.14a and Figure 4.14b show the evolution of computation time and memory consumption for varying size of the system respectively. We observed that for very small size (≤ 5), both methods give fairly comparable results in memory consumption but

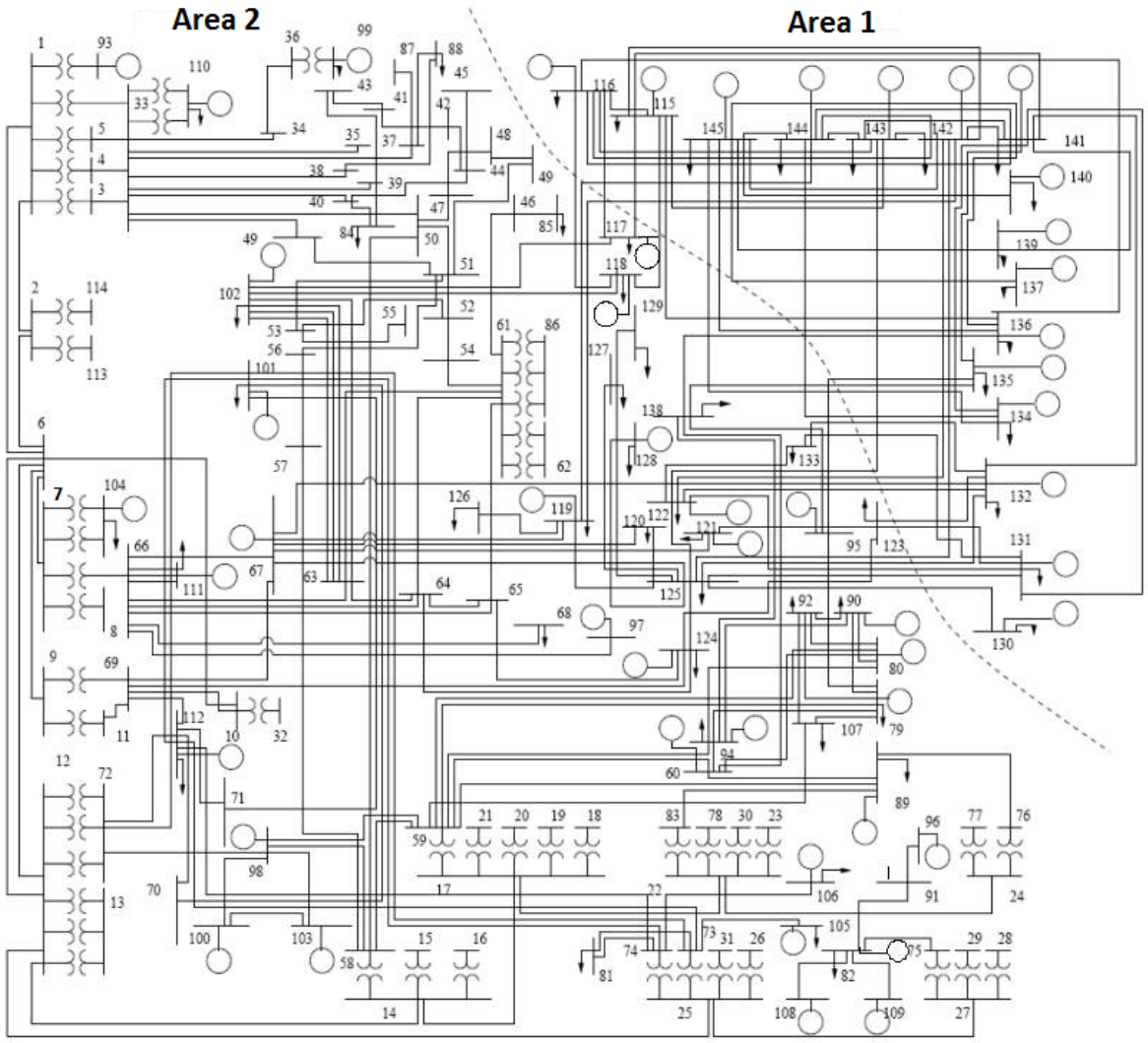

Figure 4.13 – One-line Diagram of the IEEE 50-Machine 145-Bus Power system [120].

the times required are remarkably different. Beyond 5 state variables, symbolic method's consumption rate increases tremendously.

Table 4.11 – Computation efficiency for the Tested Cases

System	No. of Coeff.	Symbolic		Proposed				
		Time(s)	Mem. (Mb)	Time (s)	Mem. (Mb)	Error (%)	MSF*	TSF**
3-Machines	35,000	1245	475	29	10	1.8e-3	49	43
16-Machines	186,434	23,130	11.4e6	49	14.7e3	7.3e-5	776	472
50-Machines	16,988,400	N/A	N/A	15,355	1,535	–	–	–

*MSF =Memory saving factor; **TSF = Time saving factor.

Figure 4.12 is a further computational analysis of the proposed method based on the number of state variables.

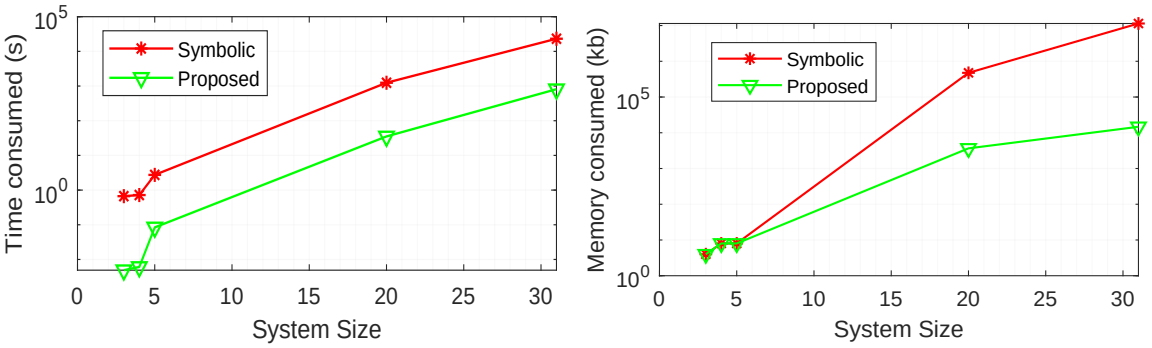

(a) Computational Time (b) Computational Memory

Figure 4.14 – Time-Memory comparison of symbolic and proposed for varying system size

Table 4.12 – Computation efficiency based on number of state variables

No. of Var.	No. of Coeff.	Symbolic	Proposed	
		Time(s)	Time(s)	TSF*
2	14	0.68	0.03	23
9	1,890	89	0.20	458
20	35,000	1,245	29	43
31	186,434	23,130	49	472
49	1,080,450	N/A	131	–
99	16,988,400	N/A	15,355	–

$$^{*}\text{TSF} = \frac{\text{Time for Symbolic}}{\text{Time for Proposed}}$$

4.4 Comments on the Computational Accuracy/Efficiency

The various tests in this chapter show that the accuracy of the proposed method is high. It is noted that the accuracy is higher for the classical models than for the detailed models, although the error in each case is infinitesimal. Where the power system is modelled classically, the computational burden is further reduced drastically if second order model is adopted. For instance, the last two rows in Table 4.12 are for the same system. While the first order model requires $15,355$s, the second order model requires only 131s; both implemented with the proposed method.

It is important to note at this point that the achieved efficiency in this work is limited by the author's programming competence. The algorithm is linear and computer-friendly; hence, it is possible to achieve very high efficiency if the code is well optimised. Although we could not compare with the method that involves building the Hessian matrix by predefined derivatives, the proposed method is envisaged to compare favourably with it if optimised. In the memory estimation for symbolic method, we did not consider the sparsity of the DAEs which will of course bring some reduction in memory usage while building the Hessians. However, the modal model (4.29), which has enough computational burden is not sparse, even with sparse DAEs. This still puts the proposed method very far from symbolic method.

Automatic differentiation (AD) could also be a strong competitor with the proposed method. Although we could not implement AD, a cursory look on both algorithms seems to suggest that our method will likely save more memory under similar program optimisation. Firstly, AD computes the nonlinear solutions and its source code simultaneously computes the derivatives, while the proposed method performs only the same nonlinear solution without any derivative at this first level. The additional memory for the 2nd and 3rd order derivatives may be significant. At the second level, with the derivatives computed by AD, operation (4.29) has to be done, and separately for 2nd and 3rd order terms. The proposed method obtains directly, the 2nd and 3rd coefficients in (4.29) in a linear way, without any derivative.

To recall the main the benefits of the proposed method over the conventional one, Figure 4.15 summarises the two pathways to evaluating the nonlinear coefficients.

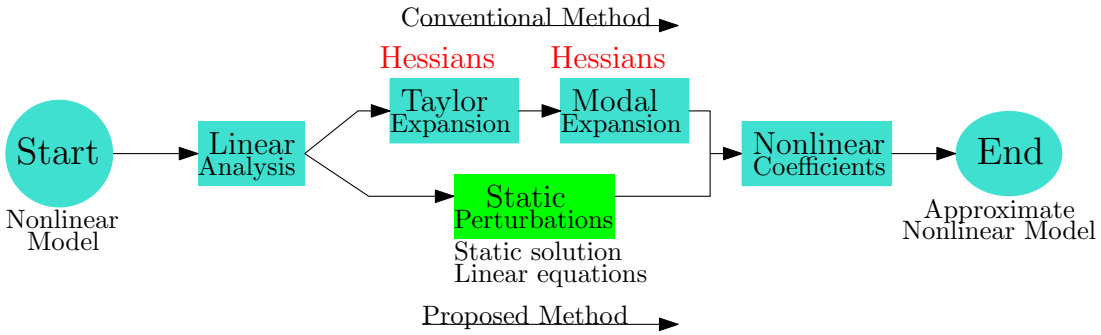

Figure 4.15 – Two pathways for computing nonlinear coefficients

4.5 Summary

In this chapter, a method is proposed for accelerating NF computation in power systems. The proposed method is an extension of a technique previously employed in structural analysis. In contrast to the conventional method, it avoids Taylor expansion which reduces time and memory in Normal Form computations. The proposed method has been developed to account for real and complex differential systems. In other words, both first and second order models of power systems were accounted for. In comparison with symbolic method, the proposed method proves to save significantly, the computation time and memory.

The method is attractive, in that both second and third order coefficients needed for the NF model are simultaneously evaluated in a linear way and any preferred coefficient can be computed selectively. Many nonlinear modal analyses, such as nonlinear interactions, stability assessments, and nonlinear participation factors usually focus on low frequency modes instead of all modes. This makes the proposed method very useful for quick nonlinear assessments. Also, since the method builds only on the same parameters used for linear analysis, it can

easily be integrated in commercial modal analysis software. Moreover, the modal deviations described by our method correspond to initialising a nonlinear system with chosen condition and investigating its solution in steady state. Therefore, using same software for linear analysis to achieve NF should be achievable.

This chapter has principally focused on the computational reduction of the NF method in power system. In the next chapter, the application of NF method in power systems will be addressed. The method developed in this chapter will be employed.

Chapter 5

Applications of Normal Form in Power Systems

"*The beauty of simplicity is the complexity it attracts.*"

Tom Robbins

Contents

Introduction

Let us recall some of the key points raised in the previous chapters. In chapter 1, it was established that the changes going on in the grid, notably the increasing bulk power transfer on the network and the integration of renewable energies, increase the nonlinearities of the grid. It was demonstrated that increase in nonlinearities leads to nonlinear modal interactions, a phenomenon beyond linear analysis and hence, the need for nonlinear modal analysis tool such as Normal Form (NF). In chapter 2, we saw the various potentials and applications of NF method in power system, as well as its computational challenges. In chapter 3, we have discussed the basic theories of NF method for first and second order system models along with more details on its computational challenges. It was identified that the higher order differentiation and the evaluations of Hessian matrices, which are compulsory with the conventional method pose serious computational difficulty. In chapter 4, a new method was developed for mitigating this computational challenge. The developed method avoids the higher order differentiation and evaluations of Hessian matrices; thereby increasing the speed of analysis and consequently, the size of the system that can be considered. In this chapter, the applications of NF in power systems will be discussed, especially with the use of the new method developed in chapter 4. The chapter is made up of basically two parts—(1) NF application based on already existing tools but now with reduced computations and (2) NF application based on new tools that are developed in this chapter. Various applications of NF in power systems were highlighted in chapter 2 but in this chapter, we focus on:

a. *Nonlinear participation factor analysis;*

b. *Detection and effects of nonlinear modal interactions;*

c. *Amplitude-dependent frequency shifts of the nonlinear dynamics; and*

d. *Transient/Mode's instability monitoring.*

The first two (i.e., a and b) are based on tools already existing while the last two are based on the tools developed in this chapter.

5.1 Nonlinear Modal Interactions and Participation Factors Analysis via Normal Form

As noted before, when controlled generators are considered, the power systems are usually represented with first order models. In designing and siting of these controls such as PSS, usually linear techniques such as state observability and controlloability are used. These

techniques lead to the definition of some indices such as participation factors and residues, which enables one to design and optimally site the controls in the power system. As we saw in chapter 1, increasing stress in the system leads to nonlinear interactions of the fundamental modes. These interactions can affect these controls, hence the quest for nonlinear equivalence of those indices (e.g. participation factors). In this section, the extension of linear participation factors to the nonlinear one is presented. Also, some already-existing indices for estimating the effects of modal interactions are presented.

5.1.1 Nonlinear Participation Factors

The inverse transform of the third order approximation can be defined from the NF transform (3.42) as

$$z_{j_0} = y_{j_0} - \sum_{k=1}^{N}\sum_{l=1}^{N} h2^{j}_{kl} y_{k_0} y_{l_0} - \sum_{p=1}^{N}\sum_{q=1}^{N}\sum_{r=1}^{N} h3^{j}_{pqr} y_{p_0} y_{q_0} y_{r_0}, \tag{5.1}$$

where y is the Jordan form variable (i.e., from $\mathbf{x} = \mathbf{U}\mathbf{y}$ or $\mathbf{y} = \mathbf{V}\mathbf{x}$, where $\mathbf{U}$ and $\mathbf{V} = \mathbf{U}^{-1}$ are right and left eigenvectors respectively), $h2$, $h3$ are NF coefficients and z, the NF state variable. The above parameters were fully defined in chapter 3. Recall also that the solution after inverse transformation was defined in (3.44) as

$$\boxed{x_i(t) = \sum_{j=1}^{N} \mu_{1_{ij}} e^{\lambda_j t} + \sum_{k=1}^{N}\sum_{l=1}^{N} \mu^{i}_{2_{kl}} e^{(\lambda_k+\lambda_l)t} + \sum_{p=1}^{N}\sum_{q=1}^{N}\sum_{r=1}^{N} \mu^{i}_{3_{pqr}} e^{(\lambda_p+\lambda_q+\lambda_r)t}}, \tag{5.2}$$

where

$$\mu_{1_{ij}} = u_{ij} z_{j_0}, \quad \mu^{i}_{2_{kl}} = z_{k_0} z_{l_0} \sum_{j=1}^{N} u_{ij} h2^{j}_{kl}, \quad \mu^{i}_{3_{pqr}} = z_{p_0} z_{q_0} z_{r_0} \sum_{j=1}^{N} u_{ij} h3^{j}_{pqr}.$$

The participation factors represent the size of the modal oscillations in a state when only that state is perturbed. Hence, the initial condition vector $x_0 = e_i$ (where all elements of e_i are zero except the i-th, which is one). By applying the initial condition $x_0 = e_i$ vector, the Jordan form initial conditions are [31]

$$y_{j_0} = v_{ji}. \tag{5.3}$$

Putting (5.3) into (5.1), the NF initial conditions become

$$z_{j_0} = v_{ji} - \sum_{k=1}^{N}\sum_{l=1}^{N} h2^{j}_{kl} v_{ki} v_{li} - \sum_{p=1}^{N}\sum_{q=1}^{N}\sum_{r=1}^{N} h3^{j}_{pqr} v_{pi} v_{qi} v_{ri} = v_{ji} + v2_{jii} + v3_{jiii}. \tag{5.4}$$

Substituting (5.4) in the inverse solution (5.2) gives

$$x_i(t) = \sum_{j=1}^{N} P_{3_{ij}} e^{\lambda_j t} + \sum_{k=1}^{N}\sum_{l=1}^{N} P^i_{3_{kl}} e^{(\lambda_k+\lambda_l)t} + \sum_{p=1}^{N}\sum_{q=1}^{N}\sum_{r=1}^{N} P^i_{3_{pqr}} e^{(\lambda_p+\lambda_q+\lambda_r)t}, \tag{5.5}$$

where P_3 stands for participation factors due to third order approximation and

$$P_{3_{ij}} = u_{ij}(v_{ji} + v2_{jii} + v3_{jiii}) \tag{5.6a}$$

$$P^i_{3_{kl}} = u2_{ikl}(v_{ki} + v2_{kii} + v3_{kiii})(v_{li} + v2_{lii} + v3_{liii}) \tag{5.6b}$$

$$P^i_{3_{pqr}} = u3_{ipqr}(v_{pi} + v2_{pii} + v3_{piii})(v_{qi} + v2_{qii} + v3_{qiii})(v_{ri} + v2_{rii} + v3_{riii}). \tag{5.6c}$$

where $u2_{ikl} = \sum_{j=1}^{N} u_{ij} h2^j_{kl}$ and $u3_{ipqr} = \sum_{j=1}^{N} u_{ij} h3^j_{pqr}$.
Therefore, 3rd order NF analysis leads to three types of participation factors: 1-eigenvalue participation factor (5.6a), which is a correction of the linear one and measures the participation of a single eigenvalue to a state; 2-eigenvalue participation factor (5.6b), which measures the participation of two eigenvalues combination to a state; and 3-eigenvalue participation factor (5.6c), which measure the participation of three eigenvalues combination to a state.

We are aware that mode-in-state participation factors are not always the same as the state-in-mode participation factors. The participation factors defined above correspond to the participation of modes in states. For details of the differences between mode-in-state and state-in-mode participation factors, the reader is kindly referred to [121].

5.1.2 Indices for Modal Interaction

In order to detect and quantify modal interactions in the system, some indices exist in literature. These indices are used in the remaining part of this chapter and are defined below.

Nonlinearity Indices [42, 71, 122]

The nonlinearity indices $N2LI(j)$, $N3LI(j)$, defined in (5.7) and (5.8), estimate the effect of the 2nd and 3rd order nonlinear terms respectively, in the approximate closed form solution. Large values indicate that the higher order terms are significant or that the difference between modal and NF variables is large, both cases indicating potential for nonlinear interaction.

$$N2LI(j) = \frac{|(y_{j_0} - z_{j_0}) + \max(h2^j_{kl} z_{k_0} z_{l_0})|}{|z_{j_0}|} \tag{5.7}$$

$$N3LI(j) = \frac{|(y_{j_0} - z_{j_0}) + \max(h2^j_{kl} z_{k_0} z_{l_0}) + \max(h3^j_{pqr} z_{p_0} z_{q_0} z_{r_0})|}{|z_{j_0}|} \tag{5.8}$$

The index "0" in the above equations indicates initial conditions.

Nonlinear Interaction Indices [71, 122]

These indices defined in (5.9) and (5.10), show whether the higher order nonlinear effects may cause strong modal interaction. Large values indicate more potential for strong nonlinear interactions.

$$N2II(j) = \frac{\max|h2^{j}_{kl} z_{k_0} z_{l_0}|}{|z_{j_0}|} \tag{5.9}$$

$$N3II(j) = \frac{\max|h3^{j}_{pqr} z_{p_0} z_{q_0} z_{r_0}|}{|z_{j_0}|} \tag{5.10}$$

As noted in [31], the indices in (5.7)—(5.10) can only be used to compare the modes for individual cases. They cannot be used as a measure to compare modes between two different cases, since they use normalised eigenvectors, which can differ between cases.

Nonlinear Modal Persistence Indices [31]

These indices estimate the extent of dominance of the mode combinations in the system response. They are defined as

$$T_{2_{set}}(j) = \frac{-4}{\text{Re.}(\lambda_k + \lambda_l)}, \qquad T_{3_{set}}(j) = \frac{-4}{\text{Re.}(\lambda_p + \lambda_q + \lambda_r)}, \tag{5.11}$$

$$Tr_2(j) = \frac{\tau(\lambda_k + \lambda_l)}{\tau(\lambda_j)}, \qquad Tr_3(j) = \frac{\tau(\lambda_p + \lambda_q + \lambda_r)}{\tau(\lambda_j)}, \tag{5.12}$$

$$\tau(\lambda) = \frac{-1}{\text{Re.}(\lambda)}, \tag{5.13}$$

where Re.$(\cdot)$ stands for *real part of* and $\tau(\cdot)$ for *time constant of*. T_{set} measures the settling time of the mode combination interacting with mode (j). Settling time here is defined as the time taken for a response to remain within 2% of the final value, and it is approximately 4 time constants. T_r is a measure of the persistence of the modal combination with respect to the dominant mode. High value of T_r indicates that the influence of the modal combination decays faster with respect to the dominant mode and vice versa. A relatively large value of $N2II * Tr_2$, $N3II * Tr_3$ tend to show a strong modal interaction of long duration for 2nd and 3rd order interactions respectively.

The study of modal interactions have been extensively reported in the past. The new idea in this thesis is the study of these interactions with fewer nonlinear terms and less burdensome computation, so-called *selective nonlinear modal interaction*. Next section will be dedicated to selective nonlinear modal interactions.

5.2 Selective Nonlinear Modal Interactions

In chapter 4, a method which facilitates the computation of the nonlinear coefficients required for NF application has been developed. The method enables computing selectively, any desired term rapidly, by avoiding the usual Taylor expansion. However, much reduction is still needed as there are still too many terms being considered in the analysis. For specific NF studies, it is possible to use some selected terms instead of all the terms. The main goal of this section is to reduce the computational burden associated with NF application to power systems, especially when it is applied to understand the significant modal interactions and the accompanying new frequencies. The section investigates further reduction of NF computation by considering fewer terms in the nonlinear approximation based on the information provided by the linear analysis. The analysis is then focused only on the considered terms. As stated before, analysis of nonlinear modal interaction is not new in power systems. What is new here is the selective application of NF to this analysis, which is made possible by the developed method.

5.2.1 Proposals for Selective NF Applications

Let us recall again from chapter 3 that the NF coefficients (i.e., $h2$ and $h3$) needed in the NF solution (5.2) are given by

$$h2^j_{kl} = \frac{C^j_{kl}}{\lambda_k + \lambda_l - \lambda_j}, \tag{5.14a}$$

$$h3^j_{pqr} = \frac{D^j_{pqr} + Cres^j_{pqr}}{\lambda_p + \lambda_q + \lambda_r - \lambda_j}. \tag{5.14b}$$

where $Cres$ is a residual term from second order transformation and is expressed as $\sum_{l=1}^{N}(C^j_{pl} + C^j_{lp})h2^p_{qr}$ and D^j_{pqr} is the original third order term. Our goal is to not compute all the coefficients but only some and set the other h-coefficients to zero. If modal interaction is the objective of study, whereby sources of unknown frequencies in time responses are explained; significant reduction of NF computation can be achieved by careful selection of relevant h-coefficients.

Careful observation of (5.14) and (5.2) shows that the indices of the NF coefficients are consistent with the indices of the mode combinations such that $h2^j_{kl} = 0$, $h3^j_{pqr} = 0$ implies that that mode combinations $\lambda_k + \lambda_l$, $\lambda_p + \lambda_q + \lambda_r$ have zero effects on the dynamics of state i. Therefore, to neglect the effect of a mode combination, the corresponding NF coefficient can be set to zero. However, the challenge remains how to decide which coefficients to set to zero. In this section, we propose two approaches that can be used to discriminate some h-coefficients, thereby reducing further the NF computations:

- real modes/eigenvalues exemption and
- mode's energy consideration.

They are discussed in the following subsections.

5.2.2 Real Modes/Eigenvalues Exemption Proposal

Let us assume that we can compute all the coefficients. Then, observation of (5.2) shows that there are interactions among the linear modes. Previous works on NF and spectral analysis prove that oscillatory modes can interact to produce new oscillations [31, 84]. However, there has not been any meaningful interpretation to interactions involving real modes or its physical phenomenon. The stability indices proposed in [55, 57] are based on the interactions associated to only oscillatory modes. With controls included in the models, there may be many of these real modes. Real modes are aperiodic and the actual interactions involving real modes may only affect the damping, but not alter the analysis of modal interaction. We propose to reduce NF computation by keeping all the linear modes in the linear part of the 3rd order approximate model, but considering only the interactions among oscillatory modes in the nonlinear part. The proposal is based on the interpretation of (5.2). Given that all modes are initially stable, (5.2) leads to the following deductions:

1. A combination of only real modes does not lead to a new frequency in the spectral.
2. A 2nd order combination of a real mode with an oscillatory mode does not lead to a new frequency in the spectral, rather a more damped version of the oscillatory mode which combined with the real mode.
3. A 3rd order combination of real and oscillatory modes may lead to a new frequency but this frequency must be the more damped version of a combination of two oscillatory modes already existing at 2nd order.

To sum up the above hypotheses, nonlinear interactions associated to real modes may be neglected without significantly altering the information needed to study modal interaction.

Application of the above hypotheses to (5.2) yields a reduced model of the the form

$$x_i(t) = \sum_{j=1}^{N} \mu_{1_{ij}} e^{\lambda_j t} + \sum_{k\geq 1}^{n}\sum_{l\geq 1}^{n} \mu^i_{2_{kl}} e^{(\lambda_k+\lambda_l)t} + \sum_{p\geq 1}^{n}\sum_{q\geq 1}^{n}\sum_{r\geq 1}^{n} \mu^i_{3_{pqr}} e^{(\lambda_p+\lambda_q+\lambda_r)t}, \tag{5.15}$$

where $i, j = 1, 2 \ldots N$, $\quad k, l, p, q, r \in$ *oscillatory modes* and $n \leq N$. Then only h-coefficients corresponding to oscillatory modes are computed. Equation (5.15) implies that all the system

modes are retained for the linear part, while for the nonlinear parts, some interactions are neglected. This is a nontrivial effort as it leads to a drastic reduction in NF computation.

Remark. *The interactions neglected in (5.15) does not mean they are exactly zero, but they are neglected on the assumption that their interactions are not nonlinearly significant. In the way NF is applied, there are always many interactions, but of interest in control are the interactions that persist [31].*

Numerical Simulations and Results for Real Mode Exemption Proposal

The test system is IEEE 9-bus power system used in the previous chapters (i.e., Figure 2.1) and has been used in the literature to study modal interaction [71, 85]. Two-axis model was used with each generator equipped with a simple exciter described in chapter 3. The loads were modelled as constant impedance. G3 is used as reference and the system modes are shown in Table 5.1. The natural frequencies of the modes in rad/s are given by the imaginary parts of the eigenvalues and are listed in column three of Table 5.1. With the linear mode-in-state participation factor analysis, the dominant states for each mode are obtained as listed in column five of Table 5.1. The states V_{m_i} and V_{r_i} are exciter parameters. Every other parameters have their usual meanings. It is a small power system containing 20 states, but large enough to demonstrate the NF problem solved in this section. As stated earlier, the

Table 5.1 – Linear analysis.

Mode #	Eigenvalue	Freq. (rad/s)	Damping (%)	Dominant States
1	-50.32	0	100	$E_{fd_1}, E_{fd_2}, E_{fd_3}$
2	-50.24	0	100	E_{fd_1}, E_{fd_2}
3	-50.21	0	100	E_{fd_2}, E_{fd_3}
4,5	$-1.02 \pm$ j13.63	13.63	7.45	$\omega_3, \delta_3, \omega_2, \delta_2$
6,7	$-0.14 \pm$ j8.94	8.94	1.52	$\omega_2, \delta_2, \omega_1, \delta_1$
8,9	$-0.84 \pm$ j4.03	4.03	20.30	$E'q_1, Vm_1$
10	-5.22	0	100	$E'd_2, E'd_3$
11,12	$-1.18 \pm$ j2.86	2.86	38	$Vm_1, Vm_2, E'q_1,$
13,14	$-1.50 \pm$ j1.98	1.98	60	$Vm_3, E'q_3, E'd_3$
15	-3.59	0	100	$E'd_3$
16	-3.25	0	100	$E'd_1$
17,18	$-0.12 \pm$ j0.01	0.01	99.52	vr_1, ω_1
19,20	$-0.11 \pm$ j0.001	0.001	99.99	vr_1, vr_2

degree of stress can be increased by changing the post-disturbance operating condition or by

changing the severity of the disturbance. Two test cases were selected for fault at Bus 4.

Case 1: Fault cleared after 0.019s. This case represents a less stressed condition.

Case 2: Fault cleared after 0.184s very near the critical clearing time[1]. This case represents stressed condition with severe nonlinear behaviour.

There are 35,000 (2nd and 3rd) coefficients in the model. NF models were built with 35,000 (full) coefficients and the reduced model discussed in next heading. In a case where linear analysis cannot explain the observations in the system response (i.e., the nonlinearity becomes significant), NF analysis is then performed with the two models, and the results compared. The transient simulations were performed with the help of PSAT software [123] to obtain the post-fault initial condition, while the algorithm described in Section 3.2.3 was followed to obtain NF initial condition. Then all NF analyses are implemented with computer programs written by the author in the MATLAB® software.

Obtaining the Reduced Model

The reduced model was obtained by skipping coefficients corresponding to the interactions of real modes as explained in Section 5.2.2. Table 5.1 shows that the studied system has 6 real modes. Reducing N by 6 leads to a total of 9,310 coefficients which translate to skipping 25,690 C, D coefficients and 25,690 $h2, h3$ coefficients, since h-coefficients are consequences of C and D coefficients (see (5.14)). For example $C_{1,1,1}$, $D_{1,1,1,1}$, $C_{1,1,2}, C_{10,15,16}\ldots$, $h2_{1,1,1}, h3_{1,1,1,1}, h2_{1,1,2}, h2_{10,15,16}\ldots$ are not computed since they involve real mode combinations. However, $C_{1,4,5}$, $D_{1,4,5,6}$, $C_{1,8,9}, C_{10,11,12}\ldots, h2_{1,4,5}, h3_{1,4,5,6}, h2_{1,8,9}, h2_{10,11,12}\ldots$ are computed since they involve only oscillatory mode combinations. The NF solution obtained with this reduced model shall be referenced as NF-9,310 against the full model referenced as NF-35,000. The computation of the remaining coefficients is easy since one just has to solve a set of linear equations as described in chapter 4.

Figure 5.1 shows drastic reduction in computation time brought by the proposed method. The time considered in Figure 5.1 is only for computing the coefficients. It can be seen that more significant reduction is achieved by skipping some interactions.

Analysis of Case 1

Figure 5.2a shows the active power response of generator 1 after fault is cleared. Generator 1 is used because it is closest to the fault point. Under this condition, the system is more or less linear. This is revealed by the FFT spectrum in Figure 5.2b which shows that nonlinear

[1] Critical clearing time is 0.185 s

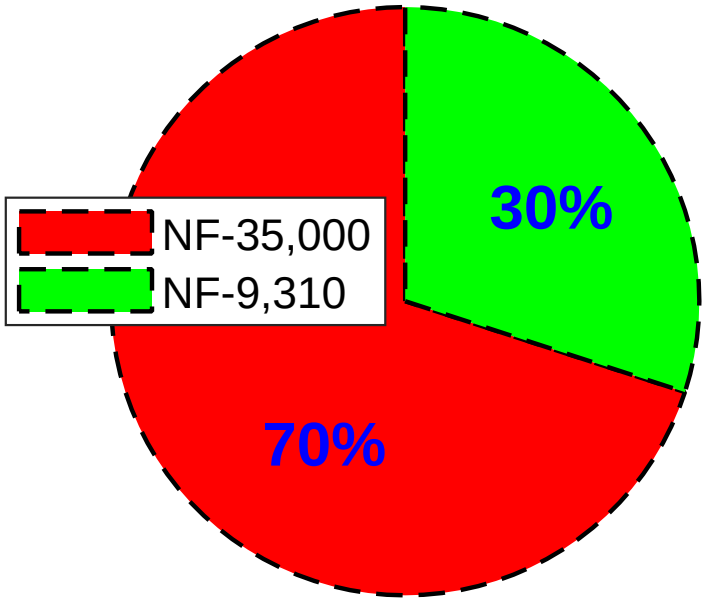

Figure 5.1 – Normal Form (NF) computation time for full and reduced models.

interactions are not strong, since the spectrum is dominated by the approximate linear modes. For example, the highest peak corresponds to a frequency of 8.9 rad/s, which is approximately mode $\lambda_{6,7}$ with frequency 8.94 rad/s in Table 5.1. This is followed by a peak with frequency 3.9 rad/s which is approximately mode $\lambda_{8,9}$ with frequency of 4.03 rad/s in Table 5.1. The frequency, 17.6 rad/s, which also appears in Figure 5.2b does not exist among the linear modes in Table 5.1 and must come from modal interaction. Note that, to compute the FFT spectrum, the instant of time for initial conditions should be chosen such that all limiting actions by controllers in the system must have ceased after the clearance of the fault.

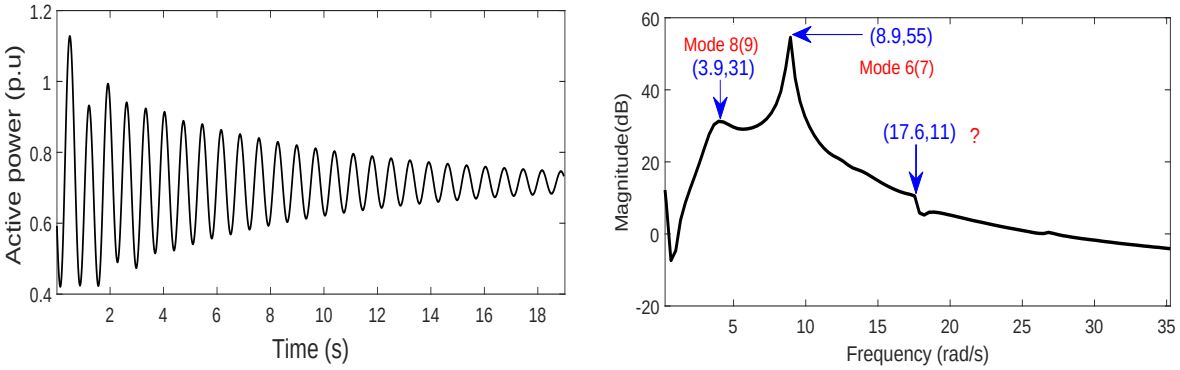

(a) (b)

Figure 5.2 – (**a**) Generator 1 active power response for case 1. (**b**) Fast Fourier transform (FFT) spectrum of generator 1 active power for case 1, showing less severe nonlinear effects.

In order to predict which mode is likely responsible for the interaction leading to the unknown frequency in Figure 5.2b, the indices discussed in Sections 5.1.2 and 5.1.2 are computed. These indices are listed in Tables 5.2 and 5.3 for 2nd and 3rd order nonlinearities respectively. In Table 5.2, among the oscillatory modes, mode 4(5) has the largest N2LI and

N2II indices. This is followed by modes 17(18) and 13(14). Others have smaller values. This observations suggest that effect of 2nd order nonlinearity on mode 4(5) may be significant. In Table 5.3, mode 4(5) also has the highest N3LI and N3II among all the oscillatory modes. However, its N3II value is very small compared to the 2nd order value. This observation suggests, perhaps a less significant interaction of 3rd order. From Tables 5.2 and 5.3, one can predict that mode 4(5) is most likely to lead to significant nonlinear interaction. A detailed NF study on mode 4(5) is likely to reveal the mode combination leading to 17.6 rad/s, observed in Figure 5.2b, but since this frequency has negligible amplitude (i.e., 11 dB), the system condition can be assumed linear.

Table 5.2 – 2nd-order NF indices for modal interaction.

Mode	**Eigenvalue**	**N2LI**	**N2II**
15	−3.59	0.315	0.314
4(5)	−1.02 ± **j13.63**	**0.443**	**0.212**
16	−3.25	0.192	0.192
17(18)	−0.12 ± j0.011	0.139	0.138
13(14)	−1.50 ± j1.98	0.245	0.108
10	−5.22	0.263	0.100
19(20)	−0.11 ± j0.001	0.061	0.061
6(7)	−0.14 ± j8.94	0.072	0.034
8(9)	−0.84 ± j4.03	0.035	0.028
1	−50.32	0.002	0.016
11(12)	−1.18 ± j2.86	0.045	0.014
3	−50.22	0.015	0.013
2	−50.24	0.002	0.001

Table 5.3 – 3rd-order NF indices for modal interaction.

Mode	**Eigenvalue**	**N3LI**	**N3II**
16	−3.25	0.177	0.069
15	−3.59	0.301	0.037
4(5)	−1.02 ± **j13.63**	**0.430**	**0.016**
10	−5.22	0.250	0.015
13(14)	−1.50 ± j1.98	0.252	0.008
6(7)	−0.14 ± j8.94	0.070	0.002
8 (9)	−0.84 ± j4.03	0.033	0.002
11(12)	−1.18 ± j2.86	0.044	0.001
3	−50.22	0.015	0.001
1	−50.32	0.002	0.001
17(18)	−0.12 ± j0.011	0.143	0.001
19(20)	−0.11 ± j0.001	0.061	0.000
2	−50.24	0.002	0.000

Analysis of Case 2

In case 2, the stress is increased and more nonlinearity is induced on the system. The active power response of generator 1 is shown in Figure 5.3a, and its FFT spectrum in Figure 5.3b. The FFT spectrum shows existence of significant nonlinear interactions whose sources have to be explained. For instance, the frequencies 3.9 rad/s, 8.9 rad/s, and 13.4 rad/s approximately correspond to the linear modes 8(9), 6(7), and 4(5) which have frequencies 4.03 rad/s, 8.94 rad/s, and 13.63 rad/s respectively, in Table 5.1. However, 17.6 rad/s frequency which had negligible amplitude in case 1 now has amplitude of 36 dB and does not correspond to any linear frequency in Table 5.1. This is also the case of 26.8 rad/s frequency, appearing with amplitude of 33dB higher than the amplitude of the linear frequency 3.9 rad/s. To unravel the sources of these frequencies in Figure 5.3b, a detailed NF analysis is performed next.

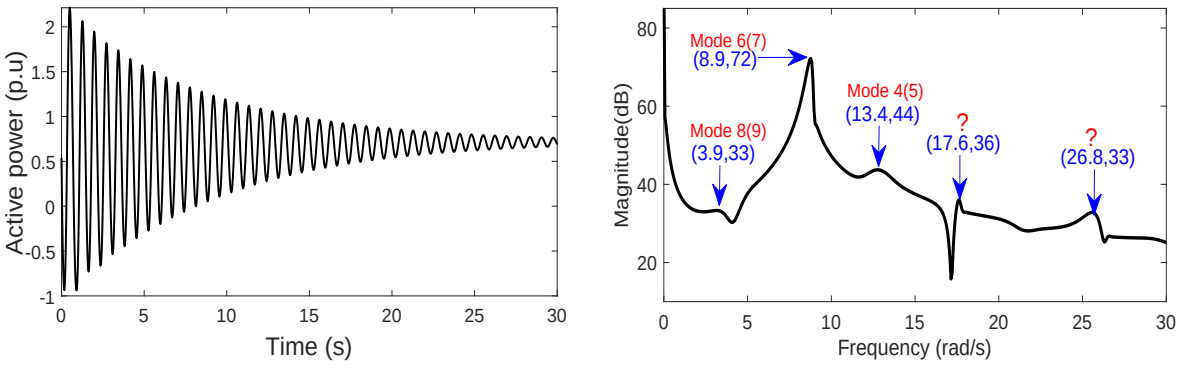

(a) (b)

Figure 5.3 – (**a**) Generator 1 active power response for case 2. (**b**) FFT spectrum of generator 1 active power for case 2, showing severe nonlinear effects.

Qualitative NF analysis of Case 2

In this section, the detailed analyses based on two NF models (i.e., NF-35,000 and NF-9,310) are compared. As earlier revealed by Tables 5.2 and 5.3, mode 4(5) is more likely to cause significant modal interactions. It was also established from Table 5.3 that 3rd order interactions for the studied system may be weak. Hence, only detailed analysis of mode 4(5) is presented, although all other modes were studied. Also, only 2nd order modal interaction coefficients ($h2_{kl}^{4,5} z_{0_k} z_{0_l}$) were examined in detail for both NF-35,000 and NF-9310 models.

The nonlinear persistence measures, T_{set}, T_r and $N2II * T_r$, together with the interaction coefficients associated with mode 4(5) are listed in Table 5.4, in descending order of the interaction coefficients. There are numerous interactions involving mode 4(5), so only first few ones are presented. The largest interaction coefficient corresponds to a combination of eigenvalues 5 and 17 (i.e., $-1.13 - \mathrm{j}13.62$), which has settling time almost equal to that of

Table 5.4 – NF-35,000—Quantitative Measures of combination Modes for Fundamental Mode 4(5).

$h2_{kl}^{4,5} z_{0_k} z_{0_l}$	k	l	$\lambda_k + \lambda_l$	T_r	T_{set}	$N2II * T_r$
5.462	5	17	$-1.13 - j13.62$	0.899	3.529	4.908
1.761	5	18	$-1.13 - j13.64$	0.899	3.529	1.582
1.579	**5**	**9**	$-1.85 - \mathbf{j17.66}$	**0.549**	**2.158**	**0.868**
1.539	5	8	$-1.85 - j9.60$	0.549	2.158	0.845
1.215	4	17	$-1.13 + j13.64$	0.899	3.529	1.092
1.063	4	9	$-1.85 + j9.60$	0.549	2.158	0.584
1.028	4	8	$-1.85 + j17.66$	0.549	2.158	0.565
0.308	4	5	-2.04	0.500	1.964	0.154
0.262	5	8	$-1.85 - j9.60$	0.549	2.158	0.144
0.258	7	9	$-0.97 - j12.97$	1.049	4.119	0.271
0.232	5	12	$-2.19 - j16.50$	0.463	1.820	0.107
0.227	**5**	**5**	$-2.04 - \mathbf{j27.26}$	**0.500**	**1.964**	**0.113**
0.201	5	9	$-1.85 - j17.66$	0.549	2.158	0.110
...	...	...	...	...	...	...

the dominant mode (i.e., 3.68 s) and large $N2II*T_r$. However, the new frequency is very near to the linear frequency 13.63 rad/s and is difficult to differentiate by FFT, if it appears in the response. Moreover, the modal persistence T_r is close to 1 (i.e., 0.899). Hence, it may not even be observed in the response. The combination of eigenvalues 5 and 9 (i.e., $-1.02 - j13.63$ $-0.84 - j4.03 = -1.85 - j17.66$) has relatively large interaction coefficient (1.579) and low T_r (0.549), with settling time, well above half that of the dominant mode (i.e., $1/2 \times 3.68$s), and relatively high $N2II * T_r$. These observations indicate that mode 4(5) is interacting nonlinearly with mode 8(9). Notice that the new frequency 17.66 rad/s is approximately observed in the FFT spectrum of Figure 5.3b (i.e., 17.6 rad/s). Also, down the table, there is a self combination of eigenvalues 5 and 5 (i.e., $-1.02 - j13.63 - 1.02 - j13.63 = -2.04$ $- j27.26$), which leads to a frequency of 27.26 rad/s, approximate value of the 26.8 rad/s appearing in the spectrum. However, its interaction coefficient is relatively small (0.227), with relatively small value of $N2II * T_r$ (0.113). This is consistent with Figure 5.3b, where 26.8 rad/s frequency has low amplitude. If the test system Figure 2.1 is considered a two-area system, it is seen that mode 4(5) which is associated with area 2 interacts with control mode 8(9) in area 1. Control-wise, in placement of PSS to damp mode 4(5), effect of its interaction with controls in area 1 should be considered in its optimisation formulation. Although, the interactions of electromechanical modes with the control modes in the same area should have more adverse effects.

The above analysis is repeated but now with NF-9,310 model and the results are listed

in Table 5.5. It is clear from the table that the reduced model identifies correctly, the same eigenvalue combinations leading to the observed frequencies in the FFT spectrum. There are some slight deviations in the values of the interaction index ($h2^{4,5}_{kl} z_{0_k} z_{0_l}$) in both cases due to different NF initial conditions.

Table 5.5 – NF-9,310—Quantitative Measures of combination Modes for Fundamental Mode 4(5).

$h2^{4,5}_{kl} z_{0_k} z_{0_l}$	k	l	$\lambda_k + \lambda_l$	T_r	T_{set}	$N2II * T_r$
6.351	5	17	$-1.13 - j13.62$	0.899	3.529	5.706
2.048	5	18	$-1.13 - j13.64$	0.899	3.529	1.840
1.843	**5**	**9**	$-1.85 - \mathbf{j17.66}$	**0.549**	**2.158**	**1.013**
1.798	5	8	$-1.85 - j9.60$	0.549	2.158	0.988
0.956	4	17	$-1.13 + j13.64$	0.899	3.529	0.859
0.840	4	9	$-1.85 + j9.60$	0.549	2.158	0.462
0.813	4	8	$-1.85 + j17.66$	0.549	2.158	0.447
0.307	**5**	**5**	$-2.04 - \mathbf{j27.26}$	**0.500**	**1.964**	**0.153**
0.306	5	8	$-1.85 - j9.60$	0.549	2.158	0.168
0.282	4	5	-2.04	0.500	1.964	0.141
0.268	5	12	$-2.19 - j16.50$	0.463	1.820	0.124
0.259	7	9	$-0.97 - j12.97$	1.049	4.119	0.272
0.234	5	9	$-1.85 - j17.66$	0.549	2.158	0.129
...	...	...	...	...	...	...

It is important to recall at this point that interactions are detected by comparing the relative magnitudes of the defined indices in each case. Hence, the actual values of these indices do not have to be the same, but the information they provide are same for the same case. These indices depend on NF initial condition which in turn depends on the number of h-coefficients considered. Note that the main idea of NF is to, at least, simplify the system nonlinearity, which implies that the values computed depend on what level the system is simplified to. So, even in *full* NF, not all h-coefficients computations are possible when resonance occurs. The NF initial conditions are determined only using the possible h-coefficients.

5.2.3 Mode's Energy Consideration

Alternatively, we can deduce the less relevant h-coefficients by exploiting the physical properties of the system modes. Recall that we established a link between the mode combinations and the h-coefficients in the previous subsection. Hence, apart from the real modes, we can search for less relevant modes (not necessarily real modes). **The assumption here is that only modes with sufficient energy can interact nonlinearly.** So the problem is reduced

to looking for modes in the system that have least/more impact on the system dynamics, so-called least/most relevant modes. In control theory, it is easy to determine the states and modes sufficient to reduce a system considering the *controllability* and *observability* of the modes [40, 103, 104].

Let the state-space representation of a linear time-invariant system (LTI) be

$$\begin{aligned} \dot{\mathbf{x}} &= \mathbf{A}\mathbf{x} + \mathbf{B}\mathbf{u} \\ \mathbf{y} &= \mathbf{C}\mathbf{x} + \mathbf{D}\mathbf{u}, \end{aligned} \tag{5.16}$$

where $\mathbf{A}$ is the state matrix, $\mathbf{B}$ and $\mathbf{D}$ are constant matrices that weight the input $\mathbf{u}$ and $\mathbf{C}$ is a matrix that weights the states $\mathbf{x}$, while $\mathbf{y}$ is the output matrix. The $\mathbf{C}$ and $\mathbf{D}$ in (5.16) should not be confused with that earlier defined for nonlinear coefficients. *Controllability* and *observability* can be measured by calculating the controllabilty and observabilty grammians [124]

$$W_c = \int_0^\infty e^{At} B B^T e^{A^T t} dt, \tag{5.17a}$$

$$W_o = \int_0^\infty e^{A^T t} C^T C e^{At} dt. \tag{5.17b}$$

There exist a unique base in which both grammians are equal and diagonal, so-called *balanced realisation* [124]. That is $W_c = W_o = diag\{\sigma_1, \sigma_2, \sigma_3, \ldots\}$ where $\sigma_1 \geq \sigma_2 \geq \sigma_3 \ldots$ are called *Hankel singular values*. The most relevant modes of the system are both controllable and observable, and they are the ones associated with the first state variable of the balance realisation [40]. To associate these modes to the states in balanced realisation, we use the mix balanced-modal truncation algorithm proposed in [104] as follow:

1. Obtain a balanced realisation as explained above (easy with a MATLAB® function).
2. Select the states for which the Hankel singular values are large.
3. Obtain the mode-in-state participation factors for the selected states [121].
4. Select modes with major participation in the selected states in 2 using the participation factors in 3.

Then only the selected modes are needed in the reduced model (5.15).

The Hankel singular values for the above test system is shown in Figure 5.4. The figure hints that the system can be modelled with only 3 or at best 5 states. The modes that participate in these 5 most relevant Hankel states, so-called relevant modes, are shown in Figure 5.5. Notice that the mode corresponding to first Hankel state (state with highest

energy) is $\lambda_{4,5}$. This is consistent with the above NF analysis, which showed mode 4(5) to be most responsible for the nonlinear modal interaction. If one focuses on the first three Hankel states, then $\lambda_{4,5}$, $\lambda_{8,9}$ and $\lambda_{11,12}$ can be retained for the study of modal interaction. Recall that the above NF analysis revealed mode 4(5) and mode 8(9) to be interacting nonlinearly. Even if all the five Hankel states are to be considered, Figure 5.5 hints that in addition to the real modes, $\lambda_{13,14}$ and $\lambda_{19,20}$ may also be skipped, thereby reducing further the computation.

The two proposals should be explored in details with various systems, to established concretely, their merits and demerits.

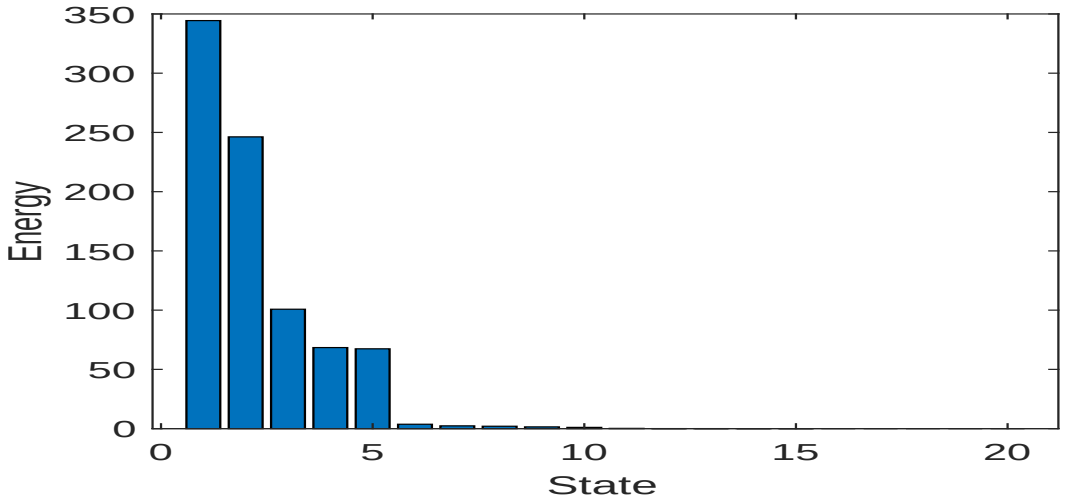

Figure 5.4 – Hankel singular values showing 5 most relevant states

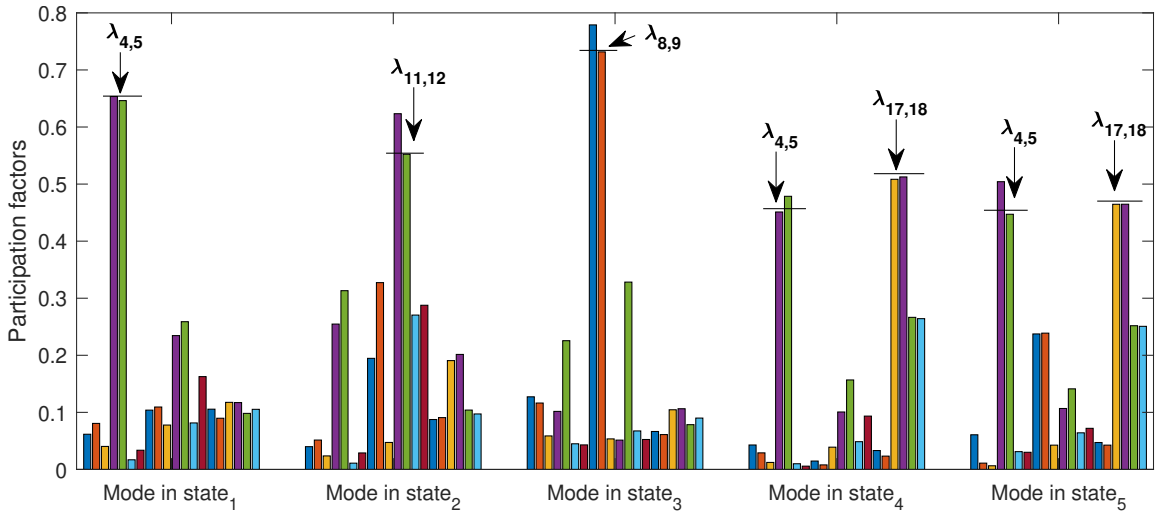

Figure 5.5 – Participation factors of modes in the 5 *hankel* states

5.2.4 Nonlinear Mode-in-state Participation Factor Analysis

A common method for siting PSS in power system is the mode-in-state participation factor analysis [121]. Also, in stability studies, attention is more on those modes that participate

actively in the stability states (i.e., voltage and angle). In this section, nonlinear participation factor analysis for the system studied in section 5.2.2 is presented just for the two angle states to emphasise the correction that NF adds to linear analysis. The three types of participation factors discussed in section 5.1.1 are implemented.

Figures 5.6a and 5.6c respectively show the 1-eigenvalue participation factors for relative angles of generators 1 and 2, which were obtained from linear analysis, 2nd NF, and 3rd NF. It can be seen that the linear analysis under-estimates the contributions of certain eigenvalues. For example, the contributions of eigenvalues 17–20 are not captured at all by the linear analysis, while the contributions of eigenvalue 15 (for generator 1) and eigenvalues 13–15 (for generator 2) are far under-estimated. This lack of information may lead to improper control designs or poor placement of PSS. The 2nd and 3rd order 1-eigenvalue corrections are similar as the effect of 3rd order interactions are not very strong in the studied case. Figures 5.6b, 5.6d show respectively, the 2-eigenvalue participation factors for generators 1 and 2.

Worthy of note is that the eigenvalue combination due to modal interactions can sometimes participate more than the dominant mode. For example, the highest participating mode to generator 2 is mode 4(5), however, in Figure 5.6d, it is clear that some interactions of this mode have more participation than single mode 4(5). Similar observation has been made in [31]. Figures 5.6e, 5.6f show respectively, the 3-eigenvalue participation factors for generators 1 and 2. Here, the 3-eigenvalue participation are not very strong as the bars are far below that of the dominant modes.

Normally, PSS is sited in the area with highest participation factor. As seen in the previous section, interaction can exist between modes in two different areas. The area of the newly formed mode is unclear, should it participate more. All these have to be factored in, while designing controls for stressed power systems. A knowledge of interacting modes could be used in nonlinear control of converters in the emerging 100% PE grids.

5.2.5 Further Discussions on the Proposed Selective NF Application

In this section, major implications of the results presented in Sections 5.2.2— 5.2.4 are discussed as follows:

- The results illustrate that the proposed method can significantly reduce the computational burden in NF applications. This is depicted with the pie chart shown in Figure 5.1, where the computation time using the proposed method occupies a sector of 30% against the conventional technique, which occupies 70%. In [31], 2nd order modal interaction was studied with a model that has 27 eigenvalues, of which 13 are real. In

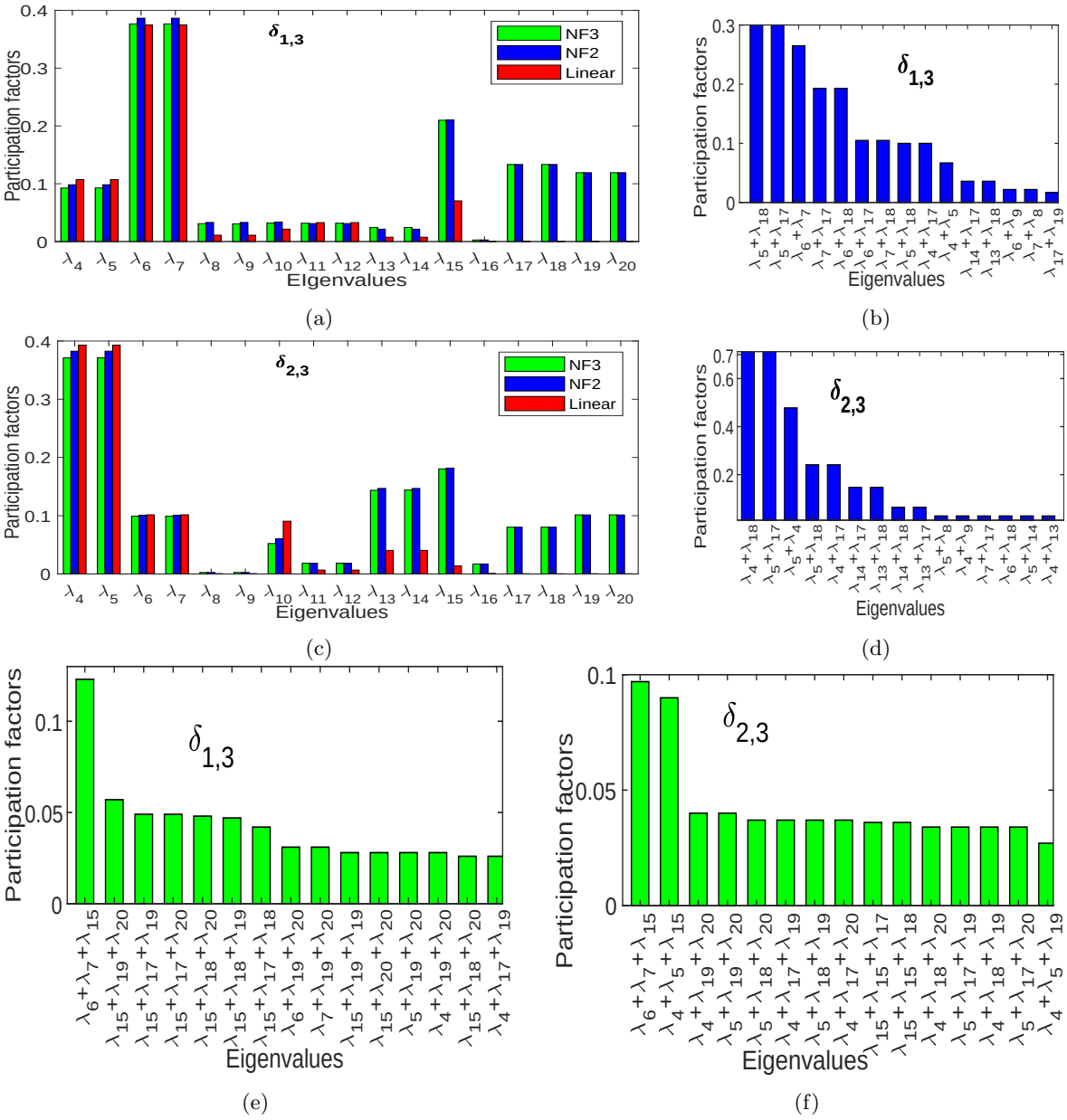

Figure 5.6 – (**a**) 1-eigenvalue mode-in-state participation factors to generator 1 relative angle. (**b**) 2-eigenvalue participation factors to generator 1 relative angle. (**c**) 1-eigenvalue participation factors to generator 2 relative angle. (**d**) 2-eigenvalue participation factors to generator 2 relative angle. (**e**) 3-eigenvalue participation factors to generator 2 relative angle. (**f**) 3-eigenvalue participation factors to generator 2 relative angle.

the interpretation of the results, the interactions involving real modes were ignored, which implies a huge computational waste. If this model is to be considered for 3rd order NF study, it will generate 108,864 coefficients. However, with the proposed method, this model will only have 9,310 coefficients, a computational saving factor of 12.

- The results show that stressed power system leads to nonlinear interactions of modes. This can be seen for example, in case 1, where less severe fault led to spectrum of Figure 5.2b with no significant interaction, whereas in case 2, where the stress increases, the nonlinearity increases and the modal interaction becomes apparent in the spectrum

of Figure 5.3b. NF analysis is able to identify these interactions as revealed in Tables 5.4 and 5.5. These observations corroborate previous research on modal interaction [31]. A significant new contribution is the use of fewer terms to perform the same analysis. This contribution is especially pertinent in view of fully PE grids. In PE grids there are several modes that decay very fast. The treatment of real modes proposed in this chapter may be extended to such very fast modes to further simplify NF application to PE grids.

- The results of the participation factor analyses in Figures 5.6a— 5.6f show the correction to the linear participation factor due to the addition of higher order terms. Reference [53] reported a case where PSS location using nonlinear participation factors outperforms the location using linear participation factor.

- As shown in Figure 5.6d, the combination modes may participate more than the fundamental modes. Hence, as the disturbance becomes significant, the stability/instability may not be completely determined by single eigenmodes without their interactions. Reference [57] has reported a case where single eigenvalue showed instability but the 3rd order interaction maintained the stability of the system.

- Since the idea proposed in this section addresses specific case of NF application (i.e., modal interaction) its potency for other NF applications such as stability studies is not guaranteed.

- The results indicate that avoiding the interactions associated to the real modes does not compromise the effectiveness of NF modal interaction analysis. This, however, does not mean that all other remaining interactions are nonlinearly significant. The Hankel energy proposal showed that even some interactions due to oscillatory modes can be discriminated.

Some Practical Concerns

It is obvious that the proposed method significantly reduces the computation needed to apply NF to power system. However, the following practical concerns are worthy of discussion:

- A major concern is the implication of the proposed method in a large system. Even with the reduction proposed in this chapter, the number of nonlinear terms will still be enormous in the case of large systems. It is important to state that the approach proposed here is one out of many steps needed to apply NF to large systems. Although general application of NF to unreduced large system remains difficult, it is good to note

that the proposed reduction is based on the physics of the modes and thus, can be applied to system of any size. We are working on several ideas, to advance NF to very large system. At the moment, reducing the network and focusing on a particular area of the network is the approach to attempt large system (already used in [61] for system with over 300 generators).

- Another valid argument could be if the usefulness of NF analysis is worth the computations involved, given that the time domain analysis could identify the interaction of nonlinear dynamics. It is good to emphasise that NF analysis just like other analytical methods, does not replace time domain analysis but complements it. Time domain analysis can identify the interactions of nonlinear dynamics but the exact natures of these interactions are unclear. Moreover, analytical parameters needed for power system control designs are not as apparent as with analytical methods. It lacks in qualitative information about the system. The nonlinear participation factor analysis helps to know from where comes the interaction. Other analytical information for the power system control designs are not exhaustively available with time domain analysis. NF analysis should be used when some phenomena are difficult to explain with the time domain analysis. Also, indices are needed based on the system condition, to know a priori that it is gainful embarking on NF analysis to avoid computational loss. These indices should be developed. We are optimistic that a well developed selective NF application will position it as always very useful tool.

Recapitulation

The previous sections were dedicated to the application of NF to the study of modal interactions. In particular, the use of NF to explain the sources of unknown frequencies due to modal interactions and the extension of the linear participation factor analysis to the nonlinear one were considered. Those concepts are not new in the literature. The significant new idea is the introduction of selective application made possible by the developed method; and allows larger systems to be considered. Selective application of NF to the study of nonlinear modal interactions are scarcely reported in literature. Moreover, such operation is not convenient with the conventional method for NF analysis. The remaining sections in this chapter will be dedicated to the developments of new tools for power system analysis based on NF, notably the detection of nonlinear frequency shift and stability monitoring. These new tools also enjoy the selective-computation capability of the computational method developed in chapter 4.

5.3 Concept of Nonlinear Frequency

Traditional power system modal analysis assumes harmonic electromechanical oscillations, which allows such oscillations to be decomposed as a sum of positively or negatively damped sinusoids. However, under large disturbance, and especially near the stability bound, electromechanical oscillations become asymmetric and their frequencies not constant. The frequency of the nonlinear system under large disturbance is then dependent on the amplitude at each time. Such frequency can be regarded as nonlinear frequency (NLF). In other words, apart from the nonlinear modal interactions, increasing stress (which increases the level of nonlinearities) also affects the frequency of the fundamental modes. This nonlinear change of frequency with respect to the amplitude of the oscillation, as we shall see, is related to the deterioration of the system stability during disturbance.

Stress, Nonlinear Frequency and the System Stability

First of all, the stress can be induced by either change of operating conditions or the severity of the disturbance. That is, increase in power transfer through the lines or severe fault case can induce stress. To make a link between the nonlinear frequency and the stability of the oscillation under stressed condition, let us consider two scenarios—effect of tie line flows and effect of large disturbance.

Effects of tie line flow on the oscillation mode

In the SMIB power system previously studied in chapter 3 (i.e. Figure 3.2), the generator output power P_e is transferred on the tie line of total impedance X_s. The system can be represented (for speed not in p.u.) by

$$\frac{2\mathcal{H}}{\omega_s}\dot{\omega} = T_m - T_e - \mathcal{D}\omega = \frac{\omega_s}{\omega}T_m - \frac{\omega_s}{\omega}T_e - \mathcal{D}\omega \tag{5.18a}$$

$$\dot{\delta} = \omega - \omega_s. \tag{5.18b}$$

Equations (5.18) can be written as

$$\dot{\omega} = \frac{\omega_s^2}{2\mathcal{H}\omega}P_m - \frac{\omega_s^2}{2\mathcal{H}\omega}P_e - \frac{\omega_s}{2\mathcal{H}}\mathcal{D}\omega \tag{5.19a}$$

$$\dot{\delta} = \omega - \omega_s \tag{5.19b}$$

$$P_e = \frac{EV}{X_s}\sin\delta, \tag{5.19c}$$

where δ is the rotor angle in radians, and ω is speed in rad/s, T_m and T_e are the mechanical and the electrical torque in p.u, P_m and P_e are mechanical input and the electrical power output in p.u., ω_s is the synchronous speed in rad/s, and $\mathcal{H}$ and $\mathcal{D}$ are the generator inertia constant and damping coefficient, respectively. As the operating point of a power system determines the oscillation modes, the oscillation behaviour will be affected by the tie line flow (P_e).

Considering constant T_m, generator internal voltage E and infinite bus voltage V, linearising (5.19) around SEP yields

$$\begin{bmatrix} \Delta\dot{\omega} \\ \Delta\dot{\delta} \end{bmatrix} = \begin{bmatrix} \frac{\omega_s^2}{2\mathcal{H}\omega_0^2}P_{e0} - \frac{\omega_s}{2\mathcal{H}}\mathcal{D} & -\frac{\omega_s^2}{2\mathcal{H}\omega_0^2}\frac{EV}{X_s}\cos\delta_0 \\ 1 & 0 \end{bmatrix} \begin{bmatrix} \Delta\omega \\ \Delta\delta \end{bmatrix} \tag{5.20}$$

Defining $K_s = \frac{\omega_s}{2\mathcal{H}}$, $K_e = \frac{EV}{X_s}\cos\delta_0$, the system oscillation modes (eigenvalues) are given by

$$\lambda_{1,2} = -\sigma \pm j\omega = \frac{-\left[-K_s\frac{\omega_s}{\omega_0^2}P_{e0} + K_s\mathcal{D}\right] \pm j\sqrt{\left[K_s\frac{\omega_s}{\omega_0^2}P_{e0} - K_s\mathcal{D}\right]^2 - 4K_s\frac{\omega_s}{\omega_0}K_e}}{2}. \tag{5.21}$$

The damping ratio becomes

$$\xi = \frac{\sigma}{\sqrt{\sigma^2+\omega^2}}. \tag{5.22}$$

Note that $\omega_s = \omega_0$ is a common and simplifying assumption in many textbooks, which makes the term $\frac{\omega_s^2}{\omega_0^2} = 1$. However, this assumption will not allow for better representation of damping effects which is intended in this section.

With varying electrical output (varying stress) in (5.21), the effects on the oscillation frequency and damping can be visualised in Figure 5.7. The parameters for plotting Figure 5.7 were discussed in section 3.2.4 with $\omega_s = \omega_0$ in (5.21). Figure 5.7 shows that as the generator

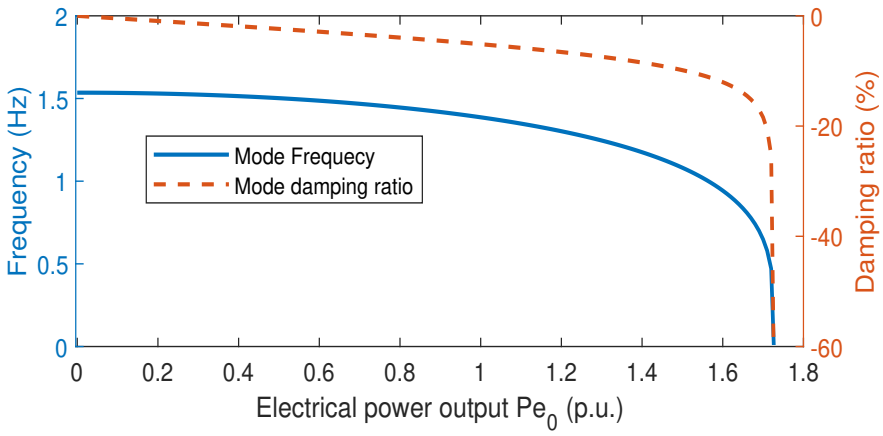

Figure 5.7 – Frequency and damping ratio variations with generator power output.

output power increases, the damping and frequency of the mode decrease simultaneously. In other words, increasing the stress on the system by increased tie line flows, decreases the mode oscillation and damping. Decreasing of damping suggests a deterioration of the oscillation stability. In fact, the figure shows decreasing damping and frequency up to a point beyond which the system stability finally deteriorates, so-called *knee point*. This phenomenon is the same even for detailed generator model. Thus, predicting the nonlinear frequency can suggest the proximity of a mode to instability.

Effects of large disturbance on the oscillation mode

With same SMIB power system (5.19), let the SEP be 15° ($\frac{\pi}{12}$ rad). With the conventional SSA, the frequency of the electromechanical mode is 7.82 rad/s (1.24 Hz). With the well known equal area criterion (EAC), the stability bound for this operating point is 165° (2.88 rad), as seen in Figure 5.8a. Now, let us consider a certain disturbance with oscillation amplitude 164.90° (i.e., 99.94% of the stability bound). The exact nonlinear response of this condition is shown in Figure 5.8b. At this point, the nonlinear oscillation is asymmetric, since the positive and negative amplitudes are not equal. At the same time, the frequency is far shifted from that obtained from SSA. Estimation of the oscillation frequency under this condition, using the two peaks indicated in the figure gives 0.65 Hz which, is 48% less than the linear frequency. Notice that the disturbance of Figure 5.8b is 99.94% close to the boundary

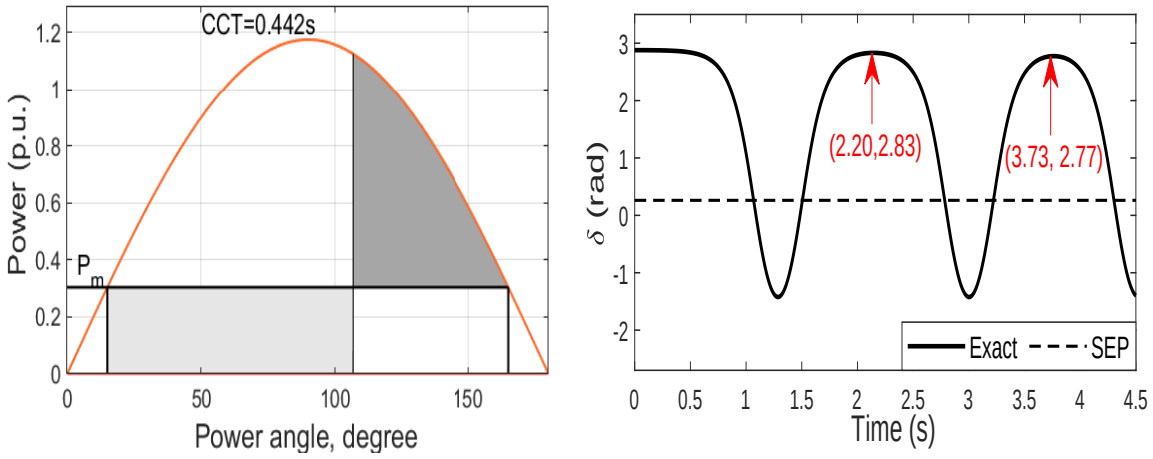

(a) Equal Area Criterion

(b) Oscillation very close boundary

Figure 5.8 – Amplitude-dependent frequency shift during large disturbance

of stability. In order words, 0.65 Hz is near to a *knee* point, beyond which instability occurs.

The above illustrations indicate that detecting the nonlinear frequency could be used in monitoring the deterioration of the system stability. This relationship between the nonlinear frequency and the power system stability has been pointed out in [125].

5.4 Detection of Frequency-Amplitude Shifts via Normal Form

Recall from chapter 3 that the second order classical modelling of power system expanded by Taylor series, up to third order, can be simplified into its normal form, called nonlinear normal mode (NNM) as

$$\forall q \neq p : R_q = 0, S_q = 0, \tag{5.23a}$$

$$\dot{R}_p = S_p, \tag{5.23b}$$

$$\dot{S}_p = -\Omega_p^2 R_p - (A^p_{ppp} + H^p_{ppp}) R_p^3 - B^p_{ppp} R_p S_p^2, \tag{5.23c}$$

where Ω is the natural frequency (linear mode), R and S, the state variables in the NF coordinate, A and B, the NF coefficients defined in chapter 3 and H, the cubic nonlinear coefficient discussed in chapter 3 and chapter 4.

It can be shown that the frequency-amplitude relation for (5.23) is given by [62]:

$$\begin{aligned} \Omega_{p_{nl}} &= \Omega_p \left(1 + \Xi_p \Pi^2\right) \\ \Xi_p &= \frac{3(A^p_{ppp} + H^p_{ppp}) + \Omega_p^2 B^p_{ppp}}{8\Omega_p^2}, \end{aligned} \tag{5.24}$$

where $\Omega_{p_{nl}}$ is a nonlinear angular frequency due to the disturbance, and depends on the amplitude Π considered. The implementation of (5.24) is illustrated next with the same SMIB power system used above. The second term in the parenthesis in (5.24) is a correction of the linear frequency Ω_p.

Remark. *To analyse the power system using NNM, the whole process presented in chapter 3 need not be completed since only specific terms are needed. Equations (5.23) contain only terms that are readily available from the beginning of the process. For instance Ω_p comes from linear analysis, A^p_{ppp} and B^p_{ppp} are just terms from quadratic change of variable see [(3.73), chapter 3], H^p_{ppp} is a nonlinear coefficient for self coupled terms, which can be selectively computed (see equation (5.28)). The above observation is a computational gain and makes this specific NF (i.e. NNM) method suitable for on-line applications.*

5.4.1 Example with SMIB Power System

Considering the SMIB power system used above, the first order model (5.19) is re-written in second order and expanded by Taylor series up to third order. Then the nonlinear coefficients are computed as explained in chapter 4 and the NF coefficients are computed for defining the NNM as explained in chapter 3. Then using the nonlinear frequency estimator (5.24), a frequency-amplitude (F-A) curve is produced for the range of amplitude 0 — 3 rads. This

curve should then be able to predict the nonlinear frequency of the system for any amplitude between 0 — 3 rads.

The F-A curve for the above description is shown in Figure 5.9. In Figure 5.8b, the maximum amplitude of the oscillation from SEP is 2.57 rad. With the analytical equation (5.24), this amplitude[2] gives a nonlinear frequency (NLF) of 4.20 rad/s, which is equivalent to 0.67 Hz and very close to the exact 0.65 Hz. The NLF 4.20 rad/s can be read easily from F-A curve for an amplitude of 2.57 rad. The F-A curve shows that the linear and nonlinear

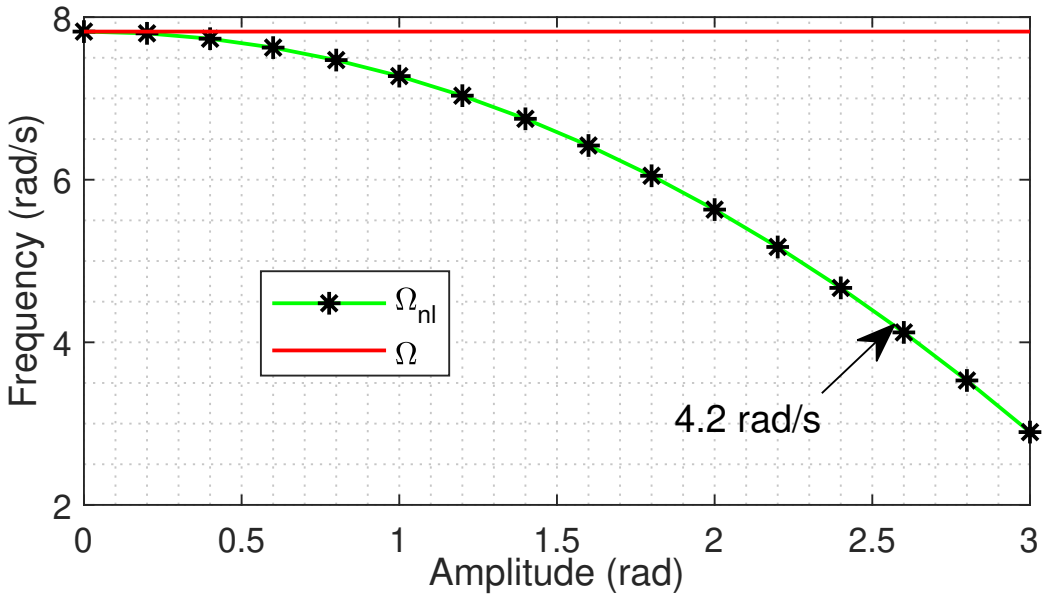

Figure 5.9 – F-A curve for the SMIB system

frequencies will be same for very small amplitudes. For larger amplitude (stressed condition), the linear analysis will not be effective, since it is based on small disturbance assumption. It can be seen that even though NF builds on the linear analysis, it adds extra information not possible with the linear analysis due to the nonlinearities accounted for.

5.4.2 Application to Multi-machine Power Systems

The power systems selected under this section are the IEEE 3-machine 9-bus system used in the previous chapters (i.e. Figure 2.1) and the IEEE 50-machine 145-bus power system used in chapter 4 (i.e. Figure 4.13).

[2] The amplitude in (5.24) is the amplitude of oscillation in NF coordinate (i.e. $R-S$ coordinate). For the SMIB example, the right eigenvector is equal to 1, hence, the amplitude in the original coordinate (i.e., $\delta-\Omega$ coordinate) is approximately the same as that of modal coordinate (i.e., $\eta-\varpi$) and approximately same in $R-S$ coordinate. For multi-machine system, the initial amplitude $\mathbf{R_0}$ ($R-S$ coordinate) can roughly be approximated as the modal amplitude $\boldsymbol{\eta_0}$ ($\eta-\varpi$ coordinate) with minimal error to avoid solving for NF initial conditions with many iterations.

As a quick reminder, the equation of motion for N generators of power system represented by 2nd order classical model can be written as (5.25).

$$M_i\ddot{\delta}_i + \bar{C}_i\dot{\delta}_i + P_{e_i} = P_{m_i} \tag{5.25a}$$

$$P_{e_i} = E_i^2\mathcal{G}_{ii} + \sum_{k=1,k\neq i}^{N} E_iE_k\left[\mathcal{G}_{ik}\cos\delta_{ik} + \mathcal{B}_{ik}\sin\delta_{ik}\right]. \tag{5.25b}$$

$M_i,\ \bar{C}_i\ , P_{e_i},\ P_{m_i},\ \delta_i$ have their meanings as defined in chapter 3. The damping constant $\bar{C}_i$ is set to zero for simplicity. To build the approximate nonlinear model of (5.25), it is expanded up to 3rd order, around a stable equilibrium point (SEP) of δ. Since loss of synchronism is determined by the relative angles $\delta_{iN} = \delta_i - \delta_N$ and not δ_i, the state variables are defined as δ_{iN} where generator N serves as a reference. Therefore, (5.25) comprises $N-1$ oscillators. The approximate model of (5.25) after setting damping to zero with equilibrium moved to the origin is of the form:

$$\boldsymbol{M\ddot{\delta} + K\delta + F2(\delta) + F3(\delta) = 0.} \tag{5.26}$$

where $\forall(i,j,k,l = 1\ldots N) : K_{ij} = \frac{\partial Pe_i}{\partial\delta_j}|_{\boldsymbol{\delta=\delta_0}},\ F2_{ijk} = \frac{1}{2}\frac{\partial^2 Pe_i}{\partial\delta_j\partial\delta_k}|_{\boldsymbol{\delta=\delta_0}},\ F3_{ijkl} = \frac{1}{6}\frac{\partial^3 Pe_i}{\partial\delta_j\partial\delta_k\partial\delta_l}|_{\boldsymbol{\delta=\delta_0}}$. The natural frequency Ω is obtained by solving the eigenvalue problem $(\mathbf{K} - \Omega_i^2\mathbf{M})\mathbf{\Phi}_i = \mathbf{0}$ and the modal model is obtained by the Jordan transformation

$$\boldsymbol{\eta = \Phi^T\delta}, \tag{5.27}$$

with its nonlinear coefficients defined $\forall(i,j,k,l,p,q,r,s = 1\ldots N)$ as:

$$G^p_{qr} = F2_{ijk}\Phi_{ip}\Phi_{jq}\Phi_{kr} \tag{5.28a}$$

$$H^p_{qrs} = F3_{ijkl}\Phi_{ip}\Phi_{jq}\Phi_{kr}\Phi_{ls}. \tag{5.28b}$$

Equations (5.28a) and (5.28b) are easily implemented without Taylor expansion of (5.26), using the method proposed in the previous chapter. Using the nonlinear coefficients, the nonlinear change of variables are defined and the NNM (5.23) are obtained for each oscillator. Then, for the desired oscillation amplitude, the nonlinear frequency is detected by (5.24).

Test on IEEE 3-Machine 9-Bus Power System

As discussed in chapter 2, the IEEE 3-machine 9-bus power system has two electromechanical modes of frequencies 13.72 rad/s (2.2 Hz) and 8.82 rad/s (1.4 Hz) for the given SEP. We consider two fault scenarios to excite the modes. A three phase fault applied at bus 9 makes

the first mode (i.e. mode 1=13.72 rad/s) dominant while a three phase fault at bus 4 makes the second mode (i.e. mode 2 = 8.82 rad/s) dominant. The faults were cleared near the critical clearing time (CCT), which are about 0.30s and 0.24s respectively. At the instant of clearing the fault, the rotor amplitudes are obtained (initial conditions) and scaled by the linear transformation (5.27), to obtain the modal amplitude needed for the analytical nonlinear frequency estimation proposed in (5.24).

The responses for the two fault conditions are presented in Figure 5.10. Figure 5.10a shows the response for the fault at bus 9. The response shows that mode 1 is predominant, since we know from chapter 2 that generator 1 (G1) and generator 2 (G2) swing together when mode 1 is excited. A *rough* estimation of the oscillation frequency from the curves using the first two peaks gives 12.50 rad/s. The estimation is rough because in the form of equations normally used in power systems, the angle differences contain harmonic terms, generally involving all fundamental frequencies of oscillation. Hence we have difficulty observing these frequencies in measured physical variables. In some situations, it is even difficult to identify the right peaks. However, in Jordan coordinate (i.e., modal model obtained after Jordan/linear transformation), all frequencies are separated [109]. Since higher order terms are included in nonlinear modal analysis, total separation of all frequencies is difficult due to nonlinear coupling. NF transformation helps to further remove these nonlinear coupling and provide clearer separation of frequencies. For this reason, the same initial condition is used to transfer the system to the modal coordinate (Figure 5.10c) and NF coordinate (Figure 5.10e). The two coordinates (i.e., $\eta - \varpi$ and $R - S$) clearly show the dominance of mode 1. The two plots seem very identical because of the level of nonlinearities, which is not evidently high. Later example will reveal the difference in the two coordinates. Note that the pre-fault condition is not included in the plots. The frequency of the response in $\eta - \varpi$ coordinate is 12.80 rad/s while the actual frequency in $R-S$ coordinate is 13.24 rad/s. With the same initial condition, the nonlinear frequency computed with the proposed equation (5.24) is 12.96 rad/s which is just 2.11% away from the actual value. Recall that in chapter 2, we observed the linear frequency ($\approx$ 13.72 rad/s) when this mode was excited because the disturbance was sufficiently small. Here, the linear frequency is decreased to 13.24 rad/s due to the disturbance. Interestingly, NF is able to predict this shift of frequency accompanying the large amplitude of the oscillation. The above observations are summarised in Table 5.6.

For the fault at bus 4, Figure 5.10b shows that mode 2 is dominant since from chapter 2 G1 and G2 swing in ant-phase with each other when mode 2 is excited. The figure also shows that mode 1 is also excited, though not at the same level as mode 2. A rough estimation of the frequency of the dominant mode from the curves gives 7.30 rad/s. As before, the system is

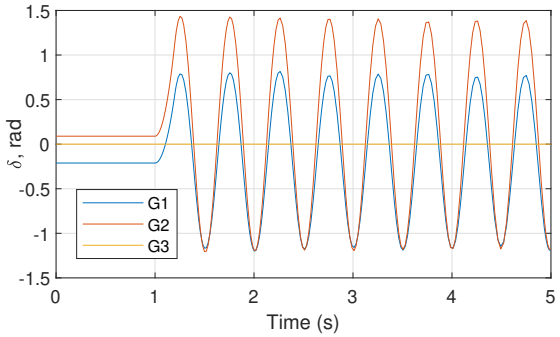

(a) Fault at Bus 9 —Original coordinate ($\delta - \omega$)

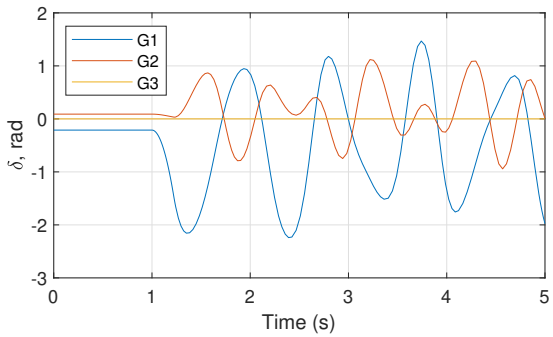

(b) Fault at Bus 4—Original coordinate ($\delta - \omega$)

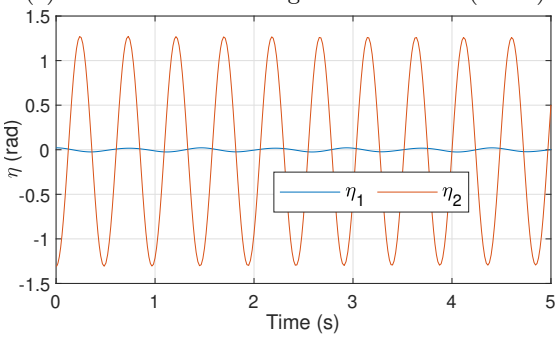

(c) Fault at Bus 9—Modal coordinate ($\eta - \varpi$)

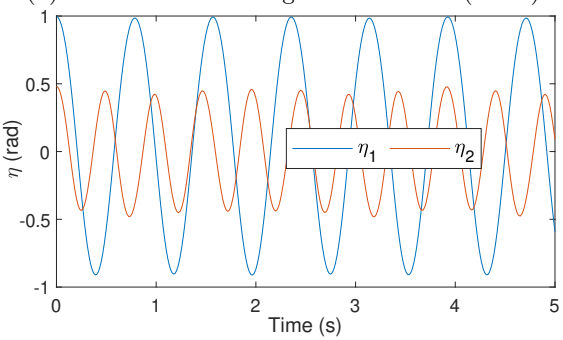

(d) Fault at Bus 4—Modal coordinate ($\eta - \varpi$)

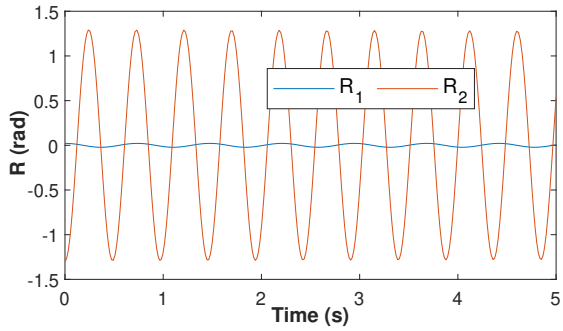

(e) Fault at Bus 9—NF coordinate ($R - S$)

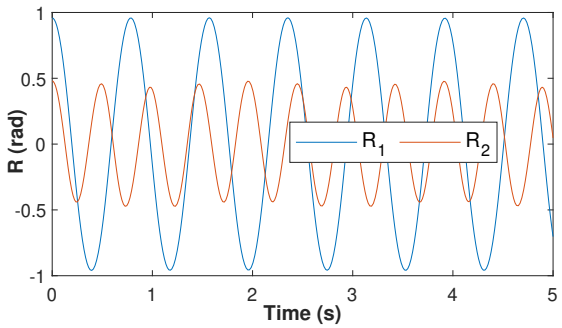

(f) Fault at Bus 4—NF coordinate ($R - S$)

Figure 5.10 – Oscillations during large disturbance for 9-Bus Power System

transferred to the modal coordinate (Figure 5.10d) and NF coordinate (Figure 5.10f), where the actual frequency of the dominant mode is obtained as 8.09 rad/s. With the analytical equation (5.24), the nonlinear frequency is estimated as 8.03 rad/s, an error of 0.05% (see Table 5.6).

Table 5.6 – Frequency–Amplitude Shifts for the 9-Bus Power System

Faulted Bus	Dominant Mode	Linear (rad/s)	Rough ($\delta - \omega$) (rad/s)	Actual ($R - S$) (rad/s)	Proposed (rad/s)	Error (%)
9	Mode 1	13.72	12.50	13.32	12.96	2.11%
4	Mode 2	8.82	7.30	8.09	8.03	0.05%

Test on IEEE 50-Machine 145-Bus Power System

Firstly, the conventional modal analysis was performed and the natural modes are listed in Table 5.7. The third, sixth, and ninth columns of Table 5.7 give the natural frequencies in Hertz (Hz). We know from previous studies that mode 44 (i.e., 2.80 rad/s) is an inter-area

Table 5.7 – Natural Modes for 145-Bus Power System

#	Ω (rad/s)	(Hz)	#	Ω (rad/s)	(Hz)	#	Ω (rad/s)	(Hz)
1	31.72	5.05	21	13.09	2.08	41	1.32	0.21
2	25.85	4.11	22	12.68	2.02	42	2.09	0.33
3	26.67	4.24	23	12.51	1.99	43	1.85	0.29
4	21.87	3.48	24	12.00	1.91	44	**2.80**	0.45
5	20.31	3.23	25	11.32	1.80	45	3.08	0.49
6	17.89	2.85	26	10.18	1.62	46	3.37	0.54
7	17.75	2.83	27	9.82	1.563	47	3.76	0.60
8	16.35	2.60	28	9.24	1.47	48	3.53	0.56
9	15.44	2.46	29	8.46	1.35	49	3.66	0.58
10	15.19	2.42	30	8.35	1.33			
11	15.09	2.40	31	8.25	1.31			
12	14.97	2.38	32	7.65	1.22			
13	14.29	2.28	33	7.95	1.27			
14	14.32	2.28	34	8.04	1.28			
15	14.05	2.24	35	6.75	1.07			
16	13.82	2.20	36	5.65	0.90			
17	13.76	2.19	37	5.34	0.85			
18	13.34	2.12	38	5.21	0.83			
19	13.36	2.13	39	4.68	0.74			
20	13.26	2.11	40	4.44	0.71			

mode with participation from all the generators, although the participations of machines to most local modes are far more than that in the inter-area mode. For example, mode 8 is a local mode with very large participation from generator 7 and close-to-zero participation from other generators. A fault at bus 7 leads to very high amplitude oscillation associated to mode 8 and leads to instability. Also, previous studies indicate that a fault at bus 1 excites both local and inter-area modes, and can lead to separation of some generators from others. In this section, two scenarios are considered—(1) fault at bus 7 with local mode 8 as dominant and (2) fault at bus 1 with significant excitation of several local and inter-area modes.

The responses due to the above two fault scenarios are shown in Figure 5.11. For fault at bus 7, Figure 5.11a indicates that generator 7 (G7) is most affected as the amplitude of oscillation is significantly high with respect to other generators. A rough estimation of the frequency of this oscillation from the figure is 14.06 rad/s. Figure 5.11c and Figure 5.11e show the transformation of the system to modal and NF coordinates respectively. Both figures indicate that mode 8 is predominantly excited. The actual frequency of mode 8 (i.e.,

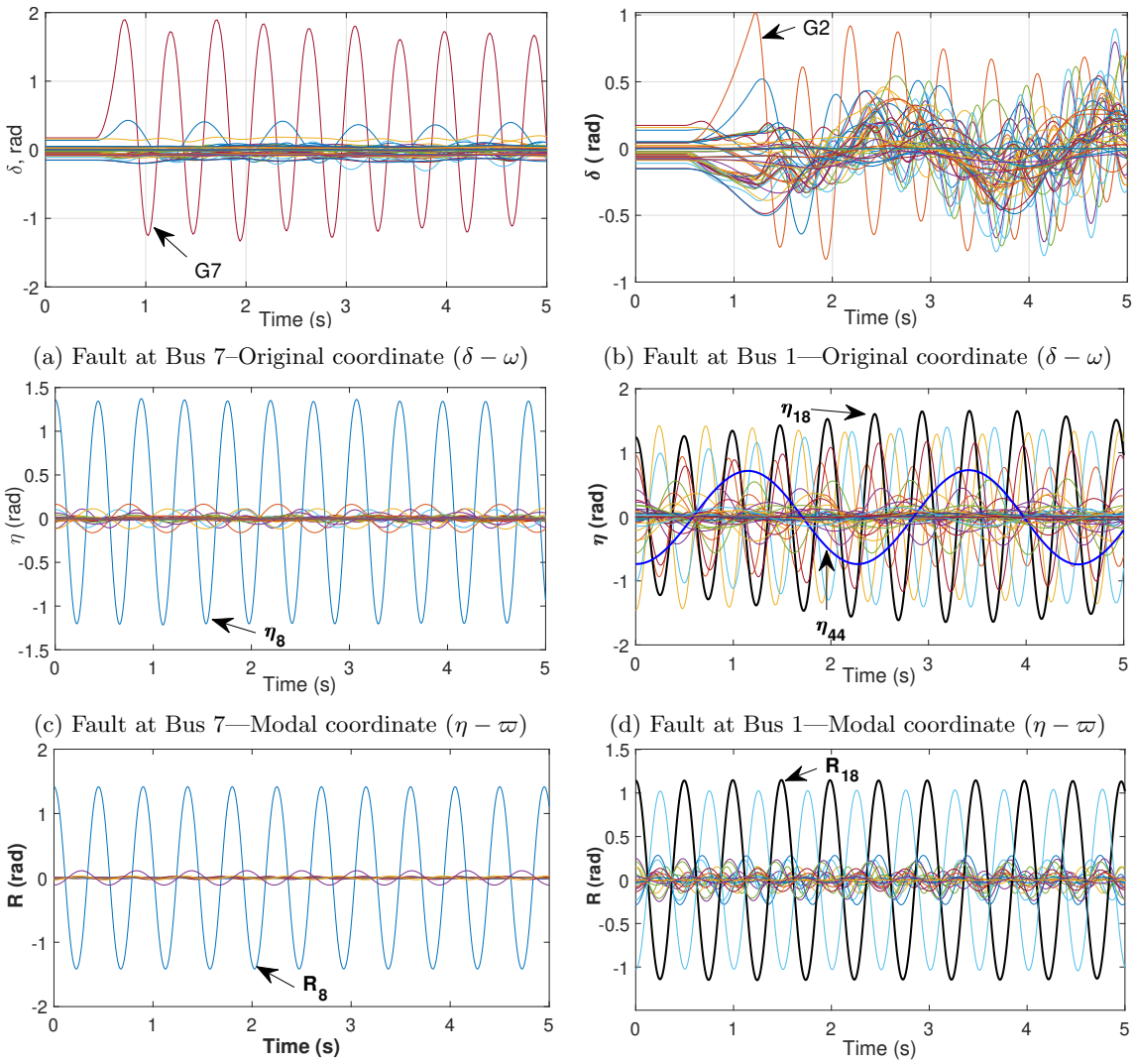

(a) Fault at Bus 7–Original coordinate ($\delta - \omega$)

(b) Fault at Bus 1—Original coordinate ($\delta - \omega$)

(c) Fault at Bus 7—Modal coordinate ($\eta - \varpi$)

(d) Fault at Bus 1—Modal coordinate ($\eta - \varpi$)

(e) Fault at Bus 7—NF coordinate ($R - S$)

(f) Fault at Bus 1—NF coordinate ($R - S$)

Figure 5.11 – Oscillation during large disturbance for 145-Bus Power System

from $R - S$ coordinate) is obtained as 14.16 rad/s. With the analytical method proposed in equation (5.24), the nonlinear frequency is calculated as 14.33, rad/s which incurs an error of 1.2%. This frequency is closer to the actual frequency, compared to the linear one which is 16.35 rad/s (see Table 5.7).

For fault at bus 1, Figure 5.11b shows that the oscillation is complicated, as many generators are affected and several modes significantly excited. Generator 2 (G2) has the highest amplitude in the first swing. A rough estimation of the oscillation frequency of the dominant mode, using G2, yields 12.27 rad/s. As in the previous cases, the system is transformed to the modal coordinate as shown in Figure 5.11d, which also show that several modes including the inter-area mode (mode 44) are significantly excited. We pay attention to Mode 18, which can be considered most excited since it shows growing oscillation. Taking mode 18 as most dominant, the frequency in the modal coordinate is estimated from the figure as 12.96 rad/s. Figure 5.11d shows clearly, that even though linear couplings are removed by the Jordan

transformation, there are still strong nonlinear couplings as we see several modes excited, almost with similar amplitudes. The system is further transformed to the NF coordinate as shown in Figure 5.11f, which becomes clearer as a result of the simplification of the nonlinearities. We see that only two most dominant modes have higher amplitudes, the rest become *slaves*. We pay attention to mode 18, which has actual frequency in this NF coordinate as 12.56 rad/s. The nonlinear frequency calculated from the proposed method is 12.30 rad/s, which is an error of 2.07%. The summary of the above analysis is presented in Table 5.8.

Table 5.8 – Frequency–Amplitude Shifts for the 145-Bus Power System

Faulted Bus	Dominant Mode	Linear (rad/s)	Rough $(\delta - \omega)$ (rad/s)	Actual $(R - S)$ (rad/s)	Proposed (rad/s)	Error (%)
7	Mode 8	16.35	14.06	14.16	14.33	1.20%
1	Mode 18	13.34	12.96	12.56	12.30	2.07%

5.4.3 Practical Significance of Frequency Shift Monitoring

Traditional power system modal analysis pays less attention to this frequency-amplitude shift phenomenon which can have some adverse effects on the system. As shown in section 5.3, both machine loading and large disturbance lead to decrease in the oscillation frequency and damping. The decrease in frequency is gradual and seems minimal initially. However, close to the knee point, it drops sharply (see Figure 5.7). Since the decrease of oscillation frequency is accompanied by decrease in damping, power system control usually focus on detecting the low damping situation, which are then addressed by the damping controllers such as PSS or other modulation-based methods. Modern power system control focuses on oscillation monitoring using real time measurements. One objective of a Wide Area Measurement System (WAMS) is to provide critical information regarding the system's oscillatory behaviour. Hauer *et al.* [126] discussed the potentials of any measurement-based approach that automatically estimates mode parameters (e.g., frequency and damping) in near real time for system operation and control applications. Such method is called *Mode Meter* methods [126]. In Mode Meter technologies, accurate monitoring of frequency is paramount since parameters of a mode can change and become close to that of another known mode in the system. This can lead to identification problem, especially if the damping is not perfectly determined. Hence, mode frequency monitoring by NF can be a complementary tool in Mode Meter technology.

A practical example is the massive breakup experienced by the western interconnection on August 10, 1996. The mechanism of failure was suggested to be a transient oscillation, under conditions of high power transfer on long paths that had been progressively weakened through a series of seemingly routine transmission line outages [126]. Measurement-based

studies revealed that the 0.25-Hz oscillation, which was indicative of the impending breakup, resulted from progressive decrease of the oscillation frequency from 0.27 Hz to 0.25 Hz, and the oscillation damping ratio, from 7.0% to 1.2% (see Figure 5.12).

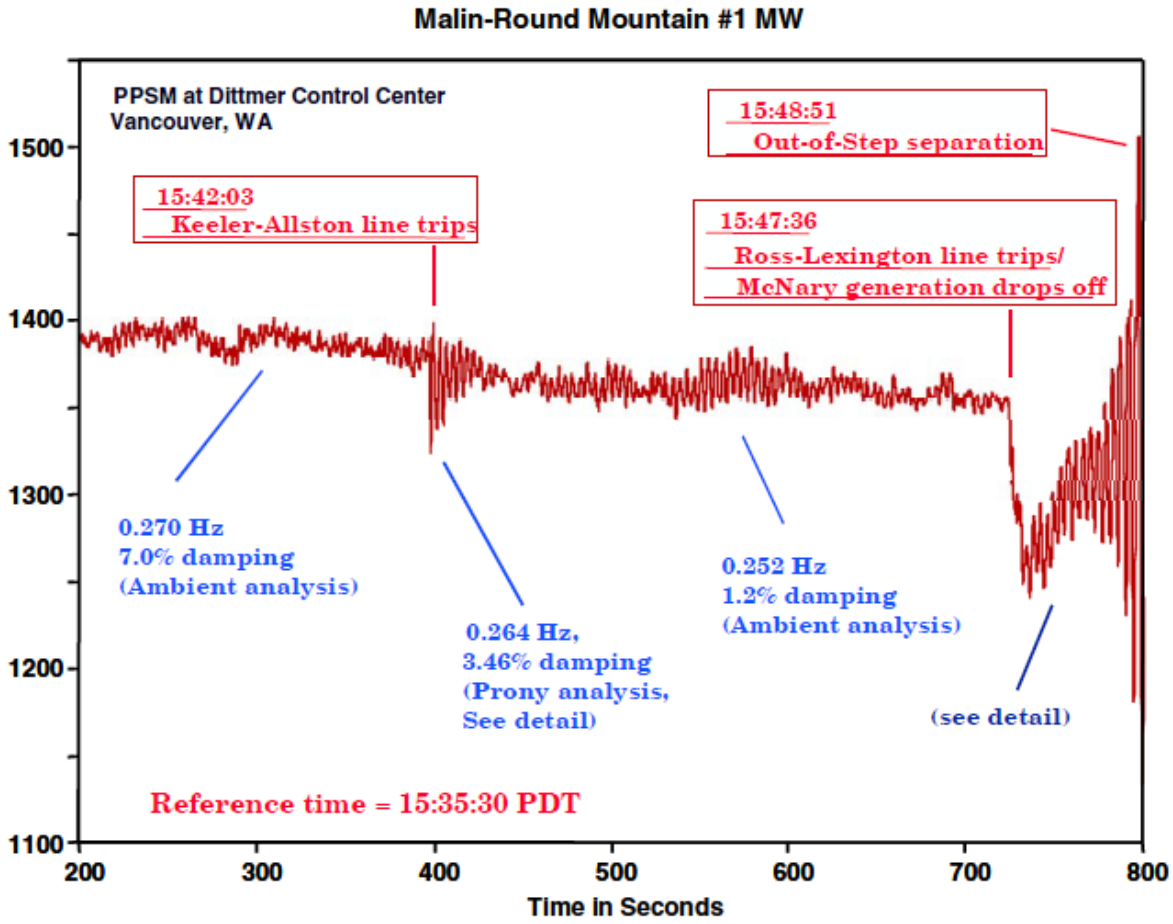

Figure 5.12 – Oscillation buildup for the WSCC breakup of August 10, 1996 [126]

5.5 Transient/Mode's Stability Estimation using Normal Form

In chapter 1, we saw that the stability of the power system following large disturbance is known as transient stability. One of the main advantages of the modal analysis is that it allows the expression of the dynamic behaviour of the power system with *modes*. The stability of the power system is in essence, the stability of the modes in the system. In this section, we will explore the application of NF to the monitoring of the oscillation mode's stability under large disturbance, so-called transient stability monitoring. In the previous chapters, nonlinear normal mode (NNM) theory was used to obtain a decoupled system, where each machine is represented by one degree-of-freedom oscillator. The decoupled system was used to obtain an analytical expression for nonlinear frequency (NLF) of electromechanical modes under disturbance in the previous section. Here, we use the expression for the NLF to define

an instability proximity index, which estimates the system's stability by investigating the proximity of NLF of each mode to the defined index during disturbance. Tests on the IEEE 3-machine and 50-machine power systems give good results and reveal the potency of the proposed method for warnings of instability.

5.5.1 Motivating Example with SMIB Power System

Still with the same SMIB power system used in the previous sections, we consider a motivating example. Recall that the SEP is $\frac{\pi}{12}$ rad and the stability bound from EAC is 2.88 rad. After certain disturbances, the system behaviour is approximated by 3rd order Taylor expansion, transformed to NNM (5.23a)—(5.23c) and finally reconstructed to the original coordinate using the processes outlined in chapter 3. The time-domain simulations (TDS) of the disturbances are shown in Figure 5.13. Figure 5.13a is a case where the rotor angle is within the stability bound and reveals that NNM3 (green curve) provides best approximation. In Figure 5.13b the rotor angle reaches the stability bound and NNM3 maintains constant value as the exact solution for sometimes before it goes unstable. The linear (dashed red curve) and NNM2 (blue curve) show stability in contrast. In Figure 5.13c, the rotor angle goes beyond the stability bound and both NNM3 and Exact (black curve) solutions show instability while NNM2 and linear solutions indicate stability.

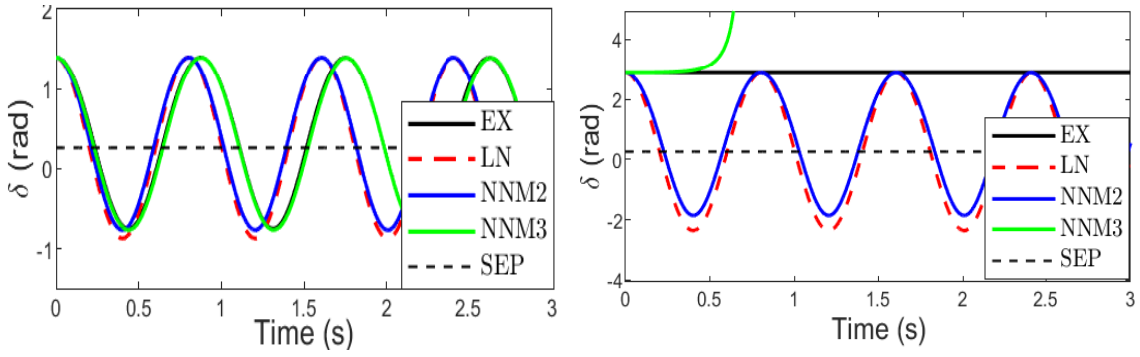

(a) Oscillation within boundary

(b) Oscillation at boundary

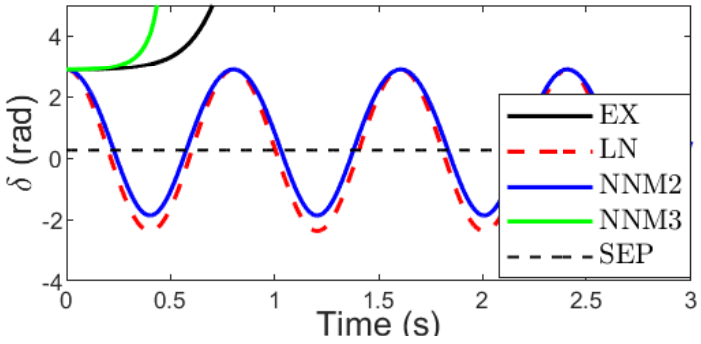

(c) Oscillation exceeds boundary

Figure 5.13 – Rotor angle for different approximations and operating points (SMIB)

The above observations show that NNM3 retains enough nonlinear characteristics of the nonlinear system and could offer a good insight into the stability of the original system. Moreover, NNM3 decouples the multi-machine system into equivalent SMIB-like oscillator systems, so that the stability of each oscillator can be accessed separately.

5.5.2 NF Stability Assessment Index

We repeat the p-th mode's frequency-amplitude relation (5.24) here for emphasis.

$$\begin{aligned} \Omega_{p_{nl}} &= \Omega_p \left(1 + \Xi_p \Pi^2\right) \\ \Xi_p &= \frac{3(A^p_{ppp} + H^p_{ppp}) + \Omega_p^2 B^p_{ppp}}{8\Omega_p^2}. \end{aligned} \tag{5.29}$$

For a stable mode, the increasing amplitude Π leads to a decreasing nonlinear frequency $\Omega_{p_{nl}}$ as shown previously in Figure 5.9. The descent of the NLF gets to a critical point (knee point) beyond which the mode looses stability. To estimate the critical NLF, it is necessary to estimate the critical amplitude. In a stable power system, if the rotor angle δ reaches its maximum, $\dot{\delta} = 0$ and the net torque on the rotor starts retarding. Therefore, if $\dot{\delta} = 0$ at the stability bound, then $\dot{R} = 0$ in the NF equation (5.23b) and invariably $\dot{S} = 0$ in (5.23c). Then for p-th mode, (5.23c) becomes

$$0 = -\Omega_p^2 R_p - (A^p_{ppp} + H^p_{ppp}) R_p^3 \tag{5.30}$$

$$\therefore \quad R_{p_{cr}} = R_p = \sqrt{\frac{-\Omega_p^2}{(A^p_{ppp} + H^p_{ppp})}}, \tag{5.31}$$

where $R_{p_{cr}}$ stands for the critical amplitude of p-th mode in the NF coordinate. One way to assess stability is to construct transient energy function, using the roots of (5.30). This however, will lead to very deceptive results for this case because (5.31) is a function of the operating modal frequency, which requires that the linear analysis be repeated for every disturbance. Alternatively, we use $R_{p_{cr}}$ from (5.31) to compute the critical NLF from (5.24). Therefore, we define a critical frequency shift (CFS) from (5.24) as:

$$CFS_{p_{cr}} = \Omega_p \left(1 + \Xi_p R_{p_{cr}}^2\right). \tag{5.32}$$

To ascertain stability:

1. Obtain the pre-fault equilibrium condition and project it to NF coordinate to obtain NNM (5.23c).

2. Using (5.31), compute critical displacement $R_{p_{cr}}$ for p-th mode satisfying (5.30) and

compute $CFS_{p_{cr}}$ with (5.32).

3. For a fault, obtain the deviations immediately the fault is cleared and transform to modal coordinate using (5.27). This is the initial condition in modal coordinate.

4. Obtain $R_{p_{cl}}$ with the technique discussed in chapter 3, where *cl* represents *after fault is cleared*. This is the initial condition in NF coordinate[3]

5. With $R_{p_{cl}}$ determined, obtain the $CFS_{p_{cl}}$ using (5.32).

6. If $CFS_{p_{cl}} < CFS_{p_{cr}}$, the post-disturbance condition is assessed to be stable otherwise it is not.

The proposed method may incur at least three kinds of error—(1) error due to model reduction; (2) error due to truncation order; and (3) error due to modal interactions. The results from classical models may not always be exact with the detail modelled power system. A third order truncation is only a compromise for computational burden; close to stability bound, higher order terms may be important. Simplification to NNM (5.23) is more valid when the initial conditions for $k \neq p$ is zero. When all the initial conditions are not zero as is the case when fault is cleared, the interaction of modes may be significant. As noted in chapter 1, the effects of modal interactions can be negative or positive. Because of the above reasons, instability determined by the proposed method may be *conservative* (true instability occurring later than the proposed) or *optimistic* (true instability occurring sooner than the proposed). Since the initial condition for $k \neq p$ is not zero for multi-machine system under disturbance, the effects of other modes will set CFS_p farther than would be for a classical SMIB power system which has only one mode. To address this challenge we introduce a shrinking factor to shrink the cumulative effects of all modes to the particular mode of interest. The shrinking factor is discussed in next paragraph.

Following the definitions in [127], the modal mass $m_p^* = \Phi_p^T \mathbf{M} \Phi_p$ is equal to the sum of (mass)× (mode displacement)^2 for each mode ($m_p^* = \sum_{q=1}^{N} m_q \Phi_{pq}^2$). Similarly, the modal stiffness $k_p^* = \Phi_p^T \mathbf{K} \Phi_p$ is the sum of the strain energy stored at each oscillator and the total strain energy indicates that $k_p^* = m_p \Omega_p^2$, where all parameters have their previously defined meanings. Therefore we define

$$STE_{p_l} = m_p \Omega_p^2 \tag{5.33a}$$

$$STE_{p_{nl}} = m_p \Omega_{p_{nl}}^2, \tag{5.33b}$$

[3]Step 4 above implies iterative solving of nonlinear equations which is not desirable for on-line application. For a motion initiated in p-th path, $R_k = 0$, $\forall k \neq p$ in [see (3.74), chapter 3]. This makes the solution of R_p very near to η_p so that further rough approximation $R_p \approx \eta_p$ can be made if the the operating point is not too far from SEP.

where STE_{p_l} is the total modal strain energy for the linear frequency of mode p and $STE_{p_{nl}}$ is the total modal strain energy for the nonlinear frequency of mode p. The shrinking factor is thus defined for p-th mode as

$$S.F = \frac{STE_{p_{nl}}}{STE_{p_l}}. \tag{5.34}$$

Therefore, for any fault condition, (5.32) is redefined as

$$CFS_{p_{cl}} = \Omega_p \left(1 + \Xi_p R_{p_{cl}}^2\right) \times S.F. \tag{5.35}$$

Then the instability proximity index (IPI), which measures how far the operating point is from instability is defined as

$$IPI_p = \left(\frac{CFS_{p_{cl}}}{CFS_{p_{cr}}} - 1\right) \times 100\%. \tag{5.36}$$

Later, the results will show that IPI gives tolerable errors for the considered model. It is important to note that the stability determined this way is limited to the validity of the approximation and the generator model used, and therefore, cannot be a global stability. Numerical simulations are presented in the following sections to test the proposed method.

Test on IEEE 3-Machine 9-Bus Power System

A three phase fault is added to bus 4 and cleared at increasing time by removing the fault until instability. The values of CFS and IPI after each clearing time are listed in Table 5.9. The critical clearing time (CCT) obtained by TDS in MATLAB® is $t < 0.24$ s. As seen from

Table 5.9 – Stability Assessment for the 9-Bus Power System (Fault at Bus 4)

T_{cl} (s)	Mode 1 (rad/s)			Mode 2 (rad/s)		
	$\text{CFS}_{1_{cl}}$	$\text{CFS}_{1_{cr}}$	IPI_1	$\text{CFS}_{2_{cl}}$	$\text{CFS}_{2_{cr}}$	IPI_2
0.05	13.71	8.55	60.35%	8.81	5.44	62%
0.15	13.65	8.55	59.65%	8.32	5.44	52.94%
0.22	13.41	8.55	56.84%	6.67	5.44	22.61%
0.24	13.30	8.55	55.56%	5.89	5.44	8.27%
0.25	13.22	8.55	54.71%	5.36	5.44	**-1.47**%

T_{cl} = clearing time. Actual CCT = 0.24 s

Table 5.9, the CCT with the proposed method is $t < 0.25$ s which is fair. The results show that mode 2 is less stable than mode 1 under the studied contingency. This can be observed from the table as the frequency of mode 2 drops faster as the stress increases while that of mode 1 decreases slowly. This is consistent with the previous simulations (Figure 5.10), which showed that mode 2 is more excited when fault is added to bus 4.

A second case is considered by adding a three phase fault to bus 9 and clearing at increasing time by removing the fault until instability occurs. The values of CFS and IPI after each clearing time are listed in Table 5.10. The table shows that the proposed method predicted instability at CCT of $t < 0.26$ s which is earlier than the TDS (i.e., 0.3 s). It can also be seen from the table that the local mode 1 is driving the instability in this case. The nonlinear frequency of mode 2 is unchanging as the stress increases. This is equally consistent with the previous simulations (Figure 5.10), where we saw that mode 1 is not significantly affected by fault at bus 9. These observations emphasise the need to monitor all modes, whether they are critical modes or not, since the stability of a mode is also dependent on the location of the disturbance.

Table 5.10 – Stability Assessment for the 9-Bus Power System (Fault at Bus 9)

T_{cl} (s)	Mode 1 (rad/s)			Mode 2 (rad/s)		
	$\text{CFS}_{1_{cl}}$	$\text{CFS}_{1_{cr}}$	IPI_1	$\text{CFS}_{2_{cl}}$	$\text{CFS}_{2_{cr}}$	IPI_2
0.15	13.00	8.55	52%	8.81	5.44	62%
0.22	10.67	8.55	25%	8.81	5.44	62%
0.24	9.58	8.55	12%	8.81	5.44	62%
0.25	9.00	8.55	4.78%	8.81	5.44	62%
0.26	8.30	8.55	**-2.9**%	8.81	5.44	62%

T_{cl} = clearing time. Actual CCT = 0.3 s

Test on IEEE 50-Machine 145-Bus Power System

In this case, we consider the two scenarios already considered in the previous section—(1) fault at bus 7 with local mode 8 as dominant and (2) fault at bus 1 with significant excitation of several local and inter-area modes.

Table 5.11 lists the results of mode stability monitoring for fault at bus 7, using the proposed method. Mode 8 is the first to exhibit instability, hence, only the stability of mode 8 is presented in Table 5.11. With TDS in MATLAB® , the first instability occurs at 0.27 s, where generator 7 goes out of synchronism with the rest (see Figure 5.14). It is found that at clearing time of 0.26 s, mode 8 goes unstable with $\text{CFS}_{8_{cl}}$ exceeding the critical value.

For the second case of fault at bus 1, only mode 18 is monitored as it encountered instability first. The results are listed in Table 5.12. The results show that the stability is lost if the fault is cleared after 0.9 s. The actual time-domain simulation in MATLAB® shows that at CCT $t \geq 1.2$ s, the system looses stability with some generators separating from others (see Figure 5.15).

Table 5.13 gives detailed comparison of proposed method with TDS, for some cases con-

Table 5.11 – Stability Assessment for the 145-Bus Power System (Fault at Bus 7)

T_{cl} (s)	Mode 8 (rad/s)		
	$\text{CFS}_{8_{cl}}$	$\text{CFS}_{8_{cr}}$	IPI_8
0.15	15.27	9.05	68.79%
0.22	11.78	9.05	30.20%
0.24	10	9.05	12.40%
0.25	9.27	9.05	2.48%
0.26	8.33	9.05	**-7.97%**

T_{cl} = clearing time. Actual CCT = 0.27 s

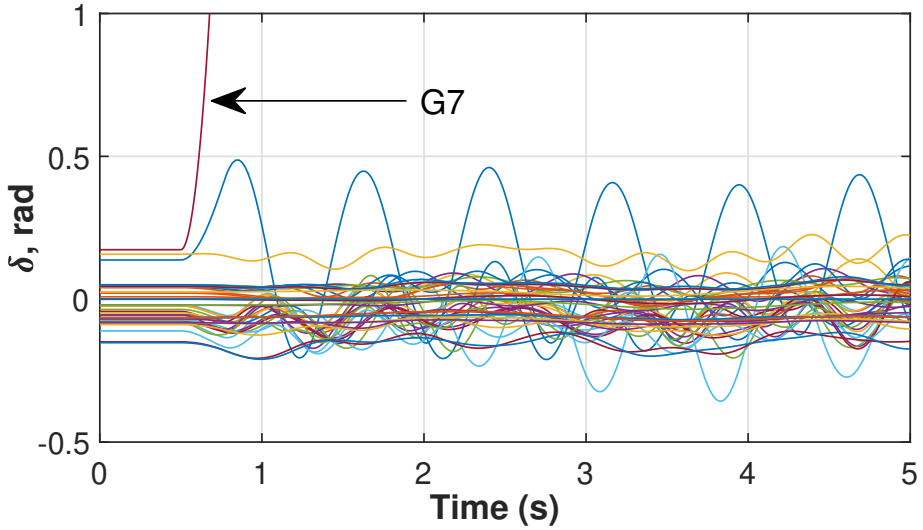

Figure 5.14 – Marginally unstable system at 0.27 s clearing time for fault at bus 7 (145-bus power system)

Table 5.12 – Stability Assessment for the 145-Bus Power System (Fault at Bus 1)

T_{cl} (s)	Mode 18 (rad/s)		
	$\text{CFS}_{18_{cl}}$	$\text{CFS}_{18_{cr}}$	IPI_{18}
0.15	13.33	8.21	62.36%
0.22	13.30	8.21	61.99%
0.40	12.88	8.21	56.90%
0.60	11.31	8.21	37.81%
0.80	8.34	8.21	1.55%
0.90	6.42	8.21	**-21.80%**

T_{cl} = clearing time. Actual CCT = 1.2 s

sidered. The errors incurred are tolerable for the case tested. However, like all NF approximations, the results are only reliable within the boundary of validity of the approximation.

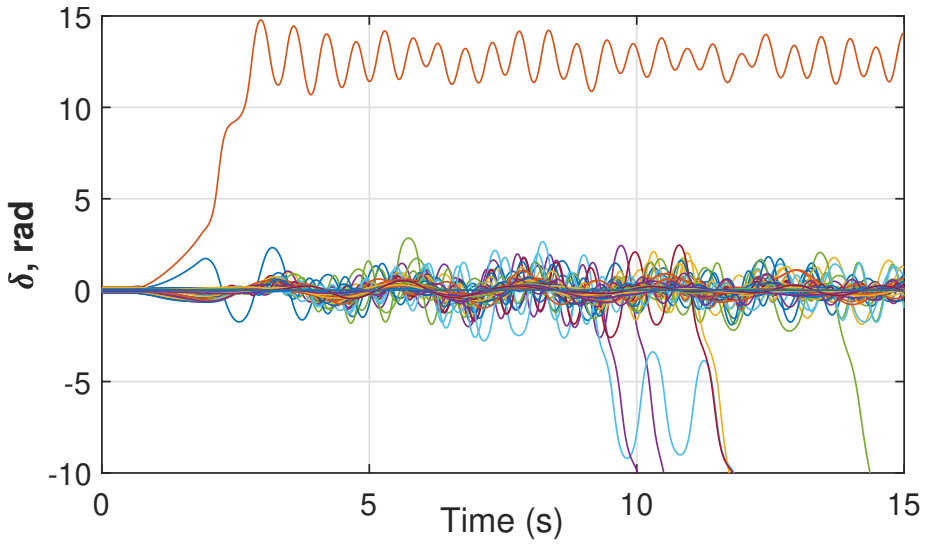

Figure 5.15 – Unstable system at 1.2 s clearing time for fault at bus 1 (145-bus power system)

Depending on the fault locations and the severity, proposed method may incur very significant error. The fact that large disturbance is discussed does not mean that the proposed method will still work when the operating point is extremely far from SEP. Also, as seen for the error in the case of fault at bus 1 of the 145-bus power system, the proposed method can be "blinded", if several modes, are significantly excited. Therefore, the proposed method should be used for warning signals of mode instability.

Table 5.13 – CCT—Proposed Method Vs TDS for some cases

Bus	Case	TDS	Proposed Method	Error
4	IEEE 9-Bus	$t < 0.24$s	$t < 0.26$s	8.30%
7	IEEE 9-Bus	$t < 0.29$s	$t < 0.32$s	10.34%
9	IEEE 9-Bus	$t < 0.30$s	$t < 0.26$s	13.30%
7	IEEE 145-Bus	$t < 0.27$s	$t < 0.26$s	3%
1	IEEE 145-Bus	$t < 1.20$s	$t < 0.90$s	25%

5.5.3 Computational complexity of the Proposed Method

Computationally, the proposed method is far simpler than conventional NF performed at first order. The approximate model is built once and only repeated whenever power flow is repeated. With 3520M 2.9GHz laptop computer, the overall time elapsed in the case of 50-machine system, for all the modes is 451s ($\approx$ 7.5 minutes), while the time to build the approximate model is 131s ($\approx$ 2 minutes). Even if it is needed to rebuild the approximate model, 7.5 minutes is not expensive and can be routinely done in power system operation. This time is drastically reduced when only some selected modes are analysed. The proposed method is suitable for on-line assessment, especially when focus is on vulnerable modes. A

computational comparison with similar works [82, 83] where the approximate model is built with first order model is shown in Table 5.14. Since the transformations are not the same, only time to build the approximate models is considered. It could be seen that the time saved by avoiding first order representation initially is huge, especially as the system size increases.

Table 5.14 – Computational benefits of proposed method

Case	[82, 83]		Proposed Method		
	No. Var.	Time (s)	No. Var.	Time (s)	TSF*
IEEE 9-bus system	5	0.120	3	0.029	4
IEEE 39-bus system	19	2.80	9	0.195	14
IEEE 145-bus system	99	15,355	49	131	117

No. var = number of variable; TSF=time saving factor

5.5.4 Practical Application of the NF-Based Stability Estimation

The proposed method has potential for on-line application and can be used by power system operators to make quick and rough estimation of modes' proximity to instability. Since NF analysis is based on truncated Taylor series approximation, the stability determined by the proposed method cannot represent a global solution. Although the proposition is based on classical model, it is important to note the following points about the method: (1) nature of electromechanical oscillation is same, irrespective of the model. Detailed model does add more information to the classical model, especially in the damping of the modes, but the frequencies do not change significantly; (2) the stability can be wrongly accessed with the proposed method but it correctly identifies the vulnerable modes due to a disturbance.

For practical application, we recommend that the proposed method be run routinely (say every 15 minutes) in the power system operation for warning signals. Once a warning flag is raised by the proposed method, other more robust approaches can be used to analyse the particular mode in detail for appropriate control actions.

5.6 Summary

In this chapter, some applications of Normal Form analysis have been explored. Tests have been done on both small and *large* power systems. The computationally-reduced method developed in the previous chapter has been used throughout the present chapter.

Firstly, proposals for further reduction of Normal Form computation, by focusing only on some selected terms are made. Two proposals were made — one which consists in neglecting interaction associated to real eigenvalues in the building of NF model and the other, which

consists in neglecting interactions associated to modes with least energy. These treatments drastically reduce the computational burden and accelerate the study of modal interaction. The extension of linear analysis to nonlinear participation factors arising from the modal interactions are also presented. The practical applications of modal interactions and possible concerns were equally discussed.

Secondly, didactic examples were used to explain the phenomenon of nonlinear frequency shifts when power systems experience disturbance. It was demonstrated that during disturbance (or increasing system stress), the frequency of an oscillation is dependent on the oscillation amplitude and can reduce, contrary to the assumption of the linear modal analysis. It was shown that the reduction of the frequency of an oscillation mode is linked to the mode's instability.

Thirdly, a method is proposed based on Normal Form, which is able to monitor an oscillation mode and detect its frequency whenever there is a disturbance. This new frequency due to disturbance is termed nonlinear frequency. Test cases showed that the proposed method captures the nonlinear frequency shift of the oscillation under disturbance with minimal error. The practical applications of the method for on-line dynamic assessments of power systems were discussed.

Finally, a mode instability monitoring method was proposed based on the nonlinear frequency, having established a relationship between the nonlinear frequency and mode's instability. The instability monitoring method consists in searching for a critical nonlinear frequency beyond which the mode loses stability, so-called critical frequency shift (CFS). With the CFS of all modes determined, an instability proximity index (IPI) was proposed which monitors how close the operating point is to instability. The comparison of the proposed method and the time-domain simulations for the tested cases showed the error of the proposed method to be fair. The potential of the proposed method for on-line applications and warning signs of mode's instability were discussed.

In the next chapter, we will connect all the developments from the first chapter to the present chapter in order to draw some conclusions.

Chapter 6

Conclusions and Future Works

"*Ends are not bad things, they just mean that something else is about to begin. And there are many things that don't really end, anyway, they just begin again in a new way. Ends are not bad and many ends aren't really an ending; some things are never-ending.*"

C. JoyBell C.

Contents

6.1 Conclusions

With all the known potentials of Normal Form method for better analysis of stressed power systems and systems exhibiting strong nonlinear behaviour, the goal of the this work has been to fast-track Normal Form application processes in order to position it as a useful tool for future grid. In this work a computationally-improved method for deriving third order Normal Form representations in the neighbourhood of equilibrium points is presented. The method has employed eigenmodes' properties and careful perturbation of the nonlinear model to avoid certain computationally-difficult steps in Normal Form analysis. Using the conventional methods for obtaining the Normal Form model requires the implementation of higher order Taylor expansion of the nonlinear model. This expansion leads to the computation of higher order Hessian matrices and the projection of the eigenmodes onto the expanded system. For systems with small number of variables, these operations are convenient; but when considering large scale systems they are computationally expensive, and even impracticable. A more efficient method has therefore been developed to extend Normal Form application to larger and future power systems. In addition to the proposed method, new proposals are made to allow for selective Normal Form application which leads to further computational reduction. Furthermore, based on the nonlinear approximate models, analytical criteria have been developed to monitor the stability of electromechanical modes and their frequency shifts during disturbance. The theory, analysis, results, and observations presented in this thesis can be summarised as follows:

1. The conventional Normal Form method and theories were first recalled. In the application of third order Normal Form in power system, firstly, the nonlinear model is expanded by Taylor series up to third order and the Hessian matrices are evaluated for the given operating point. The resulting approximate model is transformed to Jordan form, using the eigenvector/eigenvalues computed from the first order part of the Taylor expansion. The coefficients of the Jordan model, called in this thesis nonlinear coefficients, are determined. Finally, a nonlinear change of variable is defined to remove the nonlinear terms in the Jordan model, which put the resulting nonlinear approximate model in normal form. Based on this model analytical indices can be defined to understand the effect of the nonlinear interactions when the system is stressed.

2. In the case of the developed method, the linear analysis is first performed to extract the eigenvalues/eigenvectors. Then, the original nonlinear system is perturbed in such a way that certain desired modes or combinations of modes are excited using scaled eigenvectors. The scaling factor is the amplitude of the modal perturbation, and is

chosen, such that the anticipated nonlinearities due to the perturbation are within third order Taylor approximation. The static solution of the nonlinear system due to the perturbation is obtained. Different excitations allow the formulation of linear system of equations, whose coefficients correspond to the desired nonlinear coefficients and whose second member corresponds to the static solution of the nonlinear system. In this way, any desired coefficients can be computed without the actual Taylor expansion and computation of Hessian matrices. The developed method was applied to power systems represented with second order differential equations, where all quantities are real-valued, and as well as, to power systems represented with first order differential equations, where computed quantities are complex-valued.

3. The computations with the developed method are compared with computations using symbolic toolbox. The time-domain simulations for models built from the two computations were also compared. From the results presented in chapter 4, the following observations are made:

   - The proposed method is highly accurate, recording an error of $1.83e^{-3}\%$ as the highest error in all tested cases, and simulations from both the proposed and symbolic methods under severe stress conditions are matching.
   - Computations with the proposed method are very fast and memory economical, compared with symbolic method. The results showed that with increased number of variables in the system, the proposed method becomes incomparable with the symbolic method. For compared cases, the proposed method can be 776 times faster and $1.52e^{3}$ times less costly (in terms of memory) than the symbolic method. This computational economy is firstly due to the avoidance of Hessian matrices and higher order differentiation; and secondly, due to the fact that the proposed method obtains all coefficients by solving sets of linear equations which are computer-friendly. This observation is good, since the new method can now extend the size of the system that can be considered with third other Normal Form. Furthermore, future power systems will be full of power electronic converters which have several state variables, needing the use of the proposed method to obtain their normal forms.
   - The proposed method is conveniently selective; allowing one to compute only specific terms of the approximate nonlinear model without computing the rest. This observation is pertinent since it allows analysis to be focused only on some specific modes in the system with less burdensome computations. In addition, the

results in chapter 4 suggest that the nonlinearities of the system are not evenly distributed, but are localised around some certain modes in the system. This implies that selective Normal Form application can be pursued with the developed method for system with large number of variables.

- Considering power system time-domain simulation software, the perturbation of the nonlinear system with scaled eigenvectors, as required by the proposed method, corresponds simply to initialising the system with initial conditions—the scaled eigenvectors. This observation underscores the possibility of using the already existing power system software for Normal Form analysis. Moreover, there has not been any dedicated commercial software for power system Normal Form analysis.
- It is observed that with the developed method, both second and third order terms are computed simultaneously. This has advantage for third order Normal Form application; however, if only second order Normal Form is needed, it is not possible with the developed method to compute the second order terms without some third order terms. This implies that the method is specifically developed for third order Normal Form application, although the idea can be extended if necessary.
- The developed method assumes that there is no exact modal resonance. That is, all eigevalues are distinct and the system state matrix is diagonalisable. In the case of exact modal resonance, excitation of different modes independently using scaled eigenvectors becomes complicated, thereby limiting the developed method. This is though, a general problem in Normal Form application and not specific to the developed method.
- In exciting the modes to compute the coefficients, the choice of the modal deviation amplitude can affect the results. If too large amplitude is used, the level of the nonlinearities due to the perturbation exceeds third order, on which the method is based, thereby giving wrong results. On the other hand, very small value of the modal deviation amplitude does not create sufficient nonlinearities due to the perturbation, placing the system in only linear region, whereas the needed coefficients are for the nonlinear terms.
- Yet another limitation of the developed method is the assumption that the nonlinearities are smooth and static. If these assumptions become invalid, the method may break down.

4. Using the Normal Form defined for power system represented by second order differential equations, analytical index for estimating the frequency shift of electromechanical

modes under disturbance is proposed. Based on this frequency shift estimation index, an *instability proximity index (IPI)* is developed for estimating the proximity of oscillatory mode to instability. These indices were tested on small and larger power systems. From the results presented in chapter 5, the following observations are made:

- Increasing stress in the system decreases the frequencies of electromechanical modes. That is, the frequencies of the electromechanical modes shift from the fundamental values (determined by linear analysis) to another lesser value due to increased nonlinearities.
- The frequency shift is more pronounced on the dominant mode and is related to the stability of the mode. The frequency shifts increases as the stress increases till a critical point where the modes lose stability.
- Modern power system control focuses on wide-area monitoring of electromechanical oscillations using real time measurements, whereby mode parameters (e.g., frequency and damping) are automatically estimated for any current operating conditions for proper control action. The indices proposed in this work can fairly predict the frequency shifts of electromechanical modes as the stress increases. This observation is very crucial, since the indices can be used for rough on-line estimation of the system stability and for warning signals of instability in power system operation.
- Being based on classical power system model and third order approximation of the exact nonlinear model, the proposed indices have limited range of validity and hence, cannot give global stability information.

5. Finally, to further reduce Normal Form computations, selective Normal Form application is proposed. The method consists in neglecting the interactions associated to—(1) real eigenvalues and (2) modes with least energies. To determine the modes with least energies, Hankel singular values are used to determine most controllable and observable states; then participation factor analysis is used to determine modes which are related to the most relevant Hankel states. The interactions related to these modes are considered, while others are not. This selective Normal Form application technique was used to study nonlinear modal interactions and nonlinear participation factors. From the results presented in chapter 5, the following observations are made:

   - For the tested case, same nonlinear interactions are detected, both for the selective and full Normal Form application. This observation tend to suggest that real eigenvalues do not play significant role on nonlinear modal interactions. Also, it

was found that the same modes involved in nonlinear interaction are the modes having the high energies based on the Hankel singular values. This observation tends to suggest that apart from the real eigenvalues, some oscillatory modes are weak for nonlinear interactions, such that including them contributes to more computational "wastage".

- In addition to the computational reduction due to the new method for computing nonlinear coefficients, selective Normal Form application introduces another sharp reduction in computational time. This observation is especially important because when controls are considered in the generator models, many eigenvalues are real. Also, many modes are highly damped, allowing them to be neglected. This could be very useful when considering power electronic grids, where several modes are real and many oscillatory modes are highly damped.

In this thesis, it has been shown that avoiding higher order differentiation and Hessian evaluations can extend third order Normal Form analysis to larger systems, beyond what the conventional method can handle. It has also been shown that many opportunities for reducing the intractable computations in Normal Form analysis exist. From all the results in this work, it can be concluded that, with new computational technique developed, together with proper developments of the selective Normal Form application ideas proposed in this work, it will be possible to use Normal Form for studying the future and larger grids when nonlinear interactions become significant.

6.2 Future Works

Several potentially fruitful experiments were not performed due to many constraints during this research. From the observations and experience gathered in the course of this research, many potentially gainful possibilities for future work may be recommended as follows:

1. Since the developed method is non-intrusive, and requires initialisation of the original nonlinear model with choice initial conditions, it could be a very gainful adventure to try realising the proposed method with commercial power system software. The method needs a formulation of sets of linear equations, where every needed parameters are obtained from the state matrix, after linear analysis. Many standard commercial power system software such as EUROSTAG® can perform both linear analysis and time-domain simulation. Thus, it may be possible to use a time-domain simulation software to obtain the static nonlinear solution of the nonlinear model, which is needed by the developed method. If realised, such breakthrough will be both beneficial to power

system operators for detailed modal analysis, and to the researchers having interest in Normal Form analysis, since Normal Form will then be integrated as a program package into such software. Furthermore, the integration of the developed method into a commercial software will give the software a good marketing edge.

2. Although the proposed method has significantly reduced the computational burden of Normal Form, a particular aspect not directly dealt with is the burden of computing the initial condition in the Normal Form space. The determination of the initial condition is time-consuming. A more effective algorithm for solving nonlinear equations could help to ease this challenge.

3. As noted in the work, the results of the developed method is affected by the amplitude of the modal deviation. This amplitude was chosen heuristically, even though a range of values that give good results was established for the test cases used. In order to promote the method, it will be necessary to define the value of the modal deviation amplitude in advance, considering the degree of nonlinearities of the studied system. Such relationship between the degree of system nonlineaities and the right modal deviation amplitude should be developed in future.

4. The indices developed for monitoring the frequency shifts of electromechanical modes are based on the application of Normal Form to power systems represented with second order differential equations. In that case, there is no complex quantities in the formulations. Since the first-order-equation representation of power system is the standard, it could be interesting to investigate in future, the extension to power system represented with first order model, involving complex quantities.

5. Although the selective Normal Form ideas presented in this work give good results, the test case was very simple. It is recommended in future to investigate the perceived potentials with larger power systems. If the results are consistent in larger power systems, the proposal will be very essential for the future grids.

6. Whether computationally reduced or not, Normal Form analysis is not necessary if the system condition does not show strong nonlinearities. Therefore, indices are needed based on the system condition, to determine the level of nonlinearities and which order of Normal Form to be used. This will help to know a priori, if it is gainful embarking on Normal Form analysis to avoid computational loss. Thus, in future, these indices should first of all be found, or developed before proceeding with NF analysis.

7. All the developments in this work have been based on the conventional generator models. Future grids will be made up of mainly converter-control-based generators. It is necessary in future to investigate the effectiveness of the developed method, using the power electronic (PE) converter models. Moreover, the limitation of the method lies in the fact that the nonlinearities have to be static, which may not be the case for grids with 100% PE; so tests are needed.

8. The use of Normal Form method to derive a nonlinear control law for power converter control could also be a very interesting research adventure.

Bibliography

[1] S. H. Mohr, J. Wang, G. Ellem, J. Ward, and D. Giurco, "Projection of world fossil fuels by country," *Fuel*, vol. 141, pp. 120–135, 2015. [Online]. Available: http://dx.doi.org/10.1016/j.fuel.2014.10.030 3, XIII

[2] W. Dong, H. Xin, D. Wu, and L. Huang, "Small Signal Stability Analysis of Multi-Infeed Power Electronic Systems Based on Grid Strength Assessment," *IEEE Transactions on Power Systems*, vol. 34, no. 2, pp. 1393–1403, 2019. 3

[3] H. Golpîra, H. Seifi, A. R. Messina, and M. R. Haghifam, "Maximum Penetration Level of Micro-Grids in Large-Scale Power Systems: Frequency Stability Viewpoint," *IEEE Transactions on Power Systems*, vol. 31, no. 6, pp. 5163–5171, 2016. 3

[4] REN21, "REN21 - 2019 Global Status Report," Tech. Rep., 2019. [Online]. Available: https://wedocs.unep.org/bitstream/handle/20.500.11822/28496/REN2019.pdf?sequence=1{&}isAllowed=y{%}0Ahttp://www.ren21.net/cities/wp-content/uploads/2019/05/REC-GSR-Low-Res.pdf 3, XIV

[5] Y. Ni, V. Vittal, W. Kliemann, and A. A. Fouad, "NONLINEAR MODAL INTERACTION IN HVDC/AC POWR SYSTEMS WITH DC POWER MODULATION," vol. I, no. 4, 1996. 3, 4, XIV

[6] R. Zeinali Davarani, R. Ghazi, and N. Pariz, "Nonlinear modal analysis of interaction between torsional modes and SVC controllers," *Electric Power Systems Research*, vol. 91, pp. 61–70, 2012. [Online]. Available: http://dx.doi.org/10.1016/j.epsr.2012.04.017 4

[7] C.-m. Lin, ""Analysis of nonlinear modal interaction and its effect on control performance in stressed power systems using normal forms method " (1995). Retrospective Theses and Dissertations. 10924. http://lib.dr.iastate.edu/rtd/10924," 1995. [Online]. Available: http://lib.dr.iastate.edu/rtd/10924 4, 30, 34, 36

[8] E. Barocio and A. R. Messina, "Normal form analysis of stressed power systems : incorporation of SVC models," *Electrical Power and Energy Systems*, vol. 25, pp. 79–90, 2003. 4, 34

[9] H. Setiadi, A. U. Krismanto, N. Mithulananthan, and M. Hossain, "Modal interaction of power systems with high penetration of renewable energy and BES systems," *International Journal of Electrical Power & Energy Systems*, vol. 97, pp. 385–395, apr 2018. [Online]. Available: https://www.sciencedirect.com/science/article/abs/pii/S0142061517316216 4

[10] H. Amano and A. Yokoyama, "Rotor angle stability analysis using normal form method with high penetrations of renewable energy sources-energy index for multi-swing stability," in *20th Power Systems Computation Conference, PSCC 2018*. Dublin: IEEE, 2018, pp. 1–6. 4, 14, XIV, XIX

[11] J. Shair, X. Xie, L. Wang, W. Liu, J. He, and H. Liu, "Overview of emerging subsynchronous oscillations in practical wind power systems," *Renewable and Sustainable Energy Reviews*, vol. 99, pp. 159–168, 2019. [Online]. Available: https://doi.org/10.1016/j.rser.2018.09.047 4, XIV

[12] J. Quintero, V. Vittal, G. T. Heydt, and H. Zhang, "The impact of increased penetration of converter control-based generators on power system modes of oscillation," *IEEE Transactions on Power Systems*, vol. 29, no. 5, pp. 2248–2256, Sep. 2014. 4, 11, XIV, XVIII

[13] S. You, G. Kou, Y. Liu, X. Zhang, Y. Cui, M. Till, W. Yao, and Y. Liu, "Impact of High PV Penetration on the Inter-Area Oscillations in the U . S . Eastern Interconnection," *IEEE Access*, vol. 5, pp. 4361–4369, 2017. 4, XIV

[14] MIGRATE, "Horizon 2020 Work Programme 2018 - 2020." [Online]. Available: https://www.h2020-migrate.eu/ 4

[15] Migrate Deliverable 1.1, "Report on systemic issues." [Online]. Available: https://www.h2020-migrate.eu/ 5

[16] European Network of Transmission System Operators for Electricity (ENTSO-E), "Analysis of CE Inter-Area Oscillations of 19 and 24 February 2011 – Report of ENTSO-E SG SPD." [Online]. Available: https://www.entsoe.eu 4, 5, XIV, XV

[17] H. Liu, X. Xie, J. He, T. Xu, Z. Yu, C. Wang, and C. Zhang, "Subsynchronous Interaction between Direct-Drive PMSG Based Wind Farms and Weak AC Networks," *IEEE Transactions on Power Systems*, vol. 32, no. 6, pp. 4708–4720, 2017. 6, XV

[18] J. Bömer, K. Burges, C. Nabe, and M. Pöller, "All Island TSO Facilitation of Renewables Studies – Final Report for Work Package 3," 2010, study prepared for EirGrid Plc. [Online]. Available: https://www.ecofys.com 6, XV

[19] K. S. Swarup and P. B. Corthis, "ANN Approach," *IEEE Computer Applications in Power*, vol. 15, no. 3, pp. 32–38, 2002. 6, XVI

[20] R. J. Spier and M. E. Liffring, "Real-time expert systems for advanced power control (a status update) (aerospace power system testbed)," *IEEE Aerospace and Electronic Systems Magazine*, vol. 4, no. 11, pp. 33 – 38, 1989. 6, XVI

[21] Y. Wang, D. J. Hill, and G. Guo, "Robust decentralized control for multimachine power systems," *IEEE Transactions on Circuits and Systems I: Fundamental Theory and Applications*, vol. 45, no. 3, pp. 271–279, 1998. 6, XVI

[22] J. De La Ree, V. Centeno, J. S. Thorp, and A. G. Phadke, "Synchronized phasor measurement applications in power systems," *IEEE Transactions on Smart Grid*, vol. 1, no. 1, pp. 20–27, 2010. 7

[23] S. Fu, Z. Baohui, Y. Songhao, and W. Huaiyuan, "A Novel Termination Algorithm of Time-domain Simulation for Power System Transient Stability Analysis Based on Phase-plane Trajectory Geometric Characteristic." Changsha: IEEE, 2015, pp. 1422–1426. 7

[24] H.-D. Chiang, *Direct Methods for Electric Power Systems*. New Jersey: JOHN WILEY & SONS, 2011. 7

[25] G. Rogers, ""Demystifying Power Sysytem Oscillations," *IEEE Computer Applications In Power*, vol. 9, no. 3, pp. 30–35, 1999. 11, 22, XVIII

[26] M. Kouki, B. Marinescu, and F. Xavier, "Exhaustive modal analysis of large-scale interconnected power systems with high power electronics penetration," *IEEE Transactions on Power Systems*, pp. 1–1, 2020. 11, XVIII

[27] H. Poincaré, *Les mthodes nouvelles de la mcanique cleste.* Paris: Gauthiers- Villars, 1892. [Online]. Available: http://henripoincarepapers.univ-lorraine.fr/chp/hp-pdf/hp1892mna.pdf 13, 32, XIX

[28] P. M. Henri Dulac, "Solutions d'un système d'équations différentielles dans le voisinage de valeurs singulières," *Bulletin de la Socit Mathmatique de France,*, vol. 40, p. 324–383, 1912. [Online]. Available: http://www.numdam.org/article/BSMF_1912__40__324_0.pdf

[29] J. Guckenheimer and P. Holmes, *Nonlinear Oscillations, Dynamical Systems, and Bifurcations of Vector Fields*, ser. Applied Mathematical Sciences. New York, NY: Springer New York, 1983, vol. 42. [Online]. Available: http://link.springer.com/10.1007/978-1-4612-1140-2

[30] A. H. Nayfeh, *The Method of Normal Forms*, 2nd ed. Weinheim: WILEY-VCHVerlag GmbH&Co. KGaA, 2011. 13, 26, 46, XIX

[31] J. J. Sanchez-Gasca, V. Vittal, M. J. Gibbard, A. R. Messina, D. J. Vowles, S. Liu, and U. D. Annakkage, "Inclusion of higher order terms for small-signal (modal) analysis: committee report-task force on assessing the need to include higher order terms for small-signal (modal) analysis," *IEEE Transactions on Power Systems*, vol. 20, no. 4, pp. 1886–1904, 2005. 13, 28, 33, 49, 90, 99, 101, 103, 104, 113, 115

[32] V. Vittal, A. A. Fouad, and N. Bhatia, "Analysis Of The Inter-Area Mode Phenomenon In Power Systems Following Large Disturbances," *IEEE Transactions on Power Systems*, vol. 6, no. 4, pp. 1515–1521, 1991. 22

[33] G. Hirsch, "Undamped inherent inter-area oscillations in power grids," *Electrical Engineering*, vol. 88, no. 4, pp. 259–273, 2006.

[34] M. Klein, G. J. Rogers, and P. Kundur, "A fundamental study of inter-area oscillations in power systems , IEEE Transactions on," *Transactions on Power Systems*, vol. 6, no. 3, 1991. 22

[35] B. Marinescu, B. Mallem, H. Bourles, and L. Rouco, "Robust coordinated tuning of parameters of standard power system stabilizers for local and global grid objectives," in *2009 IEEE Bucharest PowerTech*, June 2009, pp. 1–7. 22

[36] N. Martins and L. T. G. Lima, "Determination of suitable locations for power system stabilizers and static var compensators for damping electromechanical oscillations in large scale power systems," *IEEE Transactions on Power Systems*, vol. 5, no. 4, pp. 1455–1469, 1990. 22

[37] C. Li, T. Qoria, F. Colas, J. Liang, W. Ming, F. Gruson, and X. Guillaud, "Coupling influence on the DQ impedance stability analysis for the three-phase grid-connected inverter," *Energies*, vol. 12, no. 19, pp. 1–16, 2019. 23

[38] T. Qoria, C. Li, K. Oue, F. Gruson, F. Colas, X. Guillaud, and T. Prevost, "Tuning of AC voltage-controlled VSC based linear quadratic regulation," in *2019 IEEE Milan PowerTech, PowerTech 2019*, no. 691800, 2019.

[39] J. Freytes, G. Bergna, J. A. Suul, S. D'Arco, F. Gruson, F. Colas, H. Saad, and X. Guillaud, "Improving small-signal stability of an mmc with ccsc by control of the

internally stored energy," *IEEE Transactions on Power Delivery*, vol. 33, no. 1, pp. 429–439, Feb 2018. 23

[40] B. Marinescu, B. Mallem, and L. Rouco, "Large-scale power system dynamic equivalents based on standard and border synchrony," *IEEE Transactions on Power Systems*, vol. 25, no. 4, pp. 1873–1882, 2010. 25, 36, 111

[41] S. K. Starrett, "Application of normal forms of vector fields to stressed power systems," Ph.D. dissertation, IOWA State University, 1994. 25

[42] G. Jang, V. Vittal, and W. Kliemann, "Effect of nonlinear modal interaction on control performance: use of normal forms technique in control design. I. General theory and procedure," *IEEE Transactions on Power Systems*, vol. 13, no. 2, pp. 401–407, 1998. 27, 100

[43] ——, "Effect of nonlinear modal interaction on control performance: use of normal forms technique in control design. II. Case studies," *Power Systems, IEEE Transactions on*, vol. 13, no. 2, pp. 401–407, 1998. 27

[44] H. Lomei, M. Assili, D. Sutanto, and K. Muttaqi, "A New Approach to Reduce the Non-Linear Characteristics of a Stressed Power System by Using the Normal Form Technique in the Control Design of the Excitation System," *IEEE Transactions on Industry Applications*, vol. 53, no. 1, pp. 492 – 500, 2017. 27, 30

[45] Meng Yue and R. Schlueter, "Nonlinear effects of a robust control design," *IEEE Transactions on Power Systems*, vol. 20, no. 1, pp. 508–510, Feb 2005. 27

[46] A. K. Singh and B. C. Pal, "Decentralized Nonlinear Control for Power Systems Using Normal Forms and Detailed Models," *IEEE Transactions on Power Systems*, vol. 33, no. 2, pp. 1160–1172, 2018. 27

[47] S. K. Starrett and A. A. Fouad, "Nonlinear measures of modal controllability and observability," *Electric Power Systems Research*, vol. 52, no. 1, pp. 65–75, 1999. 27

[48] F. X. Wu, H. Wu, Z. X. Han, and D. Q. Gan, "Validation of power system non-linear modal analysis methods," *Electric Power Systems Research*, vol. 77, no. 10, pp. 1418–1424, 2007. 28

[49] S. K. Starrett, "Nonlinear measures of mode-machine participation," *IEEE Transactions on Power Systems*, vol. 13, no. 2, pp. 389–394, 1998. 28, 30

[50] B. M. Nomikos and C. D. Vournas, "Modal Interaction and PSS Design," in *IEEE Porto Power Tech*. Porto: IEEE, 2001. 28

[51] H. Amano and T. Inoue, "A New PSS Parameter Design Using Nonlinear Stability Analysis," in *IEEE Power Engineering Society General Meeting*. Tampa: IEEE, 2007, pp. 1–8. 28, 30

[52] S. Liu, A. R. Messina, and V. Vittal, "Assessing placement of controllers and nonlinear behavior using normal form analysis," *IEEE Transactions on Power Systems*, vol. 20, no. 3, pp. 1486–1495, 2005. 28, 30

[53] ——, "A normal form analysis approach to siting power system stabilizers (PSSs) and assessing power system nonlinear behavior," *IEEE Transactions on Power Systems*, vol. 21, no. 4, pp. 1755–1762, 2006. 28, 35, 115

[54] J. Zhang, G. Li, A. N. Abd-alla, J. Y. Wen, S. J. Cheng, and S. Member, "Theoretical Analysis of the Interaction between Power System Stability Modes with the Normal Forms of Vector Fields -BjVj (G," in *International Conference on Power System Technology Theoretical*. Chongqing: IEEE, 2006. 28

[55] H. Amano, T. Kumano, and T. Inoue, "Nonlinear stability indexes of power swing oscillation using normal form analysis," *IEEE Transactions on Power Systems*, vol. 21, no. 2, pp. 825–834, 2006. 28, 54, 103

[56] H. Amano, T. Kumano, T. Inoue, and H. Taniguchi, "Proposal of nonlinear stability indices of power swing oscillation in a multimachine power system," *Electrical Engineering in Japan*, vol. 151, no. 4, pp. 16–24, 2005. [Online]. Available: http://doi.wiley.com/10.1002/eej.20070 28

[57] T. Tian, X. Kestelyn, O. Thomas, H. Amano, and A. R. Messina, "An Accurate Third-Order Normal Form Approximation for Power System Nonlinear Analysis," *IEEE Transactions on Power Systems*, vol. 33, no. 2, pp. 2128–2139, 2018. 28, 30, 31, 32, 47, 103, 115

[58] Z. Y. Zou, Q. Y. Jiang, Y. J. Cao, and H. F. Wang, "Normal form analysis of the interaction among multi-controller channels of upfc," in *Fifth World Congress on Intelligent Control and Automation (IEEE Cat. No.04EX788)*, vol. 6, June 2004, pp. 5055–5059 Vol.6. 28

[59] ——, "Normal form analysis of interactions among multiple svc controllers in power systems," *IEE Proceedings - Generation, Transmission and Distribution*, vol. 152, no. 4, pp. 469–474, July 2005. 28

[60] J. Thapar, V. Vittal, W. Kliemann, and A. A. Fouad, "Application of the normal form of vector fields to predict interarea separation in power systems," *IEEE Transactions on Power Systems*, vol. 12, no. 2, pp. 844–850, 1997. 29, 81

[61] V. Vittal, W. Kliemann, D. G. Chapman, A. D. Silk, Y. Xni, and D. J. Sobajic, "Determination of generator groupings for an islanding scheme in the manitoba hydro system using the method of normal forms," *IEEE Transactions on Power Systems*, vol. 13, no. 4, pp. 1345–1351, 1998. 29, 30, 36, 116

[62] C. Touzé, O. Thomas, and A. Chaigne, "Hardening/softening behaviour in non-linear oscillations of structural systems using non-linear normal modes," *Journal of Sound and Vibration*, vol. 273, no. 1-2, pp. 77–101, 2004. 29, 32, 45, 49, 60, 63, 81, 120

[63] C. Touzé and M. Amabili, "Nonlinear normal modes for damped geometrically nonlinear systems: Application to reduced-order modelling of harmonically forced structures," *Journal of Sound and Vibration*, vol. 298, no. 4-5, pp. 958–981, 2006. 32, 60, 63, 81

[64] V. Denis, M. Jossic, C. Giraud-Audine, B. Chomette, A. Renault, and O. Thomas, "Identification of nonlinear modes using phase-locked-loop experimental continuation and normal form," *Mechanical Systems and Signal Processing*, vol. 106, pp. 430–452, 2018. [Online]. Available: https://doi.org/10.1016/j.ymssp.2018.01.014 29

[65] I. Martínez, A. R. Messina, and V. Vittal, "Normal form analysis of complex system models: A structure-preserving approach," *IEEE Transactions on Power Systems*, vol. 22, no. 4, pp. 1908–1915, 2007. 29, 40, 65, XXIII

[66] S. Saha, A. A. Fouad, W. H. Kliemann, and V. Vittal, "Stability boundary approximation of a power system using the real normal form of vector fields," *IEEE Power Engineering Review*, vol. 17, no. 5, p. 69, 1997. 29, 40

[67] I. C. Martinez, A. R. Messina, and E. Barocio, "Higher-order normal form analysis of stressed power systems: A fundamental study," *Electric Power Components and Systems*, vol. 32, no. 12, pp. 1301–1317, 2004. 29, 30

[68] N. Kshatriya, U. Annakkage, A. Gole, and I. Fernando, "Improving the Accuracy of Normal Form Analysis," *IEEE Transactions on Power Systems*, vol. 20, no. 1, pp. 286–293, 2 2005. [Online]. Available: http://ieeexplore.ieee.org/document/1388521/ 29, 50

[69] T. K. Ram and S. Krishna, "Studies on accuracy of higher order normal forms applied to power system analysis using neumann series convergence criterion," in *2019 IEEE PES Asia-Pacific Power and Energy Engineering Conference (APPEEC)*, Macao, Dec 2019, pp. 1–6. 29

[70] C. H. Lamarque, C. Touzé, and O. Thomas, "An upper bound for validity limits of asymptotic analytical approaches based on normal form theory," *Nonlinear Dynamics*, vol. 70, p. 1931–1949, 2012. 29, 45

[71] Q. Huang, Z. Wang, and C. Zhang, "Evaluation of the effect of modal interaction higher than 2nd order in small-signal analysis," in *2009 IEEE Power and Energy Society General Meeting, PES '09*, no. 2, 2009, pp. 1–6. 30, 49, 100, 101, 104

[72] I. Martínez, A. R. Messina, and E. Barocio, "Perturbation analysis of power systems: Effects of second- and third-order nonlinear terms on system dynamic behavior," *Electric Power Systems Research*, vol. 71, no. 2, pp. 159–167, 2004. 30

[73] N. S. Ugwuanyi, X. Kestelyn, O. Thomas, B. Marinescu, and A. R. Messina, "A New Fast Track to Nonlinear Modal Analysis of Power System Using Normal Form," *IEEE Trans. on Power Systems.*, vol. 35, no. 4, pp. 3247–3257, 2020. 30

[74] N. S. Ugwuanyi, X. Kestelyn, O. Thomas, and B. Marinescu, "A Novel Method for Accelerating the Analysis of Nonlinear Behaviour of Power Grids using Normal Form Technique," in *IEEE Innovative Smart Grid Technologies Europe (ISGT Europe)*. Bucharest: IEEE, 2019.

[75] N. S. Ugwuanyi, X. Kestelyn, and B. Marinescu, "Power System Nonlinear Modal Analysis Using Computationally Reduced Normal Form Method," *Energies*, vol. 13, no. 5, p. 1249, 2020.

[76] N. S. Ugwuanyi, X. Kestelyn, O. Thomas, and B. Marinescu, "Selective Nonlinear Coefficients Computation for Modal Analysis of The Emerging Grid," in *Conférence des Jeunes chercheurs en Génie Eléctrique*, Oléron, 2019. 30

[77] R. J. Betancourt, E. Barocio, J. Arroyo, and A. R. Messina, "A real normal form approach to the study of resonant power systems," *IEEE Transactions on Power Systems*, 2006. 31

[78] S. Shaw, C. Pierre, and S. Sha, "Normal Modes for Non-Linear Vibratory Systems," *Journal of Sound and Vibration*, vol. 164, no. 1, pp. 85–124, 1993. 31, 59

[79] R. Betancourt, E. Barocio, A. Messina, and I. Martínez, "Modal analysis of inter-area oscillations using the theory of normal modes," *Electric Power Systems Research*, vol. 79, no. 4, pp. 576–585, 4 2009. 32, 81

[80] R. J. Betancourt, I. Martinez, E. Barocio, and A. Roman, "Normal mode analysis of inter-area oscillations," in *2006 IEEE PES Power Systems Conference and Exposition, PSCE 2006 - Proceedings*, 2006, pp. 1593–1600. 32

[81] V. L. Arnold, *Geometrical Methods in the Theory of Ordinary Differential Equations*, 2nd ed. New York: Springer-Verlag, 1988. 32

[82] B. Wang and K. Sun, "Nonlinear Modal Decoupling of Multi-Oscillator Systems With Applications to Power Systems," *IEEE Access*, vol. 6, pp. 9201–9217, 2018. 32, 33, 35, 40, 136

[83] B. Wang, K. Sun, and X. Xu, "Nonlinear modal decoupling based power system transient stability analysis," *IEEE Transactions on Power Systems*, vol. 34, no. 6, pp. 4889–4899, 2019. 32, 35, 40, 136

[84] A. R. Messina and V. Vittal, "Assessment of nonlinear interaction between nonlinearly coupled modes using higher order spectra," *IEEE Transactions on Power Systems*, vol. 20, no. 1, pp. 375–383, 2005. 33, 90, 103

[85] Z. Wang and Q. Huang, "Study on an improved Normal Form solution and reduced-order mode reconstruction in power system," in *IEEE Region 10 Annual International Conference, Proceedings/TENCON*. Macao: IEEE, 2016. 33, 104

[86] H. Modir Shanechi, N. Pariz, and E. Vaahedi, "General Nonlinear Modal Representation of Large Scale Power Systems," *IEEE TRANSACTIONS ON POWER SYSTEMS*, vol. 18, no. 3, 2003. 33

[87] A. Abdollahi, N. Pariz, and H. M. Shanechi, "Modal series method for nonautonomous nonlinear systems," in *Proceedings of the IEEE International Conference on Control Applications*, no. October, Singapore, 2007, pp. 759–764. 33

[88] O. Rodriguez, A. Medina, A. Roman-Messina, and C. R. Fuerte-Esquivel, "The modal series method and multi-dimensional laplace transforms for the analysis of nonlinear effects in power systems dynamics," in *2009 IEEE Power Energy Society General Meeting*, July 2009, pp. 1–8. 33

[89] Z. Wang and Q. Huang, "A Closed Normal Form Solution under Near-Resonant Modal Interaction in Power Systems," *IEEE Transactions on Power Systems*, vol. 32, no. 6, pp. 4570–4578, 2017. 33, 48

[90] M. Netto, Y. Susuki, and L. Mili, "Data-Driven Participation Factors for Nonlinear Systems Based on Koopman Mode Decomposition," *IEEE Control Systems Letters*, vol. 3, no. 1, pp. 198–203, 2019. 33, 34

[91] M. A. Hernandez-Ortega and A. R. Messina, "Nonlinear Power System Analysis Using Koopman Mode Decomposition and Perturbation Theory," *IEEE Transactions on Power Systems*, vol. 33, no. 5, pp. 5124–5134, 2018. 34, 35

[92] C. Bischof, P. Khademi, A. Mauer, and A. Carle, "Adifor 2.0: automatic differentiation of Fortran 77 programs," *IEEE computational science & engineering*, vol. 3, no. 3, pp. 18–32, 1996. 34, 35

[93] C. C. Margossian, "A review of automatic differentiation and its efficient implementation," *Wiley Interdisciplinary Reviews: Data Mining and Knowledge Discovery*, vol. 9, no. 4, pp. 1–19, 2019. 35

[94] M. Betancourt, "A Geometric Theory of Higher-Order Automatic Differentiation," p. 55, 2018. [Online]. Available: http://arxiv.org/abs/1812.11592 35, 36

[95] A. Güne¸, G. Baydin, B. A. Pearlmutter, and J. M. Siskind, "Automatic Differentiation in Machine Learning: a Survey," *Journal of Machine Learning Research*, vol. 18, pp. 1–43, 2018. [Online]. Available: http://www.jmlr.org/papers/volume18/17-468/17-468.pdf 35

[96] B. Carpenter, M. D. Hoffman, M. Brubaker, D. Lee, P. Li, and M. Betancourt, "The Stan Math Library: Reverse-Mode Automatic Differentiation in C++," 2015. [Online]. Available: http://arxiv.org/abs/1509.07164 34

[97] S. D. Engineering, "ON THE COMPUTATION OF THE COEFFICIENTS ASSOCIATED WITH HIGH ORDER NORMAL FORMS," *Journal of Sound and vibration*, vol. 232, pp. 525–540, 2000. 35

[98] V. I. Arnold and F. Takens, "A NEW APPROACH FOR OBTAINING NORMAL FORMS OF NON-LINEAR SYSTEMS," *Journal of Sound and Vibration*, vol. 210, no. 5, pp. 609–625, 1998.

[99] A. Mathematics and W. Ontario, "COMPUTATION OF NORMAL FORMS VIA A PERTURBATION TECHNIQUE," *Journal of Sound and Vibration*, vol. 211, no. 1, pp. 19–38, 1998. 35

[100] G. N. Ramaswamy, C. Evrard, G. C. Verghese, O. Fillatre, and B. C. Lesieutre, "Extensions, simplifications, and tests of synchronic modal equivalencing (sme)," *IIEEE Transactions on Power System*, vol. 12, no. 2, pp. 896–905, 1997. 36

[101] G. N. Ramaswamy, G. C. Verghese, L. Rouco, C. Vialas, and C. L. Demarco, "Synchrony, Aggregation, and Multi-Area Eigenanalysis - Power Systems, IEEE Transactions on," *IEEE Transactions on Power Systems*, vol. 10, no. 4, pp. 1986–1993, 1995.

[102] G. N. RAMASWAMY, L. Rouco, O. Fillatre, G. C. Verghese, P. PATRICK, B. C. Lesieutre, and D. Peltiers, "Synchronic Modal Equivalencing (SME) for Structure-Preserving Dynamic Equivalents PAN CIA TIC ˆ," *IEEE Trans. on power systems*, vol. 11, no. 1, pp. 19–29, 1996. 36

[103] B. Marinescu, B. Mallem, and L. Rouco, "Model reduction of interconnected power systems via balanced state-space representation," in *2007 European Control Conference, ECC 2007*, Kos, Greece, 2007, pp. 4165–4172. 36, 111

[104] M. Belhocine and B. Marinescu, "A mix balanced-modal truncations for power systems model reduction," in *2014 European Control Conference, ECC 2014*, Strasbourg, 2014, pp. 2721–2726. 36, 111

[105] Q. Cossart, F. Colas, and X. Kestelyn, "Model reduction of converters for the analysis of 100% power electronics transmission systems," in *Proceedings of the IEEE International Conference on Industrial Technology*, 2018, pp. 1254–1259. 36, 88

[106] Q. Cossart, F. Colas, and X. Kestelyn, "A priori error estimation of the structure-preserving modal model reduction by state residualization of a grid forming converter for use in 100in *15th IET International Conference on AC and DC Power Transmission (ACDC 2019)*, Feb 2019, pp. 1–6. 36

[107] Q. Cossart, "Outils et Méthodes pour l ' Analyse et la Simulation de Réseaux de Transport 100 % Électronique de Puissance," Ph.D. dissertation, L'Ecole Nationale Supérieure d'Arts et Métiers, 2019. [Online]. Available: https://pastel.archives-ouvertes.fr/tel-02464516/document 37

[108] G. Rogers, *Power system Oscillations*, M. A. Pai, Ed. New York: Springer, 2000. 40

[109] P. M. Anderson and A.-A. A. Fouad, *Power system control and stability*, 2nd ed. USA: IEEE Press, 2003. 40, 41, 123

[110] J. Machowski, J. W. Bialek, and J. R. Bumby, *POWER SYSTEM DYNAMICS Stability and Control*, 2nd ed. UK: JOHN WILEY & SONS, 2008. 42

[111] C. Touzé, M. Amabili, and O. Thomas, "Reduced-order models for large-amplitude vibrations of shells including in-plane inertia," *Computer Methods in Applied Mechanics and Engineering*, vol. 197, no. 21-24, pp. 2030–2045, 4 2008. [Online]. Available: https://linkinghub.elsevier.com/retrieve/pii/S0045782508000200 49

[112] L. Renson, G. Kerschen, and B. Cochelin, "Numerical computation of nonlinear normal modes in mechanical engineering," *Journal of Sound and Vibration*, vol. 364, pp. 177–206, 3 2016. [Online]. Available: https://linkinghub.elsevier.com/retrieve/pii/S0022460X15007543 49

[113] A. Givois, A. Grolet, O. Thomas, and J.-F. Deü, "On the frequency response computation of geometrically nonlinear flat structures using reduced-order finite element models," *Nonlinear Dynamics*, vol. 97, no. 2, pp. 1747–1781, Jul 2019. [Online]. Available: https://doi.org/10.1007/s11071-019-05021-6 56, 68, 81, XXIV

[114] C. Touzé, "A normal form approach for nonlinear normal modes. [Research Report] Publications du LMA, numéro 156, LMA. <hal-01154702>," Publications du LMA, numéro 156, LMA.<hal-01154702>, Tech. Rep., 2003. 60, 61, 63

[115] S. A. Neild and D. J. Wagg, "Applying the method of normal forms to second-order nonlinear vibration problems," *Proceedings of the Royal Society A: Mathematical, Physical and Engineering Sciences*, vol. 467, no. 2128, pp. 1141–1163, 2011. 64, 65, XXIII

[116] A. A. Muravyov and S. A. Rizzi, "Determination of nonlinear stiffness with application to random vibration of geometrically nonlinear structures," *Computers & Structures*, vol. 81, no. 15, pp. 1513–1523, 7 2003. 68, XXIV

[117] M. P. Mignolet, A. Przekop, S. A. Rizzi, and S. M. Spottswood, "A review of indirect/non-intrusive reduced order modeling of nonlinear geometric structures," *Journal of Sound and Vibration*, vol. 332, no. 10, pp. 2437–2460, 5 2013. [Online]. Available: https://www.sciencedirect.com/science/article/pii/S0022460X12008188 68, 81, XXIV

[118] PES-TR18, "IEEE Benchmark Systems for Small-Signal Stability Analysis and Control," 2015. [Online]. Available: http://www.sel.eesc.usp.br/ieee 78, XII

[119] A. K. Singh and B. C. Pal, "Ieee pes task force on benchmark systems for stability controls report on the 68-bus, 16-machine, 5-area system." [Online]. Available: http://www.sel.eesc.usp.br/ieee/ 89

[120] E. Purvine, E. Cotilla-Sanchez, M. Halappanavar, Z. Huang, G. Lin, S. Lu, and S. Wang, "Comparative study of clustering techniques for real-time dynamic model reduction," *Statistical Analysis and Data Mining*, vol. 10, no. 5, pp. 263–276, 2017. 92

[121] W. A. Hashlamoun, M. A. Hassouneh, and E. H. Abed, "New results on modal participation factors: Revealing a previously unknown dichotomy," *IEEE Transactions on Automatic Control*, vol. 54, no. 7, pp. 1439–1449, 2009. 100, 111, 112

[122] I. Dobson and E. Barocio, "Scaling of normal form analysis coefficients under coordinate change," *IEEE Transactions on Power Systems*, vol. 19, no. 3, pp. 1438–1444, 2004. 100, 101

[123] F. Milano, "An open source power system analysis toolbox," *IEEE Transactions on Power Systems*, vol. 20, no. 3, pp. 1199–1206, 2005. 105

[124] B. C. Moore, "Principal Component Analysis in Linear Systems: Controllability, Observability, and Model Reduction," *IEEE Transactions on Automatic Control*, vol. 26, no. 1, pp. 17–32, 1981. 111

[125] B. Wang and K. Sun, "Formulation and Characterization of Power System Electromechanical Oscillations," *IEEE Transactions on Power Systems*, vol. 31, no. 6, pp. 5082–5093, 2016. 119

[126] J. F. Hauer, D. J. Trudnowski, and J. G. DeSteese, "A perspective on wams analysis tools for tracking of oscillatory dynamics," in *2007 IEEE Power Engineering Society General Meeting*, 2007, pp. 1–10. 127, 128

[127] O. Matsushita, M. Tanaka, H. Kanki, M. Kobayashi, and P. Keogh, *Modal Analysis of Multi-Degree-of-Freedom Systems*. Tokyo: Springer Japan, 2017, pp. 41–78. [Online]. Available: https://doi.org/10.1007/978-4-431-55456-1_3 131

[128] R. D. Zimmerman and C. E. Murillo-Sanchez, "MATPOWER (Version 7.0) [Software]," 2019. [Online]. Available: https://matpower.org XII

[129] R. D. Zimmerman, C. E. Murillo-Sánchez, and R. J. Thomas, "Matpower: Steady-state operations, planning, and analysis tools for power systems research and education," *IEEE Transactions on Power Systems*, vol. 26, no. 1, pp. 12–19, 2011. XII

[130] S. Liu, "Assessing placement of controllers and nonlinear behavior of electrical power system using normal form information," Ph.D. dissertation, Iowa State University Ames,, 2006. [Online]. Available: https://lib.dr.iastate.edu/rtd/12800AThis XII

Appendix A

List of acronyms

AD Automatic differentiation. 34, 35

CCT critical clearing time. 123

CFS critical frequency shift. 130

DAEs differential-algebraic-equations. 20, 29, 40, 57, 65, 93, XXIII

IPI instability proximity index. 132

LMA Linear Modal Analysis. 11–15, 21, 23, 25, 26, 29, 30, XVIII–XXI

MMC Modular Multilevel Converters. 4

NF Normal Form. 6, 12–18, 26, 29, 30, 32, 35–37, 40, 45, 55, 65, XVI, XVIII, XIX, XXI–XXIII

NF2 Second order Normal Form. 29, 30, 32, 34, 36, 53–55

NF3 Third order Normal Form. 29, 30, 32, 37, 39, 45, 53–55, 66

NLF nonlinear frequency. 117

NLMA Nonlinear Modal Analysis. 12, 26, XVIII

NNM nonlinear normal mode. 15, 16, 18, XXI

PE power electronic. 23, 36

PSS power system stabilzer. 5, 22, 24, 27, 32, 83, 98, 127, XV, XX

SEP stable equilibrium point. 13, 20, 21, 71, 118, 122, XIX

SME *synchronic modal equivalencing*. 36

SMIB single-machine-infinite-bus. 29, 31, 53, 64, 84, 85, 117, 119–121, 129, 131

SSA small-signal analysis. 7, 8, 11, 82, XVIII

SVC Static VAr Compensator. 3, 4, 28

TDS time-domain simulations. 129

UPFC unified power flow controller. 28

Appendix B

Glossary

invariance in dynamic system means that a motion initiated along a manifold at time $t = 0$ remains within the manifold for every $t > 0$. That is, the ability of a motion to remain only in the path where it is initiated.. 11, 59, 64, XVIII

nonlinear coefficients After the Taylor series expansion, the resulting approximate system is put in Jordan form with decoupled linear part and coupled nonlinear parts. The coefficients of these nonlinear polynomials are referred to, in this thesis, as the *Nonlinear Coefficients*.. 14, XXI

resonance Given a system whose eigenvalues are $\{\lambda_k\}_{k=1...N}$, special combinations of these eigenvalues that equal another eigenvalue result in resonance. Resonance relation among the eigenvalues $\{\lambda_k\}_{k=1...N}$ are defined as:

$$\forall_{s=1...N} : \lambda_s = \sum_{i=1}^{N} m_i \lambda_i, \quad m_i \geq 0, \qquad \sum m_i = p \geq 2, \tag{B.1}$$

where p is the order of resonance and N is the number of eigenvalues of the system.. 44

Appendix C

Road Map for R & D of this PhD

The first work in developing this research is to include the developed method as a program package in a power system commercial software. This leads to inclusion of Normal Form analysis in an existing software. The algorithm developed in this PhD would interact mutually with specific modules of the commercial software so that one would not need to build a new model for NF studies. The integration scheme is depicted in Figure C.1.

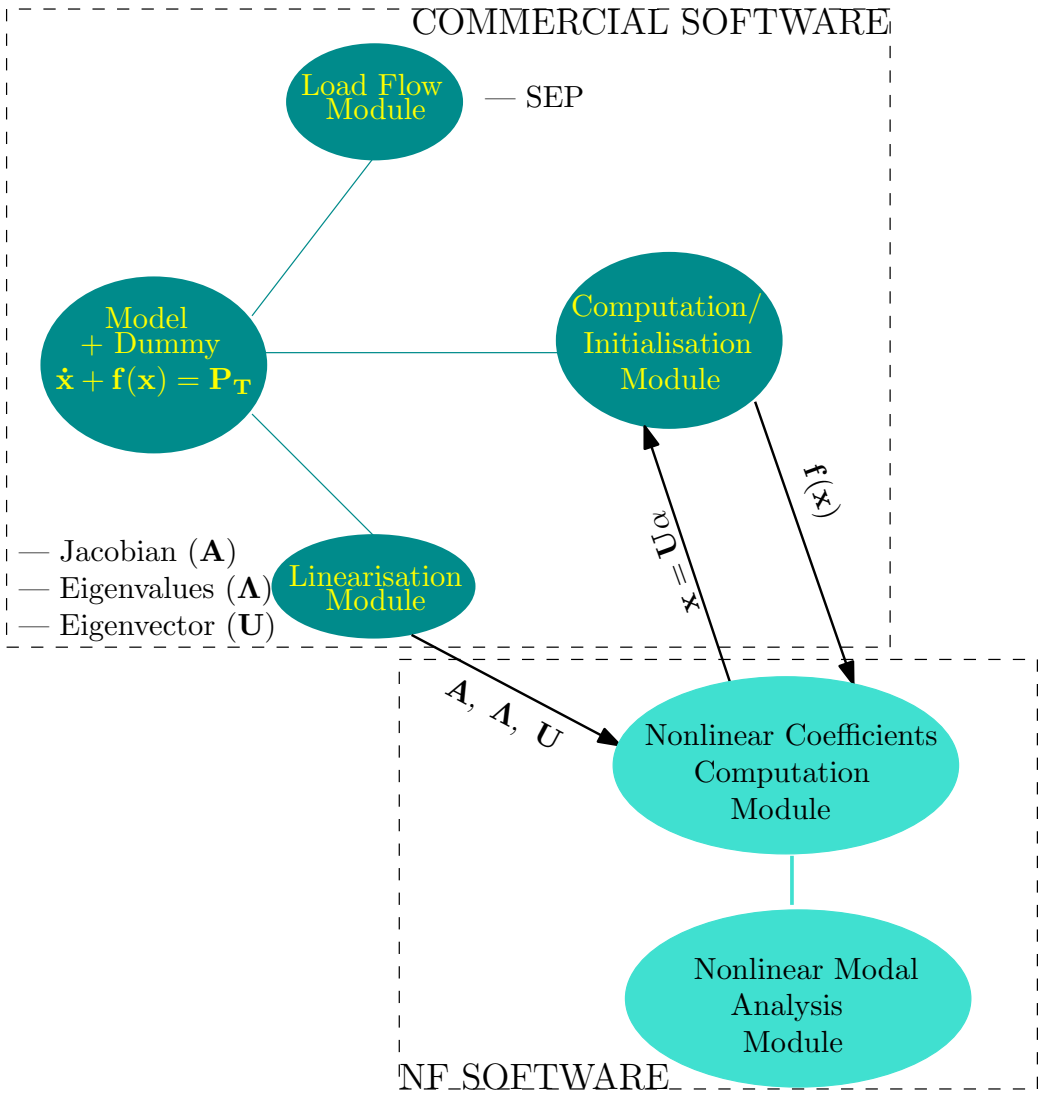

Figure C.1 – Road Map for Integration into Commercial Software

Desired features for Commercial Software are:

- Ability to linearise implemented model.
- Allows access to states after simulation/initialisation.
- Allows initialisation with user's choice values.
- Permits definition of dummy parameters.
- Interface with other software like MATLAB®.

EUROSTAG® software seems to be a good candidate.

Appendix D

Third Order Normal Form Derivation

NF main idea consists in simplifying all nonlinear terms that are not very relevant to the system dynamics in the neighbourhood of an equilibrium point. Consider the power system models represented generally as

$$\dot{\mathbf{x}} = \mathbf{f}(\mathbf{x}). \tag{D.1}$$

If the nonlinearities can be approximated by third order nonlinearities, then Taylor expansion of (D.1) yields

$$\dot{\mathbf{x}} = \mathbf{A}\mathbf{x} + \mathbf{F_2}(\mathbf{x}) + \mathbf{F_3}(\mathbf{x}) \tag{D.2}$$

where $\mathbf{x}$ and F_p are column vectors of length N, $\mathbf{A}$ is $(N \times N)$ constant matrix, and $\mathbf{F}_p$ is homogeneous polynomials of degree p in $\mathbf{x}$. Assume that $\mathbf{F}_p$ are smooth vector fields satisfying $\mathbf{F}_p(\mathbf{0}) = \mathbf{0}$ so that $\mathbf{x} = \mathbf{0}$ is a fixed (equilibrium) point.
Let the similarity transformation $\mathbf{x} = \mathbf{U}\mathbf{y}$ be applied to (D.2) in order to to obtain:

$$\dot{\mathbf{y}} = \mathbf{\Lambda}\mathbf{y} + \mathbf{F_2}(\mathbf{y}) + \mathbf{F_3}(\mathbf{y}) \tag{D.3}$$

The linear part of the system is decoupled but the nonlinear part is yet coupled. The coefficients of $\mathbf{F2}(\mathbf{y})$ and $\mathbf{F3}(\mathbf{y})$ are respectively gathered in matrices $\mathbf{C}$ and $\mathbf{D}$ called *nonlinear coefficients* in the thesis, such that for simplicity (D.3) can be written as

$$\dot{\mathbf{y}} = \mathbf{\Lambda}\mathbf{y} + \mathbf{C}(\mathbf{y}) + \mathbf{D}(\mathbf{y}) \tag{D.4}$$

The idea is to perform sequence of transformation that removes the higher order terms starting from 2, thereby reducing (D.2) to linear or simplified nonlinear system. Instead of sequential transformations, it is also possible to just perform a single nonlinear transformation and the result is the same. The non sequential transformation is given as

$$\mathbf{y} = \mathbf{z} + \mathbf{h2}(\mathbf{z}) + \mathbf{h3}(\mathbf{z}) \tag{D.5}$$

Then h_p is chosen such that the simplest possible form of the system equation is obtained (Normal Form) such as:

$$\dot{\mathbf{z}} = \mathbf{\Lambda}\mathbf{z} + \mathbf{g_2}(\mathbf{z}) + \mathbf{g_3}(\mathbf{z}) \tag{D.6}$$

$g_2(z)$ and $g_3(z)$ are included to represent respectively second and third order terms which perhaps, could not be removed *so-called resonant terms*. The terms $g_2(z)$ and $g_3(z)$ become zero when there is no resonance. To be step-wise, let us use sequential transformation instead of a single nonlinear transformation. Focusing first on the quadratic nonlinearities, let nonlinear transformation be defined as

$$\mathbf{y} = \mathbf{z} + \mathbf{h2}(\mathbf{z}) \tag{D.7}$$

$h2(z)$ is a quadratic polynomial in z such that the expanded form of (D.7) for j^{th} equation becomes

$$y_j = z_j + \sum_{k=1}^{N}\sum_{l=1}^{N} h2_{kl}^{j} z_k z_l \tag{D.8}$$

Differentiating (D.7) in time yields:

$$\dot{\mathbf{y}} = \dot{\mathbf{z}}(\mathbf{1} + \bar{\mathbf{D}}\mathbf{h2}(\mathbf{z})). \tag{D.9}$$

where $\bar{D}$ is a derivative operator.
Substituting (D.7) and (D.9) in (D.3) yields:

$$\dot{\mathbf{z}}(\mathbf{1} + \bar{\mathbf{D}}\mathbf{h2}(\mathbf{z})) = \mathbf{\Lambda}(\mathbf{z} + \mathbf{h2}(\mathbf{z})) + \mathbf{F2}(\mathbf{z} + \mathbf{h2}(\mathbf{z})) + \mathbf{F3}(\mathbf{z} + \mathbf{h2}(\mathbf{z})) \tag{D.10}$$

Assuming very small value of z then $(\mathbf{1} + \bar{\mathbf{D}}\mathbf{h2}(\mathbf{z}))^{-\mathbf{1}}$ can be expanded in Taylor series as:

$$(\mathbf{1} + \bar{\mathbf{D}}\mathbf{h2}(\mathbf{z}))^{-\mathbf{1}} = \mathbf{1} - \bar{\mathbf{D}}\mathbf{h2}(\mathbf{z}) + (\bar{\mathbf{D}}\mathbf{h2}(\mathbf{z}))^{\mathbf{2}} - (\bar{\mathbf{D}}\mathbf{h2}(\mathbf{z}))^{\mathbf{3}} + ... \tag{D.11}$$

With (D.11) truncated at third term, (D.10) can be approximated as:

$$\begin{aligned}\dot{\mathbf{z}} = \mathbf{\Lambda z}(\mathbf{1} - \bar{\mathbf{D}}\mathbf{h2}(\mathbf{z}) + (\bar{\mathbf{D}}\mathbf{h2}(\mathbf{z}))^{\mathbf{2}} + \dots) + \mathbf{\Lambda h2}(\mathbf{z})(\mathbf{1} - \bar{\mathbf{D}}\mathbf{h2}(\mathbf{z}) + \dots) + \mathbf{F2}(\mathbf{z})(\mathbf{1} - \bar{\mathbf{D}}\mathbf{h2}(\mathbf{z})) \\ + \dots\ \bar{\mathbf{D}}\mathbf{F2}(\mathbf{z})\mathbf{h2}(\mathbf{z}) + \mathbf{F3}(\mathbf{z})\end{aligned} \tag{D.12}$$

Note that any multiplications that give rise to terms higher than three have been skipped. Equation (D.12) can be sorted in ascending order as:

$$\begin{aligned}\dot{\mathbf{z}} = \mathbf{\Lambda} \boldsymbol{z} \quad &\text{(Order 1)} \\ +\mathbf{\Lambda} \boldsymbol{h2}(\boldsymbol{z}) - \mathbf{\Lambda} \boldsymbol{z} \bar{\boldsymbol{D}} \boldsymbol{h2}(\boldsymbol{z}) + \boldsymbol{F2}(\boldsymbol{z}) \quad &\text{(Order 2)} \\ -\bar{\boldsymbol{D}} \boldsymbol{h2}(\boldsymbol{z})(\mathbf{\Lambda} \boldsymbol{h2}(\boldsymbol{z}) - \mathbf{\Lambda} \boldsymbol{z} \bar{\boldsymbol{D}} \boldsymbol{h2}(\boldsymbol{z}) + \mathbf{F2}(\mathbf{z})) + \bar{\mathbf{D}}\mathbf{F2}(\mathbf{z})\mathbf{h2}(\mathbf{z}) + \mathbf{F3}(\mathbf{z}) \quad &\text{(Order 3)}\end{aligned} \tag{D.13}$$

D.1 Removing the Quadratic Terms

To simplify (D.13) the nonlinearities should be removed in sequence. The idea is to determine the coefficient of $h2(z)$ to remove the nonlinearities and put the equation in a Normal Form (simple form). Since (D.6) is the targeted Normal Form, it follows that second order terms of (D.13) should correspond to second order terms of (D.6). Therefore:

$$\boldsymbol{g_2}(\boldsymbol{z}) + \mathbf{\Lambda} \boldsymbol{z} \bar{\boldsymbol{D}} \boldsymbol{h2}(\boldsymbol{z}) - \mathbf{\Lambda} \boldsymbol{h2}(\boldsymbol{z}) = \boldsymbol{F2}(\boldsymbol{z}) \tag{D.14}$$

The operator $\boldsymbol{\mathcal{L}(h2(z))} = \mathbf{\Lambda} \boldsymbol{z} \bar{\boldsymbol{D}} \boldsymbol{h2}(\boldsymbol{z}) - \mathbf{\Lambda} \boldsymbol{h2}(\boldsymbol{z}) = \bar{\boldsymbol{D}}[\boldsymbol{h2}, \mathbf{\Lambda} \boldsymbol{z}]$ is called the *Lie or Poisson bracket*.
To show how $\mathbf{h}$ is determined, we consider a two-dimensional system as:

$$\begin{aligned}\begin{bmatrix} \dot{y}_1 \\ \dot{y}_2 \end{bmatrix} = \begin{bmatrix} \lambda_1 & 0 \\ 0 & \lambda_2 \end{bmatrix} \begin{bmatrix} y_1 \\ y_2 \end{bmatrix} + \begin{bmatrix} C_{11}^1 y_1^2 + C_{12}^1 y_1 y_2 + C_{22}^1 y_2^2 \\ C_{11}^2 y_1^2 + C_{12}^2 y_1 y_2 + C_{22}^2 y_2^2 \end{bmatrix} \\ + \begin{bmatrix} D_{111}^1 y_{3_1}^3 + D_{112}^1 y_{3_1}^2 y_{3_2} + D_{221}^1 y_{3_2}^2 y_{3_1} + D_{222}^1 y_{3_2}^3 \\ D_{111}^2 y_{2_1}^3 + D_{112}^2 y_{3_1}^2 y_{3_2} + D_{221}^2 y_{3_2}^2 y_{3_1} + D_{222}^2 y_{3_2}^3 \end{bmatrix}\end{aligned} \tag{D.15}$$

This system has been transformed already to Jordan form. That is, it is expanded form of (D.4). Noting that transformation is a change of variable, we use equation(D.15) to re-write equation(D.14) as:

$$\begin{bmatrix} g_2^1 \\ g_2^2 \end{bmatrix} + \begin{bmatrix} \frac{\partial h_2^1}{\partial z_1} & \frac{\partial h_2^1}{\partial z_2} \\ \frac{\partial h_2^2}{\partial z_1} & \frac{\partial h_2^2}{\partial z_2} \end{bmatrix} \begin{bmatrix} \lambda_1 & 0 \\ 0 & \lambda_2 \end{bmatrix} \begin{bmatrix} z_1 \\ z_2 \end{bmatrix} - \begin{bmatrix} \lambda_1 & 0 \\ 0 & \lambda_2 \end{bmatrix} \begin{bmatrix} h_2^1 \\ h_2^2 \end{bmatrix} = \begin{bmatrix} C_{11}^1 z_1^2 + C_{12}^1 z_1 z_2 + C_{22}^1 z_2^2 \\ C_{11}^2 z_1^2 + C_{12}^2 z_1 z_2 + C_{22}^2 z_2^2 \end{bmatrix} \tag{D.16}$$

Observe that this time third terms are not included since we are removing the nonlineariies in sequence. Inspection of the right hand side of equation(D.16) suggests that g_2 and $h2$ be of the form:

$$h_2^1 = h2_{11}^1 z_1^2 + h2_{12}^1 z_1 z_2 + h2_{22}^1 z_2^2 \tag{D.17}$$
$$h_2^2 = h2_{11}^2 z_1^2 + h2_{12}^2 z_1 z_2 + h2_{22}^2 z_2^2 \tag{D.18}$$
$$g_2^1 = g2_{11}^1 z_1^2 + g2_{12}^1 z_1 z_2 + g2_{22}^1 z_2^2 \tag{D.19}$$
$$g_2^2 = g2_{11}^2 z_1^2 + g2_{12}^2 z_1 z_2 + g2_{22}^2 z_2^2 \tag{D.20}$$

Equations (D.17—D.20) are then put back into equation(D.16) to obtain:

$$\begin{aligned} &\lambda_1 z_1 (2h2_{11}^1 z_1 + h2_{12}^1 z_2) + \lambda_2 z_2 (h2_{12}^1 z_1 + 2h2_{22}^1 z_2) - \lambda_1 (h2_{11}^1 z_1^2 + h2_{12}^1 z_1 z_2 + h2_{22}^1 z_2^2) \\ &\qquad = (C_{11}^1 - g2_{11}^1) z_1^2 + (C_{12}^1 - g2_{12}^1) z_1 z_2 + (C_{22}^1 - g2_{22}^1) z_2^2 \end{aligned} \tag{D.21}$$

$$\begin{aligned} &\lambda_1 z_1 (2h2_{11}^2 z_1 + h2_{12}^2 z_2) + \lambda_2 z_2 (h2_{12}^2 z_1 + 2h2_{22}^2 z_2) - \lambda_2 (h2_{11}^2 z_1^2 + h2_{12}^2 z_1 z_2 + h2_{22}^2 z_2^2) \\ &\qquad = (C_{11}^2 - g2_{11}^2) z_1^2 + (C_{12}^2 - g2_{12}^2) z_1 z_2 + (C_{22}^2 - g2_{22}^2) z_2^2 \end{aligned} \tag{D.22}$$

Equating the coefficients of z_1^2, $z_1 z_2$ and z_2^2 on both sides of (D.21) and (D.22) one can write a form of equation as:

$$\begin{bmatrix} \lambda_1 & 0 & 0 & 0 & 0 & 0 \\ 0 & \lambda_2 & 0 & 0 & 0 & 0 \\ 0 & 0 & 2\lambda_2 - \lambda_1 & 0 & 0 & 0 \\ 0 & 0 & 0 & 2\lambda_1 - \lambda_2 & 0 & 0 \\ 0 & 0 & 0 & 0 & \lambda_1 & 0 \\ 0 & 0 & 0 & 0 & 0 & \lambda_2 \end{bmatrix} \begin{matrix} h2_{11}^1 \\ h2_{12}^1 \\ h2_{22}^1 \\ h2_{11}^2 \\ h2_{12}^2 \\ h2_{22}^2 \end{matrix} = \begin{matrix} C_{11}^1 - g2_{11}^1 \\ C_{12}^1 - g2_{12}^1 \\ C_{22}^1 - g2_{22}^1 \\ C_{11}^2 - g2_{11}^2 \\ C_{12}^2 - g2_{12}^2 \\ C_{22}^2 - g2_{22}^2 \end{matrix} \tag{D.23}$$

Which can be written as:

$$\mathbf{Bh}2 = \mathbf{C} - \mathbf{g}2 \implies \mathbf{h2} = \mathbf{B}^{-1}[\mathbf{C} - \mathbf{g2}] \tag{D.24}$$

or $\mathbf{h2} = \mathbf{B}^{-1}\mathbf{C}$ if $\mathbf{g2} = \mathbf{0}$.

$$\begin{aligned} h2_{11}^1 &= \frac{C_{11}^1 - g2_{11}^1}{\lambda_1}, h2_{12}^1 = \frac{C_{12}^1 - g2_{12}^1}{\lambda_2} \\ h2_{22}^1 &= \frac{C_{22}^1 - g2_{22}^1}{2\lambda_2 - \lambda_1}, h2_{11}^2 = \frac{C_{11}^2 - g2_{11}^2}{2\lambda_1 - \lambda_2} \\ h2_{12}^2 &= \frac{C_{12}^2 - g2_{12}^2}{\lambda_1}, h2_{22}^2 = \frac{C_{22}^2 - g2_{22}^2}{\lambda_2} \end{aligned}$$

More generally, for $g_2 = 0$,

$$h2_{kl}^j = \frac{C_{kl}^j}{\lambda k + \lambda l - \lambda j} \tag{D.25}$$

Equation(D.25) satisfies the condition for eliminating the second order terms. Notice what happened. It means that as long as $\mathbf{g}_2$ is zero (*no resonance)* all values of $h2$ determined from

(D.25) will remove all second order nonlinearities in (D.13) when substituted. Then (D.13) becomes simply

$$\dot{\mathbf{z}} = \mathbf{\Lambda z} + \text{Terms of order 3 and above.} \tag{D.26}$$

If the higher order terms are neglected, (D.26) is very similar to the linear part of (D.3) except that (D.26) is in z coordinate. This is the point where second order transformation ends.

D.2 Removing the Cubic Terms

With quadratic term removed (D.13) becomes:

$$\dot{\mathbf{z}} = \mathbf{\Lambda} \boldsymbol{z} + \bar{\mathbf{D}}\mathbf{F2}(\mathbf{z})\mathbf{h2}(\mathbf{z}) + \mathbf{F3}(\mathbf{z}) \tag{D.27}$$

To remove the cubic terms of (D.27), another nonlinear transformation of order 3 is needed. Therefore:

$$\mathbf{z} = \mathbf{z} + \mathbf{h3}(\mathbf{z}) \tag{D.28}$$

$h3(z)$ is a cubic polynomial in z such that the expanded form of (D.28) for j^{th} equation becomes

$$y_j = z_j + \sum_{p=1}^{N}\sum_{q=1}^{N}\sum_{r=1}^{N} h3^j_{pqr} z_p z_q z_r. \tag{D.29}$$

Differentiating (D.28) in time and substituting in (D.27) and neglecting any term higher than three yields:

$$\dot{\boldsymbol{z}} = \mathbf{\Lambda} \boldsymbol{z}(\mathbf{1} - \bar{\boldsymbol{D}}\boldsymbol{h3}(\boldsymbol{z})) + \mathbf{\Lambda}\boldsymbol{h3}(\boldsymbol{z})(\mathbf{1} - \bar{\boldsymbol{D}}\boldsymbol{h3}(\boldsymbol{z})) + \bar{\boldsymbol{D}}\boldsymbol{F2}(\boldsymbol{z})\boldsymbol{h2}(\boldsymbol{z}) + \boldsymbol{F3}(\boldsymbol{z}) \tag{D.30}$$

$$\dot{\boldsymbol{z}} = \mathbf{\Lambda} \boldsymbol{z} - \mathbf{\Lambda}\boldsymbol{z}\bar{\boldsymbol{D}}\boldsymbol{h3}(\boldsymbol{z}) + \mathbf{\Lambda}\boldsymbol{h3}(\boldsymbol{z}) + \bar{\boldsymbol{D}}\boldsymbol{F2}(\boldsymbol{z})\boldsymbol{h2}(\boldsymbol{z}) + \boldsymbol{F3}(\boldsymbol{z}) \tag{D.31}$$

If the C and D coefficients are used in place of $F2$ and $F3$ as in [(3.37), Chapter 3], then (D.31) becomes

$$\dot{\boldsymbol{z}} = \mathbf{\Lambda} \boldsymbol{z} - \mathbf{\Lambda}\boldsymbol{z}\bar{\boldsymbol{D}}\boldsymbol{h3}(\boldsymbol{z}) + \mathbf{\Lambda}\boldsymbol{h3}(\boldsymbol{z}) + \bar{\boldsymbol{D}}\boldsymbol{C}(\boldsymbol{z})\boldsymbol{h2}(\boldsymbol{z}) + \boldsymbol{D}(\boldsymbol{z}) \tag{D.32}$$

As in the previous section, if (D.31) has to be in Normal Form, then its cubic term must correspond to the third term of (D.6). Therefore:

$$\mathbf{\Lambda}\boldsymbol{z}\bar{\boldsymbol{D}}\boldsymbol{h3}(\boldsymbol{z}) - \mathbf{\Lambda}\boldsymbol{h3}(\boldsymbol{z}) = \bar{\boldsymbol{D}}\boldsymbol{F2}(\boldsymbol{z})\boldsymbol{h2}(\boldsymbol{z}) + \boldsymbol{F3}(\boldsymbol{z}) - \boldsymbol{g_3}(\boldsymbol{z}). \tag{D.33}$$

Re-write (D.33) using (D.15) as:

$$\begin{bmatrix} \frac{\partial h^1_3}{\partial z_1} & \frac{\partial h^1_3}{\partial z_2} \\ \frac{\partial h^2_3}{\partial z_1} & \frac{\partial h^2_3}{\partial z_2} \end{bmatrix} \begin{bmatrix} \lambda_1 & 0 \\ 0 & \lambda_2 \end{bmatrix} \begin{bmatrix} z_1 \\ z_2 \end{bmatrix} - \begin{bmatrix} \lambda_1 & 0 \\ 0 & \lambda_2 \end{bmatrix} \begin{bmatrix} h^1_3 \\ h^2_3 \end{bmatrix} = \begin{bmatrix} \bar{D}F_2 h2^1 \\ \bar{D}F_2 h2^2 \end{bmatrix} + \begin{bmatrix} D^1_{111}z^3_1 + D^1_{112}z^2_1 z_2 + D^1_{221}z^2_2 z_1 + D^1_{222}z^3_2 \\ D^2_{111}z^3_{2_1} + D^2_{112}z^2_1 z_2 + D^2_{221}z^2_2 z_1 + D^2_{222}z^3_2 \end{bmatrix} - \begin{bmatrix} g^1_3 \\ g^2_3 \end{bmatrix} \tag{D.34}$$

We choose $h2$, g_3 and h_3 to be of the form below:

$$h2^1 = h2^1_{11}z^2_1 + h2^1_{12}z_1 z_2 + h2^1_{22}z^2_2 \tag{D.35}$$

$$h2^2 = h2^2_{11}z^2_1 + h2^2_{12}z_1 z_2 + h2^2_{22}z^2_2 \tag{D.36}$$

$$h^1_3 = h3^1_{111}z^3_1 + h3^1_{112}z^2_1 z_2 + h3^1_{221}z^2_2 z_1 + h3^1_{222}z^3_2 \tag{D.37}$$

$$h^2_3 = h3^2_{111}z^3_{2_1} + h3^2_{112}z^2_1 z_2 + h3^2_{221}z^2_2 z_1 + h3^2_{222}z^3_2 \tag{D.38}$$

$$g^1_3 = g3^1_{111}z^3_1 + g3^1_{112}z^2_1 z_2 + g3^1_{221}z^2_2 z_1 + g3^1_{222}z^3_2 \tag{D.39}$$

$$g^2_3 = g3^2_{111}z^3_{2_1} + g3^2_{112}z^2_1 z_2 + g3^2_{221}z^2_2 z_1 + g3^2_{222}z^3_2 \tag{D.40}$$

Therefore:

$$\frac{\partial h_3^1}{\partial z_1} = 3h3_{111}^1 z_1^3 + 2h3_{112}^1 z_1 z_2 + h3_{221}^1 z_2^2 \tag{D.41}$$

$$\frac{\partial h_3^1}{\partial z_2} = h3_{112}^1 z_1^2 + 2h3_{112}^1 z_1 z_2 + 3h3_{222}^1 z_2^2 \tag{D.42}$$

$$\frac{\partial h_3^2}{\partial z_1} = 3h3_{111}^2 z_1^3 + 2h3_{112}^2 z_1 z_2 + h3_{221}^2 z_2^2 \tag{D.43}$$

$$\frac{\partial h_3^2}{\partial z_2} = h3_{112}^2 z_1^2 + 2h3_{112}^2 z_1 z_2 + 3h3_{222}^2 z_2^2 \tag{D.44}$$

$$\frac{\partial F_2^1}{\partial z_1} = 2C_{11}^1 z_1 + C_{12}^1 z_2 \tag{D.45}$$

$$\frac{\partial F_2^1}{\partial z_2} = C_{12}^1 z_1 + 2C_{22}^1 z_2 \tag{D.46}$$

$$\frac{\partial F_2^2}{\partial z_1} = 2C_{11}^2 z_1 + C_{12}^2 z_2 \tag{D.47}$$

$$\frac{\partial F_2^2}{\partial z_2} = C_{12}^2 z_1 + 2C_{22}^2 z_2 \tag{D.48}$$

Handling the left hand side (LHS) of (D.34)

$$\begin{aligned} &3h3_{111}^1 z_1^3\lambda_1 + 2h3_{112}^1 z_1^2 z_2\lambda_1 + h3_{221}^1 z_2^2 z_1\lambda_1 + h3_{112}^1 z_1^2 z_2\lambda_2 + 2h3_{221}^1 z_2^2 z_1\lambda_2 + 3h3_{222}^1 z_1^3\lambda_2 \\ &-h3_{111}^1 z_1^3\lambda_1 - h3_{112}^1 z_1^2 z_2\lambda_1 - h3_{221}^1 z_2^2 z_1\lambda_1 - h3_{222}^1 z_2^3\lambda_1 \end{aligned} \tag{D.49}$$

$$\begin{aligned} &3h3_{111}^2 z_1^3\lambda_1 + 2h3_{112}^2 z_1^2 z_2\lambda_1 + h3_{221}^2 z_2^2 z_1\lambda_1 + h3_{112}^2 z_1^2 z_2\lambda_2 + 2h3_{221}^2 z_2^2 z_1\lambda_2 + 3h3_{222}^2 z_1^3\lambda_2 \\ &-h3_{111}^2 z_1^3\lambda_2 - h3_{112}^2 z_1^2 z_2\lambda_2 - h3_{221}^2 z_2^2 z_1\lambda_2 - h3_{222}^2 z_2^3\lambda_2 \end{aligned} \tag{D.50}$$

Collecting like terms, LHS therefore is:

$$(2h3_{111}^1\lambda_1)z_1^3 + (h3_{112}^1\lambda_1 + h3_{112}^1\lambda_2)z_1^2 z_2 + (2h3_{221}^1\lambda_1)z_2^2 z_1 + (3h3_{222}^1\lambda_2 - h3_{222}^1\lambda_1)z_2^3 \tag{D.51}$$

$$(2h3_{111}^2\lambda_1)z_1^3 + (h3_{112}^2\lambda_1 + h3_{112}^1\lambda_2)z_1^2 z_2 + (2h3_{221}^2\lambda_2)z_2^2 z_1 + (3h3_{222}^2\lambda_1 - h3_{222}^2\lambda_2)z_2^3 \tag{D.52}$$

Handling the Right hand side (RHS) of (D.34)

First we note that the expression $\bar{\mathbf{D}}\mathbf{F2h2}$ is element-wise matrix multiplication. That is, each element of $\bar{\mathbf{D}}\mathbf{F2}$ is multiplied by its corresponding element of **h2**. Thus,

$$(\bar{D}F_2h2)_{111}^1 z_1^3 + (\bar{D}F_2h2)_{112}^1 z_1^2 z_2 + (\bar{D}F_2h2)_{221}^1 z_2^2 z_1 + (\bar{D}F_2h2)_{222}^1 z_2^3 \tag{D.53}$$

$$(\bar{D}F_2h2)_{111}^2 z_{2_1}^3 + (\bar{D}F_2h2)_{112}^2 z_1^2 z_2 + (\bar{D}F_2h2)_{221}^2 z_2^2 z_1 + (\bar{D}F_2h2)_{222}^2 z_2^3 \tag{D.54}$$

$$\bar{D}F2^1 = \frac{\partial F_2^1}{\partial z_1} + \frac{\partial F_2^1}{\partial z_2} = 2C_{11}^1 z_1 + C_{12}^1 z_2 + C_{12}^1 z_1 + 2C_{22}^1 z_2 \tag{D.55}$$

$$\bar{D}F2^2 = \frac{\partial F_2^2}{\partial z_1} + \frac{\partial F_2^2}{\partial z_2} = 2C_{11}^2 z_1 + C_{12}^2 z_2 + C_{12}^2 z_1 + 2C_{22}^2 z_2 \tag{D.56}$$

We also note that $\bar{\mathbf{D}}\mathbf{F2}$ is symmetrical so $h_{12} = h_{21}$ and $C_{12} = C_{21}$. Therefore, $\bar{\mathbf{D}}\mathbf{F2h2}$ can be expressed as:

$$(2C_{11}^1 h2_{11}^1)z_1^3 + (C_{12}^1 h2_{12}^1)z_1^2 z_2 + (C_{21}^1 h2_{21}^1)z_2^2 z_1 + (2C_{22}^1 h2_{22}^1)z_2^3 \tag{D.57}$$

$$(2C_{11}^2h2_{11}^2)z - 1^3 + (C_{12}^2h2_{12}^2)z_1^2z_2 + (C_{21}^2h2_{21}^2)z_2^2z_1 + (2C_{22}^2h2_{22}^2)z_2^3 \tag{D.58}$$

Collecting like terms in RHS gives:

$$\begin{aligned}&(2C_{11}^1h2_{11}^1 + D_{111}^1 - g3_{111}^1)z_1^3 + (C_{12}^1h2_{12}^1 + D_{112}^1 - g3_{112}^1)z_1^2z_2\\&+(C_{21}^1h2_{21}^1 + D_{221}^1 - g3_{221}^1)z_2^2z_1 + (2C_{22}^1h2_{22}^1 + D_{222}^1 - g3_{222}^1)z_2^3\end{aligned} \tag{D.59}$$

$$\begin{aligned}&(2C_{11}^2h2_{11}^2 + D_{111}^2 - g3_{111}^2)z_1^3 + (C_{12}^2h2_{12}^2 + D_{112}^2 - g3_{112}^2)z_1^2z_2\\&+(C_{21}^2h2_{21}^2 + D_{221}^2 - g3_{221}^2)z_2^2z_1 + (2C_{22}^2h2_{22}^2 + D_{222}^2 - g3_{222}^2)z_2^3\end{aligned} \tag{D.60}$$

Equating the coefficients of like terms in both sides of (D.34)

$$2h3_{111}^1\lambda_1 = 2C_{11}^1h2_{11}^1 + D_{111}^1 - g3_{111}^1 \tag{D.61}$$
$$h3_{112}^1\lambda_1 + h3_{112}^1\lambda_2 = C_{12}^1h2_{12}^1 + D_{112}^1 - g3_{112}^1 \tag{D.62}$$
$$2h3_{221}^1\lambda_1 = C_{21}^1h2_{21}^1 + D_{221}^1 - g3_{221}^1 \tag{D.63}$$
$$3h3_{222}^1\lambda_2 - h3_{222}^1\lambda_1 = 2C_{22}^1h2_{22}^1 + D_{222}^1 - g3_{222}^1 \tag{D.64}$$
$$2h3_{111}^2\lambda_1 = 2C_{11}^2h2_{11}^2 + D_{111}^2 - g3_{111}^2 \tag{D.65}$$
$$h3_{112}^2\lambda_1 + h3_{112}^2\lambda_2 = C_{12}^2h2_{12}^2 + D_{112}^2 - g3_{112}^2 \tag{D.66}$$
$$2h3_{221}^2\lambda_2 = C_{21}^2h2_{21}^2 + D_{221}^2 - g3_{221}^2 \tag{D.67}$$
$$3h3_{222}^2\lambda_1 - h3_{222}^2\lambda_2 = 2C_{22}^2h2_{22}^2 + D_{222}^2 - g3_{222}^2 \tag{D.68}$$

Therefore, (D.61 —D.68) can be written as:

$$\begin{bmatrix} 2\lambda_1 & 0 & 0 & 0 & 0 & 0 & 0 & 0\\ 0 & \lambda_1+\lambda_2 & 0 & 0 & 0 & 0 & 0 & 0\\ 0 & 0 & 2\lambda_2 & 0 & 0 & 0 & 0 & 0\\ 0 & 0 & 0 & 3\lambda_2-\lambda_1 & 0 & 0 & 0 & 0\\ 0 & 0 & 0 & 0 & 3\lambda_1-\lambda_2 & 0 & 0 & 0\\ 0 & 0 & 0 & 0 & 0 & 2\lambda_1 & 0 & 0\\ 0 & 0 & 0 & 0 & 0 & 0 & \lambda_1+\lambda_2 & 0\\ 0 & 0 & 0 & 0 & 0 & 0 & 0 & 2\lambda_2 \end{bmatrix} \begin{matrix} h3_{111}^1\\ h3_{112}^1\\ h3_{221}^1\\ h3_{222}^1\\ h3_{111}^2\\ h3_{112}^2\\ h3_{221}^2\\ h3_{222}^2 \end{matrix} = \begin{matrix} 2C_{11}^1h2_{11}^1 + D_{111}^1 - g3_{111}^1\\ C_{12}^1h2_{12}^1 + D_{112}^1 - g3_{112}^1\\ C_{21}^1h2_{21}^1 + D_{221}^1 - g3_{221}^1\\ 2C_{22}^1h2_{22}^1 + D_{222}^1 - g3_{222}^1\\ 2C_{11}^2h2_{11}^2 + D_{111}^2 - g3_{111}^2\\ C_{12}^2h2_{12}^2 + D_{112}^2 - g3_{112}^2\\ C_{21}^2h2_{21}^2 + D_{221}^2 - g3_{221}^2\\ 2C_{22}^2h2_{22}^2 + D_{222}^2 - g3_{222}^2 \end{matrix} \tag{D.69}$$

Thus:

$$h3_{111}^1 = \frac{2C_{11}^1h2_{11}^1 + D_{111}^1 - g3_{111}^1}{2\lambda_1} \tag{D.70}$$
$$h3_{112}^1 = \frac{C_{12}^1h2_{12}^1 + D_{112}^1 - g3_{112}^1}{\lambda_1+\lambda_2} \tag{D.71}$$
$$h3_{221}^1 = \frac{C_{21}^1h2_{21}^1 + D_{221}^1 - g3_{221}^1}{2\lambda_2} \tag{D.72}$$
$$h3_{222}^1 = \frac{2C_{22}^1h2_{22}^1 + D_{222}^1 - g3_{222}^1}{3\lambda_2-\lambda_1} \tag{D.73}$$
$$h3_{111}^2 = \frac{2C_{11}^2h2_{11}^2 + D_{111}^2 - g3_{111}^2}{3\lambda_1-\lambda_2} \tag{D.74}$$
$$h3_{112}^2 = \frac{C_{12}^2h2_{12}^2 + D_{112}^2 - g3_{112}^2}{2\lambda_1} \tag{D.75}$$
$$h3_{221}^2 = \frac{C_{21}^2h2_{21}^2 + D_{221}^2 - g3_{221}^2}{\lambda_1+\lambda_2} \tag{D.76}$$
$$h3_{222}^2 = \frac{2C_{22}^2h2_{22}^2 + D_{222}^2 - g3_{222}^2}{2\lambda_2} \tag{D.77}$$

Assuming $g_3 = 0$, then from (D.69) we can write a general expression for h_3 as:

$$h3^{j}_{pqr} = \frac{[C_{res} + D]^{j}_{pqr}}{\lambda p + \lambda q + \lambda r - \lambda j} \tag{D.78}$$

$$\therefore \dot{\boldsymbol{z}} = \boldsymbol{\Lambda z} \tag{D.79}$$

Where C_{res} is a residual term emanating from second order transformation and which corresponds to the coefficient of $\bar{\mathbf{D}}\mathbf{F2}(\mathbf{z})\mathbf{h2}(\mathbf{z})$ while, D is the original third term corresponding to the coefficient of the term $F3(z)$

We have finally removed the third order nonlinearities and the monstrous (D.15) has been put to Normal Form!.

Appendix E

Data of Studied Power Systems

E.1 Line Data: IEEE 3-Machine Power System

Table E.1 – Line Data

Fr Bus	To Bus	R (pu)	X (pu)	Bch(pu) full
1	4	0	0.0576	0
2	7	0	0.0625	0
3	9	0	0.0586	0
4	6	0.017	0.0920	0.1580
4	5	0.01	0.0850	0.1760
6	9	0.039	0.170	0.3580
5	7	0.032	0.1610	0.3060
8	9	0.0119	0.1008	0.2090
7	8	0.0085	0.072	0.149

E.2 Bus Data: IEEE 3-Machine Power System

Table E.2 – A2: Bus Data

Bus	Type	Volt. Mag.	Ang. (deg)	Pd	Qd	Pg	Qg	Qmin	Qmax
1	Slack	1.040	0	0	0	71.9	54.6	-300	300
2	PV	1.025	9.48	0	0	163	30.4	-300	300
3	PV	1.025	4.77	0	0	85	14.2	-300	300
4	PQ	1.010	-2.26	0	0	0	0	0	0
5	PQ	0.972	-4.06	125	50	0	0	0	0
6	PQ	0.989	-3.70	90	30	0	0	0	0
7	PQ	1.011	3.84	0	0	0	0	0	0
8	PQ	0.997	0.78	100	35	0	0	0	0
9	PQ	1.018	2.03	0	0	0	0	0	0

E.3 Dynamic and Exciter Data

Table E.3 – Dynamic Data: IEEE 3-Machine Power System

Bus	R_a	X_d	X'_d	X''_d	X_q	X'_q	X''_q	T'_{do}	T''_{do}	T'_{qo}	T''_{qo}	H	D
1	0.089	0.269	0.0608	0	0.0969	0.0969	0	8.96	0	0.31	0	23.64	0.2
2	0.089	0.8958	0.1198	0	0.8645	0.1969	0	6.00	0	0.535	0	6.4	0.2
3	0.089	1.998	0.1813	0	1.2578	0.2500	0	5.89	0	0.600	0	3.01	0.2

Table E.4 – Exciter Data

KA	Tr	TE	T1	T2
20	0.6	0.02	10	2.5
20	0.6	0.02	10	2.5
20	0.6	0.02	10	2.5

E.4 Data for the 39- and 145-Bus Power Systems

The data for the 39-bus power system was extracted form [118]. For the 145-bus power system, the power flow data was extracted from MATPOWER [128, 129], while the dynamic data was taken from [130].

Appendix F

Résumé Étendu en Français

F.1 Introduction Général

Le chapitre 1 de ce manuscrit de thèse renvoie à des introductions générales. En effet, le contexte et l'énoncé du problème relatif aux travaux de recherches effectuées y sont présentés d'une part. D'autre part, la principale motivation, aussi bien les objectifs que les principales contributions de ce travail sont pour leur part, largement mis en lumière (dans ce chapitre) selon le plan de travail ci-après.

F.1.1 Contexte et Motivation

En ce qui concerne les combustibles fossiles, ils constituent l'un des agents principaux de la dégradation de l'environnement en raison des émissions dû à leur exploitation. La réduction des émissions de gaz et donc des combustibles fossiles est une préoccupation mondiale étant donné leurs retombées néfastes sur l'environnement. Du fait de plusieurs contraintes économiques, techniques et environnementales, les systèmes électriques actuels fonctionnent très près de leurs limites et donc, présentent de plus en plus des comportements non linéaires. Un système contraint est donc un systeme dont les conditions de fonctionnement sont tres proches de ses limites fonctionnelles, à l'exemple, de la limite de stabilité de sa tension. Plusieurs autres aspects peuvent induire un système electrique a fonctionnement proche de ses limites à savoir — (1) un niveau plus élevé de charges du système, (2) un transfert de puissance important à travers certaines interfaces de transmission, et (3) chargement lourd de certaines plantes. Un système d'alimentation contraint peut conduire à un comportement dynamique complexe et donc, un comportement fortement non linéaire pouvant être très difficile à expliquer.

Suite à l'épuisement des combustibles fossiles, il s'est revelé un important problème de disponibilité des ressources énergétiques traditionnelles aux profits des énergies renouvelables (REs) telles que l'énergie solaire thermique, solaire photovoltaïque, éolien et le biogaz [1]. Au fil des années, une utilisation de plus en plus accrue des énergies renouvelables est observée à des fin d'électricité comparativement aux années antérieures (voir Figure F.1). Les progrès de la science relatif à la technologie des convertisseurs au moyen de l'électronique de puissance (PE) ont rendu possible l'intégration des énergies renouvelables dans un réseau de production électrique. De plus, l'émergence de nouveaux dispositifs PE utilisé dans un systeme d'alimentation et le nombre croissant de systèmes de production d'energie distribuée dans les réseaux électriques contribuent à changer la structure du réseau traditionnel.

F.1.2 Défis Actuels et Futurs Potentiels du Reseau

La contrainte du système du fait de l'intégration des REs augmente les non-linéarités du système et, par conséquent, crée de nouveaux défis pour les systèmes électriques. Elle peut conduire à des interactions non linéaires des modes d'oscillation du système, ce qui modifie

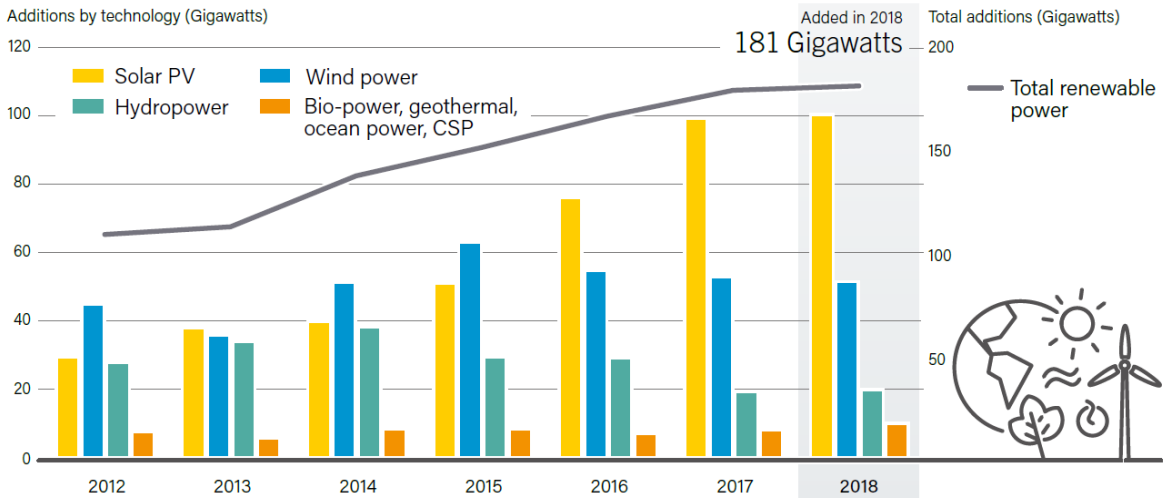

Figure F.1 – Ajouts mondiaux annuels de capacité d'énergie renouvelable, par technologie et total, 2012-2018 [4]

le comportement dynamique du système. *Mode* est le terme technique designant un modèle d'oscillation particulier (voir l'explication détaillée dans la section F.1.4). Les non-linéarités du système et les interactions modales sont affectées par les conditions de fonctionnement du système, la stratégie de contrôle et les paramètres du système de contrôle [5]. Le transport d'une grande quantité d'énergie sur de longues distances est très courantes de nos jours en raison des connexions inter-zones (par exemple Ecosse-Angleterre) et de la croissance des sources REs. De plus, la plupart des sources REs viables comme les parcs éoliens sont généralement loin du centre de charge. Le transport de grande puissance sur de longues distances entraîne des oscillations de puissance et des interactions non linéaires dans un système à haute tension AC (HVAC). Des liaisons HVDC peuvent être utilisées en substitution afin d'amortir ces oscillations. Les contrôles pour HVDC peuvent conduire à de fortes interactions non linéaires, bien que ces interactions ne soient pas toujours nécessairement négatives. Une étude antérieure de l'interaction modale non linéaire dans un système HVDC/AC avec modulation DC a indiqué qu'une interaction modale fortement non linéaire peut résulter des charges AC et DC très élevés avec des modulations de puissance DC bien réglées [5]. Étant donné que les REs injectent de l'énergie dans le réseau via des convertisseurs PE, entraînant un manque d'inertie et un couple de synchronisation dans le réseau, la deconnexion des générateurs synchrones augmenterait l'effet de non-linéarité [10] affectant ainsi la stabilité de l'angle du rotor. En plus, les convertisseurs PE pourraient former une capacité virtuelle, qui pourrait interagir avec le réseau AC pour déclencher une oscillation instable dans un système relativement faible (c'est-à-dire à haute impédance) [11].

Comme souligné dans [12, 13], en plus de contribuer à la non-linéarité, les REs et les PEs qui les accompagnent introduisent de nouveaux modes d'oscillation sur le reseau en raison du déplacement des machines synchrones. Il a été noté dans [12] que ces nouveaux modes d'oscillation sont très sensibles aux variations des paramètres de contrôle et peuvent rendre le système plus imprévisible et difficile à surveiller ou à contrôler.

Les manifestations de ces défis abondent dans les systèmes d'alimentation pratiques avec une intégration RE significative. Par exemple, le 19 février 2011, des oscillations inter-zones au sein du réseau électrique de l'Europe continentale (CE) se sont produites. Des oscillations similaires se sont reproduites le 24 février 2011. La fréquence d'oscillation était de 0,25 Hz et a duré 15 minutes (voir Figure F.2). Il n'y avait aucun indice clair sur la cause de l'oscillation au départ. Les calculs modaux dans [16] ont révélé plus tard que deux modes se superposaient à 0,25 Hz avec la participation de la Turquie, de l'Espagne/du Portugal et de l'Italie contre le nord de l'Europe. Les conclusions suivantes ont été tirées dans [16]: (1)

il y a eu une interaction des modes 0,18 Hz (mode Est-Ouest) et 0,25 Hz (mode Nord-Sud), (2) la connexion synchrone de la Turquie déplace 0,3 Hz à 0,25 Hz (nouveau mode), (3) les générateurs RE ont soustrait l'inertie du système en remplaçant les générateurs équipés de PSS. Par conséquent, le GRT italien a immédiatement renforcé le PSS en Italie.

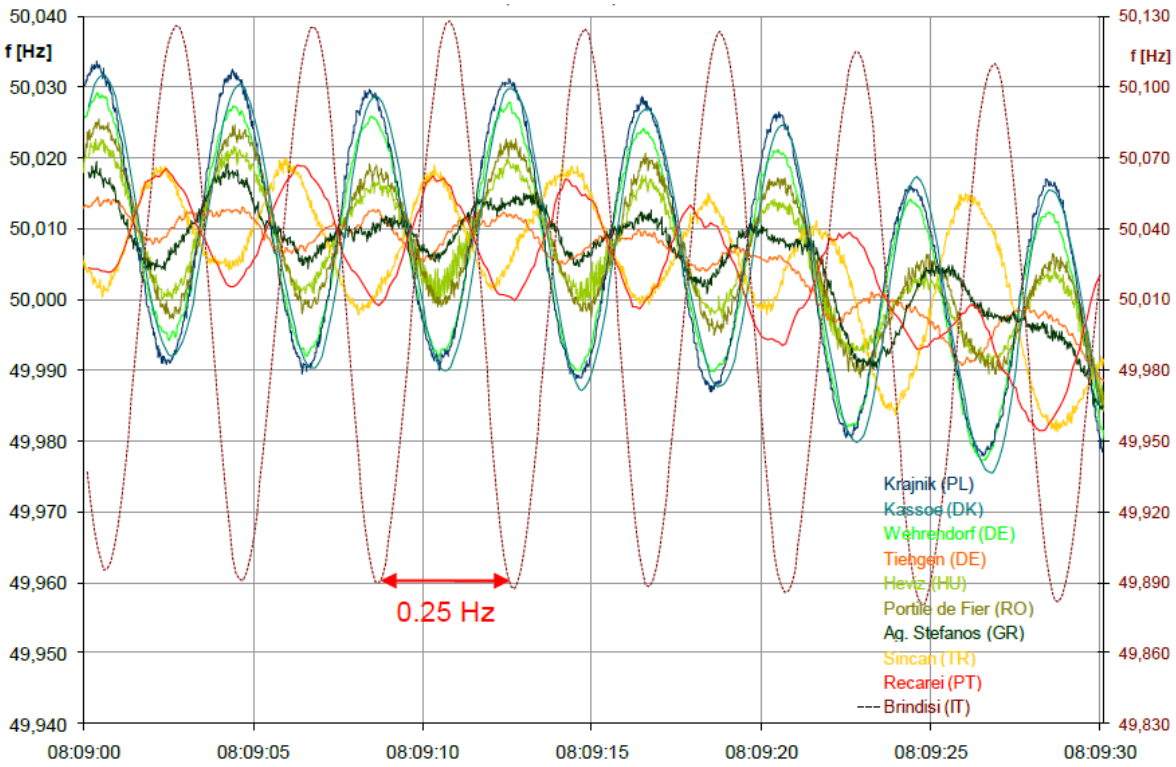

Figure F.2 – Vue détaillée de la fréquence du système (mesures) pour le 19 février 2011 — Brindisi (IT) en phase avec Sincan (TR) et Recarei (PT) en face de Portile de Fier (RO) et Kassoe (DK) [[16]

Une autre dangeureuse oscillation de 3 heures et 20 minutes de durée moyenne , s'est produite dans le système éolien de Hami, Xinjiang, Chine, le 1er juillet 2015 . Plus tard , Il a été découvert que cette oscillation était causée par l'interaction entre plusieurs convertisseurs d'éoliennes (WTC) de générateurs synchrones à aimants permanents (PMSG) et le faible réseau AC [17].

Compte tenu de tous ces changements présents et anticipés dans les systèmes électriques, il devient nécessaire d'étendre l'analyse d'un système électrique, afin de caractériser correctement son comportement dynamique et de mieux concevoir ses commandes. Pour ce faire, des outils plus sophistiqués sont neccessaires afin de faire face à l'évolution. Bien que plusieurs études soient en cours concernant l'augmentation de la non-linéarité et le comportement très complexe qui en résulte pour un système électrique, peu d'attention est accordée jusqu'ici aux interactions non linéaires pouvant révéler beaucoup d'informations cachées dans le système. Selon l'état du système, l'effet des interactions non linéaires peut lui être tantot négatif ou positif. Ce constat est d'autant plus perceptible au travers de la littérature scientifique où les effets positifs et négatifs de l'intégration des RE/PE sont présentés. Par exemple, un amortissement amélioré des oscillations dans le cas d'une partie croissante du PE interfacé de génération est rapporté dans [18].

F.1.3 La Nécessité de Développer des Outils dans la Continuité des Existants

Comme précédemment mentionné, les systèmes contraints présentent un comportement fortement non linéaire et l'intégration RE/PE dans un système électrique contribue en outre à

cette contrainte. Des outils plus sophistiqués sont alors indispensables pour palier à la complexité du système. Des outils avancés à savoir les méthodes de reconnaissance des formes [19], les méthodes des systèmes experts (ES) [20], les outils basés sur le contrôle robuste [21] sont en cours de développement pour l'étude des systèmes complexes. Ces outils sont pas à la portée d'un point de vue exploitation, d'un ingénieur moyen d'exploitation de système électrique. Dans la plus part des cas, aucun paramètres physiques quantifiables n'est disponibles permettant à l'ingénieur de prendre des décisions ou des plannings. L'outil le plus répandue pour l'étude les oscillations d'un système électrique est l'analyse modale. Des outils d'analyse modale conventionnels tels que la stabilité des petits signaux sont couramment utilisés. Cependant, ceq derniers sont linéaires et ne peuvent caractériser avec précision le comportement d'un système électrique en cas d'intégration en grand nombre de RE/PE. Il existe donc un besoin de fournir des outils alternatifs avec des fonctionnalités communes aux ingénieurs et possédant de très larges capacités. La méthode *Forme Normale (NF)* est une bonne alternative mais elle est difficile à appliquer aux systèmes avec un grand nombre de variables.

F.1.4 Modes d'oscillation

Il existe plusieurs modes d'oscillations dans un système interconnecté. Mathématiquement, un mode (ou un mode propre)/mode naturel est le terme pour une paire valeur propre/vecteur propre de la partie linéaire d'un système dynamique. Physiquement, un mode peut être considéré comme un modèle unique dans lequel l'énergie stockée dans le système est dépensée lorsque le système est perturbé. À titre d'illustration, considérons dans la Figure F.3, deux masses m_1, m_2, attachées à trois ressorts k_1, k_2 et k_{12}. Supposons que les points finaux sont fixes, ce système a deux modes naturels d'oscillation.

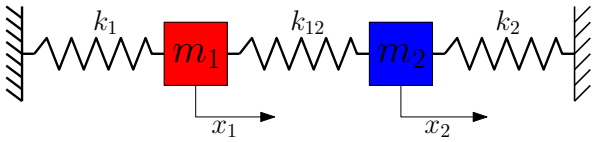

Figure F.3 – Mass-spring system exhibiting two natural modes of oscillation.

Soit les déplacements de la première masse $x_1(t)$ et ceux de la seconde masse $x_2(t)$. Les équations de mouvement du système sont données par

$$m\ddot{x}_1 = -k_1x_1 - 0.3k_1x_1^2 - 0.4k_1x_1^3 + k_{12}(x_2 - x_1) \tag{F.1a}$$

$$m\ddot{x}_2 = -k_2x_2 + 0.4k_1x_2^2 + 0.3k_1x_2^3 + k_{12}(x_1 - x_2), \tag{F.1b}$$

où des non-linéarités (choisies arbitrairement) dans les ressorts sont intentionnellement ajoutées pour les démonstrations.

Si l'on suppose que les déplacements sont suffisamment faibles et que l'équilibre du système est à l'origine, les effets des termes non linéaires (bleu dans (F.1)) peuvent être négligés et il est possible de calculer les fréquences naturelles, en Hertz, pour des ressorts et des masses identiques (c.-à-d. $k_1 = k_2 = k_{12} = k$, $m_1 = m_2 = m$) comme

$$f_1 = \frac{1}{2\pi}\sqrt{\frac{k}{m}}, \quad f_2 = \frac{1}{2\pi}\sqrt{\frac{3k}{m}}. \tag{F.2}$$

Ayant supposé un système linéaire, lorsque la masse m_1 est déplacée de x_1 vers la droite, le ressort k_1 tire la masse vers la gauche avec une force de réaction k_1x_1, et le ressort k_{12} pousse la masse vers la gauche avec une force de réaction $k_{12}(x_1 - x_2)$. De même, lorsque la masse m_2 est déplacée de x_2 vers la gauche, le ressort k_2 tire la masse vers la droite avec une force de réaction k_2x_2, et le ressort k_{12} pousse la masse vers la droite avec une force de réaction $k_{12}(x_2 - x_1)$. Supposons que $k = 5$, $m = 1$, $f_1 = 0,36\ Hz$ et $f_2 = 0,62\ Hz$. Ainsi, les deux modes sont décrits ci-dessous:

- **Mode 1** — les deux masses se déplacent ensemble à la fréquence $f_1 = 0,36\ Hz$, avec la même amplitude et dans la même direction de sorte que le ressort de connexion (k_{12}) entre elles n'est pas étiré ni compressé. Ce mouvement est illustré sur la Figure 1.5a et est obtenu en simulant le système non linéaire (F.1) avec des conditions initiales petites et égales pour $x_1,\ x_2$. La FFT de la Figure F.4b confirme la fréquence de l'oscillation.

- **Mode 2** — les deux masses se déplacent à la fréquence $f_2 = 0,62\ Hz$, avec la même amplitude mais dans des directions opposées de sorte que le ressort de connexion (k_{12}) entre elles est alternativement étiré et compressé . Dans ce cas, le centre (noeud) du ressort de connexion est fixe. Ce mouvement est illustré à la Figure F.4c et est obtenu en simulant le système non linéaire (F.1) avec des conditions initiales petites, égales mais opposées pour $x_1,\ x_2$. La FFT de la Figure F.4d confirme la fréquence de l'oscillation.

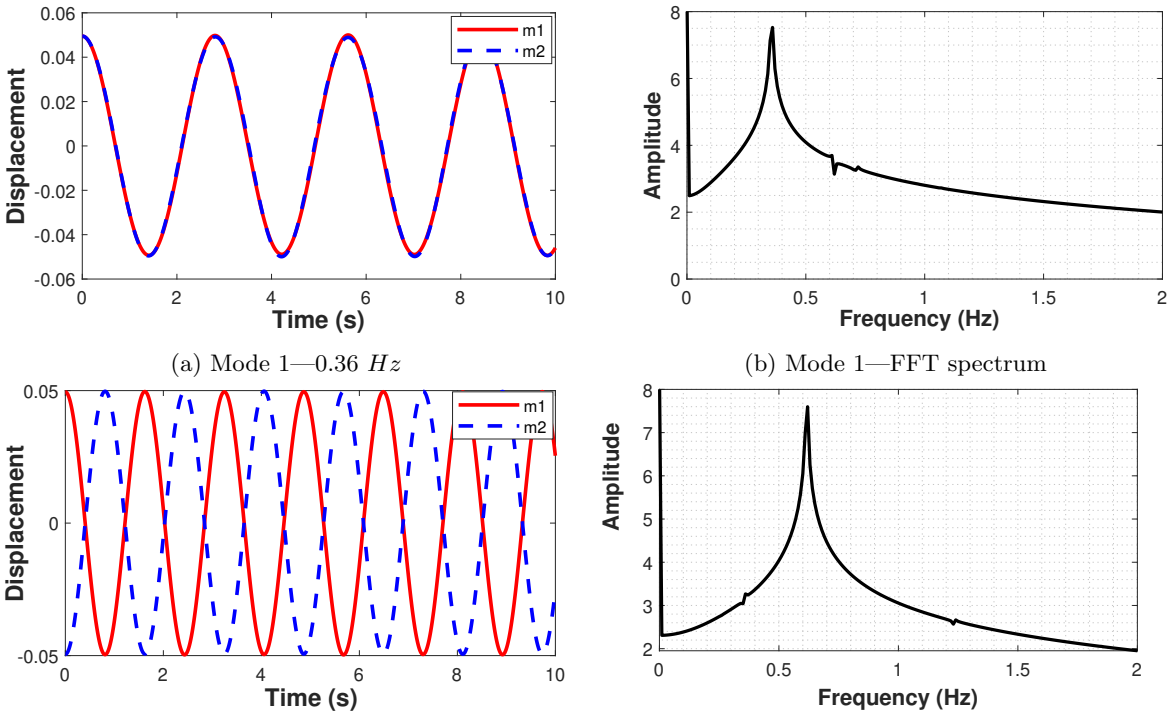

(a) Mode 1—0.36 Hz

(b) Mode 1—FFT spectrum

(c) Mode 2—0.62 Hz.

(d) Mode 2—FFT spectrum.

Figure F.4 – Natural modes of Oscillation of two-mass three-spring system.

Tout autre mouvement des corps de la Figure F.3 n'est pas naturel, mais une combinaison linéaire des deux modes naturels. Les deux modes décrits ci-dessus ont deux fréquences distinctes. Ainsi, le mode est souvent utilisé, de façon plus lâche, pour désigner une oscillation à une fréquence caractéristique.

Avec les modèles plus élaborés, les oscillations majeures dans les systèmes d'alimentation comprennent: les modes d'oscillation électromécanique, de contrôle et de torsion. Pour les modes électromécaniques, les variables les plus impliquées sontles angles internes et les vitesses de rotor des générateurs. De manière générale, les oscillations basse fréquence des réseaux électriques sont le résultat du couplage électromécanique entre le réseau de transmission et les générateurs. Les modes de contrôle sont associés au générateur ou aux unités d'excitation et à d'autres équipements de contrôle, tels que des excitateurs mal réglés, des convertisseurs HVDC et des compensateurs de var statique. Les modes d'oscillation de torsion sont associés au système de rotation de l'arbre du turbogénérateur. Le défi majeur du système électrique est les oscillations électromécaniques à basse fréquence qui peuvent être soit *locale* soit inter-zone. Lorsqu'une machine ou un groupe de machines qui ont de forts liens électriques dans une zone oscille et que leurs oscillations dominent dans la zone où elles se trouvent, on parle

d'oscillation locale. Le mode inter-zone implique des machines dans une zone se balançant contre des machines dans d'autres zones. Il a généralement une fréquence propre inférieure dans la plage de 0,1 - 0,8 Hz [25]. Cependant, avec plusieurs générateurs à commande par convertisseur (CCBG) dans le réseau, les caractéristiques ci-dessus peuvent ne pas toujours être de véritables signatures de modes électromécaniques. Cela est dû au fait que les CCBG conduisent à de nouveaux modes d'oscillation bas semblables aux modes électromécaniques d'oscillation inter-zones [12]. Ce phénomène pose un problème pour identifier clairement les modes électromécaniques réels. De nouvelles méthodes sont en cours de développement pour résoudre ce problème [26]. L'analyse des grands systèmes doit nécessairement se concentrer sur les modes critiques d'importance, généralement les modes inter-zones.

L'étude du comportement de ces modes est connue sous le nom d'analyse modale. L'outil le plus courant pour l'analyse modale est l'analyse de stabilité du petit signal (SSA) qui fournit de nombreuses informations concernant ces oscillations. Comme SSA n'explique que le comportement linéaire, il est plus précisément appelé analyse modale linéaire (LMA).

F.1.5 Interactions Modales et Modes Non Linéaires

Lorsque le système électrique est contraint, la dynamique n'est pas complètement décrite par les modes naturels. En plus des modes naturels, la dynamique peut être affectée par certaines combinaisons d'ordre supérieur des modes naturels. L'effet de ces combinaisons d'ordre supérieur est appelé *interaction modale non linéaire*. L'interaction modale non linéaire donne naissance à "d'autres modes", qui peuvent affecter de manière significative, la dynamique du système. Le concept de *mode non linéaire* permet de comprendre et d'interpréter correctement le phénomène — interaction modale non linéaire, car il aide à expliquer les "autres modes", avec le spectre propre. Le mode non linéaire est utilisé pour décrire l'extension d'un mode linéaire au régime non linéaire. Il s'agit donc d'une extension de la propriété invariance d'un mode linéaire au régime non linéaire. Physiquement, c'est le rendu de couplages modaux non linéaires, d'une manière qui, si un mouvement particulier n'est initié que sur un mode particulier; aucune énergie n'est donnée aux autres, de sorte que le mouvement ne reste que sur ce mode. L'interaction modale est essentielle et peut soit stabiliser, soit déstabiliser le système.

Lorsque l'interaction modale non linéaire se produit, la dynamique devient difficile à expliquer avec LMA. L'analyse modale qui prend en compte les interactions non linéaires des modes est connue sous le nom de NLMA.

Une illustration simple des interactions modales non linéaires peut être montrée en simulant le système (F.1) avec des conditions initiales plus élevées (c'est-à-dire des déplacements plus importants de $x_1,\ x_2$). L'effet des non-linéarités ne sera plus négligeable et l'oscillation sera composée des combinaisons linéaires (naturelles) et significatives des modes linéaires. Ceci est illustré dans la figure F.5. Il ressort clairement de la figure F.5a que le mode 1 est dominant. Au moins, la réponse ressemble à celle de la figure F.4a. Cependant, la conclusion que le mode linéaire est suffisant pour comprendre le comportement de ce système peut être trompeuse. La FFT de la figure F.5b révèle clairement la présence significative d'autres fréquences, dans ce cas, en raison de distorsions non linéaires des modes naturels. Par exemple, les deux modes linéaires sont identifiés (0,36 Hz et 0,62 Hz), le mode 2 ayant un pic plus petit. Observez qu'il existe une fréquence de 0,72 Hz (c'est-à-dire 0,36 $+0,36 = 2 \times mode1$), dont l'amplitude est élevée. Il existe également une fréquence de 1,08 Hz (c'est-à-dire 0,36 $+0,36 + 0,36 = 3 \times mode\ 1$), bien qu'avec un pic plus petit. D'une certaine manière, on peut vaguement dire qu'il existe de "nouveaux modes" dans la dynamique autres que les modes linéaires. Un terme commun habituellement utilisé pour décrire ces nouvelles fréquences est *harmoniques non linéaires*, car ce sont des multiples des modes fondamentaux. Cependant, comme nous le verrons dans les chapitres suivants, ces nouvelles fréquences ne sont pas nécessairement des multiples d'un mode fondamental mais peuvent provenir de combinaisons de modes différents. NF fournit un moyen analytique

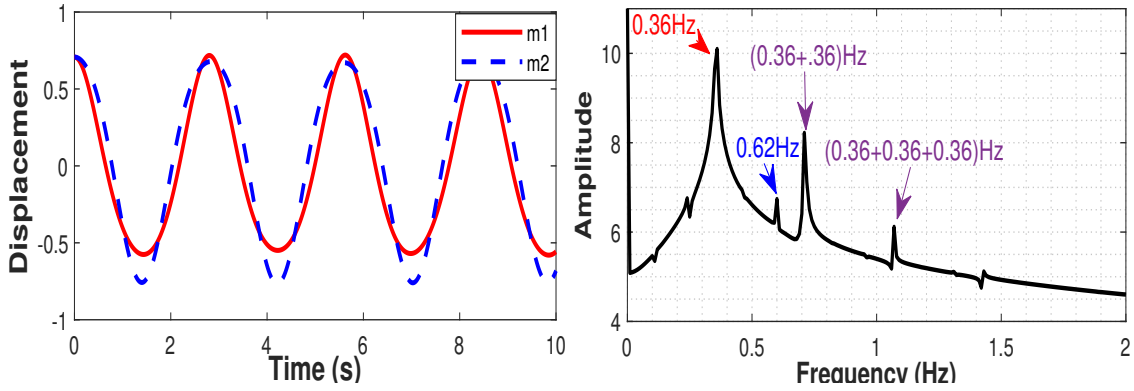

(a) Mode 1—0.36 Hz (b) FFT showing—linear and nonlinear modes.

Figure F.5 – Example of modal interactions

d'expliquer clairement les sources de ces fréquences. Lorsqu'un système électrique est stressé, ce phénomène est présent. Par conséquent, d'autres informations sont nécessaires en plus de l'analyse linéaire pour bien comprendre le comportement.

Il existe essentiellement deux approches pour détecter les interactions modales non linéaires dans un système — méthodes basées sur la simulation dans le domaine temporel et méthodes de résolution sous forme fermée. La deuxième méthode étend le LMA pour obtenir une solution de forme fermée du modèle approximatif non linéaire du système. Ensuite, il permet certaines définitions qui détectent exactement les modes d'interaction et la nouvelle fréquence. L'outil le plus courant dans la deuxième catégorie est l'outil NF. La méthode NF a l'avantage de détecter non seulement l'interaction non linéaire, mais aussi de rendre le système de telle sorte que les techniques pratiques de LMA peuvent toujours être utilisées pour décrire le système. En d'autres termes, il fournit un bon moyen d'expliquer le concept de modes non linéaires. Cependant, il a de très sérieux défis informatiques. Les deux approches peuvent être utilisées de manière complémentaire. Ainsi, la simulation dans le domaine temporel peut être utilisée pour vérifier les solutions de la méthode NF.

F.1.6 Méthode de Forme Normale

La *Forme Normale* telle qu'elle est utilisée dans ce travail est une technique mathématique qui simplifie un ensemble d'équations différentielles non linéaires en une équation simplifiée, qui peut être linéaire dans certains cas particuliers. La simplification est obtenue en introduisant des transformations de coordonnées non linéaires séquentielles. Les équations résultantes sont alors dans leur forme la plus simple (forme normale) [27–30]. Cette définition de *Forme Normale* est souvent désignée avec précision, comme Poincar é Forme Normale, d'après le travail de Poincar é [27]. Elle est basée sur l'expansion en série d'un système d'équations différentielles non linéaires. La technique NF elle-même est très ancienne mais son application de système d'alimentation à l'analyse modale non linéaire est assez à la mode. Au cours des deux dernières décennies, des chercheurs de l'université d'État de l'Iowa ont publié plusieurs publications et ont souligné la nécessité d'étudier l'analyse modale d'ordre supérieur avec la forme normale.

L'approche NF consiste à obtenir une expansion en série de Taylor d'ordre supérieur des équations non linéaires autour d'un SEP. La partie linéaire de l'expansion de la série est analysée pour extraire le contenu modal. Avec les paramètres modaux de la partie linéaire, il est possible de définir des changements de coordonnées de variables qui simplifient les parties non linéaires. L'ordre supérieur NF représente des non-linéarités suffisantes et, par conséquent, sera approprié pour étudier les développements dans le réseau actuel, et même à l'avenir. Cela a été démontré sur un réseau avec une forte pénétration de RE / PE dans [10].

L'idée de base de NF est illustrée par la figure F.6. Notez que les opérations du bloc 1 et du bloc 2 sont les mêmes opérations effectuées pour le modèle linéaire. La seule différence est que l'expansion est étendue aux commandes plus élevées. Bien que la transformation de Jordan en cas linéaire dissocie totalement le système, elle ne dissocie pas les parties non linéaires pour le modèle d'ordre supérieur. La tâche de NF est d'utiliser le bloc 3 pour supprimer ces couplages non linéaires et obtenir un système simple (au mieux un système linéaire).

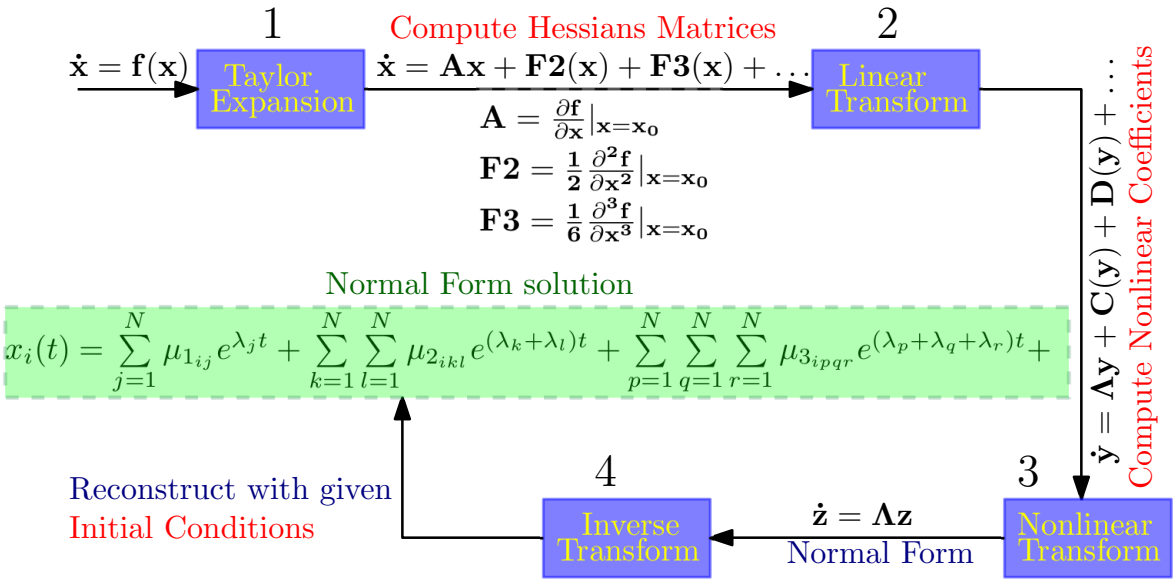

Figure F.6 – Representation of the Basic idea of Normal Form Method

Bien que le système simplifié $\dot{\mathbf{z}} = \mathbf{\Lambda}\mathbf{z}$ ressemble à un système linéaire, la solution est différente. La différence réside dans le changement de variables qui est linéaire dans LMA et non linéaire dans NF. Ainsi, la "magie" de NF est l'inclusion d'informations non linéaires dans un système dynamique linéaire. Le système simplifié qui en résulte présente de nombreux avantages et permet l'extension de nombreuses techniques linéaires. Par exemple, (1) il fournit des informations sur les interactions non linéaires des modes, ce qui aide à concevoir de meilleurs contrôles pour les systèmes électriques; (2) des facteurs de participation en mode non linéaire peuvent être définis pour un meilleur emplacement de PSS; (3) l'interaction modale donne également un aperçu de la stabilité du système non linéaire; (4) l'interaction non linéaire permet d'expliquer les sources de fréquences inconnues apparaissant dans les réponses temporelles.

Défis avec la Méthode de Forme Normale

La difficulté majeure de la NF se rencontre dans:

- *Construire le modèle approximatif et calculer ses nombreux coefficients non linéaires.* C'est-à-dire le calcul des matrices hessiennes dans le bloc 1 et les coefficients non linéaires (qui forment également des matrices hessiennes) dans le bloc 2 (voir Figure F.6).
- *Recherche de la condition initiale dans l'espace NF à partir des valeurs initiales dans l'espace physique.* C'est-à-dire la condition initiale nécessaire dans le bloc 4 pour "déplacer" le système NF vers l'espace physique.

Ce dernier implique la résolution d'un problème d'optimisation non linéaire, qui peut être difficile à converger, ou même converger vers une mauvaise solution. Le premier découle des nombreux coefficients nécessaires à l'analyse, qui doivent être calculés. Ces coefficients augmentent de façon exponentielle avec la taille du système.

F.1.7 Objectif et portée de la recherche

L'implication de tous les changements en cours dans les réseaux actuels est que les outils LMA conçus pour son analyse commencent à échouer. Pourtant, les fonctionnalités des outils LMA sont si attrayantes qu'il sera difficile de les perdre. Parmi les alternatives non linéaires, la méthode NF a reçu le plus grand intérêt de recherche jusqu'à nos jours. L'outil NF a cependant un revers majeur qui limite son application dans le système d'alimentation. C'est très coûteux en calcul. L'approche traditionnelle nécessite l'évaluation préliminaire des matrices de Hesse et l'expansion des valeurs propres, qui sont impraticables avec les méthodes standard lorsque l'on considère les systèmes à grande échelle. Le processus d'expansion des valeurs propres est très difficile et doit être accéléré. Afin d'améliorer ce problème global du système électrique et de rendre possible l'analyse modale non linéaire du futur réseau, cette thèse traite principalement d'un problème:

- **La réduction drastique des calculs nécessaires pour appliquer la méthode NF aux systèmes d'alimentation avec grand nombre de variables (ce qu'on appelle les grands systèmes).**

L'idée maîtresse du travail est donc la simplification du processus d'application NF dans le système d'alimentation. Une nouvelle méthode pour évaluer rapidement tous les coefficients polynomiaux (appelés *nonlinear coefficients* dans ce travail) nécessaires à l'application NF est proposée. On suppose que le calcul de toutes les valeurs propres est possible et que le réseau du système électrique est déjà réduit si nécessaire. La méthode proposée a été appliquée à quatre systèmes différents: les systèmes IEEE 3-, IEEE 10-, IEEE 16- et IEEE 50. Les applications connues de NF telles que l'analyse des facteurs de participation, la stabilité et les prédictions de décalage de fréquence non linéaire sont passées en revue et mises en œuvre avec un calcul considérablement réduit.

F.1.8 Contributions de cette Thèse

En réponse au problème de la recherche, cette thèse a apporté les contributions suivantes:

1. À la connaissance de l'auteur, cette thèse est la première application de NF à l'étude des réseaux électriques sans l'expansion préliminaire habituelle de la série Taylor. Cette thèse propose une méthode rapide pour obtenir le coefficient non linéaire nécessaire pour le modèle NF sans expansion de Taylor et le calcul des matrices de Hesse associées. En évitant la construction de Hessois, l'analyse NF devient rapide.

2. En termes d'application NF au modèle de système d'alimentation du second ordre, cette thèse présente le plus grand cas de test jamais réalisé, compte tenu des non-linéarités du troisième ordre. L'application de NF à un modèle de système d'alimentation de second ordre sans variables complexes, utilisant NNM est un nouveau concept mal exploité. À la connaissance de l'auteur, le plus grand cas de test signalé d'une telle application n'implique que quatre générateurs. La technique développée dans cette thèse permet d'étendre la capacité des propositions précédentes à l'étude de plus de cinquante machines en un temps de calcul commode.

3. Cette thèse présente un nouvel outil réduit en termes de calcul pour surveiller l'instabilité du mode électromécanique dans un système d'alimentation interconnecté. La méthode proposée a un potentiel d'application en ligne et peut être utilisée par les gestionnaires de réseau électrique pour faire une estimation rapide et approximative de la proximité des modes à l'instabilité.

4. La nouvelle approche de l'analyse NF proposée dans cette thèse ouvre la voie à une application sélective NF dans les réseaux électriques. Par exemple, cette thèse propose une technique NF rapide pour l'étude des interactions modales du système électrique,

qui utilise les caractéristiques des modes du système pour sélectionner soigneusement les termes pertinents à considérer dans l'analyse. Cela conduit à une analyse modale non linéaire très rapide.

5. À la connaissance de l'auteur, il n'existe pas de logiciel dédié pour l'application NF en raison de sa complexité de calcul. La méthode proposée permet de réutiliser uniquement les informations de l'analyse linéaire, pour évaluer les coefficients de tous les termes non linéaires, de manière linéaire et simple et conviviale. Ainsi, la mise en œuvre de NF avec un logiciel commercial de système d'alimentation comme EUROSTAG ®, qui a déjà des outils d'analyse linéaire et transitoire intégrés, est réalisable.

6. Bien que certaines contraintes empêchent l'expérimentation et la validation, cette thèse pose plusieurs problèmes de recherche aux futurs chercheurs. Par exemple, les critères proposés pour les applications sélectives NF peuvent être étudiés pour un réseau 100% PE. De plus, une réduction de calcul supplémentaire utilisant une technique de réalisation équilibrée a été suggérée. Cela pourrait être bien exploré pour les très grands systèmes.

Certaines des principales contributions de cette thèse sont validées par les articles suivants qui en sont issus:

- **N. S. Ugwuanyi**, X. Kestelyn, O. Thomas, B. Marinescu and A.R. Messina, "A New Fast Track to Nonlinear Modal Analysis of Power System Using Normal Form," IEEE Trans. Power Syst., 2020.
- **N. S. Ugwuanyi**, X. Kestelyn, B. Marinescu and O. Thomas, "Power System Nonlinear Modal Analysis using Computationally Reduced Normal Form Method,"Energies, vol. 13, no. 5, p. 1249, 2020.
- **N. S. Ugwuanyi**, X. Kestelyn, O. Thomas, and B. Marinescu, "A Novel Method for Accelerating the Analysis of Nonlinear Behaviour of Power Grids using Normal Form Technique," in Innovative Smart Grid Technologies Europe (ISGT Europe), 2019.
- **N. S. Ugwuanyi**, X. Kestelyn, O. Thomas, and B. Marinescu, "Selective Nonlinear Coefficients Computation for Modal Analysis of The Emerging Grid," in Conférence des Jeunes chercheurs en Génie Eléctrique, 2019.
- **N. S. Ugwuanyi**, X. Kestelyn, B. Marinescu, and O. Thomas, "Speedy Technique for Selective Nonlinear Analysis of Electromechanical Modes of Future Grids," European Journal of Electrical Engineering: **UNDER REVIEW**.

F.2 Plan de la Thèse

La thèse est divisée en 6 chapitres, et les cinq chapitres restants sont décrits comme suit.

F.2.1 Chapitre 2 — Les Revues Littéraires

Ce chapitre est dédié à la revue des applications NF dans les réseaux électriques. Le but des revues est de faire ressortir la pertinence de la forme normale comme outil dans les systèmes électriques; ses défis et les propositions existantes pour atténuer ces défis. La position de la thèse au niveau mondial est alors établie.

L'analyse linéaire est un outil puissant dans le domaine de l'ingénierie. Il révèle rapidement les caractéristiques du système avec des concepts bien connus comme les valeurs propres et les vecteurs propres. En conséquence, il a été utilisé dans divers aspects de l'ingénierie et des systèmes d'alimentation pour les conceptions de commande. Comme il offre principalement des informations *monomode*, il ne parvient pas à caractériser correctement le comportement du

système sous contrainte, car les interactions modales deviennent importantes. Pour améliorer les outils linéaires, des termes d'ordre supérieur sont inclus dans l'analyse. Cette inclusion révèle de nombreuses autres caractéristiques du système impossibles avec l'analyse linéaire. L'analyse du modèle résultant est rendue possible en utilisant des outils comme la méthode de forme normale. L'outil glspl NF a été largement utilisé dans divers aspects de l'analyse et du contrôle des systèmes électriques. Bien que puissant, NF est difficile à réaliser dans les grands systèmes en raison de sa complexité de calcul. Les grands systèmes d'alimentation peuvent d'abord être réduits avant d'appliquer l'analyse NF. Il existe différentes techniques de réduction de modèles, mais la méthode actuelle d'analyse NF est encore très difficile à suivre, même lorsque le réseau est bien réduit.

F.2.2 Chaptre 3 — Résumé des Étapes pour Appliquer NF dans le Système d'Alimentation

L'analyse de la forme normale peut être appliquée aux modèles classiques du système d'alimentation ainsi qu'au modèle détaillé. Un modèle classique peut être écrit soit comme un ensemble d'équations différentielles du premier ordre, soit comme un ensemble d'équations différentielles du second ordre. L'application de NF au modèle du second ordre est plus précise que celle du premier ordre [115], cependant, en tenant compte des contrôles d'excitation, les systèmes d'alimentation sont généralement représentés avec des modèles du premier ordre. Le modèle détaillé adopté dans ce travail est le modèle à deux axes. Le système d'alimentation DAEs est formulé sous forme d'équations différentielles uniquement adaptées à NF. Les étapes de base de l'application de NF aux réseaux électriques peuvent être résumées par la figure F.7 et décrites ci-dessous:

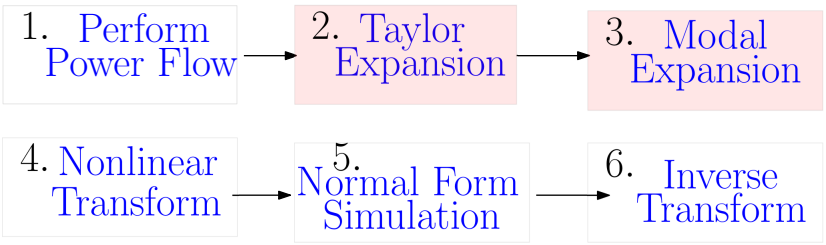

Figure F.7 – Principales étapes de l'application NF aux réseaux électriques.

1. *Formuler les DAE du système*: Les solutions de flux de puissance sont obtenues et le point d'équilibre stable (SEP) pour le système post-défaut est déterminé.

2. *Expansion de Taylor:* Les équations algébriques sont remplacées par les équations différentielles et les équations différentielles résultantes sont développées par la série de Taylor jusqu'à l'ordre souhaité autour du SEP. L'extension Taylor peut également être effectuée sur des DAE de système d'alimentation préservant la structure [65].

   Le jacobien du système (c'est-à-dire le terme de premier ordre dans l'expansion de Taylor) est utilisé pour extraire les valeurs propres et les vecteurs du système.

3. *Expansion modale:* Le système de l'étape 2 est développé sur la base des vecteurs propres obtenus à l'étape 2 et un nouveau système dynamique avec la partie linéaire de Jordan est obtenu, avec des termes non linéaires qui coupler les équations. Les coefficients des termes non linéaires, appelés*coefficients non linéaires*, doivent être calculés.

4. *Transformation de forme normale:* La partie non linéaire est encore simplifiée en appliquant la technique de forme normale, basée sur le changement non linéaire successif de variables. Cette étape conduit à l'évaluation d'autres coefficients polynomiaux, appelés coefficients NF.

5. *Conditions initiales et simulation NF:* Pour les simulations transitoires, les conditions initiales du système NF sont déterminées, généralement par combinaison de la méthode de Newton-Raphson et des techniques d'optimisation. Le système est ensuite simulé en coordonnées NF.

6. *NF inverse et transformation modale:* La dynamique d'origine peut être reconstruite en utilisant le changement de coordonnées des étapes 4 et 3.

Pour les applications de système d'alimentation, l'étape 6 est souvent utilisée uniquement comme vérification de la méthode. Pendant ce temps, la plupart des analyses sont basées sur l'analyse des informations dans les étapes 3 —4 et la condition initiale de l'étape 5. L'évaluation des coefficients NF à l'étape 4 revient finalement à une simple division des coefficients non linéaires (calculée à l'étape 3) par différentes combinaisons des valeurs propres linéaires (calculées à l'étape 2). Par conséquent, la principale charge de calcul se situe aux étapes 2 à step 3 et à l'évaluation de la condition initiale à l'étape 5. Comme on le verra, la méthode promue dans ce travail vise à simplifier considérablement les étapes 2 à 3.

F.2.3 Chapitre 4 — Méthode Développée pour Faciliter les Applications de Forme Normale

Dans cette thèse, nous proposons une méthode qui évite toutes les matrices de Hesse et obtient simultanément les coefficients non linéaires. La méthode proposée est motivée par une technique introduite dans le domaine du génie mécanique [116], et largement appliquée depuis, pour calculer les coefficients des modèles modaux non linéaires d'ordre réduit des structures mécaniques discrétisées par une méthode des éléments finis [113, 117]. L'effort dans la section suivante est d'exploiter les similitudes entre les systèmes mécaniques et électriques du second ordre, afin d'adapter cette technique pour les études de réseaux électriques.

Motivation: Pour une meilleure compréhension de la méthode proposée, considérons un exemple de motivation simple. La figure F.8 montre une masse reliée à un corps rigide par un ressort de raideur K. La masse repose sur certains rouleaux, de sorte qu'elle peut se déplacer. Supposons qu'une force externe F_{ext} provoque le mouvement de la masse, ce qui entraîne à

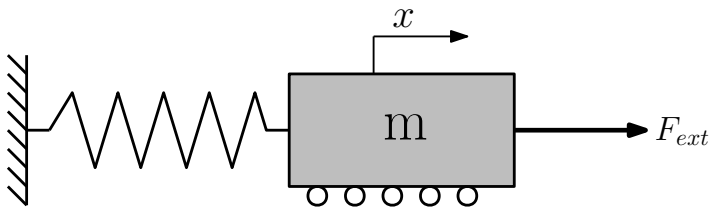

Figure F.8 – Un système masse-ressort

son tour le ressort à s'étendre sur une distance x. Le comportement non linéaire du ressort peut être modélisé comme:

$$m\ddot{x} + f(x) = F_{ext}. \tag{F.3}$$

Le système (F.3) peut être approximé avec des non-linéarités jusqu'au troisième ordre comme

$$m\ddot{x} + Kx + \beta x^2 + \gamma x^3 = F_{ext}, \tag{F.4}$$

où β, γ sont des coefficients inconnus. Essayons de résoudre les coefficients inconnus en prenant la partie rigidité (c'est-à-dire en supposant une condition stationnaire) de (F.4). Mais comme il contient deux inconnues dans une equation, la résolution de β, γ est mathématiquement difficile; nécessitant peut-être, des itérations. On suppose que nous connaissons la plage de x pour laquelle l'approximation (F.4) est valide et nous pouvons toujours calculer $f(x)$; alors il est possible de résoudre (F.4) linéairement pour obtenir les coefficients inconnus.

Choisissons deux valeurs arbitraires de x, d'amplitude égale mais de signe opposé (c'est-à-dire $\pm x \equiv x,\ -x$) dans la plage de valeurs de x. Ensuite, il est possible d'obtenir deux equations différentes, une pour chaque valeur de x as

$$Kx^{\pm} + \beta x^{2\pm} + \gamma x^{3\pm} = F_{ext}^{\pm} \implies \begin{cases} Kx^{+} + \beta x^{2+} + \gamma x^{3+} = F_{ext}^{+} \\ Kx^{-} + \beta x^{2-} + \gamma x^{3-} = F_{ext}^{-}, \end{cases} \tag{F.5}$$

où les exposants positifs et négatifs sont utilisés pour faire référence à l'equation relative à x et $-x$ respectivement. Ainsi, F_{ext}^{+} et F_{ext}^{-} correspondent respectivement à $f(x)$ et $f(-x)$ dans la partie statique de (F.3) . La forme plus compacte $\pm$ sera désormais utilisée là où le sens n'est pas déroutant.

Le système d'equations (F.5) est linéaire et totalement défini et peut ensuite être résolu pour trouver les coefficients inconnus β et γ. L'opération ci-dessus est exactement l'idée proposée dans ce travail, sauf que la méthode proposée traite du champ vectoriel au lieu de l'equation scalaire comme (F.4).

Résumé du chaptire: Dans ce chapitre, une méthode est proposée pour accélérer le calcul de la NF dans les réseaux électriques. La méthode proposée est une extension d'une technique précédemment utilisée en analyse structurale. Contrairement à la méthode conventionnelle, elle évite l'expansion de Taylor qui réduit le temps et la mémoire dans les calculs de forme normale. La méthode proposée a été développée pour tenir compte des systèmes différentiels réels et complexes. En d'autres termes, les modèles de premier et de second ordre des systèmes électriques ont été pris en compte. Par rapport à la méthode symbolique, la méthode proposée s'avère économiser de manière significative, le temps de calcul et la mémoire.

La méthode est intéressante, dans la mesure où les coefficients du deuxième et du troisième ordre nécessaires pour le modèle NF sont évalués simultanément de manière linéaire et tout coefficient préféré peut être calculé de manière sélective. De nombreuses analyses modales non linéaires, telles que les interactions non linéaires, les évaluations de stabilité et les facteurs de participation non linéaires se concentrent généralement sur les modes basse fréquence au lieu de tous les modes. Cela rend la méthode proposée très utile pour des évaluations non linéaires rapides. De plus, comme la méthode ne s'appuie que sur les mêmes paramètres que ceux utilisés pour l'analyse linéaire, elle peut facilement être intégrée dans un logiciel d'analyse modale commercial. De plus, les écarts modaux décrits par notre méthode correspondent à l'initialisation d'un système non linéaire avec la condition choisie et à l'étude de sa solution en régime permanent. Par conséquent, l'utilisation du même logiciel pour l'analyse linéaire pour atteindre la NF devrait être réalisable.

Ce chapitre a principalement porté sur la réduction des calculs de la méthode NF dans le système électrique. Dans le chapitre suivant, l'application de la méthode NF dans les réseaux électriques sera abordée. La méthode développée dans ce chapitre sera utilisée.

F.2.4 Chapitre 5 — Applications de Forme Normale dans les Systèmes d'Alimentation

Dans ce chapitre, certaines applications de l'analyse de forme normale ont été explorées. Des tests ont été effectués sur des systèmes d'alimentation petits et *grands*. La méthode à calcul réduit développée dans le chapitre précédent a été utilisée tout au long du présent chapitre.

Premièrement, des propositions de réduction supplémentaire du calcul de la forme normale, en se concentrant uniquement sur certains termes sélectionnés, sont faites. Deux propositions ont été faites — une qui consiste à négliger les interactions associées aux valeurs propres réelles dans la construction du modèle NF et l'autre qui consiste à négliger les interactions associées aux modes avec le moins d'énergie. Ces traitements réduisent considérablement la charge de calcul et accélèrent l'étude de l'interaction modale. L'extension de l'analyse linéaire aux facteurs de participation non linéaires résultant des interactions modales est également

présentée. Les applications pratiques des interactions modales et les préoccupations possibles ont également été discutées.

Deuxièmement, des exemples didactiques ont été utilisés pour expliquer le phénomène des décalages de fréquence non linéaires lorsque les systèmes électriques subissent des perturbations. Il a été démontré que pendant la perturbation (ou l'augmentation de la contrainte du système), la fréquence d'un mode d'oscillation dépend de l'amplitude d'oscillation et peut diminuer, contrairement à l'hypothèse de l'analyse modale linéaire. Il a été montré que la réduction de la fréquence d'un mode d'oscillation est liée à l'instabilité du mode.

Troisièmement, une méthode basée sur la forme normale est proposée, qui permet de surveiller un mode d'oscillation et de détecter sa fréquence en cas de perturbation. Cette nouvelle fréquence due aux perturbations est appelée fréquence non linéaire. Les cas de test ont montré que la méthode proposée capture la fréquence non linéaire de l'oscillation sous perturbation avec une erreur minimale. Les applications pratiques de la méthode d'évaluation dynamique en ligne des réseaux électriques ont été discutées.

Enfin, une méthode de surveillance de l'instabilité du mode a été proposée sur la base de la fréquence non linéaire, ayant établi une relation entre la fréquence non linéaire et l'instabilité du mode. La méthode de surveillance de l'instabilité consiste à rechercher une fréquence critique non linéaire au-delà de laquelle le mode perd de sa stabilité, appelé décalage de fréquence critique (CFS). Le CFS de tous les modes étant déterminé, un indice de proximité d'instabilité (IPI) a été proposé qui surveille la proximité du point de fonctionnement à l'instabilité. La comparaison de la méthode proposée et des simulations dans le domaine temporel pour les cas testés a montré que l'erreur de la méthode proposée était juste. Le potentiel de la méthode proposée pour les applications en ligne et les signes avant-coureurs de l'instabilité du mode ont été discutés.

Dans le prochain chapitre, nous relierons tous les développements du premier chapitre au présent chapitre afin de tirer quelques conclusions.

F.3 Conclusions et Travaux Futurs

F.3.1 Conclusions

La théorie, l'analyse, les résultats, et les observations présentées dans cette thèse peuvent être résumées comme suit:

1. La méthode et les théories conventionnelles de la forme normale ont d'abord été rappelées. Dans l'application de la forme normale du troisième ordre dans le système électrique, tout d'abord, le modèle non linéaire est étendu par la série Taylor jusqu'au troisième ordre et les matrices de Hesse sont évaluées pour le point de fonctionnement donné. Le modèle approximatif résultant est transformé en forme de Jordan, en utilisant le vecteur propre/valeurs propres calculé à partir de la partie de premier ordre de l'expansion de Taylor. Les coefficients du modèle de Jordan, appelés dans cette thèse coefficients non linéaires, sont déterminés. Enfin, un changement de variable non linéaire est défini pour supprimer les termes non linéaires du modèle de Jordan, qui mettent le modèle approximatif non linéaire résultant sous une forme normale. Sur la base de ce modèle, des indices analytiques peuvent être définis pour comprendre l'effet des interactions non linéaires lorsque le système est stressé.

2. Dans le cas de la méthode développée, l'analyse linéaire est d'abord effectuée pour extraire les valeurs propres/vecteurs propres. Ensuite, le système non linéaire d'origine est perturbé de telle sorte que certains modes ou combinaisons de modes souhaités sont excités à l'aide de vecteurs propres à l'échelle. Le facteur d'échelle est l'amplitude de la perturbation modale, et est choisi de telle sorte que les non-linéarités anticipées dues à la perturbation se trouvent dans l'approximation de Taylor du troisième ordre. La

solution statique du système non linéaire due à la perturbation est obtenue. Différentes excitations permettent de formuler un système d'équations linéaire dont les coefficients correspondent aux coefficients non linéaires souhaités et dont le deuxième membre correspond à la solution statique du système non linéaire. De cette façon, tous les coefficients souhaités peuvent être calculés sans l'expansion de Taylor et le calcul réels des matrices de Hesse. La méthode développée a été appliquée aux systèmes de puissance représentés avec des équations différentielles de second ordre, où toutes les quantités sont à valeur réelle, ainsi qu'aux systèmes de puissance représentés avec des équations différentielles de premier ordre, où les quantités calculées sont à valeur complexe.

3. Les calculs avec la méthode développée sont comparés aux calculs utilisant la boîte à outils symbolique. Les simulations dans le domaine temporel des modèles construits à partir des deux calculs sont également comparées. A partir des résultats présentés au chapitre 4, les observations suivantes sont faites:

   - La méthode proposée est très précise, enregistrant une erreur de $1,83e^{-3}$ % comme l'erreur la plus élevée dans tous les cas testés, et les simulations des méthodes proposées et symboliques dans des conditions de stress sévères correspondent.
   - Les calculs avec la méthode proposée sont très rapides et économiques en mémoire, comparés à la méthode symbolique. Les résultats ont montré qu'avec l'augmentation du nombre de variables dans le système, la méthode proposée devient incomparable avec la méthode symbolique. Pour des cas comparés, la méthode proposée peut être 776 fois plus rapide et $1,52e^{3}$ fois moins coûteuse (en termes de mémoire) que la méthode symbolique. Cette économie de calcul est d'abord due à l'évitement des matrices de Hesse et des différenciations d'ordre supérieur; et deuxièmement, du fait que la méthode proposée obtient tous les coefficients en résolvant des ensembles d'équations linéaires qui sont faciles à utiliser par ordinateur. Cette observation est bonne, car la nouvelle méthode peut désormais étendre la taille du système qui peut être considérée avec une troisième autre forme normale. De plus, les futurs systèmes d'alimentation seront remplis de convertisseurs électroniques de puissance qui ont plusieurs variables d'état, nécessitant l'utilisation de la méthode proposée pour obtenir leurs formes normales.
   - La méthode proposée est commodément sélective, permettant de calculer uniquement les termes spécifiques du modèle non linéaire approximatif sans calculer le reste. Cette observation est pertinente car elle permet à l'analyse de se concentrer uniquement sur certains modes spécifiques du système avec des calculs moins lourds. De plus, les résultats du chapitre 4 suggèrent que les non-linéarités du système ne sont pas réparties uniformément, mais sont localisées autour de certains modes dans le système. Cela implique que l'application sélective de la forme normale peut être poursuivie avec la méthode développée pour un système avec un grand nombre de variables.
   - En considérant le logiciel de simulation de domaine temporel du système électrique, la perturbation du système non linéaire avec des vecteurs propres à l'échelle, comme requis par la méthode proposée, correspond simplement à l'initialisation du système avec les conditions initiales — les vecteurs propres à l'échelle. Cette observation souligne la possibilité d'utiliser le logiciel du système d'alimentation déjà existant pour l'analyse de la forme normale. De plus, il n'y a pas de logiciel dédié pour l'analyse de la forme normale du système d'alimentation.
   - On observe qu'avec la méthode développée, les termes du deuxième et du troisième ordre sont calculés simultanément. Cela présente un avantage pour la demande de formulaire normal de troisième ordre; cependant, si seule la forme normale du second ordre est nécessaire, il n'est pas possible avec la méthode développée de

calculer les termes du second ordre sans certains termes du troisième ordre. Cela implique que la méthode est spécifiquement développée pour les applications de forme normale de troisième ordre, bien que l'idée puisse être étendue si nécessaire.

- La méthode développée suppose qu'il n'y a pas de résonance modale exacte. Autrement dit, toutes les valeurs propres sont distinctes et la matrice d'état du système est diagonalisable. Dans le cas d'une résonance modale exacte, l'excitation de différents modes indépendamment à l'aide de vecteurs propres à l'échelle devient compliquée, limitant ainsi la méthode développée. Il s'agit cependant d'un problème général dans l'application de formulaire normal et non spécifique à la méthode développée.
- En excitant les modes de calcul des coefficients, le choix de l'amplitude de l'écart modal peut affecter les résultats. Si une amplitude trop grande est utilisée, le niveau des non-linéarités dues à la perturbation dépasse le troisième ordre sur lequel la méthode est basée, donnant ainsi des résultats erronés. D'un autre côté, une très faible valeur de l'amplitude de l'écart modal ne crée pas de non-linéarités suffisantes en raison de la perturbation, plaçant le système uniquement dans une région linéaire alors que les coefficients nécessaires sont pour les termes non linéaires.
- Une autre limitation de la méthode développée est l'hypothèse que les non-linéarités sont lisses et statiques. Si ces hypothèses deviennent invalides, la méthode peut échouer.

4. En utilisant la forme normale définie pour le système d'alimentation représenté par des équations différentielles du second ordre, un indice analytique pour estimer le décalage de fréquence des modes électromécaniques sous perturbation est proposé. Sur la base de cet indice d'estimation de décalage de fréquence, un autre indice de proximité d'instabilité est développé pour estimer la proximité du mode oscillatoire à l'instabilité. Ces indices ont été testés sur de petits et grands réseaux électriques. A partir des résultats présentés au chapitre 5, les observations suivantes sont faites:

   - L'augmentation des contraintes dans le système diminue les fréquences des modes électromécaniques. C'est-à-dire que les fréquences des modes électromécaniques passent des valeurs fondamentales (déterminées par analyse linéaire) à une autre valeur moindre en raison de l'augmentation des non-linéarités.
   - Le décalage de fréquence est plus prononcé sur le mode dominant et est lié à la stabilité du mode. Les décalages de fréquence augmentent à mesure que la contrainte augmente jusqu'à un point critique où les modes perdent leur stabilité.
   - Le contrôle du système d'alimentation moderne se concentre sur la surveillance étendue des oscillations électromécaniques à l'aide de mesures en temps réel, où les paramètres de mode (par exemple, la fréquence et l'amortissement) sont automatiquement estimés pour toutes les conditions de fonctionnement actuelles pour une action de contrôle appropriée. Les indices proposés dans ce travail peuvent assez bien prédire les décalages de fréquence des modes électromécaniques à mesure que la contrainte augmente. Cette observation est très cruciale, car les indices peuvent être utilisés pour une estimation approximative en ligne de la stabilité du système et pour des signaux d'avertissement d'instabilité dans le fonctionnement du système électrique.
   - Étant basés sur un modèle de système d'alimentation classique et une approximation du troisième ordre du modèle non linéaire exact, les indices proposés ont une plage de validité limitée et ne peuvent donc pas fournir des informations sur la stabilité globale.

5. Enfin, pour réduire encore les calculs de forme normale, une application sélective de forme normale est proposée. La méthode consiste à négliger les interactions associées

aux — (1) valeurs propres réelles et (2) modes aux énergies les plus faibles. Pour déterminer les modes avec le moins d'énergie, les valeurs singulières de Hankel sont utilisées pour déterminer les états les plus contrôlables et observables; l'analyse des facteurs de participation est ensuite utilisée pour déterminer les modes qui sont liés aux états de Hankel les plus pertinents. Les interactions liées à ces modes sont prises en compte, tandis que d'autres ne le sont pas. Cette technique d'application sélective de forme normale a été utilisée pour étudier les interactions modales non linéaires et les facteurs de participation non linéaires. A partir des résultats présentés au chapitre 5, les observations suivantes sont faites:

- Pour le cas testé, les mêmes interactions non linéaires sont détectées, à la fois pour l'application sélective et la forme normale complète. Cette observation tend à suggérer que les valeurs propres réelles ne jouent pas un rôle significatif sur les interactions modales non linéaires. En outre, il a été constaté que les mêmes modes impliqués dans l'interaction non linéaire sont les modes ayant les hautes énergies basées sur les valeurs singulières de Hankel. Cette observation tend à suggérer qu'en dehors des valeurs propres réelles, certains modes oscillatoires sont faibles pour les interactions non linéaires, de sorte que leur inclusion contribue à davantage de "gaspillage" de calcul.
- En plus de la réduction de calcul due à la nouvelle méthode de calcul des coefficients non linéaires, l'application sélective de forme normale introduit une autre forte réduction du temps de calcul. Cette observation est particulièrement importante car lorsque les contrôles sont pris en compte dans les modèles de générateur, de nombreuses valeurs propres sont réelles. De plus, de nombreux modes sont fortement amortis, ce qui permet de les négliger. Cela pourrait être très utile lorsque l'on considère les réseaux électroniques de puissance, où plusieurs modes sont réels et de nombreux modes oscillatoires sont fortement amortis.

Dans cette thèse, il a été démontré qu'éviter la différenciation d'ordre supérieur et les évaluations de Hesse peuvent étendre l'analyse de forme normale du troisième ordre à des systèmes plus grands, au-delà de ce que la méthode conventionnelle peut gérer. Il a également été démontré qu'il existe de nombreuses possibilités de réduire les calculs intraitables dans l'analyse de forme normale. De tous les résultats de ce travail, on peut conclure que, avec la nouvelle technique de calcul développée, ainsi que les développements appropriés des idées d'application de forme normale sélective proposées dans ce travail, il sera possible d'utiliser la forme normale pour étudier l'avenir et plus réseaux lorsque les interactions non linéaires deviennent significatives.

F.3.2 Travaux Futurs

Plusieurs expériences potentiellement fructueuses n'ont pas été réalisées en raison de nombreuses contraintes au cours de cette recherche. D'après les observations et l'expérience recueillies au cours de cette recherche, de nombreuses possibilités potentiellement lucratives pour les travaux futurs peuvent être recommandées comme suit:

1. Étant donné que la méthode développée n'est pas intrusive et nécessite l'initialisation du modèle non linéaire d'origine avec des conditions initiales de choix, il pourrait être très intéressant d'essayer de réaliser la méthode proposée avec un logiciel de système d'alimentation commercial. La méthode nécessite une formation d'ensembles d'équations linéaires, où tous les paramètres nécessaires sont obtenus à partir de la matrice d'état, après une analyse linéaire. De nombreux logiciels standard de systèmes d'alimentation commerciaux tels que EUROSTAG ® peuvent effectuer à la fois une analyse linéaire et une simulation dans le domaine temporel. Ainsi, il peut être possible d'utiliser un logiciel de simulation dans le domaine temporel pour obtenir la solution

statique non linéaire du modèle non linéaire, qui est requise par la méthode développée. Si elle est réalisée, une telle percée sera à la fois bénéfique pour les opérateurs de réseaux électriques pour une analyse modale détaillée, et pour les chercheurs intéressés par l'analyse de la forme normale, puisque la forme normale sera ensuite intégrée en tant que progiciel dans un tel logiciel.

2. Bien que la méthode proposée ait considérablement réduit la charge de calcul de la forme normale, un aspect particulier non directement traité est la charge de calcul de la condition initiale dans l'espace de la forme normale. La détermination de la condition initiale prend du temps. Un algorithme plus efficace pour la résolution d'équations non linéaires pourrait aider à résoudre ce problème.

3. Comme indiqué dans l'article, les résultats de la méthode développée sont affectés par l'amplitude de l'écart modal. Cette amplitude a été choisie heuristiquement, même si une plage de valeurs donnant de bons résultats a été établie pour les cas de test utilisés. Afin de promouvoir la méthode, il sera nécessaire de définir à l'avance la valeur de l'amplitude de l'écart modal, compte tenu du degré de non-linéarité du système étudié. Une telle relation entre le degré de non-linéarité du système et l'amplitude correcte de l'écart modal devrait être développée à l'avenir.

4. Les indices développés pour surveiller les décalages de fréquence des modes électromécaniques sont basés sur l'application de la forme normale aux réseaux électriques représentés par des équations différentielles du second ordre. Dans ce cas, il n'y a pas de quantités complexes dans les formulations. Étant donné que la représentation par équation du premier ordre du système d'alimentation est la norme, il pourrait être intéressant d'étudier à l'avenir, l'extension au système d'alimentation représentée avec un modèle du premier ordre, impliquant des quantités complexes.

5. Bien que les idées sélectives de forme normale présentées dans ce travail donnent de bons résultats, le cas de test était très simple. Il est recommandé à l'avenir d'étudier les potentiels perçus avec des systèmes d'alimentation plus importants. Si les résultats sont cohérents dans les grands réseaux électriques, la proposition sera très essentielle pour les futurs réseaux.

6. Qu'elle soit réduite ou non par calcul, l'analyse de forme normale n'est pas nécessaire si la condition du système ne montre pas de fortes non-linéarités. Par conséquent, des indices sont nécessaires en fonction de l'état du système, pour déterminer le niveau de non-linéarités et l'ordre de forme normale à utiliser. Cela aidera à savoir a priori, s'il est rentable de se lancer dans l'analyse de forme normale pour éviter une perte de calcul. Ainsi, à l'avenir, ces indices devraient d'abord être trouvés ou développés avant de procéder à l'analyse NF.

7. Tous les développements de ce travail ont été basés sur les modèles de générateurs conventionnels. Les futurs réseaux seront constitués principalement de générateurs à commande par convertisseur. Il est nécessaire à l'avenir d'étudier l'efficacité de la méthode développée en utilisant les modèles de convertisseurs électroniques de puissance (PE). De plus, la limitation de la méthode réside dans le fait que les non-linéarités doivent être statiques, ce qui peut ne pas être le cas pour les réseaux avec 100 % PE; des tests sont donc nécessaires.

8. L'utilisation de la méthode de la forme normale pour dériver une loi de commande non linéaire pour la commande du convertisseur de puissance pourrait également être une aventure de recherche très intéressante.

Nnaemeka UGWUANYI

Contributions pour le positionnement de la méthode de forme normale comme outil d'analyse de future système d'alimentation

Résumé: Compte tenu de plusieurs contraintes économiques, techniques et environnementales, les systèmes électriques actuels fonctionnent très près de leurs limites, ce qui fait qu'ils présentent de plus en plus des comportements non linéaires. De plus, le transfert d'une grande quantité d'énergie sur de longues distances n'est pas rare aujourd'hui, cela conduit à des interactions non linéaires, conduisant à un réel défit; celui de l'utilisation des outils traditionnels d'analyse du système électrique en présence de fortes non linéarités. En outre, la forte pénétration des énergies renouvelables et de l'électronique de puissance qui l'accompagne viennent augmenter ces non linéarités du système électrique. En conséquence, les outils d'analyse modale bien établis utilisés par le passé deviennent insuffisants pour l'analyse du système électrique aujourd'hui et celui du futur; d'où le besoin d'outils alternatifs. L'inclusion de termes d'ordres supérieurs dans l'analyse modale, possible avec la méthode de forme normale (NF), augmente les informations qu'elle fournit et permet de mieux étudier les aspects dynamiques sur un système d'alimentation présentant un comportement fortement non linéaire. Cependant, la méthode NF nécessite au préalable la décomposition de Taylor du système non linéaire, qui produit plusieurs matrices et coefficients de Hesse d'ordre supérieur, une opération non réalisable avec les méthodes standard lorsque l'on considère les systèmes à grande échelle. Dans cette thèse, pour répondre à cette problématique, une méthode numérique efficace pour accélérer ces calculs, en évitant l'expansion de Taylor habituelle, est développée. Les nouveaux calculs consistent à définir les vecteurs propres linéaires comme champ inconnu dans le système non linéaire initial, ce qui conduit à résoudre des équations linéaires uniquement pour obtenir tous les coefficients nécessaires. De cette façon, le calcul du modèle non linéaire jusqu'au troisième ordre et l'analyse modale non linéaire deviennent simples et réalisables avec un temps de calcul raisonnable. De plus, des indices basés sur la NF pour la stabilité du système électrique et la surveillance du fonctionnement sont proposés et testés sur plusieurs systèmes.

Mots clés: Réduction du calcul, analyse modale non linéaire, méthode de forme normale, analyse du système d'alimentation.

Abstract: Given several economic, technical and environmental constraints, today's power systems are operated very close to their limits, which means they exhibit nonlinear behaviour more than in the past. In addition, the transfer of large amount of power over long distances common nowadays leads to nonlinear interactions, a phenomenon which challenges the traditional power system analysis tools. Furthermore, high penetration of renewable energies and the accompanying power electronics, which are evident in today's power systems, increase the nonlinearities of the systems. As a result, the well-established modal analysis tools become insufficient for the analysis of present and future power systems; making the development of alternative tools necessary. The inclusion of higher order terms in modal analysis, possible with Normal Form (NF) method, augments the information it provides, and enables better dynamic studies of systems exhibiting high nonlinear behaviour. However, NF method requires the preliminary Taylor expansion of the nonlinear system, which generates several higher order Hessian matrices and coefficients to be computed, an operation impracticable with standard methods, when considering large scale systems. In this thesis, to answer to this problem, an efficient numerical method for accelerating those computations, by avoiding the usual Taylor expansion is developed. The new computations consist in prescribing the linear eigenvectors as unknown field in the initial nonlinear system, which leads to solving linear-only equations to obtain all needed coefficients. In this way, the computation of the nonlinear model up to third order, and nonlinear modal analysis become fast, and achievable in a convenient computation time. Moreover, NF-based indices for power system stability and operation monitoring are proposed and tested on several systems.

Keywords: Computation reduction, nonlinear modal analysis, normal form method, power system analysis.